Title
Is the unique localization of TIMP-3 a consequence of interactions with heparan sulfate proteoglycans?

Author
Taniguchi, Gary Takeru

Publication Date
2000

Peer reviewed|Thesis/dissertation

Is the Unique Localization of TIMP-3 a Consequence of Interactions with Heparan Sulfate Proteoglycans?

by

Gary Takeru Taniguchi

DISSERTATION

Submitted in partial satisfaction of the requirements for the degree of

DOCTOR OF PHILOSOPHY

in

Pharmaceutical Chemistry

in the

GRADUATE DIVISION

of the

UNIVERSITY OF CALIFORNIA SAN FRANCISCO

[redacted]

Date University Librarian

Degree Conferred: .....

ther, Robert, my moth
band, Larry, whose supp
wor

To
my father, Robert, my mother, Aiko, my brother, Glen, and my husband, Larry, whose support and love have helped make this work possible

Ackno

My most thanks and gra

Sara Hawkes, Ph.D. for he

her guidance in scientific in

taught me to become a v

given me the foundation fo

would like to thank my

thesis Patricia C. Babbitt, P

time throughout my scie

writing of this thesis.

I would also like to thank

Jeffrey Kimbrel, Ph.D., Thomas

for helping me to build a

I would like to thank former

at Veteran Laboratories, Lisa

Jessica Kishiyama, Ph.D., Hong

Dr. Kaishi Wang, Ph.D., an

support and patience.

I would like to thank Dylan Ed

Nick Sexis and many TIMP

Hessler, Ph.D. for providing

the key components in th

Acknowledgements

My utmost thanks and gratitude go to my advisor and mentor, Susan P. Hawkes, Ph.D. for her support and patience through difficult times, guidance in scientific investigation and writing. Her supervision has taught me to become a very critical and analytical scientist and has given me the foundation for better scientific writing.

I would like to thank my thesis advisors and orals committee members, Patricia C. Babbitt, Ph.D. and Robert Stern, M.D., for their guidance throughout my scientific education at UCSF and in the production of this thesis.

I would also like to thank my other orals committee members, Deanna Kroetz, Ph.D., Thomas Meehan, Ph.D., and Wolfgang Sadee, Ph.D., for helping me to build an interesting and productive project.

I would like to thank former and current members of the Hawkes and Meehan laboratories, Lisa Ahlberg-Randall, Ph.D., Van Hoang, Narendra Kishnani, Ph.D., Hongxia Li, Michael W. Oakley, Ester Vogt, Ph.D., Keshi Wang, Ph.D., and Alan Wolfe, for their friendship, support, and patience.

I would like to thank Dylan Edwards, Ph.D. for the generous gift of BHK-21 cells and many TIMP cDNA constructs, and Richard A. Williamson, Ph.D. for providing the N-TIMP-2 structure files, all of which were key compenents in the success of this project.

...uld especially like to thi...
...-Quantum Analytics ...
...for the chromatograph...
...My thanks also go to Al...
...ric and guidance towa...
...Finally, I would like to e...
...gratitude to my best f...
...support during unusually c...
...years.

I would especially like to thank Gerry Farren, Ph.D. and Dona Smith from Link-Quantum Analytics for their generous loan of an HPLC system for the chromatographic analyses presented in this thesis.

Many thanks also go to Alan Herman, Ph.D. for his mentorship at Amgen Inc. and guidance towards graduate school.

Finally, I would like to especially extend my appreciation and eternal gratitude to my best friend, partner, and husband, Larry, for his support during unusually difficult times and patience throughout these years.

Is the Unique Localizat

Interactions with He

Gary Ta

e processes of meta

ar matrix or basa

metalloproteinases, MM

e invasive processes. T

ycans and fibronectin

et al. demonstrated in

prototype matrix meta

ers of MDCK cells throug

tissue inhibitor of m

s that are the natural

ers. TIMP-3 is unique to

only one that localizes

and TIMP-4 are found

ed media of cultured c

s and Hawkes determ

extracellular matrix a

Is the Unique Localization of TIMP-3 a Consequence of Interactions with Heparan Sulfate Proteoglycans?

Gary Takeru Taniguchi

Abstract

For the processes of metastasis and angiogenesis to occur, the extracellular matrix or basal laminae must undergo degradation. Matrix metalloproteinases, MMPs, are the key enzymes involved in these invasive processes. They function by degrading collagens, proteoglycans and fibronectin of the extracellular matrix. Recently, Hotary *et al.* demonstrated in an *in vitro* model that the MT-MMPs, membrane-type matrix metalloproteinases, increase the invasive properties of MDCK cells through a three-dimensional matrix (1). The TIMPs, tissue inhibitor of metalloproteinases, are multifunctional proteins that are the natural inhibitors of the MMPs and are also cytokines. TIMP-3 is unique to the four-member TIMP family in that it is the only one that localizes to the extracellular matrix. TIMP-1, TIMP-2, and TIMP-4 are found in body fluids *in vivo* and *in vitro* in the conditioned media of cultured cells.

Blenis and Hawkes determined that the interactions with TIMP-3 and the extracellular matrix are likely to be electrostatic (2). Kishnani

it MMPs demonstrated t

ose agarose beads and do

ses 3). The data presente

ence alignments and pe

ts that the basic linear s

ail of TIMP-3 forms a basic

present on the surface of t

ction with heparan sulfa

ed electrostatically. From

ds from Arg20 to Lys 5

ding ears localizing it to th

ssing dimeric TIMP-2 a

ive region from Arg20 to L

ion in the extracellular mat

ssion of TIMP-2 from the

ion.

ibition experiments we

ther characterization of b

ency data suggests that

ence is less than its a

siological significance of

ibute properties to stu

and Hawkes demonstrated that TIMP-3 binds to heparan sulfate-coated agarose beads and does not bind to polylysine-coated agarose beads (3). The data presented in this thesis demonstrate, by creating sequence alignments and performing homology modeling of the four TIMPs, that the basic linear sequence of amino acids from Arg20 to Lys52 of TIMP-3 forms a basic surface on the TIMP-3 molecule that is not present on the surface of the other TIMPs. Modeling of the TIMP-3 projection with heparan sulfate demonstrated that the two could interact electrostatically. From these data, we postulate that the basic region from Arg20 to Lys 52 of TIMP-3 binds to heparan sulfate proteoglycans localizing it to the extracellular matrix. By creating and expressing chimeric TIMP-2 and TIMP-3 proteins, we demonstrated that the region from Arg20 to Lys52 is necessary for the localization of TIMP-3 in the extracellular matrix but it is not sufficient to change the localization of TIMP-2 from the conditioned media to the extracellular matrix.

Purification experiments were performed to provide pure proteins for further characterization of binding, growth, and inhibitory activity. Preliminary data suggests that the affinity of MMP-2 for the C3 and C3-L chimeras is less than its affinity for TIMP-2.

The biological significance of the chimeras was tested by examining the growth properties to study the effect localization has on cell

...raction. TIMP-3 inhibits

...NA sequence that the ch...

...focal microscopy dem...

...eparan sulfate in the ex...

...ization by confocal mic...

...ociation of TIMP-3 on th...

...localization of TIMP-3 a...

...ect could directly influe...

...ast ADAMs, and may be...

...raction with cell surface

...eins and glypicans.

...Huxley K, Allen E, Puntur...

...sion and morphogenesis:...

...rich membrane-type matr...

...al Cell Biology 2000;14...

...Bass J, Hawkes SP. Char...

...fold protein in the extrace...

...ases J Biol Chem 1984;2...

...Kashiwagi N. Characteriza...

...Proteinases-3 (TIMP-3), ...

...Human and Avian Cells...

...Press San Francisco; 1994.

proliferation. TIMP-3 inhibited proliferation. In addition, the more TIMP-3 sequence that the chimera contains, the slower the growth.

Confocal microscopy demonstrated the co-localization of TIMP-3 and heparan sulfate in the extracellular matrix. In addition, the co-localization by confocal microscopy provides the first definitive demonstration of TIMP-3 on the cell surface.

The localization of TIMP-3 at the cell surface places it in a position where it could directly influence cell surface molecules such as MT-MMPs and ADAMs, and may be directly controlled by the cell through its interaction with cell surface heparan sulfate proteoglycans such as syndecans and glypicans.

1. Hotary K, Allen E, Punturieri A, Yana I, Weiss SJ. Regulation of cell invasion and morphogenesis in a three-dimensional type I collagen matrix by membrane-type matrix metalloproteinases 1, 2, and 3. Journal of Cell Biology 2000;149(6):1309-23.

2. Blenis J, Hawkes SP. Characterization of a transformation-sensitive protein in the extracellular matrix of chicken embryo fibroblasts. J Biol Chem 1984;259(18):11563-70.

3. Kishnani N. Characterization of Tissue Inhibitor of Metalloproteinases-3 (TIMP-3) from the Extracellular Matrices of Cultured Human and Avian Cells [Ph.D.]. San Francisco: University of California San Francisco; 1994.

TABLE

Chapter 1 **Introduction**

1 Preface

2 The Extracellular

3 Extracellular M

3.1 Plasmin

3.2 Matrix Met

4 Tissue Inhibito

4.1 Growth Fac

4.2 Induction o

4.3 TIMP-2 Is a
MMP-2

4.4 TIMPs as T-

4.5 TIMP-3 Elec
Extracellular

5 Heparan Sulfate

5.1 Composition
Proteoglycan

5 Overview

7 Bibliography

Chapter 2 **Sequence Analysis of TIMP-3**

3 Introduction

4 Materials and Me

TABLE OF CONTENTS

Chapter 1	**Introduction**	**1**
1.1	Preface	2
1.2	The Extracellular Matrix and Basal Laminae	5
1.3	Extracellular Matrix Degrading Enzymes	6
1.3.1	Plasmin	6
1.3.2	Matrix Metalloproteinases	8
1.4	Tissue Inhibitor of Metalloproteinases	15
1.4.1	Growth Promoting Activity of TIMPs	17
1.4.2	Induction of Apoptosis by TIMP-3	18
1.4.3	TIMP-2 Is an Activator and Inhibitor of MMP-2	19
1.4.4	TIMPs as Therapeutics?	21
1.4.5	TIMP-3 Electrostatically Interacts with the Extracellular Matrix	23
1.5	Heparan Sulfate Proteoglycans	25
1.5.1	Composition of Heparan Sulfate Proteoglycans	27
1.6	Overview	29
1.7	Bibliography	31
Chapter 2	**Sequence Analysis and Homology Modeling of TIMP-3**	**63**
2.1	Introduction	64
2.2	Materials and Methods	74

2.2.1	Protein Sequence Searches	74
2.2.2	Multiple Sequence Alignments	75
2.2.3	Projections of N-TIMPs	76
2.2.4	Projections of Full TIMPs	77
2.3	Results and Discussion	78
2.3.1	Sequence Alignments of the Four Human TIMPs	78
2.3.2	Homology Modeling of N-TIMP-1, N-TIMP-3, and N-TIMP-4 Utilizing the N-TIMP-2 NMR Structure	80
2.3.3	Modeling of TIMP-3 with Heparan Sulfate	83
2.3.4	Homology Modeling of TIMP-1, TIMP-3, and TIMP-4 Utilizing the Full TIMP-2 X-ray Crystal Structure	88
2.4	Bibliography	93
Chapter 3	**Construction and Expression of the Wild-Type and Chimeric TIMPs**	**101**
3.1	Introduction	102
3.2	Materials and Methods	106
3.2.1	Construction of the Chimeras by PCR	106
3.2.2	Cloning and Sequence Confirmation	111
3.2.3	Transient Expression in COS-1 Cells for Confirmation of Activity	112
3.2.4	Generation of Stably Transfected BHK-21 Cell Lines and Expression of Wild-type and Chimeric Proteins	114

3.2.5	Transfection of COS-1 and BHK-21 Cells	115
3.2.6	Maintenance of COS-1 Cells Prior to Transfection	116
3.2.7	Maintenance of BHK-21 Cells	116
3.2.8	Induction of Stably Transfected BHK-21 Cells	117
3.2.9	Western Blots	117
3.2.10	Analysis of pNUThuTIMP-3 BHK-21 in VP-SFM	119
3.3	Results	120
3.3.1	PCR Results	120
3.3.2	Cloning and Sequence Confirmation of PCR Products	123
3.3.3	Ligation into pXMT2 for Transient Transfection of COS-1 Cells	128
3.3.4	Stable Transfection of BHK-21 Cells	134
3.3.5	Reverse Zymography Analysis of Conditioned Media and ECM of C3 and C2 Chimeras	142
3.3.6	Western Blots of the C3 and C2 Chimeras	146
3.3.7	Significance of the C3 and C2 Chimeras	150
3.3.8	Construction of the New Chimeras, C2cT3, T3cT2 and C3-L	154
3.3.9	The C2cT3 Chimera Partially Localizes in the ECM	155
3.3.10	The T3cT2 Chimera Does Not Localize to the Conditioned Media	158

3.3.1.1 The Loca
Similar t
Chimera

3.3.1.2 Gelatin z
from BHK
TIMP-3 a

3.4 Discussion

3.5 Bibliography

Chapter 4 Purification of Chimeras

4.1 Introduction

4.2 Materials and

4.2.1 Collection
Preparat

4.2.2 Ion Exchan

4.2.3 Gel Filtratio

4.3 Results and Dis

4.4 Bibliography

Chapter 5 Co-localization Sulfate by Confo

5.1 Introduction

5.2 Materials and M

5.2.1 Maintenance

BHK-21 Cell
heparinase I

3.3.11	The Localization of the C3-L Chimera is Similar to that Displayed by the C3 Chimera	160
3.3.12	Gelatin zymography of Conditioned Media from BHK-21 Cells Expressing TIMP-2 and TIMP-3 and the C2 and C3 Chimeras	163
3.4	Discussion	168
3.5	Bibliography	174
Chapter 4	**Purification of TIMP-3 and the C3 and C3-L Chimeras**	**178**
4.1	Introduction	179
4.2	Materials and Methods	181
4.2.1	Collection of Conditioned Media and Preparation of Extracellular Matrix	181
4.2.2	Ion Exchange Chromatography	181
4.2.3	Gel Filtration Chromatography	182
4.3	Results and Discussion	182
4.4	Bibliography	197
Chapter 5	**Co-localization of TIMP-3 and Heparan Sulfate by Confocal Microscopy**	**199**
5.1	Introduction	200
5.2	Materials and Methods	201
5.2.1	Maintenance of BHK-21 Cells	201
5.2.2	BHK-21 Cell Growth and Treatment with heparinase III	202

5.2.3	Cell Growth and Treatment with Heparan Sulfate, Heparinase III and Chondroitinase ABC	202
5.2.4	Staining with Anti-chicken TIMP-3 Polyclonal Antibody and Anti-human Heparan Sulfate Monoclonal Antibody	204
5.2.5	Confocal Microscopy	205
5.3	Results	206
5.3.1	Confocal Microscopy of Untransfected and pNUThuTIMP-3 Transfected BHK-21 Cells	207
5.3.2	Confocal Microscopy of pNUThuTIMP-3 BHK-21 Cells Incubated with Heparinase III	209
5.3.3	Confocal Microscopy of pNUThuTIMP-3 BHK-21 Cells Incubated with Heparan Sulfate, Heparinase III, and Chondroitinase ABC	212
5.3.4	Reverse Zymography of Incubation Solutions and Extracellular Matrix from pNUThuTIMP-3 BHK-21 Cells Incubated in Heparan Sulfate, Heparinase III, and Chrondroitinase ABC	215
5.4	Discussion	217
5.5	Bibliography	222
Chapter 6	**Growth Effects of the Wild-Type and Chimeric TIMPs**	**225**
6.1	Introduction	226
6.2	Materials and Methods	228
6.2.1	Seeding and growth of BHK-21 cell lines	228
6.2.2	Cell Proliferation Assay	229

6.3	Results	229
6.4	Discussion	235
6.5	Bibliography	238
Chapter 7	**Conclusion**	**242**
7.1	Conclusion	243
7.2	Bibliography	250
Appendix		**255**
A-1	Extracellular Matrix and Conditioned Media Collection	256
A-2	Reverse Zymography Method (includes SDS-PAGE and zymography methods)	259

Domain arrangeme

Sequence alignmen

Sequence alignmen

Schematic structure

Sequence alignment

Homology modeling o
N-TIMP-4 based on t

The N-TIMP-3 project

Schematic of distance
heparin and the hydro
and lysines of TIMP-3

TIMP-3 models show
the proposed hepara-
opposite faces of the

Homology modeling o
based on the TIMP-2

Alignment of huTIMP
sequences that were

Flow diagram for clo
type and chimeric TI

Schematic of 3-step

0.7% agarose gel of
chimera DNA cons

0.7% agarose gel of
chimera DNA cons

0.7% agarose gel of
chimera DNA cons

List of Figures

1.1	Domain arrangements of the vertebrate MMPs	13
2.1	Sequence alignment of the 38 TIMP sequences	65
2.2	Sequence alignment of the four human TIMPs	68
2.3	Schematic structure of TIMP-3	70
2.4	Sequence alignment of the four mature human TIMPs	79
2.5	Homology modeling of N-TIMP-1, N-TIMP-3, and N-TIMP-4 based on the N-TIMP-2 NMR Structure	82
2.6	The N-TIMP-3 projection with heparin	84
2.7	Schematic of distances between oxygens on the heparin and the hydrogens on the amines of arginines and lysines of TIMP-3	85
2.8	TIMP-3 models showing the MMP-binding domain and the proposed heparan sulfate binding domain on opposite faces of the TIMP-3	89
2.9	Homology modeling of TIMP-1, TIMP-3, and TIMP-4 based on the TIMP-2 X-ray crystal structure	90
3.1	Alignment of huTIMP-2 and huTIMP-3 showing the sequences that were exchanged highlighted in yellow	102
3.2	Flow diagram for cloning and expression of the wild-type and chimeric TIMPs	104
3.3	Schematic of 3-step PCR for chimera construction	107
3.4a	0.7% agarose gel of PCR products from Step 1 of the C3 chimera DNA construction	121
3.4b	0.7% agarose gel of PCR products from Step 1 of the C2 chimera DNA construction	121
3.5a	0.7% agarose gel of PCR products from Step 2 of the C3 chimera DNA construction	121

3.5b	0.7% agarose gel of PCR products from Step 2 of the C2 chimera DNA construction	121
3.6a	1.0% agarose gel of PCR products from Step 3 of C3 chimera DNA construction	122
3.6b	1.0% agarose gel of PCR products from Step 3 of C2 chimera DNA construction	122
3.7	1.0% agarose gel of *Xho*I and *Eco*RI restriction digest of C3 chimera pCR2.1 clones	125
3.8	1.0% agarose gel of *Xho*I and *Eco*RI restriction digest of the C3 chimera and huTIMP-3 pCR2.1 clones	125
3.9	1.0% agarose gel of *Xho*I and *Eco*RI restriction digest of the huTIMP-3 and C3 chimera pCR2.1 clones	125
3.10	Agarose gel of *Nar*I restriction digest of the huTIMP-3 and C3 chimera pCR2.1 clones.	126
3.11	Agarose gel of of the C2 chimera pCRBlunt clones	126
3.12	Agarose gel of the huTIMP-2 pCRBlunt clones	126
3.13	Agarose gel of the C3 chimera pXMT2 clones	129
3.14	Agarose gel of the huTIMP-3 pXMT2 clones	129
3.15	Agarose gel of the C2 chimera pXMT2 clones	129
3.16	Agarose gel of the huTIMP-2 pXMT2 clones	129
3.17	15% SDS-PAGE of conditioned media and extracellular matrix and reverse zymography of conditioned media and extracellular matrix from transiently transfected COS-1 cells	131
3.18	Reverse zymogram of conditioned media from pNUThuTIMP-3 BHK cells uninduced and induced in FBS DMEM/F-12 medium or virus production serum-free medium (VP-SFM)	136
3.19	Schematic diagram of the pNUT vector	137

3.20	Agarose gel of *Xma*I and *Kpn*I restriction digests of pNUThuTIMP-3 clones	140
3.21	Agarose gel of *Xma*I and *Kpn*I restriction digests of pNUTC3 clones	140
3.22	Agarose gel of *Xma*I and *Kpn*I restriction digests of pNUThuTIMP-2 clones	140
3.23	Agarose gel of *Xma*I and *Kpn*I restriction digests of pNUTC2 clones	140
3.24	Agarose gel of *Xma*I and *Kpn*I restriction digests of pNUT clones	141
3.25	17% SDS-PAGE of conditioned media and extracellular matrix and 17% reverse zymography of conditioned media and extracellular matrix from uninduced and induced BHK-21 cells	144
3.26	Western blots of conditioned media from transfected BHK-21 cells	148
3.27	Western blot of conditioned media and extracellular matrix from pNUTC3, pNUTC3-L, pNUTT3cT2, pNUTC2, and pNUTC2cT3 transfected BHK-21 cells	148
3.28	Structure of TIMP-2 with Regions I, II, and III	152
3.29	Reverse zymogram of conditioned media and extracellular matrix from BHK-21 cells transfected with pNUTC2cT3	156
3.30	Reverse zymogram of ECM and CM from BHK-21 cells transfected with pNUTT3cT2	159
3.31	Reverse zymography of ECM and CM from BHK-21 cells transfected with pNUTC3 and pNUTC3-L	162
3.32	Zymography of conditioned media from untransfected and transfected BHK-21 cells	165
4.1	Ion exchange chromatogram of concentrated ECM from pNUThuTIMP-3 BHK-21 cells	184

4.2	Reverse zymogram of eluted fractions from ion exchange chromatography of concentrated ECM from pNUThuTIMP-3	184
4.3	Ion exchange chromatogram of concentrated 5% FBS DMEM/F-12 conditioned media from pNUTC3 BHK-21 cells	185
4.4	Reverse zymogram of eluted fractions from ion exchange chromatography of concentrate 5% FBS DMEM/F-12 CM from pNUTC3 BHK-21 cells	185
4.5	Gel filtration chromatogram of concentrated VP-SFM CM from pNUTC3 BHK-21 cells chromatographed in 25 mM MES (pH 6.0), 0.025% Brij 35, 0.02% NaN3	188
4.6	Reverse zymogram of eluted fractions from gel filtration of concentrated VP-SFM CM from pNUTC3 BHK-21 cells Chromatographed in 25 mM MES (pH 6.0), 0.025% Brij 35, 0.02% NaN3	188
4.7	Gel filtration chromatogram of concentrated VP-SFM CM from pNUTC3 BHK-21 cells chromatographed in 0.5 M NaCl, 25 mM MES (pH 6.0), 0.025% Brij 35, 0.02% NaN3	191
4.8	Reverse zymogram of eluted fractions from gel filtration of concentrated VP-SFM CM from pNUTC3 BHK-21 cells chromatographed in 0.5 M NaCl, 25 mM MES (pH 6.0), 0.025% Brij 35, 0.02% NaN3	191
4.9	Gel filtration chromatogram of concentrated VP-SFM CM from pNUTC3 BHK-21 cells chromatographed in 1.0 M NaCl, 25 mM Tris (pH 7.0), 0.025% Brij 35, 0.02% NaN3	193
4.10	Reverse zymogram of eluted fractions from gel filtration of concentrated VP-SFM CM from pNUTC3 BHK-21 cells chromatographed in 1.0 M NaCl, 25 mM Tris (pH 7.0), 0.025% Brij 35, 0.02% NaN3	193

4.11	Gel filtration chromatogram of concentrated VP-SFM CM from pNUTC3-L BHK-21 cells chromatographed in 1.0 M NaCl, 25 mM Tris (pH 7.0), 0.025% Brij 35, 0.02% NaN3	194
4.12	Reverse zymogram of eluted fractions from gel filtration of concentrated VP-SFM CM from pNUTC3-L BHK-21 cells chromatographed in 1.0 M NaCl, 25 mM Tris (pH 7.0), 0.025% Brij 35, 0.02% NaN3	194
5.1	Confocal microscopy images of untransfected BHK-21 and pNUThuTIMP-3 transfected BHK-21	208
5.2	Confocal microscopy images of TIMP-3 transfected BHK-21 and TIMP-3 transfected BHK-21 treated with heparinase III	211
5.3	Confocal microscopy images of TIMP-3 transfected BHK-21 treated with PBS, heparan sulfate, heparinase III, and chondroitinase ABC	213
5.4	Reverse zymogram of extracellular matrix and incubation solutions from pNUThuTIMP-3 transfected BHK-21 cells treated with PBS, heparan sulfate, heparinase III, and chondroitinase ABC	216
6.1	Growth curves for transfected BHK-21 cells seeded at 100,000 cells/well in 2.5% FBS DMEM/F-12	231
6.2	Growth curves for transfected BHK-21 cells seeded at 200,000 cells/well in 2.5% FBS DMEM/F-12	232
6.3	Growth curves for transfected BHK-21 cells seeded at 50,000 cells/well in 1.0% FBS DMEM/F-12	233
6.4	Growth curves for transfected BHK-21 cells seeded at 25,000 cells/well in 0.5% FBS DMEM/F-12	234
7.1	Potential cell surface interactions of TIMP-3 with MT-MMP, MMP-2, and TACE by its localization through heparan sulfate proteoglycans	249

List of Tables

1.1	Normal and pathological roles of MMPs and TIMPs	9
1.2	MMP substrates	11
1.3	Vertebrate members of the MMP family	13
2.1	Biochemical Properties of the human TIMPs	73
2.2	Sequence accession numbers for the TIMPs	75
2.3	Net charge of the three regions of TIMP-3 and the homologous regions in TIMP-1, TIMP-2 and TIMP-4.	80
3.1	Primers for the C3 chimera	110
3.2	Primers for the C2 chimera	111
3.3	Additional primers for C2cT3, T3cT2 and C3-L chimeras	111
3.4	Calculated molecular weights and relative mobilities	130
3.5	Expected size of DNA fragments generated with *Xma*I	138
3.6	Expected size of DNA fragments generated with *Kpn*I	139

Abbreviations

Å	angstrom
µg	microgram or micrograms
µl	microliter or microliters
µM	micromolar
Ab	antibody
ADAM	A Disintegrin And Metalloproteinase
aFGF	acidic fibroblast growth gactor
BES	N,N-bis(2-hydroxyethyl)-2-aminoethanesulfonic acid
bFGF	basic fibroblast growth factor
BHK	baby hamster kidney
bp	base pair or base pairs
C. *elegans*	*Caenorhabditis elegans*
C2	Chimera composed of TIMP-2 with Ala23 to Tyr64 replaced with Val23 to His60 of TIMP-3
C2cT3	C2 chimera with the C-terminal 10 amino acids exchanged with the C-terminal 10 amino acids of TIMP-3
C3	Chimera composed of TIMP-3 with Val23 to His60 replaced with Ala23 to Tyr64 of TIMP-2
C3-L	C3 chimera with NDIYGN, the 1st loop of TIMP-2 removed
CAPS	3-[cyclohexylamino]-1-propanesulfonic acid
cDNA	complementary deoxyribonucleic acid
chkTIMP	chicken Tissue Inhibitor of Metalloproteinase

CM	conditioned media
cm	centimeter
COS-1	*Cercopithecus aethiops*, African green monkey, SV40 transformed kidney fibroblasts
CTX or cTX	C-terminus of TIMP-X
D. melanogaster	*Drosophila melanogaster*
Da	Dalton
DMEM	Dulbecco's Modified Eagle Medium
DNA	deoxyribonucleic acid
dNTP	2'-deoxynucleoside 5'-triphosphate
E. coli	*Escherichia coli*
ECM	extracellular matrix
EDTA	ethylenediaminetetraacetic acid
EGF	epidermal growth factor
EGTA	ethylene glycol-bis(beta-aminoethyl ether)-N,N,N',N'-tetraacetic acid
EPA	erythroid potentiating activity
et al.	et alia - and others
F-12	Ham's F-12 Nutrient mixture
FBS	fetal bovine serum
FGF	fibroblast growth factor
FGFR	fibroblast growth factor receptor
FHs 173 We	human embryonic fibroblasts

g	gram or grams
GAG	glycosaminoglycan
GCG	Genetics Computer Group
GPI	glycosylphosphatidylinositol
HER2	human epidermal growth factor receptor-2
HPLC	high performance liquid chromatograph or chromatography
HRP	horseradish peroxidase
HSPG	heparan sulfate proteoglycan
huTIMP	human Tissue Inhibitor of Metalloproteinase
IL	interleukin
kDa	kilo Dalton
LB	Luria broth
mAb	monoclonal antibody
MCF	Michigan Cancer Foundation
MES	2-(N-morpholino)ethanesulfonic acid
mg	milligram or micrograms
MIDAS	Molecular Interactive Display And Simulation
ml	milliliter or milliliters
mM	millimolar
mm	millimeter
MMP	matrix metalloproteinase
Mr	relative mobility

mRNA	messenger ribonucleic acid
MS	Microsoft
MT-MMP	membrane-type matrix metalloproteinase (e.g. MT1-MMP, MT2-MMP)
MT*X* or $_{M}$T*X*	mid-section of TIMP-X
MW	molecular weight
nm	nanometer
NT*X* or $_{N}$T*X*	N-terminus of TIMP-X
OB	oligosaccharide-binding or oligonucleotide-binding
ODN	oligodeoxynucleotide
pAb	polyclonal antibody
PAI	plasminogen activator inhibitor
PBS	phosphate buffered saline
PBS-CMF	phosphate-buffered saline - calcium and magnesium free
PBS-T	phosphate-buffered saline - Tween-20
PCR	polymerase chain reaction
PDB	protein data bank
PDGF	platelet derived growth factor
PES	polyethersulfone
Pfu	*Pyrococcus furiosus*
PgsD-677	*Cricetulus griseus* (Chinese hamster) ovary cell mutant deficient in the polymerization of heparan sulfate
pI	isoelectric point

PIMA	pattern-induced multiple alignment
ProMMP	proenzyme form of the matrix metalloproteinase
PVDF	polyvinylidenedifluoride
rpm	rotations per minute
SDS	sodium dodecyl sulfate
SDS-PAGE	sodium dodecyl sulfate - polyacrylamide gel electrophoresis
SV	simian virus
T3cT2	TIMP-3 with the C-terminal 10 amino acids exchanged with the C-terminal 10 amino acids of TIMP-2
Taq	*Thermus aquaticus*
TE	Tris-EDTA
TGFß	transforming growth factor beta
TIMP	tissue inhibitor of metalloproteinase
TNF	tumor necrosis factor
tPA	tissue-type plasminogen activator
TPA	tumor promoting factor
Tris	Tris(hydroxymethyl) aminomethane
UK	United Kingdom
UCSF	University of California at San Francisco
uPA	urokinase-type plasminogen activator
uPAR	urokinase-type plasminogen activator receptor
UV	ultraviolet

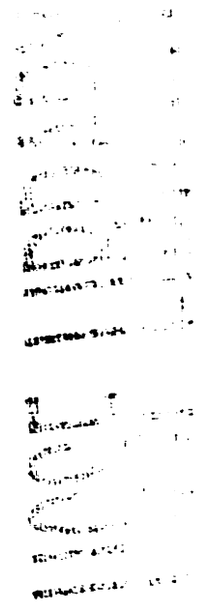

Chapter 1

Introduction

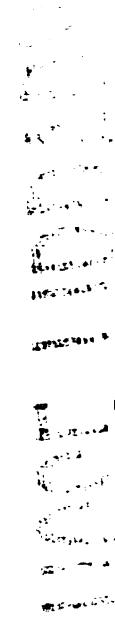

1.1 Preface

In most cases of cancer-related deaths, the primary tumor is not the cause but it is rather the metastases to vital organs. If the neoplasm were confined to a single site, surgeons might be able to remove the tumor without recurrence of disease. When left untreated, whether from neglect or unresponsive therapy, most malignant tumors will metastasize. Current chemotherapy for cancer targets the cell cycle hoping to kill the proliferating tumor cells. All are based on the premise that cancerous tissue growth rate is higher than most normal tissue growth rates and will 'die off' before the normal tissue. The taxane class and platinum-based agents are a two of the cytotoxic therapies prescribed today (1). The taxane class of chemotherapy drugs inhibits mitotic progression that induces apoptosis (2). The platinum agents form DNA adducts that may also be activating programmed cell death (1). Recently, protein-based therapeutics such as monoclonal antibodies in conjunction with chemotherapy are being prescribed for cancer treatment. An anti-CD-20 antibody is being used to treat HER2-positive (human epidermal growth factor receptor-2) breast cancer (3). CD-20 positive B-cell non-Hodgkin's lymphoma is being treated with a monoclonal antibody to CD-20 (4). Each of these monoclonal antibodies is believed to induce apoptosis by crosslinking the cell-surface receptors and triggering an apoptotic pathway (3-5).

Because treatment with these agents sometimes results in drug-resistant tumor progression, possibly due to 'genetic instability resulting in rapid biological diversification', cellular heterogeneity of the tumor, and/or homeostatic mechanisms induced by metastatic cells, new therapies are continually being developed (6).

Therapeutics under investigation include kinase inhibitors, viral vectors to introduce oncogenes or tumor suppressor genes, anti-angiogenic agents such as angiostatin, endostatin, interferons alpha and beta, and matrix metalloproteinase (MMP) inhibitors (7-11). Investigators are screening small molecules to inhibit kinases to halt cellular signals that may lead to apoptosis (7). Viral vectors are being utilized to introduce genes that will replace damaged DNA repair genes and/or induce apoptosis (8, 9). Although their mode of action is not understood, the angiogenesis inhibitors, angiostatin and endostatin halt neovascularization (12, 13). Angiostatin is a 55 kDa fragment of plasminogen, and endostatin is a 20 kDa C-terminal fragment of type XVIII collagen (14-16). Interferons alpha and beta are cytokines that down-regulate angiogenic factors (10). For tumor growth to proceed past 1 mm in diameter, angiogenesis is required to feed the growing tumor. Otherwise the tumor will not grow and will involute (12, 17). The MMP inhibitors include synthetic inhibitors (hydroxamic acid and phosphinic acid based inhibitor and peptide-based inhibitors), and the

natural inhibitor of MMPs, and the TIMPs, tissue inhibitor of matrix metalloproteinase (18-23). The goal in using these synthetic inhibitors or recombinant TIMPs is primarily to target the inhibition of MMPs that degrade the extracellular matrix (ECM) or basal lamina preventing tumor angiogenesis and metastasis.

The processes of metastasis and angiogenesis both involve the local degradation of surrounding stroma and/or basal lamina for migration and proliferation. (Refer to reviews by Fidler, I.J., Woodhouse E.C. *et al.*, and Kleiner, D.E. and Stetler-Stevenson, W.G. for further information on tumor growth, metastasis and angiogenesis (6, 24, 25).) In the process of angiogenesis, the surrounding matrix undergoes remodeling while the vascular endothelium proliferates to form new capillaries. In the process of metastasis, cells must detach from the primary tumor, intravasate into the lymphatic or capillary system, migrate and extravasate to establish new tumors. Each of these steps in the metastatic process involves the degradation of both ECM and/or basal lamina that provides a path and sites for migration by cell attachment and detachment through cell surface molecules such as the integrins (26).

1.2 The Extracellular Matrix and Basal Laminae

The ECM is an intricate meshwork of proteins and complex carbohydrates that underlies epithelial cells and surrounds mesenchymal cells (27). The basal lamina is a specialized form of ECM that underlies all epithelial cell sheets and tubes, surrounds individual muscle cells, fat cells and Schwann cells and surrounds the endothelial cells of capillaries (28). Basal lamina is a strong, elastic and dense meshwork of different types of collagens, predominantly type IV, VI, and XVIII collagen, laminin, entactin, thrombospondin, tenascin, fibronectin, heparan sulfate proteoglycans such as perlecan, agrin, and chondroitin sulfate proteoglycans such as versican (27-32). The ECM provides a site for cell migration, attachment and signaling involving differentiation, proliferation and morphogenesis through its interaction with integrins, cadherins, selectins, and other cell surface receptors and ligands (27, 33-36). In addition, the ECM is believed to modulate and/or act as a 'storehouse' for cytokines and growth factors (33-36). For example, acidic fibroblast growth factor (aFGF), basic fibroblast growth factors (bFGF), vascular endothelial growth factor (VEGF), and platelet derived growth factor (PDGF), bind to heparan sulfate proteoglycans in the ECM and on the cell surface, which modulate and concentrate their activities (37, 38).

1.3 Extracellular Matrix Degrading Enzymes

Serine proteases, such as plasmin, and the MMPs have been implicated as the key enzymes involved in ECM degradation both in normal physiological processes and pathological tissue damage (25, 39-41). These enzymes have been found in the surrounding stroma and associated with the cell membrane (24-26, 42). NOTE: Because they are beyond the scope of this thesis, other ECM degrading proteases such as cathepsins, meprins, and thrombin will not be discussed (43).

1.3.1 Plasmin

Plasmin is expressed as the inactive zymogen, plasminogen, that can be activated by the urokinase-type (uPA) or the tissue-type (tPA) plasminogen activators (41). The cell surface receptor for uPA (uPAR) has been demonstrated to focalize plasmin activation near the cell surface (44). The uPAR also interacts with integrins and vitronectin that is thought to focalize invasion at the leading edge of migrating cells (41). The plasminogen activators are inhibited by plasminogen activator inhibitors-1 and -2 (PAI-1 and PAI-2, respectively), while plasmin is inhibited by α_2-anti-plasmin (41). PAI-1 not only inhibits uPA but also blocks binding of vitronectin and integrins with the uPAR-uPA complex (41). Interestingly, high levels of PAI-1, uPA, and uPAR correlate with poor patient prognosis (41). This may be similar to the

TIMP-2/MMP-2/MT1-MMP-2 complex where TIMP-2 is not only an inhibitor but forms a complex with MT1-MMP and proMMP-2 to activate MMP-2 (45, 46). That is, the complex of PAI-1, uPA, and uPAR may form a complex that activates plasmin. In addition to degrading ECM components, plasmin has been demonstrated to activate MMPs such as MMP-1, MMP-3, MMP-9 and MMP-13 (26, 47). It is of interest to note that MMP-2, MMP-3, MMP-7, and MMP-12 can cleave plasminogen to produce angiostatin (15, 48, 49). MMP-3 has also been demonstrated to modulate plasmin activity by proteolytically cleaving a plasminogen-binding domain of uPA (50, 51).

Although, the uPA cascade has been implicated in the metastatic process, inhibition of uPA and plasmin with PAI-2 and aprotinin, respectively, does not affect invasiveness of epidermal growth factor induced human squamous carcinoma cells (52). However, recombinant and synthetic MMP inhibitor completely suppresses invasiveness. Other cancer cell models and models of vascular wound healing have shown that uPA is necessary, but not sufficient for invasiveness and that MMPs may be the key enzymes degrading the basal laminae (52-55). Although plasmin can degrade ECM, the uPA cascade may actually be a pathway for MMP activation and subsequent degradation of ECM.

1.3.2 Matrix Metalloproteinases

The MMPs are a family of zinc-dependent extracellular endopeptidases also referred to as matrixins. For review on the MMPs refer to Woessner, J.F., Nagase *et al.*, Kleiner *et al.*, Parks *et al.* and Curran *et al.* (24, 56-59). The MMPs in concert with their natural inhibitors, the TIMPs, are involved in normal physiological processes such as wound healing, embryo implantation, and ovulation. Table 1.1 lists normal physiological processes where a controlled balance of MMPs and TIMPs is believed to be a significant factor. Table 1.1 also lists pathological diseases such as rheumatoid arthritis, osteoarthritis, atherosclerosis, and tumor metastasis where an imbalance of MMPs and TIMPs has been observed. (60-72). Recently, Denhardt, D. T. compiled a list of the characterization of MMPs and TIMPs in human malignancies (73). Although most of the MMPs have been implicated in some form of malignant cancer, this compilation of data and information from other recent reviews of MMPs and TIMPs, implicate MT1-MMP, MMP-2 and MMP-9 as key enzymes in the metastatic phenotype. Unusually high amounts of MT1-MMP, MMP-2, and MMP-9 mRNA expression and/or activity have been observed in cancer of the breast, prostate, stomach, colon, head and neck, lung, skin, pancreas, bladder, brain, ovaries, and liver (24, 42, 56, 73). Because MMP-2 and MMP-9 have broad enzymatic activities towards many ECM

Table 1.1: Normal and pathological roles of MMPs and TIMPs.

Normal Processes	Pathological Processes
Embryogenesis	Rheumatoid arthritis
Salivary gland morphogenesis	Osteoarthritis
Mammary development and involution	Cancer invasion
Ovulation	Tumor metastasis
Blastocyst implantation	Periodontal disease
Endometrial cycling	Fibrotic lung disease
Cervical dilatation	Liver cirrhosis
Fetal membrane rupture	Corneal ulceration
Uterine involution	Gastric ulcer
Bone growth	Skin Diseases
Bone remodeling	Otosclerosis
Tooth eruption	Atherosclerosis
Hair follicle cycle	Abdominal aortic aneurysm
Angiogenesis	Dilated cardiomyopathy
Wound/fracture healing	Glomerulunephritis
Macrophage function	Encephalomyelitis
Neutrophil function	Neural disease
Apoptosis	Diabetes mellitus (74, 75)
	Macular degeneration of the eye (76)
	Cystic fibrosis (77)
	Asthma (78)
	Emphysema (79)
	Guillain-Barre syndrome (80)

*From Nagase *et al.* unless otherwise indicated (81).

components, more specifically type IV collagen, it is not surprising that these two enzymes would be found in metastatic diseases (see Table 1.2). It is of interest to note that in many cases, the levels of TIMP-1 and/or TIMP-2 were also elevated compared to controls (24, 42, 56, 73).

The MMPs are secreted in their zymogen form. Once active the MMPs digest several different types of extracellular proteins, such as collagens, gelatins, proteoglycans, etc., shown in Table 1.2. The direct results of their enzymatic activity are not just degradation of the ECM but also the activation of other MMPs. In addition, MMPs have been reported to digest extracellular proteins exposing their cryptic activities. The cleavage of plasminogen with MMP-3, -7, -9 and -12 results in angiostatin, which inhibits angiogenesis (15, 48, 49). Matrilysin, MMP-7, can process cell-associated Fas ligand to soluble Fas ligand resulting in the induction of apoptosis of human embryonic kidney 293 cells by the soluble Fas ligand (82). Laminin-5 proteolysis by MT1-MMP and/or MMP-2 stimulates migration of breast epithelial cells (83). The authors suggest that the proteolysis results in integrin interactions with the fragments of laminin-5 that alters cell signaling and migration.

Table 1.2: MMP substrates

Enzyme	MMP	Substrates
Collagenases		
Interstitial collagenase	MMP-1	Collagens I, II, III, Vii, and X, gelatins, entactin, aggrecan, link protein
Neutrophil collagenase	MMP-8	Collagens I, II and III, aggrecan, link protein
Collagenase 3	MMP-13	Collagens I, II, III, VII, and X
Collagenase 4	MMP-18	Collagens I, II
Gelatinases		
Gelatinase A	MMP-2	Gelatins, collagens I, IV, V, VII, X, and XI, fibronectin, laminin, aggrecan, elastin, large tenascin C, vitronectin, ß-amyloid protein precursor
Gelatinase B	MMP-9	Gelatins, collagens IV, V, XIV, aggrecan, elastin, entactin, vitronectin
Stromelysins		
Stromelysin 1	MMP-3	Aggrecan, gelatins, fibronectin, laminin, collagen III, IV, IX and X, large tenascin-C, vitronectin, activates proMMP-1
Stromelysin 2	MMP-10	Aggrecan, fibronectin, collagen III, IV, IX, and X, activates proMMP-1
Membrane-type MMPs		
MT1-MMP	MMP-14	Activates proMMP-2, gelatin, collagens
MT2-MMP	MMP-15	Activates proMMP-2
MT3-MMP	MMP-16	Activates proMMP-2
MT4-MMP	MMP-17	pro-TNFα peptide, fibrinogen, fibrin (84)
MT5-MMP	MMP-24	Activates proMMP-2 (85)
MT6-MMP	MMP-25	Activates proMMP-2 (86)
Others		
Matrilysin	MMP-7	Aggrecan, fibronectin, laminin, gelatins, collagen IV, elastin, entactin, small tenascin-C, vitronectin, activates proMMP-1
Stromelysin 3	MMP-11	Weak activity for fibronectin, laminin, collagen IV, aggrecan, gelatins, Alpha-1-antiprotease
Metalloelastase	MMP-12	Elastin
(No name)	MMP-19	type IV collagen, gelatin, fibronectin, laminin, nidogen, and large tenascin-C isoform
Enamelysin	MMP-20	Amelogenin
XMMP (Xenopus)	MMP-21	?
CMMP (Chicken)	MMP-22	?
(No name)	MMP-23	? (87)
Endometase	MMP-26	Gelatin, a1-proteinase inhibitor (88)

Compiled from Nagase *et al.* and Kleiner *et al.* (24, 81) and various sources as indicated.

Currently, 26 members of the MMP family have been identified and subdivided into subfamilies; collagenases, gelatinases, stromelysins, and the membrane-type as shown in Table 1.3, Figure 1.1. (NOTE: MMP-4, -5 and -6 are not in the table because no references could be found.) The family shares a common structure of having at least two domains (Table 1.3): a pro-domain of about 80 amino acids with a conserved PRCG(V/N)PD sequence where the cystine ligates the catalytic zinc maintaining the latent proMMP and a catalytic domain of about 170 amino acids with the zinc-binding motif HEXXHXXGXXH (89). Recently, MMP-26 was discovered to have a catalytic domain with a unique "cysteine-switch" pro-peptide sequence, PHCGVPDGSD, and a zinc-binding motif, VATHEIGHSLGLQH (88). Within the catalytic domain are conserved structural metal binding sites for 2-3 calcium ions and a zinc ion which are necessary for activity and stability (89). MMP-2 and MMP-9 contain three repeats of a fibronectin type II domain inserted in the catalytic domain that binds with collagens and gelatins (90, 91). All but MMP-7 and MMP-23 have a hemopexin domain that is required for collagenases to cleave triple helical interstitial collagens (92). MMP-23 has a Cys and Pro rich and IL-1 receptor-like region at the C-terminus (93). The six membrane bound MT-MMPs have a 'linker', transmembrane and cytoplasmic domain at th e C-terminus. The MT-MMPs, MMP-11, MMP-21 and MMP-23 contain

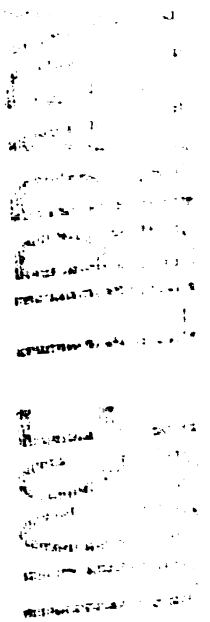

Table 1.3: Vertebrate members of the MMP family

Protein	MMP	Domain Composition
Collagenase 1	MMP-1	B
Gelatinase A	MMP-2	C
Stromelysin 1	MMP-3	B
Matrilysin	MMP-7	A
Collagenase 2	MMP-8	B
Gelatinase B	MMP-9	D
Stromelysin 2	MMP-10	B
Stromelysin 3	MMP-11	E
Macrophage elastase	MMP-12	B
Collagenase 3	MMP-13	B
MT1-MMP	MMP-14	F
MT2-MMP	MMP-15	F
MT3-MMP	MMP-16	F
MT4-MMP	MMP-17	F
Collagenase 4	MMP-18	B
(Not named)	MMP-19	B
Enamelysin	MMP-20	B
XMMP (Xenopus)	MMP-21	G
CMMP (Chicken)	MMP-22	B
(Not named)	MMP-23	H
MT5-MMP (94)	MMP-24	F
MT6-MMP (95)	MMP-25	F
Endometase (88, 96)	MMP-26	A

*Updated from Nagase and Woessner (57).

Figure 1.1: Domain arrangements of the vertebrate MMPs.

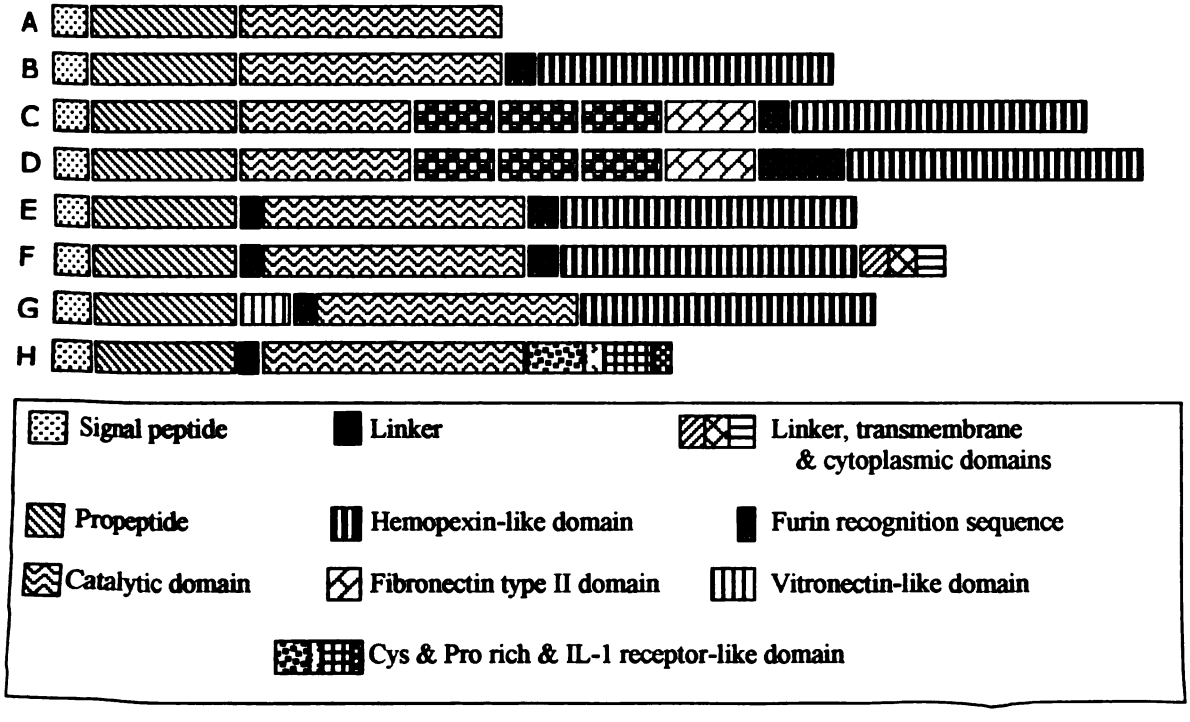

a furin-sensitive cleavage site between the pro-domain and the catalytic domain. Some have postulated that furin trafficking may be regulated by the actin cytoskeletal network that concentrates furins for focal MMP activation (42). MMP-11 has been shown to be dependent on intracellular furin activation (97). In contrast, MT1-MMP was still activated when furin gene expression was suppressed by anti-sense oligonucleotides (98). Further research is needed to address furin activation of MMPs.

MMPs are regulated at several levels: expression; activation; and inhibition. Many of the MMP genes are inducible (57). Control of the expression of MMPs may be mediated via differential transcriptional regulation by growth factors, cytokines, oncogenes, chemical agents such as phorbol esters, physical stress, hormones, cell-matrix and cell-cell interactions (56, 57). Activation of the secreted zymogens is regulated. The activation process is believed to occur through the initial cleavage before the conserved cysteine in the pro-domain, which disrupts the zinc-cysteine interaction of the pro-domain with the catalytic domain (57, 89). The pro-domain is finally cleaved leaving the active mature enzyme (57, 89). This final cleavage has been found to be autocatalytic in the activation of MMP-2 and MMP-9 (99-101). Most MMPs can be activated by serine protease such as plasmin and urokinase-type plasminogen activator (26, 102-104). MMPs can

activate other MMPs. For example, MMP-3 has been demonstrated to activate proMMP-1, while MMP-2, MMP-3, and MMP-13 can activate proMMP-9 (26, 104). The activation of MMP-2 is the most understood MMP activation pathway and will be discussed in detail later in this chapter.

1.4 Tissue Inhibitor of Metalloproteinases

The TIMPs, tissue inhibitors of metalloproteinases, are the major endogenous regulators of MMP activity (73, 105, 106). Although the MMPs are inhibited by α_2-macroglobulins, their inhibition is nonspecific and only in the fluid phase and not in tissue (106). The TIMPs are 21-28 kDalton proteins that reversibly and specifically inhibit the MMPs through a 1:1 stoicheometric, non-covalent complex formation (106). The four members of the TIMP family are able to inhibit most of the MMPs, but with different specificity and affinity (106). (NOTE: A more *in* depth study of TIMP structure and TIMP/MMP interactions will be discussed in Chapter 2.) The TIMPs share a 45-60% similarity and a 36-50% identity to each other containing twelve highly conserved cysteines that form 6 disulfide bridges (calculated using the gap program from the Genetics Computer Group version 10.0 software). The disulfides of TIMP-1 and TIMP-2 form a two-domain structure with 3 disulfides in the N-terminal domain and 3 disulfides in the C-terminal

main (107). Becaus

served and because a

e N-terminus, it is ass

sulfide linkages (107).

Subtle differences in

ecific binding and inhib

K values between

e TIMP-MMP complex

ecificity of the TIMPs a

e affinity appears to

monstrated by creati

C-terminus, that the

MP could be manipu

e N-terminal domain

ive-site pocket in the

e C-terminal tail of

minal hemopexin-l

ker et al. and Overa

ity was due to cha

MPs and the C-termina

e four TIMPs have

e Chapter 2, Figure

domain (107). Because the spacing of the cysteines is highly conserved and because activity is dependent on the intact disulfides in the N-terminus, it is assumed that TIMP-3 and TIMP-4 share similar disulfide linkages (107).

Subtle differences in their structure give each TIMP unique and specific binding and inhibitory properties, discussed in Chapter 2 (89, 108). K_i values between 10^{-9} to 10^{-12} M have been demonstrated for the TIMP-MMP complexes using peptide substrates (109). The specificity of the TIMPs appears to be in the N-terminal domain and the affinity appears to be in the C-terminal domain. Meng *et al.* demonstrated by creating mutants of TIMP-2 at position 2 at the amino terminus, that the specificity of TIMP-1 towards MMP-1, MMP-2, MMP-3 could be manipulated (110). Butler *et al.* demonstrated that the N-terminal domain of TIMP-1, TIMP-2, and TIMP-3 binds to the active-site pocket in the N-terminal domains of MMP-2 and MMP-9, and the C-terminal tail of TIMP-1, TIMP-2, and TIMP-3 binds to the C-terminal hemopexin-like domains of MMP-2 and MMP-9 (111). Butler *et al.* and Overall *et al.* reported that the differences in their affinity was due to charge differences in the C-terminal tail of the TIMPs and the C-terminal tail of MMPs (111, 112).

The four TIMPs have been cloned from several different species (see Chapter 2, Figure 2.1). TIMP-1 and TIMP-2 are secreted from

many cell types and are found in body fluids *in vivo* and the conditioned media of cultured cells (113, 114). TIMP-1 is found in ovary, bone and uterine tissue and is inducible by several cytokines and chemokines such as bFBF, EGF, TGFß, IL-1, IL-6, phorbol ester, and progesterone (115). TIMP-2 to appears to be constitutively expressed in many different tissues (115). The most recently discovered member, TIMP-4, is less characterized but has been found in brain, heart and skeletal muscle and breast tissue and localizes to the conditioned media of cultured cells (116). TIMP-3, which is inducible by phorbol esters, TGFß, dexamethasone and PDGF, is unique to the family in that it localizes to the ECM or basal lamina in kidney, breast, colon, eye, and lung (115-120).

1.4.1 Growth Promoting Activity of TIMPs

The TIMPs not only demonstrate MMP inhibitory activity but also growth promoting activity. TIMP-1 and erythroid potentiating activity, EPA, were both discovered in 1985 and found to be the same protein (113, 121, 122). TIMP-2 has been reported to have cell proliferative activity in many human, bovine and mouse cell lines (123-127). TIMP-3 has also been reported to have growth promoting activity in chicken embryo fibroblasts (128). Point mutations of TIMP-1 that abolishes MMP inhibitory activity still retains erythroid potentiating activity (122). Hayakawa *et al.* demonstrated that reduction and

alkylation of TIMP-1 and TIMP-2 destroys their MMP inhibitory activity while retaining their growth promoting activities (126). By adding an N-terminal alanine to TIMP-2 that abolishes MMP inhibitory activity, Wingfield *et al.* demonstrated that the growth modulating property is independent of the inhibitory activity (129). Recently, Zhao *et al.* demonstrated that TIMP-1 shows cell cycle-associated accumulation in the nuclei of human gingival fibroblasts (130). In addition, TIMP-1 has been found to bind to the cell surface and translocates to the nucleus of MCF-7 breast carcinoma cells (131). It is of interest to note that the TIMP structures have an oligosaccharide- or oligonucleotide-binding domain that could possibly bind to DNA (132).

1.4.2 Induction of Apoptosis by TIMP-3

In contrast to growth promoting activity, TIMP-3 has been recently shown to induce apoptotic cell death in many cancer cell lines and in rat vascular smooth muscle cells (133-137). Although, in 1992, Yang and Hawkes reported that TIMP-3 stimulates the proliferation of chicken embryo fibroblasts, this could be interpreted as apoptosis because DNA synthesis is slowed by addition of TIMP-3 to transformed chicken embryo fibroblasts (128). Smith *et al.* reported that apoptosis of human carcinoma cells was induced by the stabilization of the TNFalpha receptor on the cell surface by TIMP-3 (133). TIMP-3 appeared to be preventing the shedding of the TNFalpha receptor from

the surface of the cells. A year later, it was discovered that TIMP-3 and not TIMP-1 or TIMP-2 inhibits TNFalpha converting enzyme (TACE), which cleaves the membrane bound pro TNFalpha from the cell surface producing the active cytokine (138). In contrast, TIMP-1 and TIMP-2 inhibit apoptosis (139). Li *et al.* demonstrated that TIMP-1 inhibits MCF10A cell death induced by hydrogen peroxide, adriamycin, or X-ray irradiation (139). The inhibition of apoptosis occurrs after the MCF10A cells detach and, therefore, is not dependent on the stabilization of the matrix by TIMP-1. B16F10 melanoma cells are also protected from apoptosis by TIMP-2 (137).

1.4.3 TIMP-2 Is an Activator and Inhibitor of MMP-2

Investigators have recently determined that TIMP-2 is not only an inhibitor of MMPs but also an activator of MMP-2 (140). Because of the extensive characterization of MMP-2 and TIMP-2 interactions and the discovery and characterization of the membrane-type matrix metalloproteinases (MT-MMPs) investigators have developed a clearer understanding of the activation of MMP-2 (26, 109, 111, 112, 140, 141). TIMP-2 and MT1-MMP have been demonstrated to be secreted as a complex and show temporal and spatially co-regulated expression in mouse development (142, 143). The complex of MT1-MMP and TIMP-2 has been referred to as a "receptor" for proMMP-2 resulting in MMP-2 activation (140). Investigators report that TIMP-2 binds to

MT1-MMP followed by binding of proMMP-2 (45, 46). The MT1-MMP cleaves the proMMP-2 at Asn37-Leu38 and the resulting Δ1-37MMP-2 is autocatalytically activated by cleavage at Asn80-Tyr81 (99). Activation also requires the C-terminal domain of proMMP-2 but it is not necessary for activity (45). By utilizing truncated forms of MMP-2 and MT1-MMP without a transmembrane domain, Butler *et al.* deduced that the N-terminal domain of MT1-MMP binds the N-terminal domain of TIMP-2 and the C-terminal domain of TIMP-2 interacts with the C-terminal domain of proMMP-2 to localize it to the cell surface for activation (140). TIMP-2 and TIMP-3, but not TIMP-1, are effective inhibitors of MT1-MMP (99). TIMP-4 also binds tightly to the C-terminal hemopexin-like domain of MMP-2 but has not been demonstrated to bind any of the MT-MMPs (111, 144). Both TIMP-2 and TIMP-3 bind to MT1-MMP and proMMP-2 but only TIMP-2 can activate MMP-2 (111). At low levels of TIMP-2 added to TIMP-2-depleted membranes expressing MT1-MMP, proMMP-2 activation is increased (140). But, at higher levels of TIMP-2, MT1-MMP is inhibited by TIMP-2 and does not activate proMMP-2 (140). Because of the cell surface interactions of TIMP-1 and similar expression patterns of TIMP-1 and MMP-9, there is speculation that proMMP-9 may be activated similarly by forming a complex with TIMP-1 and another MT-MMP (131).

Similar to local proteolysis exhibited by the uPA receptor/uPA/plaminogen activation cascade, the cell surface localization MT1-MMP and activation of MMP-2 may be a way of focalizing proteolysis of ECM. Human melanoma cells and 3T3 cells overexpressing MT1-MMP activate MMP-2 and degrade ECM that is localized predominantly to 'invadopodia' (145, 146). αVβ3 integrin has been shown to bind to the hemopexin domain of MMP-2 focalizing the degradation (147). Deryugina *et al.* recently demonstrated that MCF7 breast carcinoma cells expressing both αVβ3 integrin and MT1-MMP increase adhesion and migration on vitronectin by localizing MMP-2 at the cell surface (148). Further investigation is underway to study potential tyrosine phosphorylation sites in the cytoplasmic domain of the MT-MMPs (26).

1.4.4 TIMPs as Therapeutics?

Because of their ability to inhibit and activate MMPs, induce proliferation or apoptosis, investigators struggle with an apparent paradox of the TIMPs. The TIMPs appear to be an excellent biological drug for anti-angiogenic and/or anti-metastatic therapy. TIMP-1, TIMP-2, and TIMP-3 have all been reported to inhibit angiogenesis (149-151). Several reports over the past 10 years demonstrate the ability of the TIMPs to inhibit invasion of many different cancerous cell types (39, 56, 137, 152-160). In rat bladder cancer cell lines, MMP-2

nsfected into MYU3L

nsfection of TIMP-1 c

ates their invasive

nstrate that T

tocarcinogenesis by

ause TIMP-1 and TIM

ptosis, and because T

TIMP-2 as a therapeu

t appear to have c

TIMP-2 activation by

hanism by which TIM

136, 149, 165). T

s (133, 138). Inh

tion of apoptosis co

unique characteristic

the critical factor tha

3 to the ECM pla

ct and affect cell s

transfected into MYU3L cells enhance their invasive potential while transfection of TIMP-1 or TIMP-2 into highly metastatic LMC19 cells reduces their invasiveness (161, 162). TIMP-1 transgenic mice demonstrate that TIMP-1 inhibits T-cell lymphoma and hepatocarcinogenesis by tumor vascularization (163, 164). However, because TIMP-1 and TIMP-2 promote cell growth and rescue cells from apoptosis, and because TIMP-2 activates proMMP-2, the use of TIMP-1 or TIMP-2 as a therapeutic may exacerbate the disease. TIMP-3 does not appear to have contraindicative activities. TIMP-3 inhibits proMMP-2 activation by MT1-MMP, which may contribute to the mechanism by which TIMP-3 inhibits angiogenesis and cellular invasion (111, 136, 149, 165). TIMP-3 also induces apoptosis of cancerous cell lines (133, 138). Inhibition of angiogenesis and invasiveness, and induction of apoptosis could have a potent effect on cancerous tissue. The unique characteristic of ECM localization displayed by TIMP-3 may be the critical factor that determines its activities. The localization of TIMP-3 to the ECM places it in a location where it could directly interact and affect cell surface molecules (21, 134-137).

1.4.5 TIMP-3 Electrostatically Interacts with the Extracellular Matrix

In 1984, Blenis and Hawkes first characterized the ECM localization of chicken TIMP-3 by utilizing chaotropes, high salt, and ionic and non-ionic detergents to extract it from the ECM (117). Non-ionic detergents such as NP-40 and Triton X-100 are unable to extract TIMP-3 from the ECM except in the presence of high salt, 0.5 M KCl, or reducing agents such as 10% ß-mercaptoethanol. High concentration of chaotropic agents such as 6 M guanidine-HCl or 6 M urea with 10% ß-mercaptoethanol is necessary to extract TIMP-3. Strong anionic detergents such as sodium dodecyl sulfate (SDS) will extract TIMP-3 from the ECM. In an attempt to inhibit TIMP-3 production by utilizing antisense oligodeoxynucleotides (ODN), Kishnani and Hawkes determined that exposure of transformed chicken embryo fibroblasts to ODNs caused TIMP-3 to relocate from the ECM to the conditioned media (166). The amount of TIMP-3 activity detected in the conditioned media was ODN-sequence independent, directly proportional to the ODN concentration, and not due to increased TIMP-3 expression. Kishnani hypothesized that the change in location of TIMP-3 is due to electrostatic interactions between the negatively charged ODNs and the basic amino acids of TIMP-3. This hypothesis was investigated by exposing chicken embryo fibroblasts to several

arged and uncharged

alization of TIMP-3.

ly-anionic molecules

sulfate, poly-glutama

GAGs) such as chondr

ronate, and hepar

thionine. Poly-cat

rgest effect on the lo

ysine and poly-arg

n of the poly-anions.

also displayed the st

he conditioned media.

TIMP-3 was a binding e

hicken embryo fibrobl

pharose beads and pol

heparan sulfate coated

ations from the poly-

ng these data, Kish

ine displaces the TIM

harged species in the

harged amino acids

ites of heparan su

charged and uncharged polymers, to determine their effect on the localization of TIMP-3. The polymers included poly-cationic and poly-anionic molecules such as poly-lysine, poly-arginine, poly-aspartate, poly-glutamate, and poly-acrylate, glycosaminoglycans (GAGs) such as chondroitin sulfates A, B, and C, dextran sulfate, hyaluronate, and heparan sulfate, and uncharged poly-alanine and poly-histidine. Poly-cationic and poly-anionic molecules exhibited the strongest effect on the localization of TIMP-3 to the conditioned media. Poly-lysine and poly-arginine have a stronger effect when compare to any of the poly-anions. Of the GAGs, heparan sulfate and dextran sulfate displayed the strongest effect on the localization of TIMP-3 to the conditioned media. To determine if the change in location of TIMP-3 was a binding effect or a displacement effect, the ECM from chicken embryo fibroblasts was exposed to heparan sulfate-coated agarose beads and poly-lysine-coated agarose beads. Elutions from heparan sulfate coated agarose beads contained TIMP-3 activity, while elutions from the poly-lysine coated agarose beads had no activities. From these data, Kishnani and Hawkes hypothesized that the poly-lysine displaces the TIMP-3 from the ECM by binding to the negatively charged species in the ECM, thus preventing binding of the positively charged amino acids of TIMP-3. In contrast, negatively charged sulfates of heparan sulfate bind to the positively charged lysines and

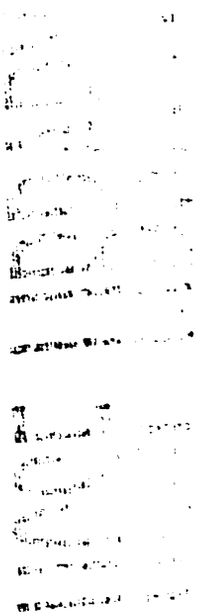

arginines of TIMP-3 and extract it from the ECM to the conditioned media. They noted that three short stretches of 9-11 amino acids that contain a high density of positive charge from lysines and arginines and are uninterrupted by negative charge may be involved in binding of TIMP-3 to polyanionic polymers.

From these data and sequence analysis and homology modeling demonstrated and discussed in Chapter 2 a hypothesis was constructed. The hypothesis states that basic Region I, Arg20 to lys52, on the surface of TIMP-3 binds to heparan sulfate chains on heparan sulfate proteoglycans (HSPGs) in the ECM, localizing TIMP-3 to the ECM.

1.5 Heparan Sulfate Proteoglycans

Heparan sulfates are the heterogeneously N- and O-sulfated polysaccharide components of proteoglycans that are common constituents of the ECM and cell surface (167). HSPGs are involved in cell adhesion, migration, proliferation and differentiation (37, 168). The heparan sulfate chains of HSPGs bind to various proteases, protease inhibitors, cytokines and growth factors such as MMP-7, anti-thrombin III, aFGF, bFGF, VEGF, hepatocyte growth factor, keratinocyte growth factor, and TGF-ß (169). Heparan sulfate chains also bind to structural proteins in the ECM such as fibrillar collagen,

fibronectin, and laminin (170). In each case HSPGs appear to function as a way of accumulating or localizing heparan sulfate-binding molecules to enhance and/or promote ligand-receptor, protease-inhibitor and protease-substrate interactions. MMP-7 has been demonstrated to bind to and co-localize with heparan sulfate in the basement membrane and around epithelial cells (171). The investigators suggest this may function to sequester the enzyme for activation or focalized proteolysis. Heparan sulfate and heparin catalyze the binding of anti-thrombin III to thrombin and factor Xa inhibiting coagulation (172). Heparin is a highly sulfated form of heparan sulfate. A specific pentasaccharide sequence of the heparin chains actually causes a conformational change of the anti-thrombin III, enabling it to bind (173). Heparan sulfate chains of HSPGs bind to lipoprotein lipase and enhance the binding of lipoproteins to the cell surface to facilitate uptake or receptor binding (174, 175). Thrombospondin-1, which is involved in platelet aggregation and regulation of cell adhesion, migration, and proliferation, binds to heparan sulfate on the cell surface and in the ECM (176-178). The fibroblast growth factors, FGFs, are probably the most intensively studied HSPG-binding proteins. The FGFs, which stimulate angiogenesis, proliferation and differentiation, have been implicated in many forms of cancer (6, 10, 179-181). Heparan sulfate is believed to

be essential for the complex formation of the FGF and the FGF receptor, FGFR, resulting in signal transduction (182, 183). Different FGFs and FGFRs may also have unique specificity towards to different heparan sulfate sequences and sulfation patterns (182).

1.5.1 Composition of Heparan Sulfate Proteoglycans

The following is a summary of HSPG composition from papers by Zhang *et al.* and Esko *et al.* (184, 185). They are composed of a protein core with one or more covalently attached GAG chains. The GAGs attach to conserved SGXG or SG sequences that are usually preceded by acidic amino acids. Although chondroitin sulfate also attaches to SGXG or SG sites, repeating SG sequences and adjacent acidic residues appear to signal for heparan sulfate synthesis. The heparan sulfate chains are synthesized in the Golgi complex by the stepwise attachment of saccharide units to form the tetrasaccharide glucosamine-β1,3-D-galactose-β1,3-D-galactose–β1,4-D-xylose. The chains are elongated by the addition of alternating glucuronate and N-acetylglucosamine. The chains can be anywhere between 30 to 200 disaccharide units. Sulfation occurs by the interdependent reactions of N-deacetylase and N-sulfotransferases. In addition, glucuronate is epimerized to iduronate, and glucosamine and iduronate are sulfated by O-sulfotransferases. Isoenzyme variations and their expression levels appear to give rise to the different sulfation patterns on the

heparan sulfate chains attributed to the specific binding of ligands. HSPGs appear at the cell surface shortly after synthesis where they are excreted in the case of ECM HSPGs or anchored in the membrane (186).

The predominant HSPG in the basal lamina is perlecan, followed by agrin and type XVIII collagen (32). Perlecan consists of a core protein of approximately 400kDa with 3-4 heparan sulfate chains attached in the N-terminal domain of the protein. Agrin and type XVIII collagen are 200-210 kDa and 180 kDa proteins, respectively (32). Two families of HSPGs, Syndecans-1 through -4, 33 kDa proteins with 3-4 glycanation sites, and glypicans-1 through -6, 60-65 kDa proteins with 2-3 glycanation sites, and two unrelated HSPGs, CD44E and the TGFß-receptor betaglycan have been identified on the cell surface (37, 187). The syndecans, CD-44E, and TGFß-receptor betaglycan have single membrane-spanning transmembrane domains. The glypicans are tethered to the cell surface through glycosylphosphatidylinositol (GPI) (37, 187, 188). Some of the cell surface HSPGs are enyzymatically shed possibly by ADAMs or in the case of GPI-anchored HSPGs by specific phospholipases (186).

Syndecan-1 is the most extensively studied of the cell surface HSPGs (189). The loss of syndecan-1 expression and different expression patterns of integrins and E-cadherin correlates with the loss

of cell differentiation when normal tissues are compared with cancerous tissue such as squamous cell carcinomas of the head, neck, lung and cervix (189). Syndecan-1 expression is lower in the malignant transformation of several of these epithelial cells. Syndecan-1 has been demonstrated to mediate the binding and activity of FGF-2 but not FGF-1 to FGFR-1 (190). Recently, Fitzgerald *et al.* demonstrated that the shedding of syndecan-1 and -4 is inhibited by TIMP-3 (191). The localization of TIMP-3 in the ECM may provide TIMP-3 with the ability to directly regulate the shedding process. If TIMP-3 also binds to the heparan sulfate chains of syndecan-1, this interaction may provide a way for the cell to have direct control over TIMP-3 action.

1.6 Overview

Chapter 2 will demonstrate that a basic Region I, Arg20 to Lys52, on the surface of the TIMP-3 molecule determined by sequence alignments and molecular modeling could bind to heparan sulfate. A chimera was constructed to test if this basic Region I could be exchanged with the homologous region of TIMP-2 to create a TIMP-3 chimera, C3, that localizes to the conditioned media instead of the ECM in cultured cells. The reverse chimera was also constructed to determine if this basic Region I could be exchanged into TIMP-2 to

reate a TIMP-2 chime

onditioned media in C

re reported in Chapte

MP-3 and the ch

emonstration of the c

nfocal microscopy w

oliferation assay of

meric TIMP-3 and TI

Chapter 6.

The experiments pre

localized to the ECM

egion I, Arg20 to Lys5

create a TIMP-2 chimera, C2, that localizes to the ECM instead of the conditioned media in cultured cells. The results of these experiments are reported in Chapter 3. The preliminary results from purification of TIMP-3 and the chimeras will be discussed in Chapter 4. Demonstration of the co-localization of TIMP-3 and heparan sulfate by confocal microscopy will be reported in Chapter 5. Preliminary cell proliferation assay of BHK-21 cells transfected with wild-type and chimeric TIMP-3 and TIMP-2 proteins will be reported and discussed in Chapter 6.

The experiments presented in this thesis demonstrate that TIMP-3 is localized to the ECM and cell surface by the interaction of basic Region I, Arg20 to Lys52, of TIMP-3 with heparan sulfate.

1.7 Bibliography

1. Ferrante K, Winograd B, Canetta R. Promising new developments in cancer chemotherapy. Cancer Chemotherapy and Pharmacology 1999;43 Suppl(1):S61-8.

2. De Brabander M, Geuens G, Nuydens R, Willebrords R, De Mey J. Taxol induces the assembly of free microtubules in living cells and blocks the organizing capacity of the centrosomes and kinetochores. Proceedings of the National Academy of Sciences of the United States of America 1981;78(9):5608-612.

3. Le XF, Vadlamudi R, McWatters A, Bae DS, Mills GB, Kumar R, et al. Differential signaling by an anti-p185(HER2) antibody and heregulin [In Process Citation]. Cancer Res 2000;60(13):3522-31.

4. Harjunpaa A, Junnikkala S, Meri S. Rituximab (anti-CD20) therapy of B-cell lymphomas: direct complement killing is superior to cellular effector mechanisms. Scand J Immunol 2000;51(6):634-41.

5. Shan D, Ledbetter JA, Press OW. Signaling events involved in anti-CD20-induced apoptosis of malignant human B cells. Cancer Immunol Immunother 2000;48(12):673-83.

6. Fidler IJ. Critical determinants of cancer metastasis: rationale for therapy. Cancer Chemother Pharmacol 1999;43 Suppl:S3-10.

7. Sedlacek HH. Kinase inhibitors in cancer therapy: a look ahead. Drugs 2000;59(3):435-76.

8. Comis RL, Finley RS. Future directions in the treatment of non-small cell lung cancer. Semin Oncol 1999;26(6 Suppl 18):14-8.

9. Kouraklis G. Gene therapy for cancer: from the laboratory to the patient. Dig Dis Sci 2000;45(6):1045-52.

10. Fidler IJ. Angiogenesis and cancer metastasis. Cancer Journal from Scientific American 2000;6 Suppl 2(8):S134-41.

11. Cirri L, Donnini S, Morbidelli L, Chiarugi P, Ziche M, Ledda F. Endostatin: a promising drug for antiangiogenic therapy. Int J Biol Markers 1999;14(4):263-7.

12. Fidler IJ, Ellis LM. The implications of angiogenesis for the biology and therapy of cancer metastasis [comment]. Cell 1994;79(2):185-8.

13. Folkman J. Seminars in Medicine of the Beth Israel Hospital, Boston. Clinical applications of research on angiogenesis [see comments]. New England Journal of Medicine 1995;333(26):1757-63.

14. Gately S, Twardowski P, Stack MS, Patrick M, Boggio L, Cundiff DL, et al. Human prostate carcinoma cells express enzymatic activity that converts human plasminogen to the angiogenesis inhibitor, angiostatin. Cancer Res 1996;56(21):4887-90.

15. Lijnen HR, Ugwu F, Bini A, Collen D. Generation of an angiostatin-like fragment from plasminogen by stromelysin-1 (MMP-3). Biochemistry 1998;37(14):4699-702.

16. Zatterstrom UK, Felbor U, Fukai N, Olsen BR. Collagen XVIII/endostatin structure and functional role in angiogenesis [In Process Citation]. Cell Struct Funct 2000;25(2):97-101.

17. Folkman J. How is blood vessel growth regulated in normal and neoplastic tissue? G.H.A. Clowes memorial Award lecture. Cancer Research 1986;46(2):467-73.

18. Docherty AJ, O'Connell JP. Synthetic Metalloproteinase Inhibitors. Tissue Inhibitors of Metalloproteinases in Development and Disease 2000;Proceedings of the Inhibitors of Metalloproteinases Conference(1996):189-202.

19. Skotnicki JS, Zask A, Nelson FC, Albright JD, Levin JI. Design and synthetic considerations of matrix metalloproteinase inhibitors. Annals of the New York Academy of Sciences 1999;878(6):61-72.

20. Kahari VM, Saarialho-Kere U. Matrix metalloproteinases and their inhibitors in tumour growth and invasion. Annals of Medicine 1999;31(1):34-45.

21. Edwards DR, Beaudry PP, Laing TD, Kowal V, Leco KJ, Leco PA, et al. The roles of tissue inhibitors of metalloproteinases in tissue remodelling and cell growth. Int J Obes Relat Metab Disord 1996;20 Suppl 3:S9-15.

22. Blavier L, Henriet P, Imren S, Declerck YA. Tissue inhibitors of matrix metalloproteinases in cancer. Annals of the New York Academy of Sciences 1999;878:108-19.

23. Baker AH, Ahonen M, Keaheari VM. Potential applications of tissue inhibitor of metalloproteinase (TIMP) overexpression for cancer gene therapy. Advances in Experimental Medicine and Biology 2000;465:469-83.

24. Kleiner DE, Stetler-Stevenson WG. Matrix metalloproteinases and metastasis. Cancer Chemotherapy and Pharmacology 1999;43 Suppl:S42-51.

25. Woodhouse EC, Chuaqui RF, Liotta LA. General mechanisms of metastasis. Cancer 1997;80(8 Suppl):1529-37.

26. Murphy G, Gavrilovic J. Proteolysis and cell migration: creating a path? Current Opinion in Cell Biology 1999;11(5):614-21.

27. Hay ED. Cell Biology of Extracellular Matrix. 3rd ed. New York: Plenum Publishing Corp.; 1992.

28. Alberts B, Bray D, Lewis J, Raff M, Roberts K, Watson JD. Molecular Biology Of The Cell. 3rd ed. New York: Garland Publishing, Inc.; 1994.

29. Sage H. Collagens of basement membranes. J Invest Dermatol 1982;79 Suppl 1:51s-59s.

30. D'Ardenne AJ, Burns J, Sykes BC, Kirkpatrick P. Comparative distribution of fibronectin and type III collagen in normal human tissues. J Pathol 1983;141(1):55-69.

31. Sanes JR, Engvall E, Butkowski R, Hunter DD. Molecular heterogeneity of basal laminae: isoforms of laminin and collagen IV at the neuromuscular junction and elsewhere. J Cell Biol 1990;111(4):1685-99.

32. Halfter W, Dong S, Schurer B, Cole GJ. Collagen XVIII is a basement membrane heparan sulfate proteoglycan. J Biol Chem 1998;273(39):25404-12.

33. Schmeichel KL, Weaver VM, Bissell MJ. Structural cues from the tissue microenvironment are essential determinants of the human mammary epithelial cell phenotype. J Mammary Gland Biol Neoplasia 1998;3(2):201-13.

34. Bissell MJ, Weaver VM, Lelievre SA, Wang F, Petersen OW, Schmeichel KL. Tissue structure, nuclear organization, and gene expression in normal and malignant breast. Cancer Res 1999;59(7 Suppl):1757-1763s; discussion 1763s-1764s.

35. Lukashev ME, Werb Z. ECM signalling: orchestrating cell behaviour and misbehaviour. Trends Cell Biol 1998;8(11):437-41.

36. Boudreau N, Bissell MJ. Extracellular matrix signaling: integration of form and function in normal and malignant cells. Curr Opin Cell Biol 1998;10(5):640-6.

37. Tumova S, Woods A, Couchman JR. Heparan sulfate proteoglycans on the cell surface: versatile coordinators of cellular functions. Int J Biochem Cell Biol 2000;32(3):269-88.

38. Einspanier R, Gabler C, Bieser B, Einspanier A, Berisha B, Kosmann M, et al. Growth factors and extracellular matrix proteins in interactions of cumulus-oocyte complex, spermatozoa and oviduct. J Reprod Fertil Suppl 1999;54:359-65.

39. Thorgeirsson UP, Lindsay CK, Cottam DW, Gomez DE. Tumor invasion, proteolysis, and angiogenesis. J.Neurooncol. 1993;18:89-103.

40. Abramson SR, Woessner JF, Jr. Characterization of rat matrilysin and its cDNA. Annals of the New York Academy of Sciences 1994;732(6):362-4.

41. Andreasen PA, Kjøller L, Christensen L, Duffy MJ. The urokinase-type plasminogen activator system in cancer metastasis: a review. International Journal of Cancer 1997;72(1):1-22.

42. Ellerbroek SM, Stack MS. Membrane associated matrix metalloproteinases in metastasis. Bioessays 1999;21(11):940-9.

43. Chen WT. Membrane proteases: roles in tissue remodeling and tumour invasion. Current Opinion in Cell Biology 1992;4(5):802-9.

44. Chapman HA. Plasminogen activators, integrins, and the coordinated regulation of cell adhesion and migration. Current Opinion in Cell Biology 1997;9(5):714-24.

45. Murphy G, Willenbrock F, Ward RV, Cockett MI, Eaton D, Docherty AJ. The C-terminal domain of 72 kDa gelatinase A is not required for catalysis, but is essential for membrane activation and modulates interactions with tissue inhibitors of metalloproteinases [published erratum appears in Biochem J 1992 Jun 15;284(Pt 3):935]. Biochem.J. 1992;283:637-641.

46. Ward RV, Atkinson SJ, Reynolds JJ, Murphy G. Cell surface-mediated activation of progelatinase A: demonstration of the involvement of the C-terminal domain of progelatinase A in cell surface binding and activation of progelatinase A by primary fibroblasts. Biochem.J. 1994;304:263-269.

47. Hahn-Dantona E, Ramos-DeSimone N, Sipley J, Nagase H, French DL, Quigley JP. Activation of proMMP-9 by a plasmin/MMP-3 cascade in a tumor cell model. Regulation by tissue inhibitors of metalloproteinases. Annals of the New York Academy of Sciences 1999;878:372-87.

48. Patterson BC, Sang QA. Angiostatin-converting enzyme activities of human matrilysin (MMP-7) and gelatinase B/type IV collagenase (MMP-9). J Biol Chem 1997;272(46):28823-5.

49. Dong Z, Kumar R, Yang X, Fidler IJ. Macrophage-derived metalloelastase is responsible for the generation of angiostatin in Lewis lung carcinoma. Cell 1997;88(6):801-10.

50. Ugwu F, Lemmens G, Collen D, Lijnen HR. Modulation of cell-associated plasminogen activation by stromelysin-1 (MMP-3). Thrombosis and Haemostasis 1999;82(3):1127-31.

51. Ugwu F, Van Hoef B, Bini A, Collen D, Lijnen HR. Proteolytic cleavage of urokinase-type plasminogen activator by stromelysin-1 (MMP-3). Biochemistry 1998;37(20):7231-6.

52. Rosenthal EL, Johnson TM, Allen ED, Apel IJ, Punturieri A, Weiss SJ. Role of the plasminogen activator and matrix metalloproteinase systems in epidermal growth factor- and scatter factor-stimulated invasion of carcinoma cells. Cancer Research 1998;58(22):5221-5230.

53. Carmeliet P, Moons L, Dewerchin M, Rosenberg S, Herbert JM, Lupu F, et al. Receptor-independent role of urokinase-type plasminogen activator in pericellular plasmin and matrix metalloproteinase proteolysis during vascular wound healing in mice. Journal Of Cell Biology 1998;140(1):233-245.

54. Deryugina EI, Bourdon MA, Reisfeld RA, Strongin A. Remodeling of collagen matrix by human tumor cells requires activation and cell surface association of matrix metalloproteinase-2. Cancer Res 1998;58(16):3743-50.

55. Kim J, Yu W, Kovalski K, Ossowski L. Requirement for specific proteases in cancer cell intravasation as revealed by a novel semiquantitative PCR-based assay. Cell 1998;94(3):353-62.

56. Curran S, Murray GI. Matrix metalloproteinases in tumour invasion and metastasis. J Pathol 1999;189(3):300-8.

57. Nagase H, Woessner JF, Jr. Matrix metalloproteinases. Journal of Biological Chemistry 1999;274(31):21491-4.

58. Woessner JF, Jr. The family of matrix metalloproteinases. Annals of the New York Academy of Sciences 1994;732(6):11-21.

59. Parks WC. Matrix metalloproteinases in repair. Wound Repair and Regeneration 1999;7(6):423-32.

60. Baker T, Tickle S, Wasan H, Docherty A, Isenberg D, Waxman J. Serum metalloproteinases and their inhibitors: markers for malignant potential. Br.J.Cancer 1994;70:506-512.

61. Gohji K, Fujimoto N, Fujii A, Komiyama T, Okawa J, Nakajima M. Prognostic significance of circulating matrix metalloproteinase-2 to tissue inhibitor of metalloproteinases-2 ratio in recurrence of urothelial cancer after complete resection. Cancer Res 1996;56(14):3196-8.

62. Gohji K, Fujimoto N, Ohkawa J, Fujii A, Nakajima M. Imbalance between serum matrix metalloproteinase-2 and its inhibitor as a predictor of recurrence of urothelial cancer. Br J Cancer 1998;77(4):650-5.

63. Lee MA, Palace J, Stabler G, Ford J, Gearing A, Miller K. Serum gelatinase B, TIMP-1 and TIMP-2 levels in multiple sclerosis. A longitudinal clinical and MRI study [see comments]. Brain 1999;122(Pt 2)):191-7.

64. Arai M, Niioka M, Maruyama K, Wada N, Fujimoto N, Nomiyama T, et al. Changes in serum levels of metalloproteinases and their inhibitors by treatment of chronic hepatitis C with interferon. Dig Dis Sci 1996;41(5):995-1000.

65. Manicourt DH, Fujimoto N, Obata K, Thonar EJ. Levels of circulating collagenase, stromelysin-1, and tissue inhibitor of matrix metalloproteinases 1 in patients with rheumatoid arthritis. Relationship to serum levels of antigenic keratan sulfate and systemic parameters of inflammation. Arthritis Rheum. 1995;38:1031-1039.

66. Nishida T. Kinetics of tissue and serum matrix metalloproteinase-3 and tissue inhibitor of metalloproteinases-1 in intervertebral disc degeneration and disc herniation. Kurume Medical Journal 1999;46(1):39-50.

67. Scully SP, Berend KR, Qi WN, Harrelson JM. Collagenase specificity in chondrosarcoma metastasis. Brazilian Journal of Medical and Biological Research 1999;32(7):885-9.

68. Watanabe Y, Yamaguchi R, IwakiEgawa S, Shimamori Y, Fujimoto Y, Matsuno H. Activation of progelatinase B in synovial fluids of patients with rheumatoid arthritis, with reference to stromelysin-1 and tissue inhibitor of matrix metalloproteinase-1. Clinical and Experimental Rheumatology 1999;17(4):401-6.

69. Waubant E, Goodkin DE, Gee L, Bacchetti P, Sloan R, Stewart T, et al. Serum MMP-9 and TIMP-1 levels are related to MRI activity in relapsing multiple sclerosis [see comments]. Neurology 1999;53(7):1397-401.

70. Yazawa N, Kikuchi K, Ihn H, Fujimoto M, Kubo M, Tamaki T, et al. Serum levels of tissue inhibitor of metalloproteinases 2 in patients with systemic sclerosis. Journal of the American Academy of Dermatology 2000;42(1 Pt 1):70-5.

71. Yoshihara Y, Obata K, Fujimoto N, Yamashita K, Hayakawa T, Shimmei M. Increased levels of stromelysin-1 and tissue inhibitor of metalloproteinases-1 in sera from patients with rheumatoid arthritis. Arthritis Rheum. 1995;38:969-975.

72. Zucker S, Mian N, Drews M, Conner C, Davidson A, Miller F, et al. Increased serum stromelysin-1 levels in systemic lupus

erythematosus: lack of correlation with disease activity. J Rheumatol 1999;26(1):78-80.

73. Denhardt DT. On the Paradoxical Ability of TIMPs Either to Inhibit of to Promote the Development and Progression of the Malignant Phenotype. In: Hawkes SP, Edwards DR, Khokha R, editors. Tissue Inhibitors of Metalloproteinases in Development and Disease: Proceedings of the Inhibitor of Metalloproteinases Conference, Banff, Alberta, Canada, September 25-29, 1996. Amsterdam, The Netherlands: Harwood Academic Publishers; 2000. p. 260.

74. Ishimura E, Nishizawa Y, Shoji S, Mori H. Serum type III, IV collagens and TIMP in patients with type II diabetes mellitus. Life Sci 1996;58(16):1331-7.

75. Del Prete D, Anglani F, Forino M, Ceol M, Fioretto P, Nosadini R, et al. Down-regulation of glomerular matrix metalloproteinase-2 gene in human NIDDM. Diabetologia 1997;40(12):1449-54.

76. Weber BH, Vogt G, Pruett RC, Stohr H, Felbor U. Mutations in the tissue inhibitor of metalloproteinases-3 (TIMP3) in patients with Sorsby's fundus dystrophy. Nat Genet 1994;8(4):352-6.

77. Delacourt C, Le Bourgeois M, D'Ortho MP, Doit C, Scheinmann P, Navarro J, et al. Imbalance between 95 kDa type IV collagenase and tissue inhibitor of metalloproteinases in sputum of patients with cystic fibrosis. Am.J.Respir.Crit.Care Med. 1995;152:765-774.

78. Holgate ST. Asthma: a dynamic disease of inflammation and repair. Ciba Found Symp 1997;206:5-28; discussion 28-34, 106-10.

79. Finlay GA, LR OD, Russell KJ, EM DA, Masterson JB, FitzGerald MX, et al. Matrix metalloproteinase expression and production by alveolar macrophages in emphysema. Am J Respir Crit Care Med 1997;156(1):240-7.

80. Craeange A, Sharshar T, Planchenault T, Christov C, Poron F, Raphaeel JC, et al. Matrix metalloproteinase-9 is increased and correlates with severity in Guillain-Barrae syndrome. Neurology 1999;53(8):1683-91.

81. Nagase H, Das SK, Dey SK, Fowlkes JL, Huang W, Brew K. Matrix Metalloproteinases (MMPs) and Tissue Inhibitors of Metalloproteinases (TIMPs): Physiologial Roles and Structural Basis of MMP Inhibition by TIMP-1. In: Hawkes SP, Edwards DR, Khokha R, editors. Tissue Inhibitors of Metalloproteinases in Development and Disease: Proceedings of the Inhibitor of Metalloproteinases Conference, Banff, Alberta, Canada, September 25-29, 1996. Amsterdam, The Netherlands: Harwood Academic Publishers; 2000. p. 260.

82. Powell WC, Fingleton B, Wilson CL, Boothby M, Matrisian LM. The metalloproteinase matrilysin proteolytically generates active soluble

Fas ligand and potentiates epithelial cell apoptosis. Current Biology 1999;9(24):1441-7.

83. Koshikawa N, Giannelli G, Cirulli V, Miyazaki K, Quaranta V. Role of cell surface metalloprotease MT1-MMP in epithelial cell migration over laminin-5. Journal of Cell Biology 2000;148(3):615-24.

84. English WR, Puente XS, Freije JM, Knauper V, Amour A, Merryweather A, et al. Membrane type 4 matrix metalloproteinase (MMP17) has tumor necrosis factor-alpha convertase activity but does not activate pro-MMP2. Journal of Biological Chemistry 2000;275(19):14046-55.

85. Pei D. Identification and characterization of the fifth membrane-type matrix metalloproteinase MT5-MMP. J Biol Chem 1999;274(13):8925-32.

86. Pei D. Leukolysin/MMP25/MT6-MMP: a novel matrix metalloproteinase specifically expressed in the leukocyte lineage. Cell Research 1999;9(4):291-303.

87. Velasco G, Pendas AM, Fueyo A, Knauper V, Murphy G, Lopez-Otin C. Cloning and characterization of human MMP-23, a new matrix metalloproteinase predominantly expressed in reproductive tissues and lacking conserved domains in other family members. J Biol Chem 1999;274(8):4570-6.

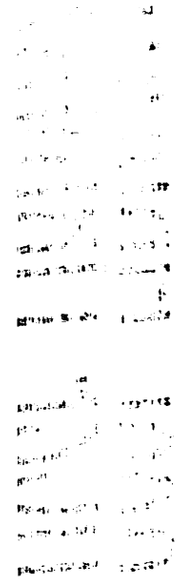

88. Park HI, Ni J, Gerkema FE, Liu D, Belozerov VE, Sang QX. Identification and Characterization of Human Endometase (Matrix Metalloproteinase-26) from Endometrial Tumor. J Biol Chem 2000.

89. Bode W, Fernandez-Catalan C, Tschesche H, Grams F, Nagase H, Maskos K. Structural properties of matrix metalloproteinases. Cellular and Molecular Life Sciences 1999;55(4):639-52.

90. Steffensen B, Wallon UM, Overall CM. Extracellular matrix binding properties of recombinant fibronectin type II-like modules of human 72-kDa gelatinase/type IV collagenase. High affinity binding to native type I collagen but not native type IV collagen. J.Biol.Chem. 1995;270:11555-11566.

91. Banyai L, Tordai H, Patthty L. Structure and domain-domain interactions of the gelatin binding site of human 72-kilodalton type IV collagenase (gelatinase A, matrix metalloproteinase 2). J Biol Chem 1996;271(20):12003-8.

92. Lauer-Fields JL, Tuzinski KA, Shimokawa K, Nagase H, Fields GB. Hydrolysis of triple-helical collagen peptide models by matrix metalloproteinases. Journal of Biological Chemistry 2000;275(18):13282-90.

93. Gururajan R, Grenet J, Lahti JM, Kidd VJ. Isolation and characterization of two novel metalloproteinase genes linked to the

Cdc2L locus on human chromosome 1p36.3. Genomics 1998;52(1):101-6.

94. Llano E, Pendaas AM, Freije JP, Nakano A, Kneauper V, Murphy G, et al. Identification and characterization of human MT5-MMP, a new membrane-bound activator of progelatinase a overexpressed in brain tumors. Cancer Research 1999;59(11):2570-6.

95. Velasco G, Cal S, Merlos-Suaarez A, Ferrando AA, Alvarez S, Nakano A, et al. Human MT6-matrix metalloproteinase: identification, progelatinase A activation, and expression in brain tumors. Cancer Research 2000;60(4):877-82.

96. Benoit De Coignac A, Elson G, Delneste Y, Magistrelli G, Jeannin P, Aubry JP, et al. Cloning of MMP-26 A novel matrilysin-like proteinase. Eur J Biochem 2000;267(11):3323-3329.

97. Pei D, Weiss SJ. Furin-dependent intracellular activation of the human stromelysin-3 zymogen. Nature 1995;375:244-247.

98. Sato T, Kondo T, Fujisawa T, Seiki M, Ito A. Furin-independent pathway of membrane type 1-matrix metalloproteinase activation in rabbit dermal fibroblasts. Journal of Biological Chemistry 1999;274(52):37280-4.

99. Will H, Atkinson SJ, Butler GS, Smith B, Murphy G. The soluble catalytic domain of membrane type 1 matrix metalloproteinase cleaves the propeptide of progelatinase A and initiates autoproteolytic

activation. Regulation by TIMP-2 and TIMP-3. J Biol Chem 1996;271(29):17119-23.

100. Ries C, Lottspeich F, Dittmann KH, Petrides PE. HL-60 leukemia cells produce an autocatalytically truncated form of matrix metalloproteinase-9 with impaired sensitivity to inhibition by tissue inhibitors of metalloproteinases. Leukemia 1996;10(9):1520-6.

101. Bergmann U, Tuuttila A, Stetler-Stevenson WG, Tryggvason K. Autolytic activation of recombinant human 72 kilodalton type IV collagenase. Biochemistry 1995;34:2819-2825.

102. Birkedal-Hansen H, Moore WG, Bodden MK, Windsor LJ, Birkedal-Hansen B, DeCarlo A, et al. Matrix metalloproteinases: a review. Crit.Rev.Oral Biol.Med. 1993;4:197-250.

103. Kleiner DE, Jr., Stetler-Stevenson WG. Structural biochemistry and activation of matrix metalloproteases. Curr Opin Cell Biol 1993;5(5):891-7.

104. Murphy G, Atkinson S, Ward R, Gavrilovic J, Reynolds JJ. The role of plasminogen activators in the regulation of connective tissue metalloproteinases. Ann N Y Acad Sci 1992;667:1-12.

105. Woessner JF, Jr. TIMPs as Multifunctional Molecules. In: Hawkes SP, Edwards DR, Khokha R, editors. Tissue Inhibitors of Metalloproteinases in Development and Disease: Proceedings of the Inhibitor of Metalloproteinases Conference, Banff, Alberta, Canada,

September 25-29, 1996. Amsterdam, The Netherlands: Harwood Academic Publishers; 2000. p. 260.

106. Brew K, Dinakarpandian D, Nagase H. Tissue inhibitors of metalloproteinases: evolution, structure and function. Biochim Biophys Acta 2000;1477(1-2):267-83.

107. Williamson RA, Marston FA, Angal S, Koklitis P, Panico M, Morris HR, et al. Disulphide bond assignment in human tissue inhibitor of metalloproteinases (TIMP). Biochem.J. 1990;268:267-274.

108. Bode W, Fernandez-Catalan C, Grams F, Gomis-Reuth FX, Nagase H, Tschesche H, et al. Insights into MMP-TIMP interactions. Annals of the New York Academy of Sciences 1999;878:73-91.

109. Willenbrock F, Murphy G. Structure-function relationships in the tissue inhibitors of metalloproteinases. Am.J.Respir.Crit.Care Med. 1994;150:S165-S170.

110. Meng Q, Malinovskii V, Huang W, Hu Y, Chung L, Nagase H, et al. Residue 2 of TIMP-1 is a major determinant of affinity and specificity for matrix metalloproteinases but effects of substitutions do not correlate with those of the corresponding P1' residue of substrate. J Biol Chem 1999;274(15):10184-9.

111. Butler GS, Apte SS, Willenbrock F, Murphy G. Human tissue inhibitor of metalloproteinases 3 interacts with both the N- and C-

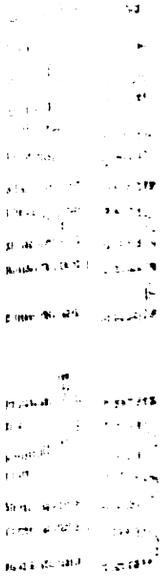

terminal domains of gelatinases A and B. Regulation by polyanions. Journal of Biological Chemistry 1999;274(16):10846-51.

112. Overall CM, King AE, Sam DK, Ong AD, Lau TT, Wallon UM, et al. Identification of the tissue inhibitor of metalloproteinases-2 (TIMP-2) binding site on the hemopexin carboxyl domain of human gelatinase A by site-directed mutagenesis. The hierarchical role in binding TIMP-2 of the unique cationic clusters of hemopexin modules III and IV. J Biol Chem 1999;274(7):4421-9.

113. Docherty AJ, Lyons A, Smith BJ, Wright EM, Stephens PE, Harris TJ, et al. Sequence of human tissue inhibitor of metalloproteinases and its identity to erythroid-potentiating activity. Nature 1985;318(6041):66-9.

114. Stetler-Stevenson WG, Krutzsch HC, Liotta LA. Tissue inhibitor of metalloproteinase (TIMP-2). A new member of the metalloproteinase inhibitor family. J Biol Chem 1989;264(29):17374-8.

115. Edwards DR, Leco KJ, Leco PA, Lim MS, Phillips BW, Raja J, et al. Regulation of TIMP Gene Expression. In: Hawkes SP, Edwards DR, Khokha R, editors. Tissue Inhibitors of Metalloproteinases in Development and Disease: Proceedings of the Inhibitor of Metalloproteinases Conference, Banff, Alberta, Canada, September 25-29, 1996. Amsterdam, The Netherlands: Harwood Academic Publishers; 2000. p. 260.

116. Leco KJ, Apte SS, Taniguchi GT, Hawkes SP, Khokha R, Schultz GA, et al. Murine tissue inhibitor of metalloproteinases-4 (TIMP-4): cDNA isolation and expression in adult mouse tissues. FEBS Lett 1997;401(2-3):213-7.

117. Blenis J, Hawkes SP. Characterization of a transformation-sensitive protein in the extracellular matrix of chicken embryo fibroblasts. J Biol Chem 1984;259(18):11563-70.

118. Pavloff N, Staskus PW, Kishnani NS, Hawkes SP. A new inhibitor of metalloproteinases from chicken: ChIMP-3. A third member of the TIMP family. J.Biol.Chem. 1992;267:17321-17326.

119. Leco KJ, Khokha R, Pavloff N, Hawkes SP, Edwards DR. Tissue inhibitor of metalloproteinases-3 (TIMP-3) is an extracellular matrix-associated protein with a distinctive pattern of expression in mouse cells and tissues. J.Biol.Chem. 1994;269:9352-9360.

120. Hawkes SP, Shubayev V, Hoang V, Taniguchi GT. Localization of TIMP-3 in Extracellular Matrix of Human Tissues. In: Hawkes SP, Edwards DR, Khokha R, editors. Tissue Inhibitors of Metalloproteinases in Development and Disease: Proceedings of the Inhibitor of Metalloproteinases Conference, Banff, Alberta, Canada, September 25-29, 1996. Amsterdam, The Netherlands: Harwood Academic Publishers; 2000. p. 260.

121. Gasson JC, Bersch N, Golde DW. Characterization of purified human erythroid-potentiating activity. Prog Clin Biol Res 1985;184:95-104.

122. Chesler L, Golde DW, Bersch N, Johnson MD. Metalloproteinase inhibition and erythroid potentiation are independent activities of tissue inhibitor of metalloproteinases-1. Blood 1995;86(12):4506-15.

123. Bertaux B, Hornebeck W, Eisen AZ, Dubertret L. Growth stimulation of human keratinocytes by tissue inhibitor of metalloproteinases. J.Invest.Dermatol. 1991;97:679-685.

124. Hayakawa T, Yamashita K, Tanzawa K, Uchijima E, Iwata K. Growth-promoting activity of tissue inhibitor of metalloproteinases-1 (TIMP-1) for a wide range of cells. A possible new growth factor in serum. FEBS Lett. 1992;298:29-32.

125. Stetler-Stevenson WG, Bersch N, Golde DW. Tissue inhibitor of metalloproteinase-2 (TIMP-2) has erythroid-potentiating activity. FEBS Lett. 1992;296:231-234.

126. Hayakawa T, Yamashita K, Ohuchi E, Shinagawa A. Cell growth-promoting activity of tissue inhibitor of metalloproteinases-2 (TIMP-2). J.Cell Sci. 1994;107:2373-2379.

127. Saika S, Kawashima Y, Okada Y, Tanaka SI, Yamanaka O, Ohnishi Y, et al. Recombinant TIMP-1 and -2 enhance the proliferation

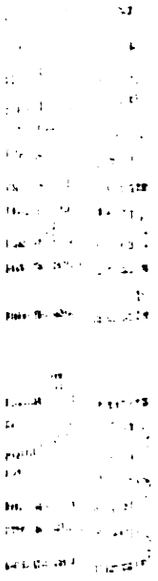

of rabbit corneal epithelial cells in vitro and the spreading of rabbit corneal epithelium in situ. Curr Eye Res 1998;17(1):47-52.

128. Yang TT, Hawkes SP. Role of the 21-kDa protein TIMP-3 in oncogenic transformation of cultured chicken embryo fibroblasts. Proc.Natl.Acad.Sci.U.S.A. 1992;89:10676-10680.

129. Wingfield PT, Sax JK, Stahl SJ, Kaufman J, Palmer I, Chung V, et al. Biophysical and functional characterization of full-length, recombinant human tissue inhibitor of metalloproteinases-2 TIMP-2 produced in Escherichia coli. Comparison of wild type and amino-terminal alanine appended variant with implications for the mechanism of TIMP functions. Journal of Biological Chemistry 1999;274(30):21362-8.

130. Zhao WQ, Li H, Yamashita K, Guo XK, Hoshino T, Yoshida S, et al. Cell cycle-associated accumulation of tissue inhibitor of metalloproteinases-1 (TIMP-1) in the nuclei of human gingival fibroblasts. J Cell Sci 1998;111(Pt 9)):1147-53.

131. Ritter LM, Garfield SH, Thorgeirsson UP. Tissue inhibitor of metalloproteinases-1 (TIMP-1) binds to the cell surface and translocates to the nucleus of human MCF-7 breast carcinoma cells. Biochemical and Biophysical Research Communications 1999;257(2):494-499.

132. Williamson RA, Martorell G, Carr MD, Murphy G, Docherty AJ, Freedman RB, et al. Solution structure of the active domain of tissue inhibitor of metalloproteinases-2. A new member of the OB fold protein family. Biochemistry 1994;33:11745-11759.

133. Smith MR, Kung H, Durum SK, Colburn NH, Sun Y. TIMP-3 induces cell death by stabilizing TNF-alpha receptors on the surface of human colon carcinoma cells. Cytokine 1997;9(10):770-80.

134. Bian J, Wang Y, Smith MR, Kim H, Jacobs C, Jackman J, et al. Suppression of in vivo tumor growth and induction of suspension cell death by tissue inhibitor of metalloproteinases (TIMP)-3. Carcinogenesis 1996;17(9):1805-11.

135. Ahonen M, Baker AH, Kahari VM. High level expression of tissue inhibitors of metalloproteinases-1,-2 and -3 in melanoma cells achieved by adenovirus mediated gene transfer. Adv Exp Med Biol 1998;451:69-72.

136. Baker AH, George SJ, Zaltsman AB, Murphy G, Newby AC. Inhibition of invasion and induction of apoptotic cell death of cancer cell lines by overexpression of TIMP-3. Br J Cancer 1999;79(9-10):1347-55.

137. Valente P, Fasina G, Melchiori A, Masiello L, Cilli M, Vacca A, et al. TIMP-2 over-expression reduces invasion and angiogenesis and

protects B16F10 melanoma cells from apoptosis (vol 75, pg 246, 1998). International Journal of Cancer 1999;80(3):485.

138. Amour A, Slocombe PM, Webster A, Butler M, Knight CG, Smith BJ, et al. TNF-alpha converting enzyme (TACE) is inhibited by TIMP-3. FEBS Lett 1998;435(1):39-44.

139. Li G, Fridman R, Kim HR. Tissue inhibitor of metalloproteinase-1 inhibits apoptosis of human breast epithelial cells. Cancer Research 1999;59(24):6267-75.

140. Butler GS, Butler MJ, Atkinson SJ, Will H, Tamura T, van Westrum SS, et al. The TIMP2 membrane type 1 metalloproteinase "receptor" regulates the concentration and efficient activation of progelatinase A. A kinetic study. J Biol Chem 1998;273(2):871-80.

141. Upadhyay J, Shekarriz B, Nemeth JA, Dong Z, Cummings GD, Fridman R, et al. Membrane type 1-matrix metalloproteinase (MT1-MMP) and MMP-2 immunolocalization in human prostate: change in cellular localization associated with high-grade prostatic intraepithelial neoplasia. Clinical Cancer Research 1999;5(12):4105-10.

142. Imai K, Ohuchi E, Aoki T, Nomura H, Fujii Y, Sato H, et al. Membrane-type matrix metalloproteinase 1 is a gelatinolytic enzyme and is secreted in a complex with tissue inhibitor of metalloproteinases 2. Cancer Res 1996;56(12):2707-10.

143. Apte SS, Fukai N, Beier DR, Olsen BR. The matrix metalloproteinase-14 (MMP-14) gene is structurally distinct from other MMP genes and is co-expressed with the TIMP-2 gene during mouse embryogenesis. J Biol Chem 1997;272(41):25511-7.

144. Bigg HF, Shi YE, Liu YE, Steffensen B, Overall CM. Specific, high affinity binding of tissue inhibitor of metalloproteinases-4 (TIMP-4) to the COOH-terminal hemopexin-like domain of human gelatinase A. TIMP-4 binds progelatinase A and the COOH-terminal domain in a similar manner to TIMP-2. J Biol Chem 1997;272(24):15496-500.

145. Belien AT, Paganetti PA, Schwab ME. Membrane-type 1 matrix metalloprotease (MT1-MMP) enables invasive migration of glioma cells in central nervous system white matter. J Cell Biol 1999;144(2):373-84.

146. Nakahara H, Howard L, Thompson EW, Sato H, Seiki M, Yeh Y, et al. Transmembrane/cytoplasmic domain-mediated membrane type 1-matrix metalloprotease docking to invadopodia is required for cell invasion. Proc Natl Acad Sci U S A 1997;94(15):7959-64.

147. Brooks PC, Stromblad S, Sanders LC, von Schalscha TL, Aimes RT, Stetler-Stevenson WG, et al. Localization of matrix metalloproteinase MMP-2 to the surface of invasive cells by interaction with integrin alpha v beta 3. Cell 1996;85(5):683-93.

148. Deryugina EI, Bourdon MA, Jungwirth K, Smith JW, Strongin AY. Functional activation of integrin alpha V beta 3 in tumor cells expressing membrane-type 1 matrix metalloproteinase. International Journal of Cancer 2000;86(1):15-23.

149. Anand-Apte B, Pepper MS, Voest E, Montesano R, Olsen B, Murphy G, et al. Inhibition of angiogenesis by tissue inhibitor of metalloproteinase-3. Invest Ophthalmol Vis Sci 1997;38(5):817-23.

150. Johnson MD, Kim HR, Chesler L, Tsao-Wu G, Bouck N, Polverini PJ. Inhibition of angiogenesis by tissue inhibitor of metalloproteinase. J.Cell Physiol. 1994;160:194-202.

151. Takigawa M, Nishida Y, Suzuki F, Kishi J, Yamashita K, Hayakawa T. Induction of angiogenesis in chick yolk-sac membrane by polyamines and its inhibition by tissue inhibitors of metalloproteinases (TIMP and TIMP-2). Biochem.Biophys.Res.Commun. 1990;171:1264-1271.

152. Albini A, Melchiori A, Santi L, Liotta LA, Brown PD, Stetler-Stevenson WG. Tumor cell invasion inhibited by TIMP-2 [see comments]. J.Natl.Cancer Inst. 1991;83:775-779.

153. DeClerck YA, Yean TD, Chan D, Shimada H, Langley KE. Inhibition of tumor invasion of smooth muscle cell layers by recombinant human metalloproteinase inhibitor. Cancer Res. 1991;51:2151-2157.

154. Testa JE, Quigley JP. Reversal of misfortune: TIMP-2 inhibits tumor cell invasion [editorial; comment]. J.Natl.Cancer Inst. 1991;83:740-742.

155. DeClerck YA, Perez N, Shimada H, Boone TC, Langley KE, Taylor SM. Inhibition of invasion and metastasis in cells transfected with an inhibitor of metalloproteinases. Cancer Res. 1992;52:701-708.

156. Khokha R, Zimmer MJ, Graham CH, Lala PK, Waterhouse P. Suppression of invasion by inducible expression of tissue inhibitor of metalloproteinase-1 (TIMP-1) in B16-F10 melanoma cells. J.Natl.Cancer Inst. 1992;84:1017-1022.

157. Melchiori A, Albini A, Ray JM, Stetler-Stevenson WG. Inhibition of tumor cell invasion by a highly conserved peptide sequence from the matrix metalloproteinase enzyme prosegment. Cancer Res. 1992;52:2353-2356.

158. Imren S, Kohn DB, Shimada H, Blavier L, DeClerck YA. Overexpression of tissue inhibitor of metalloproteinases-2 retroviral-mediated gene transfer in vivo inhibits tumor growth and invasion. Cancer Res 1996;56(13):2891-5.

159. Valente P, Fassina G, Melchiori A, Masiello L, Cilli M, Vacca A, et al. TIMP-2 over-expression reduces invasion and angiogenesis and protects B16F10 melanoma cells from apoptosis. Int J Cancer 1998;75(2):246-53.

160. Keaheari VM, Saarialho-Kere U. Matrix metalloproteinases and their inhibitors in tumour growth and invasion. Annals of Medicine 1999;31(1):34-45.

161. Kawamata H, Kameyama S, Kawai K, Tanaka Y, Nan L, Barch DH, et al. Marked acceleration of the metastatic phenotype of a rat bladder carcinoma cell line by the expression of human gelatinase A. International Journal of Cancer 1995;63(4):568-75.

162. Kawamata H, Kawai K, Kameyama S, Johnson MD, Stetler-Stevenson WG, Oyasu R. Over-expression of tissue inhibitor of matrix metalloproteinases (TIMP1 and TIMP2) suppresses extravasation of pulmonary metastasis of a rat bladder carcinoma. Int.J.Cancer 1995;63:680-7XX4X.

163. Kruger A, Fata JE, Khokha R. Altered tumor growth and metastasis of a T-cell lymphoma in TIMP-1 transgenic mice. Blood 1997;90(5):1993-2000.

164. Martin DC, Sanchez-Sweatman OH, Ho AT, Inderdeo DS, Tsao MS, Khokha R. Transgenic TIMP-1 inhibits simian virus 40 T antigen-induced hepatocarcinogenesis by impairment of hepatocellular proliferation and tumor angiogenesis. Lab Invest 1999;79(2):225-34.

165. Baker AH, Zaltsman AB, George SJ, Newby AC. Divergent effects of tissue inhibitor of metalloproteinase-1, -2, or -3 overexpression on

rat vascular smooth muscle cell invasion, proliferation, and death in vitro. TIMP-3 promotes apoptosis. J Clin Invest 1998;101(6):1478-87.

166. Kishnani N. Characterization of Tissue Inhibitor of Metalloproteinases-3 (TIMP-3) from the Extracellular Matrices of Cultured Human and Avian Cells [Ph.D.]. San Francisco: University of California San Francisco; 1994.

167. Stringer SE, Gallagher JT. Heparan sulphate. Int J Biochem Cell Biol 1997;29(5):709-14.

168. Bernfield M, Götte M, Park PW, Reizes O, Fitzgerald ML, Lincecum J, et al. Functions of cell surface heparan sulfate proteoglycans. Annual Review of Biochemistry 1999;68(20):729-77.

169. Tanaka Y, Kimata K, Adams DH, Eto S. Modulation of cytokine function by heparan sulfate proteoglycans: sophisticated models for the regulation of cellular responses to cytokines. Proc Assoc Am Physicians 1998;110(2):118-25.

170. Gallagher JT. Heparan sulphate and protein recognition. Binding specificities and activation mechanisms. Adv Exp Med Biol 1995;376:125-34.

171. Yu WH, Woessner JF, Jr. Heparan sulfate proteoglycans as extracellular docking molecules for matrilysin (matrix metalloproteinase 7). Journal of Biological Chemistry 2000;275(6):4183-91.

172. Desai UR, Petitou M, Bjork I, Olson ST. Mechanism of heparin activation of antithrombin. Role of individual residues of the pentasaccharide activating sequence in the recognition of native and activated states of antithrombin. J Biol Chem 1998;273(13):7478-87.

173. Kusche M, Bäckström G, Riesenfeld J, Petitou M, Choay J, Lindahl U. Biosynthesis of heparin. O-sulfation of the antithrombin-binding region. Journal of Biological Chemistry 1988;263(30):15474-84.

174. Berryman DE, Bensadoun A. Heparan sulfate proteoglycans are primarily responsible for the maintenance of enzyme activity, binding, and degradation of lipoprotein lipase in Chinese hamster ovary cells. Journal of Biological Chemistry 1995;270(41):24525-31.

175. Sendak RA, Bensadoun A. Identification of a heparin-binding domain in the distal carboxyl-terminal region of lipoprotein lipase by site-directed mutagenesis. J Lipid Res 1998;39(6):1310-5.

176. Majack RA, Cook SC, Bornstein P. Control of smooth muscle cell growth by components of the extracellular matrix: autocrine role for thrombospondin. Proceedings of the National Academy of Sciences of the United States of America 1986;83(23):9050-4.

177. Phan SH, Dillon RG, McGarry BM, Dixit VM. Stimulation of fibroblast proliferation by thrombospondin. Biochemical and Biophysical Research Communications 1989;163(1):56-63.

178. Bagavandoss P, Kaytes P, Vogeli G, Wells PA, Wilks JW. Recombinant truncated thrombospondin-1 monomer modulates endothelial cell plasminogen activator inhibitor 1 accumulation and proliferation in vitro. Biochemical and Biophysical Research Communications 1993;192(2):325-32.

179. Halaban R. Growth factors and melanomas. Semin Oncol 1996;23(6):673-81.

180. Ellis LM, Fidler IJ. Angiogenesis and metastasis. Eur J Cancer 1996;32A(14):2451-60.

181. Kornmann M, Beger HG, Korc M. Role of fibroblast growth factors and their receptors in pancreatic cancer and chronic pancreatitis. Pancreas 1998;17(2):169-75.

182. Ornitz DM. FGFs, heparan sulfate and FGFRs: complex interactions essential for development. Bioessays 2000;22(2):108-12.

183. Lin X, Buff EM, Perrimon N, Michelson AM. Heparan sulfate proteoglycans are essential for FGF receptor signaling during Drosophila embryonic development. Development 1999;126(17):3715-23.

184. Zhang L, David G, Esko JD. Repetitive Ser-Gly sequences enhance heparan sulfate assembly in proteoglycans. Journal of Biological Chemistry 1995;270(45):27127-35.

185. Esko JD, Zhang L. Influence of core protein sequence on glycosaminoglycan assembly. Current Opinion in Structural Biology 1996;6(5):663-70.

186. Yanagishita M, Hascall VC. Cell surface heparan sulfate proteoglycans. Journal of Biological Chemistry 1992;267(14):9451-4.

187. Veugelers M, De Cat B, Ceulemans H, Bruystens AM, Coomans C, Deurr J, et al. Glypican-6, a new member of the glypican family of cell surface heparan sulfate proteoglycans. Journal of Biological Chemistry 1999;274(38):26968-77.

188. Lopez-Casillas F, Cheifetz S, Doody J, Andres JL, Lane WS, Massague J. Structure and expression of the membrane proteoglycan betaglycan, a component of the TGF-beta receptor system. Cell 1991;67(4):785-95.

189. Inki P, Jalkanen M. The role of syndecan-1 in malignancies. Annals of Medicine 1996;28(1):63-7.

190. Filla MS, Dam P, Rapraeger AC. The cell surface proteoglycan syndecan-1 mediates fibroblast growth factor-2 binding and activity. J Cell Physiol 1998;174(3):310-21.

191. Fitzgerald ML, Wang Z, Park PW, Murphy G, Bernfield M. Shedding of syndecan-1 and -4 ectodomains is regulated by multiple signaling pathways and mediated by a TIMP-3-sensitive metalloproteinase. Journal of Cell Biology 2000;148(4):811-24.

Chapter 2

Sequence Analysis and Molecular Modeling of TIMP-3

2.1 Introduction

Currently, there are 38 known TIMP sequences from different species including *Drosophila melanogaster* (*D. melanogaster*) and *Caenorhabditis elegans* (*C. elegans*), Figure 2.1. Five structures of TIMP-1 and TIMP-2 have been solved by NMR or X-ray crystallography alone or bound to MMP-3 or MT1-MMP (1-6). Neither of the *D. melanogaster* or *C. elegans* TIMPs has been expressed and characterized to determine if they inhibit MMPs (7). However, in *C. elegans*, Wada *et al.* found that at least one of the three putative MMP gene products, MMP-C31, exhibit gelatinase activity and two of the three, MMP-C31 and MMP-H19, cleave a fluorescence-quenching peptide used for detecting MMP activity (8). In addition, TIMP-1 and TIMP-2 inhibit MMP-C31 and MMP-H19.

In 1996, only 13 TIMP sequences were known and the structure of the N-terminal domain of TIMP-2 had been solved by nuclear magnetic resonance, NMR (1). In the same year, transcripts for a new TIMP, TIMP-4, were detected in human and mouse, in kidney, placenta, colon and testes but not in liver, brain, lung, thymus, and spleen (9, 10). A comparison of TIMP-4 with the other three TIMPs (Figure 2.2) demonstrate that the family has the conserved sequences **CXCXPXHPQXXXCXXXXVIRAK** and **YXIKXXKMXXG** in the N-terminal

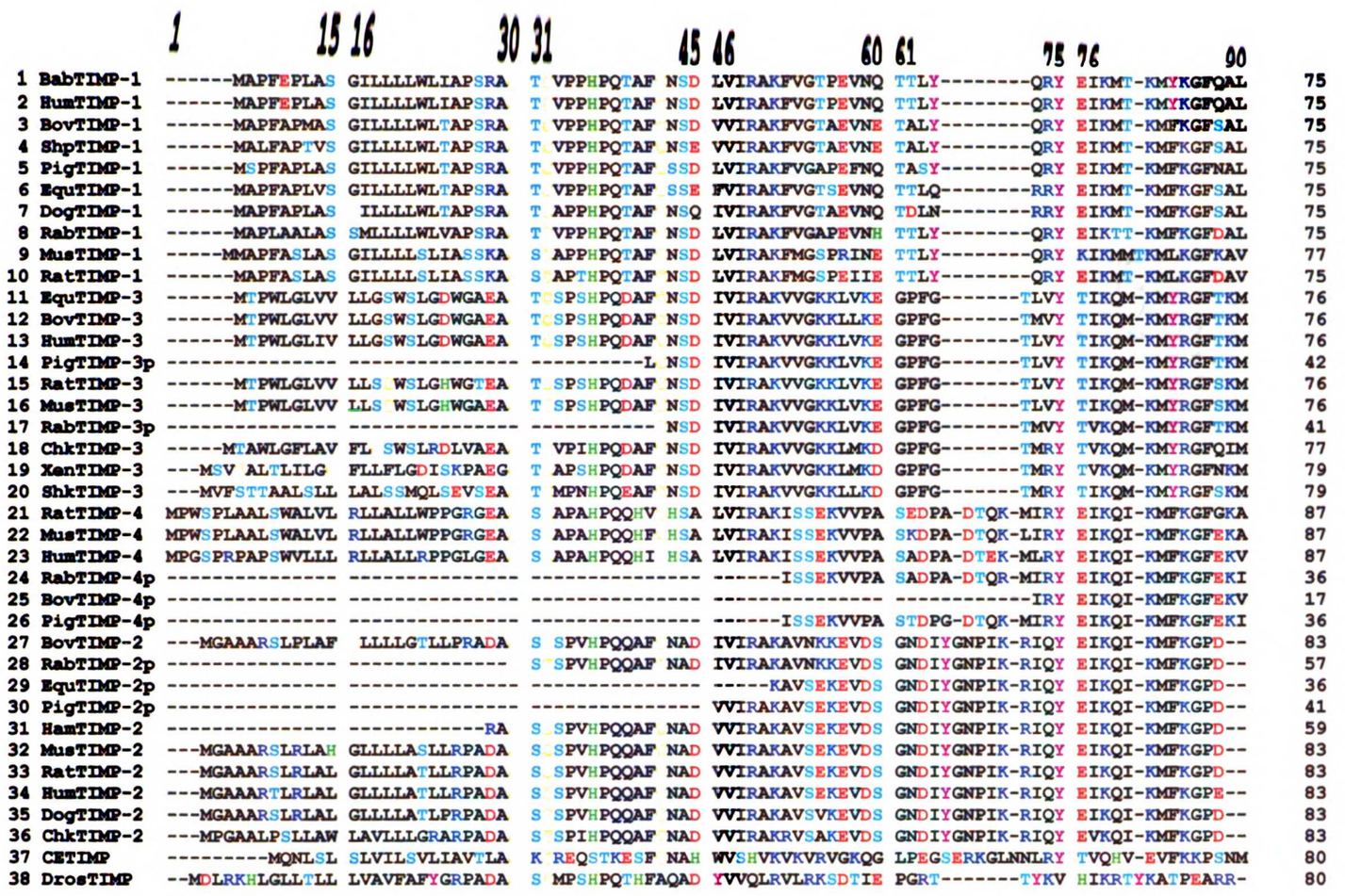

Figure 2.1. Sequence Alignment of the 38 TIMP Sequences. The alignment was made using ClustalW 1.8 using the defaults with a Gap opening penalty of 10.0 and a Gap extension penalty of 0.05. Partial sequences - 'p' at the end of the sequence name. See last page of figure for abbreviations. Arg(R) & Lys(K)- blue, Asp(D) & Glu(E)- red, Ser(S) & Thr(T)- cyan, His(H)- green, Tyr(Y)- pink, Cys( )- yellow

```
                 91        105 106       120 121       135 136       150 151       165 166       180
 1 RabTIMP-1     GDAADIRFVYTPAME SV GYFHRSHNRSEE FLIAGKLQDGLLHIT T SFVAPWNSLSLAQ RRGFTKT-YTVG EE TVFP LSIP KLQS  164
 2 HumTIMP-1     GDAADIRFVYTPAME SV GYFHRSHNRSEE FLIAGKLQDGLLHIT T SFVAPWNSLSLAQ RRGFTKT-YTVG EE TVFP LSIP KLQS  164
 3 BovTIMP-1     RDAPDIRFIYTPAME SV GYFHRSQNRSEE FLIAGQLSNGHLHIT T SFVAPWNSMSSAQ RRGFTKT-YAAG EE TVFP SSIP KLQS  164
 4 ShpTIMP-1     RDAPDIRFIYTPAME SV GYFHRSQNRSEE FLIAGQLSNGHLHIT T SFVAPWNSMSSAQ RRGFTKT-YAAG EE TVFP SSIP KLQS  164
 5 PigTIMP-1     GDAPDIRFIYTPAME SV GYFHRSQNRSQE FLIAGQLWNGHLHIT T SFVAPWNSLSSAQ RQGFTEI-YAAG EE TVFP TSIP KLQS  164
 6 EquTIMP-1     GDAPDTWFVYTPAME SL GYFHRSENRSEE FLIAGQLLDEKLYIT T SFVAPWNSLSSAQ RQGFTKT-YAAG GE SVFP SSIP KLQS  164
 7 DogTIMP-1     GNASDIRFVDTPALE SV GYLHRSQNRSEE FLVAGNLRDGHLQIN T SFVAPWSSLSTAQ RRGFTKT-YAAG EG TVFT SSIP KLQS  164
 8 RabTIMP-1     GHATDIRFVYTPAME SV GYSHKSQNRSEE FLIAGQLRNGLLHIT T SFVVPWNSLSFSQ RSGFTKT-YAAG DM TVFA ASIP HLES  164
 9 MusTIMP-1     GNAADIRYAYTPVME SL GYAHKSQNRSEE FLITGRLRNGKFHIN A SFLVPWRTLSPAQ QRVFSKKNYSAG GV TVFP LSIP KLES  167
10 RatTIMP-1     GNATGFRFAYTPAME SL GYVHKSQNRSEE FLIAGRLRNGNLHIT A SFLVPWHNLSPAQ QKAFVKT-YSAG GV TVFP SAIP KLES  164
11 EquTIMP-3     ---PHVQYIHTEASE SL GLKLEVN-KYQY LLTGRVY-DGKMYTG L NFVERWDQLTLSQ RKGLNYR--YHLG N KIKS YYLP YVTS  159
12 BovTIMP-3     ---PHVQYIHTEASE SL GLKLEVN-KYQY LLTGRVY-DGKMYTG L NFVERWDQLTLSQ RKGLNYR--YHLG N KIKS YYLP FVTS  159
13 HumTIMP-3     ---PHVQYIHTEASE SL GLKLEVN-KYQY LLTGRVY-DGKMYTG L NFVERWDQLTLSQ RKGLNYR--YHLG N KIKS YYLP FVTS  159
14 PigTIMP-3p    ---PHVQYIHTEASE SL GLKLEVN-KYQY LLTGRVY-DGKMYTG L NFVERWDQLTLSQ RKGLNYR--YHLG N KIKS YYLP FVTS  125
15 RatTIMP-3     ---PHVQYIHTEASE SL GLKLEVN-KYQY LLTGRVY-EGKMYTG L NFVERWDHLTLSQ RKGLNYR--YHLG N KIKS YYLP FVTS  159
16 MusTIMP-3     ---PHVQYIHTEASE SL GLKLEVN-KYQY LLTGRVY-EGKMYTG L NFVERWDHLTLSQ RKGLNYR--YHLG N KIKS YYLP FVTS  159
17 RabTIMP-3     ---PHVQYIHTEASE SL GLKLEVN-KYQY LLTGRVY-DGKVYTG L NFVERWDQLTLSQ RKGLNYR--YHLG N KIKS YYLP FVTS  124
18 ChkTIMP-3     ---PHVQYIYTEASE SL GVKLEVN-KYQY LITGRVY-EGKVYTG L NWYEKWDRLTLSQ RKGLNHR--YHLG G KIRP YYLP FATS  160
19 XenTIMP-3     ---PQVQYIYTEASE SL GVKLEVN-KYQY LITGRVY-EGKVYTG L NLIERWEKLTFAQ RKGLNHR--YPLG T KIKP YYLP FITS  162
20 ShkTIMP-3     ---QQVQYIYTEAAE SL GVRLQVN-KFQY LITGRVF-DGEVYTG V NFIVPWDRLTLSQ RKGLNHR--YQYG N KIKP YYLP FVTA  162
21 RatTIMP-4     ---KDIQYVYTPFDS SL GVKLETNSQKQY LLTGQILSDGKVFIH L NYIEPWEDLSLVQ RESLNHH--YHQN G QITT YAVP TITA  172
22 MusTIMP-4     ---KDIQYVYTPFDS SL GVKLETNSHKQY LLTGQILSDGKVFIH L NYIEPWEDLSLVQ RESLNHH--YHQN G QITT YAVP TISA  172
23 HumTIMP-4     ---KDVQYIYTPFDS SL GVKLEANSQKQY LLTGQVLSDGKVFIH L NYIEPWEDLSLVQ RESLNHH--YHLN G QITT YTVP TISA  172
24 RabTIMP-4p    ---KDVQYIYTPFDS SL GVKLEANSQKQY LLTGQVLSDGKVFIH L NYIEPWEDLSLVQ RESLNHH--YHLN V QITT YTVP TISA  121
25 BovTIMP-4p    ---NDIQYIYTPFDS SL GVKLEANSQKQY LLTGQILSDGKVFVH L NYIEPWENLSFLQ RESLNHR--YHLN G QITT YAVP TISA  102
26 PigTIMP-4p    ---SDIQYIYTPFDS SL GVKLETNSQKQY LLTGQILSDGKVFIH L NYIEPWENLSFLQ RESLNHY--HHLN G QITT YVVP TISA  121
27 BovTIMP-2     ---QDIEFIYTAPAA AV GVSLDIGGKKEY LIAGKAEGNGNMHIT L DFIVPWDTLSATQ KKSLNHR--YQMG E KITR PMIP YISS  168
28 RabTIMP-2     ---QDIEFIYTAPSS AV GVSLDIGGKKEY LIAGKAEGNGNMHIT L DFIVPWDTLSATQ KKSLNHR--YQMG E KITR PMIP YISS  142
29 EquTIMP-2p    ---KDIEFIYTAPSS AV GVSLDVGGKKEY LIAGKADGNGKMHIT L DFIVPWDTLST-- ---------------- ----------------   91
30 PigTIMP-2p    ---KDIEFIYTAPSS AV GVSLDIGGKKEY LIAGKAEGHGKMHIT L DFIVPWDTLSTTQ KKSLNHR--YQMG E KITR PMIP YISS  126
31 HamTIMP-2     ---KDIEFIYTAPSS AV GVSLDVGGKKEY LIAGKAEGDGKMHIT L DFIVPWDTLSTTQ KKSLNHR--YQMG E KITR PMIP YISS  144
32 MusTIMP-2     ---KDIEFIYTAPSS AV GVSLDVGGKKEY LIAGKAEGDGKMHIT L DFIVPWDTLSITQ KKSLNHR--YQMG E KITR PMIP YISS  168
33 RatTIMP-2     ---KDIEFIYTAPSS AV GVSLDVGGKKEY LIAGKAEGDGKMHIT L DFIVPWDTLSITQ KKSLNHR--YQMG E KITR PMIP YISS  168
34 HumTIMP-2     ---KDIEFIYTAPSS AV GVSLDVGGKKEY LIAGKAEGDGKMHIT L DFIVPWDTLSTTQ KKSLNHR--YQMG E KITR PMIP YISS  168
35 DogTIMP-2     ---KDIEFIYTAPSS AV GVSLDIGGKKEY LIAGKAEGNGKMHIT L DFIVPWDTLSSTQ KKSLNHR--YQMG E KITR PMIP YISS  168
36 ChkTIMP-2     ---QDIEFIYTAPST EV GQPLDTGGKKEY LIAGKSEGDGKMHIT L DLVATWDSVSPTQ KKSLNQR--YQMG E KISR LSIP FVSS  168
37 CETIMP        T--TLPDEIFTPSEA PA GLKIAAG--HEY LLAGRVEGPNALYTV L GQVLPDDRS---Q TS---------FEN- --VLEWKNVPQTLQS  151
38 DrosTIMP      --MLRDGRLSTPQDD AM GINLDLG--KVY IVAGRMP-----TLN I SYYKEYTRMTITE RHGFSGG--YAKATN TVTP FGER FKGR  159
```

Figure 2.1. Sequence Alignment of the 38 TIMP Sequences. (continued)

```
                181         195 196         210 211         225 226         240
 1 RabTIMP-1    G--TH LWTDQ-LLQ GSEKGFQSRHLA LP REPGL TWQSLRTRI A----------  207
 2 HumTIMP-1    G--TH LWTDQ-LLQ GSEKGFQSRHLA LP REPGL TWQSLRSQI A----------  207
 3 BovTIMP-1    D--TH LWTDQ-LLT GSDKGFQSRHLA LP REPGL TWQSLRAQM A----------  207
 4 ShpTIMP-1    D--TH LWTDQ-LLT GSDKGFQSRHLA LP REPGM TWQSLRPRG A----------  207
 5 PigTIMP-1    D--TH LWTDQ-LLT GSDKGFQSRHLA MP REPGM TWQSLRPRV A----------  207
 6 EquTIMP-1    D--TD LWTDQ-LLT GSDKGFQSRYLA LP REPGL TWQSLRPRT A----------  207
 7 DogTIMP-1    D--TH LWTDQ-FLT GSDKGFQSRHLA LP REPGI TWQSLPRMA ----------  206
 8 RabTIMP-1    D--TH LWTDS-SLG -SDKGFQSRHLA LP QEPGL AWESLRPRK D----------  206
 9 MusTIMP-1    D--TH LWTDQ-VLV GSED-YQSRHFA LP RNLGL TWRSLGAR- ----------  207
10 RatTIMP-1    D--SH LWTDQ-ILM GSEKGYQSDHFA LP RNPDL TWQYLGVSM TRSLPLAKAEA  217
11 EquTIMP-3    K--NE LWTDM-LSN FGYPGYQSKHYA IR QKGGY SWYRGWAPP DKSIINATDP-  211
12 BovTIMP-3    K--NE LWTDM-FSN FGYPGYQSKHYA IR QKGGY SWYRGWAPP DKSIINATDP-  211
13 HumTIMP-3    K--NE LWTDM-LSN FGYPGYQSKHYA IR QKGGY SWYRGWAPP DKSIINATDP-  211
14 PigTIMP-3p   K--NE LWTDM-LSN FGYPGYQSKHYA IR ---------- ----------  152
15 RatTIMP-3    K--KE LWTDM-LSN FGYPGYQSKHYA IR QKGGY SWYRGWAPP DKSISNATDP-  211
16 MusTIMP-3    K--NE LWTDM-LSN FGYPGYQSKHYA IR QKGGY SWYRGWAPP DKSISNATDP-  211
17 RabTIMP-3    K--NE LWTDM-LSN FGYPGYQSKHYA IR ---------- ----------  151
18 ChkTIMP-3    K--NE IWTDM-LSN FGHSGHQAKHYA IQ RVEGY SWYRGWAPP DKTIINATDP-  212
19 XenTIMP-3    K--NE LWTDM-LSN FGYPGYQSKNYA IK QKEGY SWYRGWAPP DKTTINTTDP-  214
20 ShkTIMP-3    K--NE FWTDM-LSD QGYMGHQAKHYV IR QKEGY SWYRGAAPP DKTRINATDP-  214
21 RatTIMP-4    P--DE LWTNW-LLE RMLYGYQAQHYV MK HVDGI SWYRGHLHL RKEYVDIVQP-  224
22 MusTIMP-4    P--NE LWTDW-LLE RKLYGYQAQHYV MK HVDGI SWYRGHLHL RKEYVDIIQP-  224
23 HumTIMP-4    P--NE LWTDW-LLE RKLYGYQAQHYV MK HVDGT SWYRGHLPL RKEFVDIVQP-  224
24 RabTIMP-4p   P--NE LWTDW-LLE RKLYGYQAQHYV MK HADGT SWYQGRLPL RKEFVDI----  170
25 BovTIMP-4p   P--NE L--------- ---------- ---------- ----------  107
26 PigTIMP-4p   P--NE LWTDW-LLE QKLYGYQAQHYV MK HADGT SWYQGRLHL RKEFVDI----  170
27 BovTIMP-2    P--DE LWMDW-VTE KNINGHQAKFFA IK RSDGS AWYRGAAPP KQEFLDIEDP-  220
28 RabTIMP-2    P--DE LWMDW-VTE KNINRHQAKFFA IK RSDGS AWYRGAAPP KQEFLDIEDP-  194
29 EquTIMP-2p   ---------- ---------- ---------- ----------   91
30 PigTIMP-2p   P--DE LWMDW-VTE ---------- ---------- ----------  138
31 HamTIMP-2    P--DE LWMDW-VTE KSINGHQAKFFA IK RSDGS AWYRGAAPP KQEFLDIEDP-  196
32 MusTIMP-2    P--DE LWMDW-VTE KSINGHQAKFFA IE RSDGS AWYRGAAPP KQEFLDIEDP-  220
33 RatTIMP-2    P--DE LWMDW-VTE KSINGHQAKFFA IK RSDGS AWYRGAAPP KQEFLDIEDP-  220
34 HumTIMP-2    P--DE LWMDW-VTE KNINGHQAKFFA IK RSDGS AWYRGAAPP KQEFLDIEDP-  220
35 DogTIMP-2    P--DE LWMDW-VTE KSINGHQAKFFA IK RSDGS AWYRGAAPP KQEFLDIEDP-  220
36 ChkTIMP-2    S--DE LWTDW-AME KIVGGRQAKHYA IK RSDGS AWYRGWAPP KQEFLDIEDP-  220
37 CETIMP       ---------- ------QVKSIK -- ---------- ----------  158
38 DrosTIMP     NYADT KWSPFGK E TNYSA MPHKVQTVW GVISR RWRRTQLYR K MSMP-----  210
```

Abbreviations
Bab – baboon
Bov – bovine
CE – *Caenorhabditis elegans*
Chk – chicken
Dog – dog
Dros – *Drosophil melanogaster*
Equ – *Equus cabalus*
Ham – hamster
Hum – human
Mus – *Mus musculus*
Pig – pig
Rab – rabbit
Rat – rat
Shk – shark
Shp – sheep
Xen – *Xenopus laevis*

Figure 2.1. Sequence Alignment of the 38 TIMP Sequences. (continued)

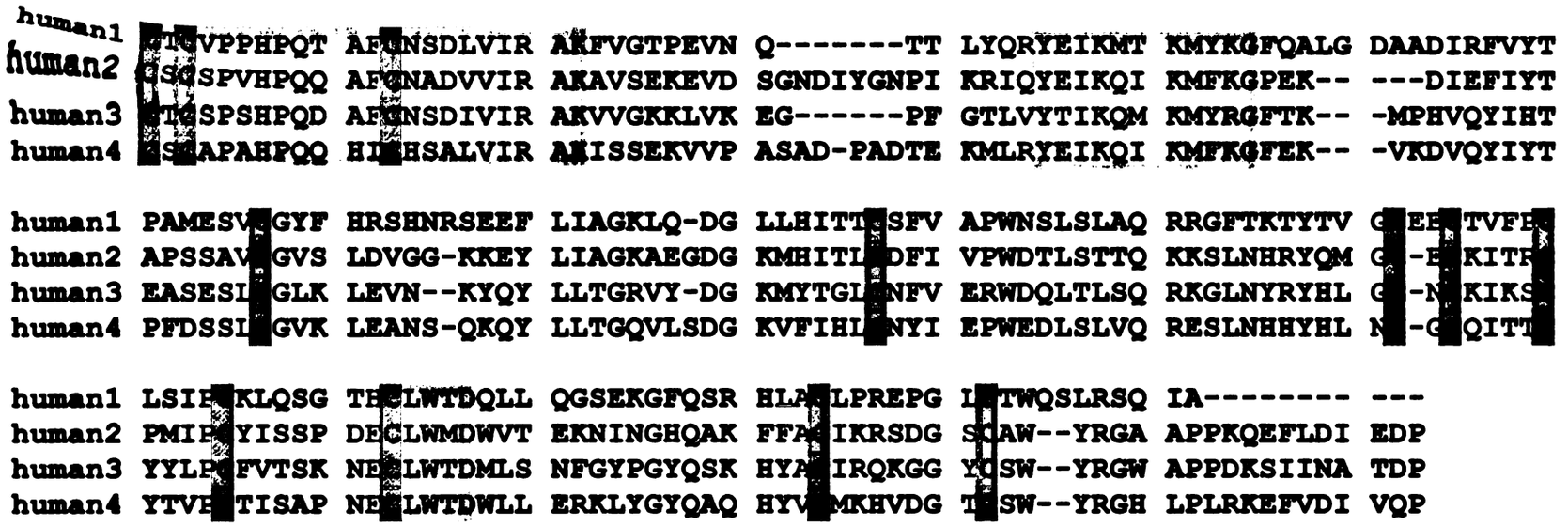

Figure 2.2: Sequence alignment of the four human TIMPs. Conserved cysteines are highlight with dark gray. Regions containing highly conserved sequences are highlighted in light gray.

region and **CLWXD** toward the C-terminus. Woessner proposed in 1991 that the first highly conserved 22 amino acids of TIMPs were responsible for MMP inhibition (11).

The TIMPs form a two-domain structure, as illustrated for TIMP-3 in Figure 2.3, with 3 disulfides (Cys1-Cys68, Cys3-Cys95, Cys13-Cys120) in the N-terminal domain and 3 disulfides (Cys122-Cys169, Cys127-Cys132, Cys140-Cys161) in the C-terminal domain. Disulfide assignments had only been made for TIMP-1 in 1990 by Williamson *et al.* and were later confirmed for TIMP-2 (5, 12). Coulomb *et al.* determined that for TIMP inhibitory activity, at least the first 3 disulfides must be intact (13). They reported that a truncated form of TIMP-1 consisting of amino acids 1-122 with the first two disulfides (Cys1-Cys70 and Cys3-Cys99) is inactive, whereas the N-terminal domain of TIMP-1, comprising the first 126 amino acids, (including the Cys13-Cys124) is an active inhibitor of MMPs (14). In 1993, DeClerck *et al.* using a partial trypsin digest demonstrated by partial trypsin digestion of TIMP-2 that the N-terminal domain of TIMP-2, comprising amino acids 1-126, is necessary for inhibitory activity (15). By peptide mapping they demonstrated that the Cys13-Cys126 disulfide is necessary for MMP inhibition. It is interesting to note that in the *current* three-dimensional structures, the Cys13-Cys126 disulfide does

Figure 2.3: Schematic structure of TIMP-3 showing conserved cysteines (green), arginines and lysines (cyan), and aspartates and glutamates (red).

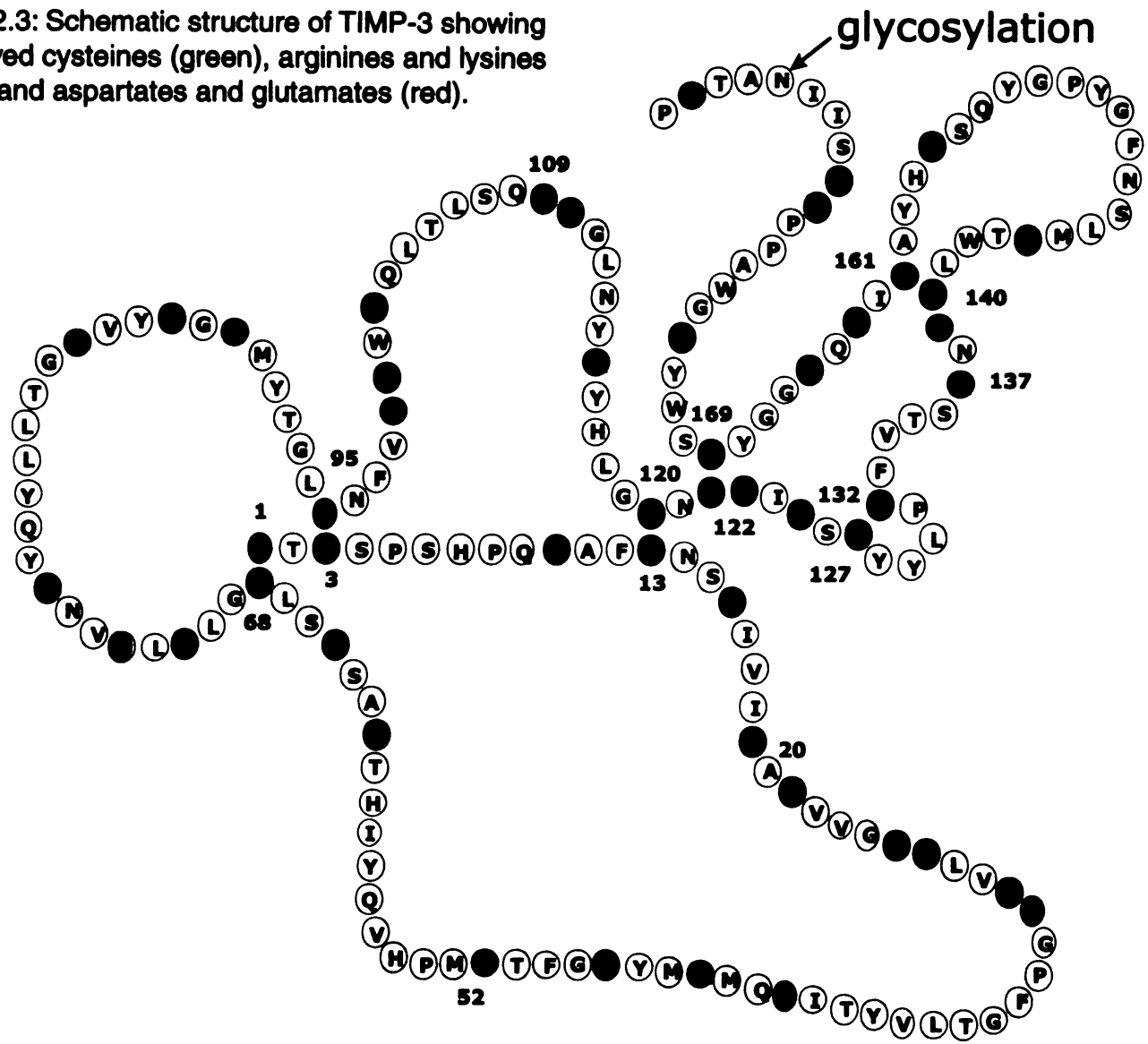

not directly interact with the MMP active site pocket but appears to be more structural.

In 1994, Williamson *et al.* reported the NMR solved structure of the N-terminal domain of TIMP-2 (1). The truncated N-TIMP-2 protein contains six beta strands and two alpha helices. The beta strands are arranged in anti-parallel beta sheets forming a common Greek Key topology. The beta barrel formed by strands A through E is homologous to the OB fold identified in oligosaccharide- or oligonucleotide-binding proteins. The N-TIMP-2 structure shares a very close beta-barrel topology with the OB fold proteins, Staphylococcal nuclease and the B subunit of heat-labile enterotoxin. The investigators postulate that two surface regions consisting of conserved positively charged residues Arg20, Lys22, Lys48 and Lys51 forms a hydrophilic convex surface at the back of the beta barrel, and a hydrophobic concave surface consisting of conserved residues Phe103, Leu85, Trp107, Gln114, Leu118, Tyr122 and His7. It is surprising that they did not speculate on the highly conserved cysteines, more precisely Cys1, Cys3, Cys72, and Cys101 protruding from the concave surface that were later found to chelate the zinc in the MMP active site.

The C-terminal domains of TIMPs do not appear to be involved in direct inhibition of the MMPs but appear to be important in increasing

binding to certain MMPs (16). Through the use of truncated TIMP-1 and TIMP-2, Δ127-184TIMP-1 and Δ128-194TIMP-2 and Δ186-144TIMP-2, the investigators found that TIMP-2 binds more rapidly to MMP-2 than TIMP-1 and that the last 9 amino acids of TIMP-2 are largely responsible for this interaction. Further studies by the same group of investigators demonstrated that the N-terminal domain of MMP-3 interacts with the N-terminal domain of TIMP-1, and the hemopexin-like domain of MMP-2 interacts with the C-terminal domain of TIMP-2, respectively (17). They also demonstrated that TIMP-1 shows faster binding and greater specificity to MMP-3, and TIMP-2 shows faster binding and specificity to MMP-2. Howard *et al.* and Kleiner *et al.* separately deduced that there are two distinct interactions between TIMP-2 and MMP-2 by Scatchard analysis and cross-linking, respectively (18, 19).

Biochemically, the TIMPs are similar. All TIMPs have twelve conserved cysteines that are assumed to be organized as six disulfides although this has only been confirmed for TIMP-1 and TIMP-2. Because the spacing of the cysteines is highly conserved and because activity is dependent on the intact disulfides in the N-terminus, it is assumed that TIMP-3 and TIMP-4 share similar disulfide linkages. They are all small proteins (M_r 20kDa-30kDa) in size (Table 2.1). TIMP-1 is N-glycosylated at Asn30 and Asn78 (20), whereas TIMP-2

and TIMP-4 are both unglycosylated proteins. TIMP-3 is expressed unglycosylated and N-glycosylated, at Asn184, and both forms are found in the ECM and are active inhibitors of MMPs. From this information, one can deduce that localization is not critically dependent on glycosylation although a role for this post-translational modification cannot be eliminated. TIMP-3 is the most basic of the four TIMPs, with

Table 2.1: Biochemical Properties of the human TIMPs.

	TIMP-1	TIMP-2	TIMP-3	TIMP-4
Localization	CM	CM	ECM	CM
Size (M_r)	20.7kD (~29)	21.8kD (~20)	21.7kD (~23)	22.4kD (~22)
N-glycosylation	+	-	-(+)	-
Disulfides	6	6	6	6
% similarity/identity to TIMP-3[a]	51.7/39.9	60.2/47.3	-	57.4/50.5
pI	8.5[b]/6.5[c]	6.5[b]	9.2[b]	7.3[b]

All calculations were made using the mature human form of the protein.
a - calculated using GAP program from Genetics Computer Group, Inc.
b – calculated using peptidesort from Genetics Computer Group, Inc.
c – Reported pI for purified glycosylated bovine TIMP-1 (20).

a pI of 9.2, and one of the most basic proteins in the ECM.

Because the interactions of chicken TIMP-3 with ECM appeared to be electrostatic, Kishnani and Hawkes noted three short stretches of 9-11 amino acids that contain a high density of positive charge from lysines and arginines, uninterrupted by negative charge, in the N-terminus of TIMP-3 between Arg20 to Arg48, and a longer stretch from Arg 103 to Lys137 not present in TIMP-1 or TIMP-2 (21). With the identification of a fourth member of the TIMP family, it was possible to refine the analysis of sequence alignments of the human

TIMPs to locate conserved regions of positive or negative charge. In addition, homology modeling of TIMP-1, TIMP-3 and TIMP-4 was performed utilizing the NMR solved structure of truncated TIMP-2 (1). By utilizing these analytical tools, a highly basic linear sequence has been identified on the surface of the TIMP-3 molecule that appears as a groove that could bind a polyanion such as heparan sulfate. It is postulated that this basic surface could be the critical feature that differentiates it from the other TIMPs and localizes it to the ECM by binding to HSPGs.

2.2 Materials and Methods

2.2.1 Protein Sequence Searches – Sequences searches were performed on a Digital AlphaServer 2100 using blastp from the Genetics Computer Group (GCG) software Version 10.0 (Genetics Computer Group) or through the internet, using blastp with the default parameters, at http://www.ncbi.nlm.nih.gov/BLAST/ (22). TIMP sequence searches were performed using the all non-redundant GenBank CDS translations+PDB+SwissProt+PIR+PRF database. Further sequence searching was performed using SHOTGUN V2.0a after determining a set of distantly related members of the TIMP family (23). Distances were determined from alignments of each member of the TIMP families. The most distant from each member

was then used in the SHOTGUN blast to locate any other possible TIMPs or new TIMPs in the databases.

2.2.2 Multiple Sequence Alignments – The sequences were downloaded using the FETCH program (GCG Ver. 10.0) and the sequence accession number (Table 2.2).

Table 2.2: Sequence accession numbers for the TIMPs

species subspecies	**common name**	**Name used in alignments**	**accession number**
Papio hamadryas cynocephalu	baboon	BabTIMP-1	L37295
Bos taurus	bovine	BovTIMP-1	S70841
Bos taurus	bovine	BovTIMP-2	M32303
Bos taurus	bovine	BovTIMP-3	U77588
Bos taurus	bovine	BovTIMP-4	AAD02097
Caenorhabditis elegans		CETIMP	U53336
Gallus gallus	chicken	ChkTIMP-2	AF004664
Gallus gallus	chicken	ChkTIMP-3	M94531
Canis familiaris	dog	DogTIMP-1	AB016817
Canis familiaris	dog	DogTIMP-2	AF112115
Cricetulus longicaudatus	hamster	HamTIMP-2	S38624
Drosophila melanogaster		DrosTIMP	AJ010067
Equus caballus	horse	EquTIMP-1	U95039
Equus caballus	horse	EquTIMP-2	AJ010315
Equus caballus	horse	EquTIMP-3	AJ243283
Homo sapiens	human	HumTIMP-1	X03124
Homo sapiens	human	HumTIMP-2	S48568
Homo sapiens	human	HumTIMP-3	S78453
Homo sapiens	human	HumTIMP-4	U76456
Mus musculus	mouse	MusTIMP-1	M28312
Mus musculus	mouse	MusTIMP-2	M93954
Mus musculus	mouse	MusTIMP-3	L27424
Mus musculus	mouse	MusTIMP-4	(10)
Oryctolagus cuniculus	rabbit	RabTIMP-1	J04712
Oryctolagus cuniculus	rabbit	RabTIMP-2	AAB35920
Oryctolagus cuniculus	rabbit	RabTIMP-3	AAC95006
Oryctolagus cuniculus	rabbit	RabTIMP-4	AAC95007
Ovis aries	sheep	ShpTIMP-1	S67450
Rattus norvegicus	rat	RatTIMP-1	U06179
Rattus norvegicus	rat	RatTIMP-2	S72594
Rattus norvegicus	rat	RatTIMP-3	U27201
Rattus norvegicus	rat	RatTIMP-4	P81556
Scyliorhinus torazame	shark	ShkTIMP-3	AAD26150
Sus scrofa	pig	PigTIMP-1	S96211
Sus scrofa	pig	PigTIMP-2	AF156030
Sus scrofa	pig	PigTIMP-3	AF156031
Sus scrofa	pig	PigTIMP-4	AF156032
Xenopus laevis	frog	XenTIMP-3	AF042493

Each sequence was converted from GCG format to FASTA format using READSEQ. The FASTA files were concatenated in a text file using Microsoft Word 97 on a Pentium II/233 MHz computer running Windows 2000. ClustalW, at the Baylor College of Medicine Search Launcher web page, was used to align the 38 TIMP sequences (https://www.sacs.ucsf.edu/secure/cgi-bin/clustalw.pl) (24, 25). The ClustalW default conditions of a gap opening penalty of 10.0 and a gap extension penalty of 5.0 were used. The maximal linkage alignment was used for further analysis by formatting and highlighting in MS Word 97 (Microsoft Corp.).

For alignment of the four human TIMPs, PIMA 1.4, Pattern-Induced Multiple Alignment, software was utilized at the web site http://dot.imgen.bcm.tmc.edu:9331/multi-align/multi-align.html (26). The Class 1 matrix default gap of 6.67 and default gap extension penalty of 1.33 were used. Coloring and formatting were performed in MS Word 97 (Microsoft Corp.).

2.2.3 Projections of N-TIMPs – The ^{1}H NMR solved coordinates for the truncated N-huTIMP-2 (amino acids 1-127) were kindly provided by Dr. Richard A. Williamson (University of Kent, U.K.) in PDB format. The N-TIMP-1, N-TIMP-3 and N-TIMP-4 models were constructed by substituting amino acids from the TIMP-2 sequence with the corresponding homologous amino acids from each TIMP using

the *swapaa* command in MIDAS, Molecular Interactive Display And Simulation (27). The N-huTIMP-2 model and the other TIMP projections were viewed in MIDAS and CONIC (27, 28). The heparin PDB file, hep2.pdb, was downloaded from the Protein Data Bank (29). The distance calculations between hydrogens on the amines of arginines and lysines and the oxygens on the sulfates of heparin were carried out using the distance command in MIDAS. Images were prepared utilizing Target Image File Format from the MIDAS output and further formatting in Adobe PhotoShop 5.5 and Illustrator 8.0 (Adobe Corp.).

2.2.4 Projections of Full TIMPs – The protein data bank, pdb, file for X-ray crystallography solved TIMP-2, 1br9.pdb, was downloaded from the Protein Data Bank (5). The TIMP-1, TIMP-3 and TIMP-4 models were constructed by substituting amino acids from the TIMP-2 sequence with the corresponding homologous amino acids from each TIMP using swapaa in MIDAS, Molecular Interactive Display And Simulation (27). The TIMP-2 model and the other TIMP projections were viewed in MIDAS and CONIC (27, 28). Images were prepared by creating protein data bank files through MIDAS. The images were oriented and colored utilizing RasMol Version 2.7.1 (Glaxo Welcome) and formatted in Adobe PhotoShop 5.5 and Illustrator 8.0 (Adobe Corp.).

2.3 Results and Discussion

2.3.1 Sequence Alignments of the Four Human TIMPs

In order to investigate the structural features of TIMP-3 that may differentiate it from TIMP-1, TIMP-2, and TIMP-4 that cause it to localize to the ECM, a sequence alignment was prepared utilizing the four known human TIMP sequences, Figure 2.4. All TIMPs share the conserved 12 cysteines (6 disulfides). TIMP-3 has 51.7% similarity and 39.9% identity to TIMP-1, 60.2% similarity and 47.3% identity to TIMP-2 and 57.4% similarity and 50.5% identity to TIMP-4. All four proteins have conserved sequences CXCXPXHPQXXXCXXXXVIRAK and YXIKXXKMXXG in the N-terminal domain, and CLWXD in the C-terminal domain, Figure 2.4. The greatest similarity between TIMP-3 and TIMP-1, TIMP-2, and TIMP-4 is in the N-terminal sequence of the proteins. Because TIMP-3 has such a high pI (9.2), the distribution of basic and acidic residues within the four TIMPs was compared. Unique to TIMP-3 are three basic linear sequences of amino acids in the primary structure, Figure 2.4. These regions are highly conserved in the ten TIMP-3 sequences from different species, Figure 2.1. TIMP-3 is the only sequence that has highly positively charged regions from arg20 to lys52 (Region I), arg109 to lys137 (Region II), and lys157 to arg173 (Region III), Figure 2.4. Table 2.3 shows the net charge of these regions in all of the TIMPs. Region I

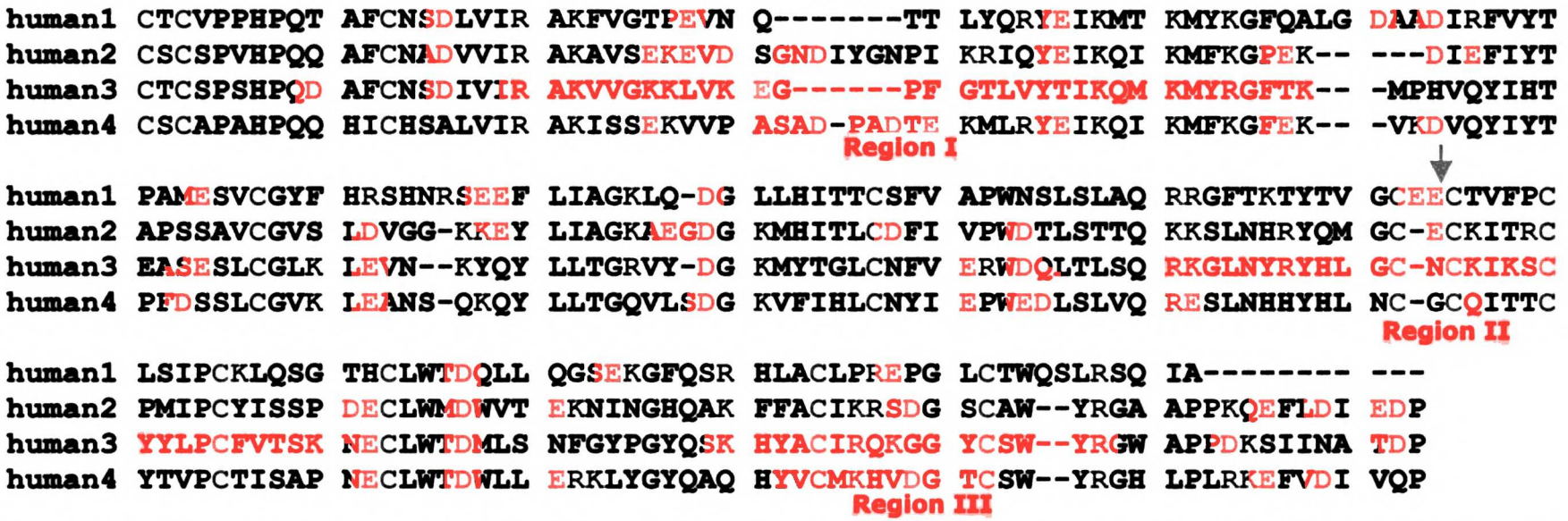

Figure 2.4: Sequence alignment of the four mature human TIMPs. Negatively charged amino acids, asp and glu, are colored red. Positively charged amino acids, lys and arg, are colored blue. Cysteines are colored green. Cyan arrow indicates where Williamson *et al*. made the truncation on TIMP-2 (3). Yellow highlights show basic regions of TIMP-3.

and II of TIMP-3 are clearly much more basic than the corresponding regions in the other TIMPs. None of the three sequences, Regions I, II, and III, in TIMP-3 contain putative heparan sulfate binding motifs such as the linear sequences XBBXBX or XBBBXXBX (B – basic residure, X – hydropathic residue) defined by Weintraub and Cardin (30). Furthermore, there are no sequence similarities to either acidic fibroblast growth factor (aFGF) or basic fibroblast growth factor (bFGF), which bind to heparan sulfate. Neither of these related proteins contains heparan sulfate-binding motifs. However, the regions of aFGF and bFGF, that are thought to bind heparan sulfate, are composed of two sequence-separated beta sheets that create a basic surface (31, 32). Similarly, the ECM-binding domain of TIMP-3 may be determined by its three-dimensional structure (33).

Table 2.3: Net charge of the three regions of TIMP-3 and the homologous regions in TIMP-1, TIMP-2 and TIMP-4.

	Net Charge		
	Region I	Region II	Region III
TIMP-1	+4	+2	+2
TIMP-2	+3	+3	+3
TIMP-3	+8	+6	+4
TIMP-4	+3	0	+1

2.3.2 Homology Modeling of N-TIMP-1, N-TIMP-3, and N-TIMP-4 Utilizing the N-TIMP-2 NMR Structure

The first basic Region I, Arg20 to lys52, was further analyzed using the ^{1}H NMR solved N-TIMP-2 model (amino acids 1-127) (1). Using

the N-TIMP-2 model and the sequence alignments, projected models of N-TIMP-1, 3 & 4 were made in MIDAS and viewed using CONIC, Figure 2.5, (27, 28). The projections assume that the TIMPs will have a similar fold because of the two-domain structure, conserved cysteine linkages that have a highly conserved spacing, and the fact that MMP-inhibitory activity is dependent on correct folding. In addition, the similar profiles for the binding and inhibition of MMPs also would suggest that they have similar structure. It should also be noted that the first loop, glu34 to asn38 of TIMP-2, can be accommodated by a similar loop of glu34 to glu37 in TIMP-4, and tighter loops formed by gln3 to thr32 in TIMP-1, the gly32 to pro33 in TIMP-3. The projection of N-TIMP-3 shows an uninterrupted surface region that is highly basic. This region is the first basic Region I, arg20 to lys52, seen in the sequence alignments, Figure 2.4. In the N-TIMP-2 structure, this region is composed of two anti-parallel beta sheets separated by a long loop, NGIYGN. By comparing the N-TIMP projection in Figure 2.5, this analogous region on the other N-TIMP projections is either lacking some of the basic residues and is interrupted by acidic residues as in N-TIMP-1, or has a basic residue replaced by an acidic residue and is interrupted by more acidic residues as in N-TIMP-2 and N-TIMP-4. The single negative charge in Region I of the N-TIMP-3 projection is located near the first loop of TIMP-3 and as a result does not interrupt

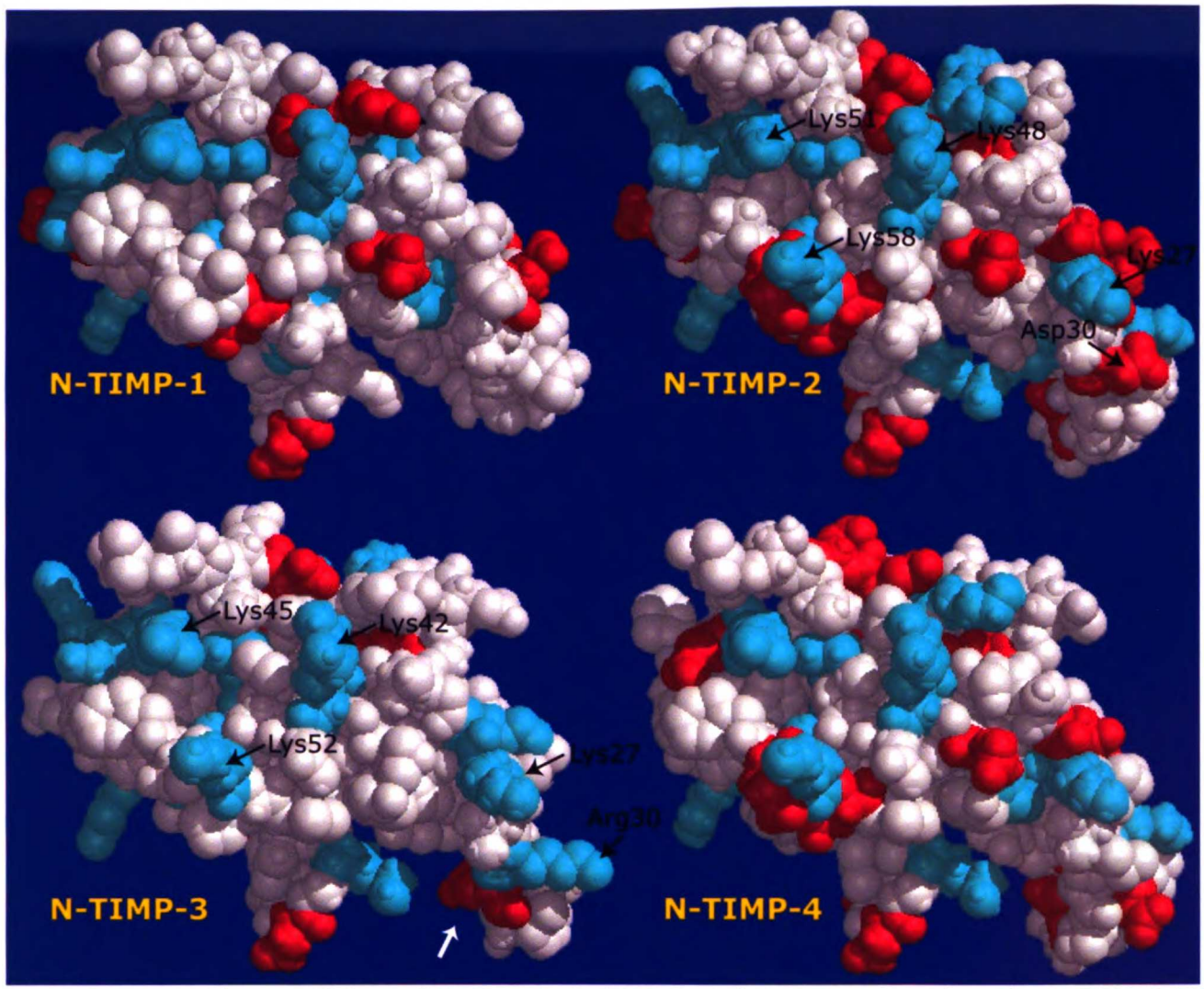

Figure 2.5: Homology modeling of N-TIMP-1, N-TIMP-3, and N-TIMP-4 based on the N-TIMP-2 NMR structure. Lysines and arginines are colored cyan. Aspartates and glutamates are colored red. The white arrow near the N-TIMP-3 indicates the single negative charge in Region I, Figure 2.4.

the basic surface region noted above (indicated by the white arrow in Figure 2.5).

2.3.3 Modeling of TIMP-3 with Heparan Sulfate

When rotated in MIDAS, this region forms a highly basic surface that appears to form a groove that could accommodate a molecule such as heparan sulfate. Figure 2.6 shows a heparin molecule as it might appear with the N-TIMP-3 projection. Heparin is a more sulfated form of heparan sulfate. The 6 disaccharide heparin model is the only three-dimensional structure available (29). Mulloy *et al.* determined that regardless of the sulfate substitution pattern the overall polysaccharide structures are similar (34).

Figure 2.7 shows a schematic of the distances from oxygens on the sulfates of heparin compared to distances of hydrogens of the amines on arginines and lysines of the N-TIMP-3 projection. The differences of these distances are well within the 3.0 Å limit for electrostatic interactions. Models comparing chondroitin sulfate, keratan sulfate and hyaluronate were constructed and did not appear to be able form as many close electrostatic interactions as heparan sulfate (data not shown).

Although, these homology models of N-TIMP-1, N-TIMP-3, and N-TIMP-4 were not energetically minimized, they do provide important information that can be used to make hypotheses about TIMP

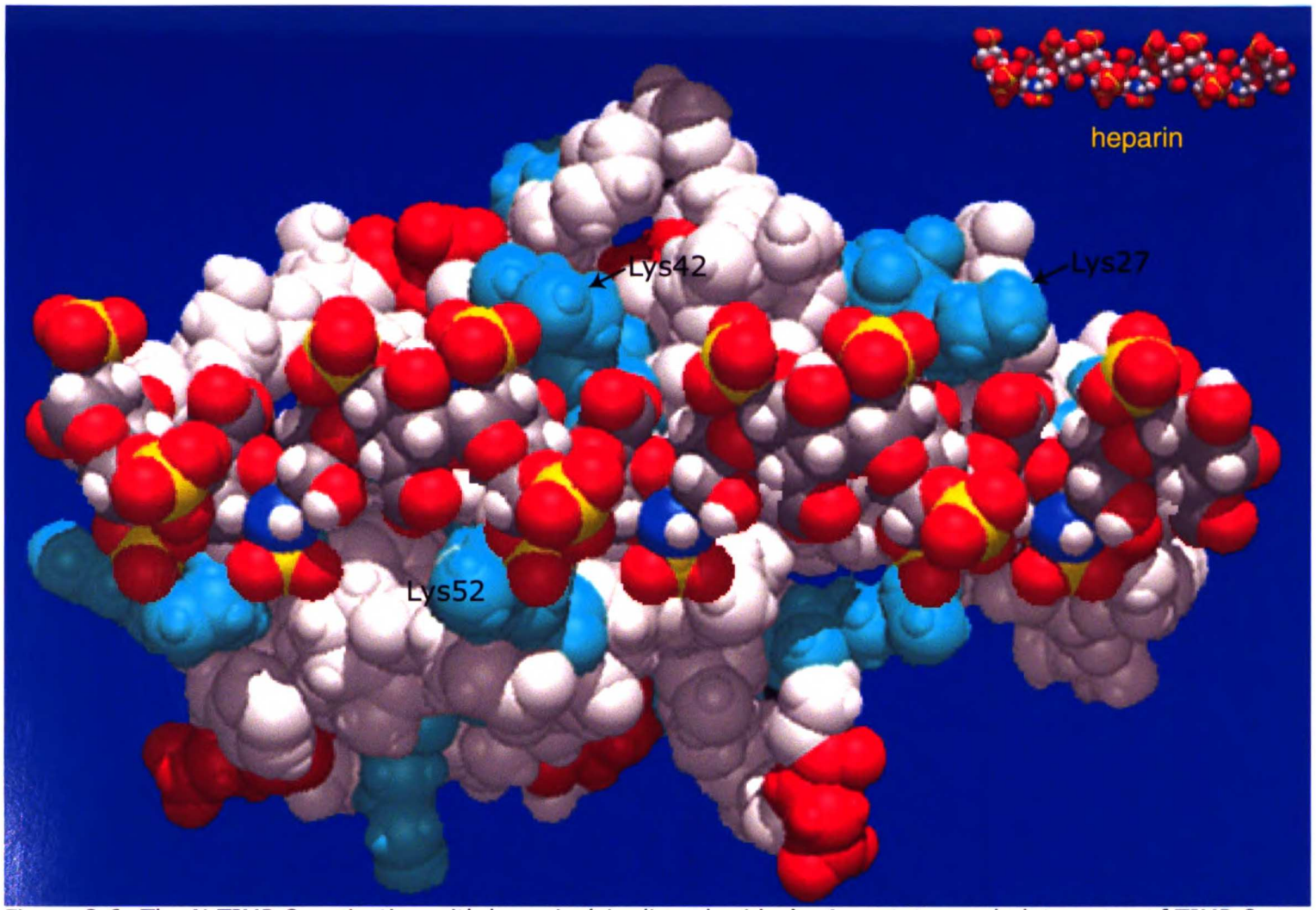

Figure 2.6: The N-TIMP-3 projection with heparin (six disaccharides). Aspartates and glutamates of TIMP-3 are colored red. Lysines and arginines of TIMP-3 are colored cyan. Oxygens of heparin are colored red. Sulfurs of heparin are colored yellow. Nitrogens of hepain are colored blue. Carbons of heparin are colored grey.

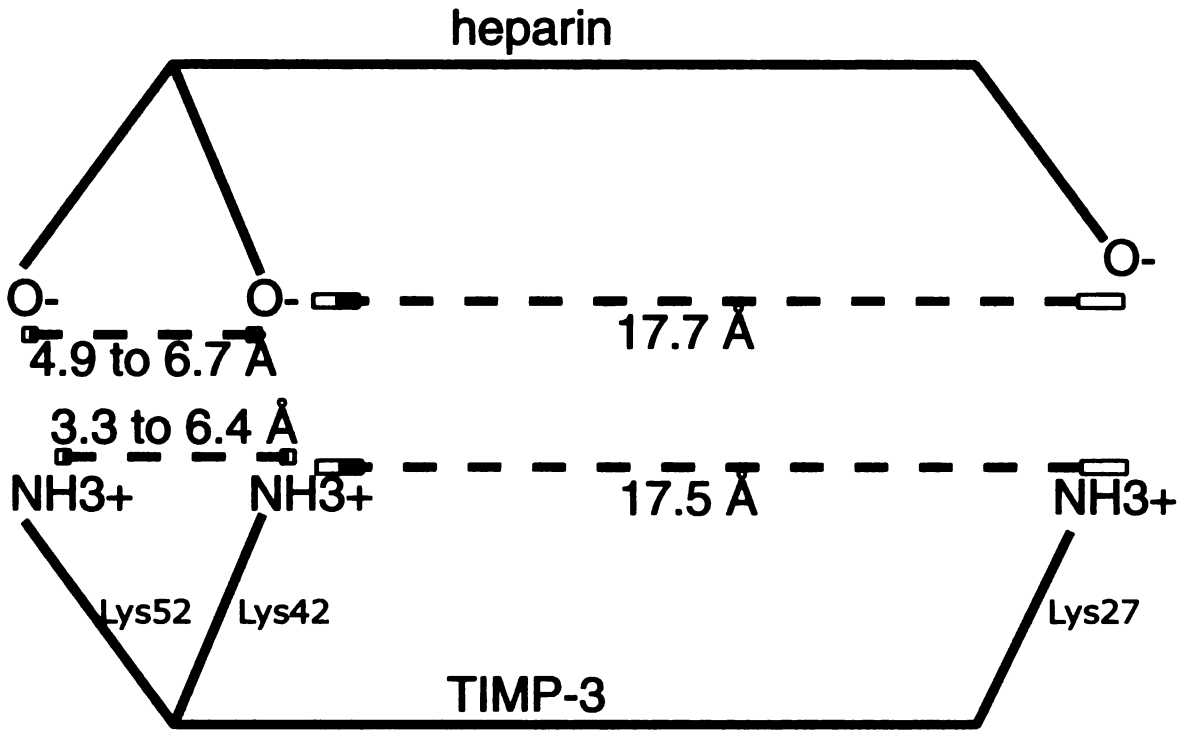

Figure 2.7: Schematic of distances between oxygens on sulfates of heparin and the hydrogens on the amines of lysines of TIMP-3.

structure/function relationships. This analysis provides the basis for the chimeras constructed in Chapter 3. The chimeras were designed to determine if the first basic region, Region I, of TIMP-3 localizes TIMP-3 to the ECM through potential interactions with heparan sulfate.

After the sequence analysis and N-TIMP homology models were made in 1996, additional sequences for TIMPs from different species were reported. More significantly, a TIMP-1/cdMMP-3 (cd – catalytic domain) 2.8 Å structure by X-ray crystallography (2), a TIMP-2/cdMT1-MMP 2.75 Å structure by X-ray crystallography (3), a full TIMP-2 2.1 Å structure by X-ray crystallography (5), and an N-TIMP-1 NMR structure (6) were solved. For TIMP-2, Cys1 to Pro5, Cys72, and Cys101 appear to be key amino acids involved in chelation of the active-site zinc and binding to the active site pocket of MMP-3 and MT1-MMP (3, 4). Homologous amino acids were determined to be involved in TIMP-1 binding to MMP-3 (2). The N-terminus from Cys1 to Pro5, the strand C connector loop (Ser68-Val71) and the disulfide of Cys1 to Cys72 comprise most of the intermolecular inhibitory contacts with MMP-3. The Cys1 interacts with the catalytic zinc through the carbonyl oxygen. The N-terminal α-amino group is thought to form a hydrogen bond with one of the carboxylate oxygen atoms of the catalytic Glu219 of MMP-2 (35). The Ser2 in TIMP-2 and the Thr2 in TIMP-1 extends into the S1′ pocket, hydrogen bonding to the other

Glu219 carboxylate. Mutagenesis experiments have shown that changes to this amino acid results in discrimination between different MMPs (36). The N-TIMP-2 and N-TIMP-1 structures overlay very closely with the exceptions of the longer strand A to strand B loop of N-TIMP-2 and the longer strand C connector loop of N-TIMP-1 (3, 6). When the full TIMP-2 structure is compared to full TIMP-1 bound to MMP-3, investigators note a slight turn between the two N- and C-terminal domains. Since there are few C-terminal contacts with MMP-3, it is uncertain whether this is a conformational change do to binding to MMP-3 or is a consequence of the particular crystallization.

The authors of the TIMP/MMP complex references describe several connecting loops of the TIMPs (3, 35, 37). In TIMP-2 there is a long strand A to strand B hairpin loop, NDIYGN in Figure 2.5, that folds over the rim of the active-site cleft of the MT1-MMP (3). The authors note that "in spite of the relatively large overall interface between the strand A to strand B loop and the molecular MMP surface, most of the intermolecular contacts do not seem to be designed for optimal complementarity" (35). In fact, the shorter strand A to strand B loop of TIMP-1 does not make contact with MMP-3 (2). The other edge loops are believed to be involved in very few intermolecular contacts. Bode *et al.* suggests that the C-terminal edge loops may be flexible

(35). Furthermore, the C-terminal tail appears to have different possible conformations (35).

When the N-TIMP projections were performed, the first highly conserved 22 amino acids of TIMPs were believed to be responsible for MMP inhibition (11). These amino acids of the TIMP structure appear on the opposite side from the proposed heparan binding domain. This region of the TIMP-1 and TIMP-2 was confirmed to be responsible for MMP inhibition (2, 3). Figure 2.8 demonstrates that the binding domain for MMP inhibition is on the opposite side of the TIMP molecule from that containing the proposed basic groove that binds to heparan sulfate.

2.3.4 Homology Modeling of the TIMP-1, TIMP-3, and TIMP-4 Utilizing the Full TIMP-2 X-ray Crystal Structure

Homology models of TIMP-1, TIMP-3, and TIMP-4 were constructed utilizing the full TIMP-2 structure, Figure 2.9. These also suggest that TIMP-3 contains an uninterrupted surface region that is highly basic and unique to TIMP-3 (compare TIMP structures in Figure 2.9). This region is the first basic Region I, arg20 to lys52, seen in the sequence alignments, Figure 2.4. As demonstrated with the N-TIMP homology models, this analogous region on the other full TIMP projections is either lacking some of the basic residues and is interrupted by acidic residues as in TIMP-1, or has a basic residue replaced by an acidic

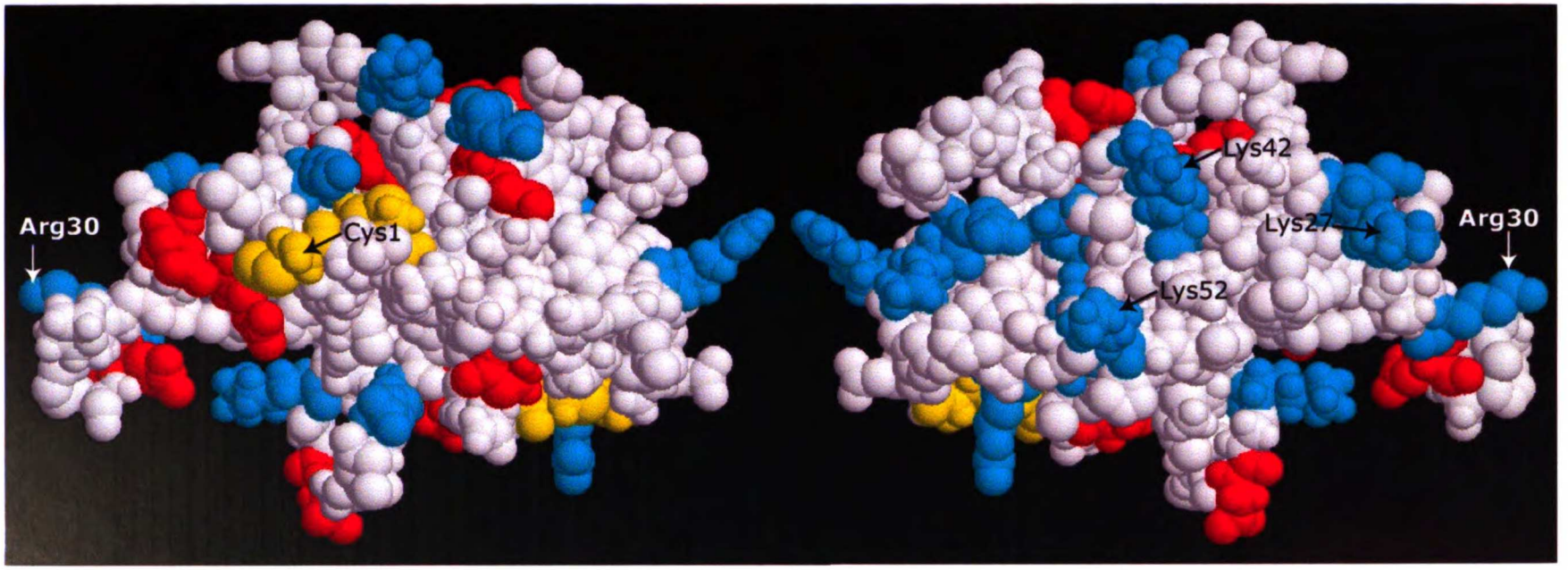

Figure 2.8: TIMP-3 models showing the MMP-binding domain and the proposed heparan sulfate binding domain on opposite faces of the TIMP-3. Molecule is rotated 180° around the Y-axis. Aspartates and glutamates are colored red. Arginines and lysines are colored cyan. Cysteines are colored yellow. Cys1 that chelates the active site zinc of MMPs and Arg30 near the 1st loop are indicated with arrows.

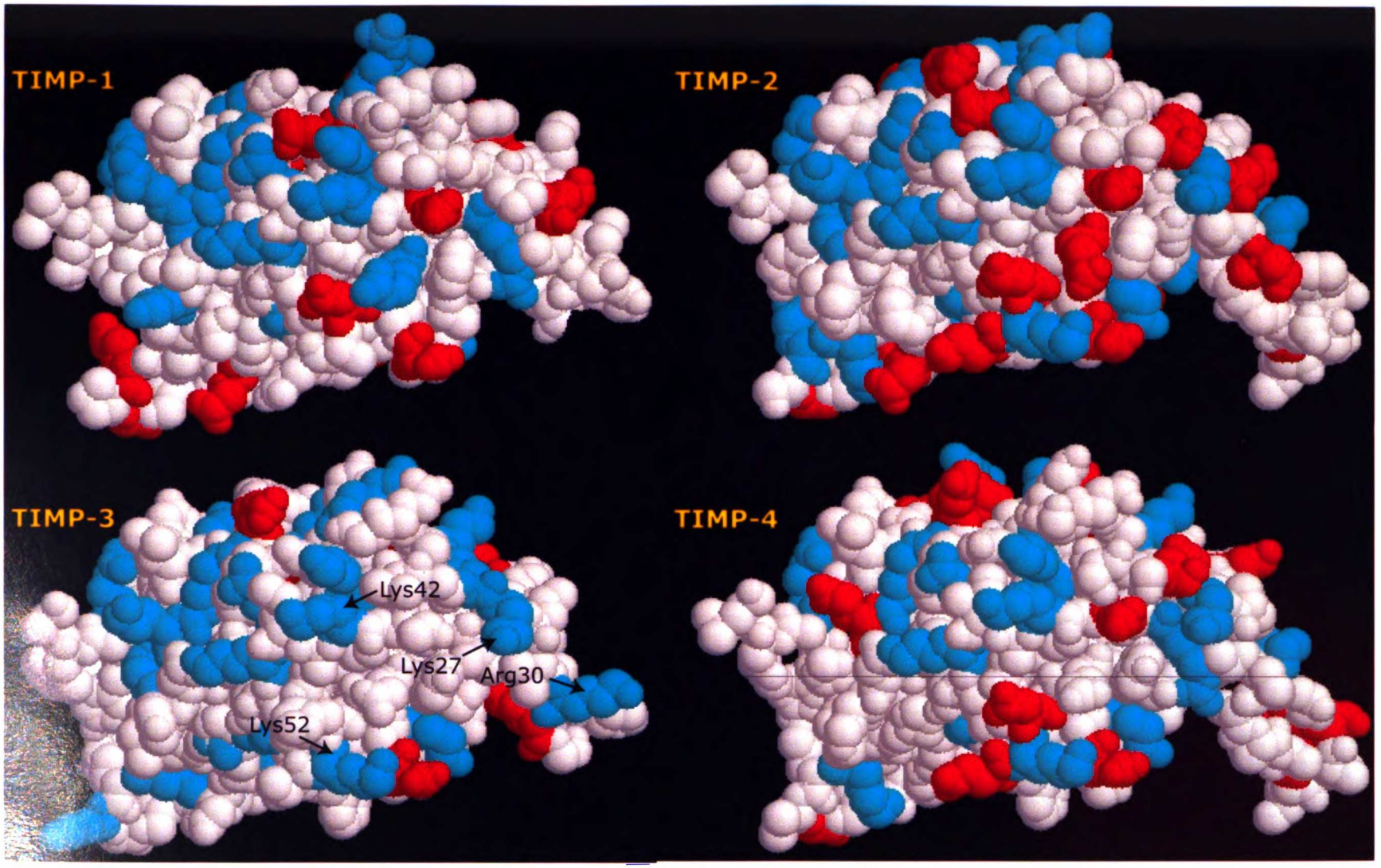

Figure 2.9: Homology modeling of TIMP-1, TIMP-3, and TIMP-4 based on the TIMP-2 X-ray crystal structure. Lysines and arginines are colored cyan. Aspartates and glutamates are colored red.

residue and is interrupted by more acidic residues as in TIMP-2 and TIMP-4, Figure 2.9. Furthermore, when rotated in MIDAS, this region forms a highly basic surface that appears to form a groove that could accommodate a molecule such as heparan sulfate.

In addition to solution structures, recent chimera constructs and mutagenesis studies of MMPs with TIMP-2 and TIMP-3 have shown that TIMP-2 and TIMP-3 can bind to MMP-2 and MMP-9 through both their respective N- and C-terminal domains (38). The N-terminal domains of TIMP-2 and TIMP-3 can each bind to the active-site pockets in the N-terminal domains of MMP-2 and MMP-9, and the C-terminal tails of TIMP-2 and TIMP-3 can each bind to the C-terminal hemopexin-like domains of MMP-2 and MMP-9 (38). These data confirm the binding studies of TIMP-2 and MMP-2 by Kleiner *et al.* in 1991 and Howard *et al.* in 1992 that first suggested the existence of two binding sites (18, 19). TIMP-2 also binds more tightly to MMP-2 than TIMP-3, possibly because of the greater number of negatively charged amino acids in the C-terminal tail of TIMP-2 that could interact with the positively charged amino acids in the hemopexin-like domain of MMP-2 (39). Much of this information has contributed to understanding the mechanism of MMP-2 activation and formation of the MT1-MMP/TIMP-2/proMMP-2 ternary complex (40, 41).

This chapter has described sequence alignment analyses and construction of a TIMP-3 homology model utilizing the N-TIMP-2 structure to investigate the structural features of the TIMP-3 molecule that may contribute to its localization in the ECM. In addition, potential electrostatic interactions were determined by analyzing the TIMP-3 model and a heparin structure. These calculations predict that it is conceivable for TIMP-3 to interact with heparan sulfate through the positively charged amines of lysines and arginines of TIMP-3 and the negatively charged sulfates of heparan sulfate. Recently, Butler *et al.* determined that polyanions, such as heparan sulfate, heparin, and dextran sulfate enhances inhibition of MMP-2 by TIMP-3 (38). In addition MMP-2 contains a putative heparan sulfate binding site in its C-terminus (38). A truncated MMP-2, Δ418-631MMP-2, does not show increased inhibition by TIMP-3 when incubated with heparin, suggesting that a heparin binding site is required for both proteins (38). The same investigators briefly suggest that modeling of TIMP-3 shows a basic groove that could bind to heparan sulfate. These data support the hypothesis that basic Region I on the surface of TIMP-3 binds to HSPGs in the ECM and localizes the protein to the ECM.

2.4 Bibliography

1. Williamson RA, Martorell G, Carr MD, Murphy G, Docherty AJ, Freedman RB, *et al.* Solution structure of the active domain of tissue inhibitor of metalloproteinases-2. A new member of the OB fold protein family. Biochemistry 1994;33:11745-11759.

2. Gomis-Ruth FX, Maskos K, Betz M, Bergner A, Huber R, Suzuki K, *et al.* Mechanism of inhibition of the human matrix metalloproteinase stromelysin-1 by TIMP-1. Nature 1997;389(6646):77-81.

3. Fernandez-Catalan C, Bode W, Huber R, Turk D, Calvete JJ, Lichte A, *et al.* Crystal structure of the complex formed by the membrane type 1-matrix metalloproteinase with the tissue inhibitor of metalloproteinases-2, the soluble progelatinase A receptor. Embo J 1998;17(17):5238-48.

4. Muskett FW, Frenkiel TA, Feeney J, Freedman RB, Carr MD, Williamson RA. High resolution structure of the N-terminal domain of tissue inhibitor of metalloproteinases-2 and characterization of its interaction site with matrix metalloproteinase-3. J Biol Chem 1998;273(34):21736-43.

5. Tuuttila A, Morgunova E, Bergmann U, Lindqvist Y, Maskos K, Fernandez-Catalan C, *et al.* Three-dimensional structure of human

tissue inhibitor of metalloproteinases-2 at 2.1 A resolution. J Mol Biol 1998;284(4):1133-40.

6. Wu B, Arumugam S, Gao G, Lee GI, Semenchenko V, Huang W, *et al.* NMR structure of tissue inhibitor of metalloproteinases-1 implicates localized induced fit in recognition of matrix metalloproteinases. Journal of Molecular Biology 2000;295(2):257-68.

7. Pohar N, Godenschwege TA, Buchner E. Invertebrate tissue inhibitor of metalloproteinase: structure and nested gene organization within the synapsin locus is conserved from Drosophila to human. Genomics 1999;57(2):293-6.

8. Wada K, Sato H, Kinoh H, Kajita M, Yamamoto H, Seiki M. Cloning of three Caenorhabditis elegans genes potentially encoding novel matrix metalloproteinases. Gene 1998;211(1):57-62.

9. Greene J, Wang M, Liu YE, Raymond LA, Rosen C, Shi YE. Molecular cloning and characterization of human tissue inhibitor of metalloproteinase 4. J Biol Chem 1996;271(48):30375-80.

10. Leco KJ, Apte SS, Taniguchi GT, Hawkes SP, Khokha R, Schultz GA, *et al.* Murine tissue inhibitor of metalloproteinases-4 (Timp-4): cDNA isolation and expression in adult mouse tissues. FEBS Lett 1997;401(2-3):213-7.

11. Woessner JFJ. Matrix Metalloproteinases and Their Inhibitors in Connective Tissue Remodeling. FASEB J. 1991;5, May:2145-2154.

12. Williamson RA, Marston FA, Angal S, Koklitis P, Panico M, Morris HR, *et al.* Disulphide bond assignment in human tissue inhibitor of metalloproteinases (TIMP). Biochem.J. 1990;268:267-274.

13. Coulombe B, Skup D. In vitro synthesis of the active tissue inhibitor of metalloproteinases encoded by a complementary DNA from virus-infected murine fibroblasts. J Biol Chem 1988;263(3):1439-43.

14. Murphy G, Houbrechts A, Cockett MI, Williamson RA, O'Shea M, Docherty AJ. The N-terminal domain of tissue inhibitor of metalloproteinases retains metalloproteinase inhibitory activity [published erratum appears in Biochemistry 1991 Oct 22;30(42):10362]. Biochemistry 1991;30:8097-8102.

15. DeClerck YA, Yean TD, Lee Y, Tomich JM, Langley KE. Characterization of the functional domain of tissue inhibitor of metalloproteinases-2 (TIMP-2). Biochem.J. 1993;289:65-69.

16. Willenbrock F, Crabbe T, Slocombe PM, Sutton CW, Docherty AJ, Cockett MI, *et al.* The activity of the tissue inhibitors of metalloproteinases is regulated by C-terminal domain interactions: a kinetic analysis of the inhibition of gelatinase A. Biochemistry 1993;32:4330-4337.

17. Nguyen Q, Willenbrock F, Cockett MI, O'Shea M, Docherty AJ, Murphy G. Different domain interactions are involved in the binding of

tissue inhibitors of metalloproteinases to stromelysin-1 and gelatinase A. Biochemistry 1994;33:2089-2095.

18. Howard EW, Banda MJ. Binding of tissue inhibitor of metalloproteinases 2 to two distinct sites on human 72-kDa gelatinase. Identification of a stabilization site. J.Biol.Chem. 1991;266:17972-17977.

19. Kleiner DEJ, Unsworth EJ, Krutzsch HC, Stetler-Stevenson WG. Higher-order complex formation between the 72-kilodalton type IV collagenase and tissue inhibitor of metalloproteinases-2. Biochemistry 1992;31:1665-1672.

20. Kishi J, Hayakawa T. Purification and characterization of bovine dental pulp collagenase inhibitor. Journal of Biochemistry 1984;96(2):395-404.

21. Kishnani N. Characterization of Tissue Inhibitor of Metalloproteinases-3 (TIMP-3) from the Extracellular Matrices of Cultured Human and Avian Cells [Ph.D.]. San Francisco: University of California San Francisco; 1994.

22. Zhang J, Madden TL. PowerBLAST: a new network BLAST application for interactive or automated sequence analysis and annotation. Genome Res 1997;7(6):649-56.

23. Pegg SC, Babbitt PC. Shotgun: getting more from sequence similarity searches. Bioinformatics 1999;15(9):729-40.

24. Smith RF, Wiese BA, Wojzynski MK, Davison DB, Worley KC. BCM Search Launcher--an integrated interface to molecular biology data base search and analysis services available on the World Wide Web. Genome Research 1996;6(5):454-62.

25. Thompson JD, Higgins DG, Gibson TJ. CLUSTAL W: improving the sensitivity of progressive multiple sequence alignment through sequence weighting, position-specific gap penalties and weight matrix choice. Nucleic Acids Research 1994;22(22):4673-80.

26. Smith RF, Smith TF. Pattern-induced multi-sequence alignment (PIMA) algorithm employing secondary structure-dependent gap penalties for use in comparative protein modelling. Protein Engineering 1992;5(1):35-41.

27. Ferrin TE, Huang CC, Jarvis LE, Langridge R. The MIDAS Display System. J. Mol. Graphics 1988;6(1):13-27,36-37.

28. Huang CC, Pettersen EF, T.E. Klein TE, Ferrin TE, Langridge R. Conic: A Fast Renderer for Space-Filling Molecules with Shadows. J. Mol. Graphics 1991;9(4):230-236.

29. Mulloy B, Forster MJ, Jones C, Davies DB. N.m.r. and molecular-modelling studies of the solution conformation of heparin. Biochemical Journal 1993;293(Pt 3)(5):849-58.

30. Cardin AD, Demeter DA, Weintraub HJ, Jackson RL. Molecular design and modeling of protein-heparin interactions. Methods in Enzymology 1991;203(1):556-83.

31. Ogura K, Nagata K, Hatanaka H, Habuchi H, Kimata K, Tate S, *et al.* Solution structure of human acidic fibroblast growth factor and interaction with heparin-derived hexasaccharide. Journal of Biomolecular Nmr 1999;13(1):11-24.

32. Pye DA, Gallagher JT. Monomer complexes of basic fibroblast growth factor and heparan sulfate oligosaccharides are the minimal functional unit for cell activation. Journal of Biological Chemistry 1999;274(19):13456-61.

33. Margalit H, Fischer N, Ben-Sasson SA. Comparative analysis of structurally defined heparin binding sequences reveals a distinct spatial distribution of basic residues. Journal of Biological Chemistry 1993;268(26):19228-31.

34. Mulloy B, Forster MJ, Jones C, Drake AF, Johnson EA, Davies DB. The effect of variation of substitution on the solution conformation of heparin: a spectroscopic and molecular modelling study. Carbohydrate Research 1994;255(3):1-26.

35. Bode W, Fernandez-Catalan C, Grams F, Gomis-Reuth FX, Nagase H, Tschesche H, *et al.* Insights into MMP-TIMP interactions. Annals of the New York Academy of Sciences 1999;878:73-91.

36. Huang W, Meng Q, Suzuki K, Nagase H, Brew K. Mutational study of the amino-terminal domain of human tissue inhibitor of metalloproteinases 1 (TIMP-1) locates an inhibitory region for matrix metalloproteinases. J Biol Chem 1997;272(35):22086-91.

37. Bode W, Fernandez-Catalan C, Tschesche H, Grams F, Nagase H, Maskos K. Structural properties of matrix metalloproteinases. Cellular and Molecular Life Sciences 1999;55(4):639-52.

38. Butler GS, Apte SS, Willenbrock F, Murphy G. Human tissue inhibitor of metalloproteinases 3 interacts with both the N- and C-terminal domains of gelatinases A and B. Regulation by polyanions. Journal of Biological Chemistry 1999;274(16):10846-51.

39. Overall CM, King AE, Sam DK, Ong AD, Lau TT, Wallon UM, *et al.* Identification of the tissue inhibitor of metalloproteinases-2 (TIMP-2) binding site on the hemopexin carboxyl domain of human gelatinase A by site-directed mutagenesis. The hierarchical role in binding TIMP-2 of the unique cationic clusters of hemopexin modules III and IV. J Biol Chem 1999;274(7):4421-9.

40. Butler GS, Butler MJ, Atkinson SJ, Will H, Tamura T, van Westrum SS, *et al.* The TIMP2 membrane type 1 metalloproteinase "receptor" regulates the concentration and efficient activation of progelatinase A. A kinetic study. J Biol Chem 1998;273(2):871-80.

41. Cao J, Sato H, Takino T, Seiki M. The C-terminal region of membrane type matrix metalloproteinase is a functional transmembrane domain required for pro-gelatinase A activation. J.Biol.Chem. 1995;270:801-805.

Chapter 3

Construction and Expression of the Wild-Type and Chimeric TIMPs

3.1 Introduction

In the previous chapter, using sequence analysis and molecular modeling, it was hypothesized that the first basic region, Region I, of TIMP-3 binds to heparan sulfate and thereby localizes the protein to the ECM. The region is composed of a linear sequence of amino acids that forms two beta sheets separated by a short loop. In order to test the hypothesis *in vitro*, a chimera of TIMP-2 and TIMP-3 was made by exchanging this linear sequence of TIMP-3 with the homologous linear sequence of TIMP-2, highlighted in Figure 3.1. The reverse chimera was constructed to determine if incorporating the basic region, Region I (Val23-His60), of TIMP-3 into the TIMP-2 structure would be sufficient to convert it to an ECM-binding protein. As stated in the previous chapter, because both TIMP-1 and TIMP-2 have very similar tertiary structures with the six conserved disulfides and because TIMP activity is dependent on the tertiary structure, it is assumed that TIMP-3 and the chimeras would exhibit a similar folded tertiary structure (1-5).

```
human2 CSCSPVHPQQ AFCNADVVIR AKAVEKEEVD SGNDIYGNPI KRIQYEIKQI KMFKGPEK-- ---DIEFIYT
human3 CTCSPSHPQD AFCNSDIVIR AKVVGKKLVK EG------PF GTLVYTIKQM KMYRGFTK-- -MPHVQYIHT

human2 APSSAVCGVS LDVGG-KKEY LIAGKAEGDG KMHITLCDFI VPWDTLSTTQ KKSLNHRYQM GC-ECKITRC
human3 EASESLCGLK LEVN--KYQY LLTGRVY-DG KMYTGLCNFV ERWDQLTLSQ RKGLNYRYHL GC-NCKIKSC

human2 PMIPCYISSP DECLWMDWVT EKNINGHQAK FFACIKRSDG SCAW--YRGA APPKQEFLDI EDP
human3 YYLPCFVTSK NECLWTDMLS NFGYPGYQSK HYACIRQKGG YCSW--YRGW APPDKSIINA TDP
```

Figure 3.1: Alignment of huTIMP-2 and huTIMP-3 showing the sequences that were exchanged highlighted in yellow.

The chimeras were constructed utilizing the TIMP-2 sequence because the tertiary structure of the N-terminal domain of TIMP-2 was solved, it is constitutively expressed, and, unlike TIMP-1, TIMP-2 is not glycosylated. In addition, a comparison of the amino acids of the TIMP-2 and TIMP-3 sequences, demonstrates that an exchange of the beta sheets should result in predominantly similar or identical amino acid interactions with the core of the protein that should not disrupt the structure. Although TIMP-4 is also found in the conditioned media in cell culture, it was only recently discovered and, therefore, not as well characterized as TIMP-2.

The alignment of human TIMP-2 and TIMP-3, Figure 3.1, diagrams the regions that were exchanged between the two proteins. Val23 to His60 of TIMP-3 were replaced with Ala23 to Tyr64 from TIMP-2 to construct a TIMP-3/TIMP-2 chimera, designated C3, and the reverse exchange was made for TIMP-2 to construct a TIMP-2/TIMP-3 chimera designated C2.

The cDNAs for the chimeras were constructed by using the polymerase chain reaction (PCR) with overlapping primers. The flow diagram on the following page illustrates the process for cloning and expression of the wild-type and chimeric TIMPs, Figure 3.2. Initially, the PCR products were placed into a PCR product-cloning vector

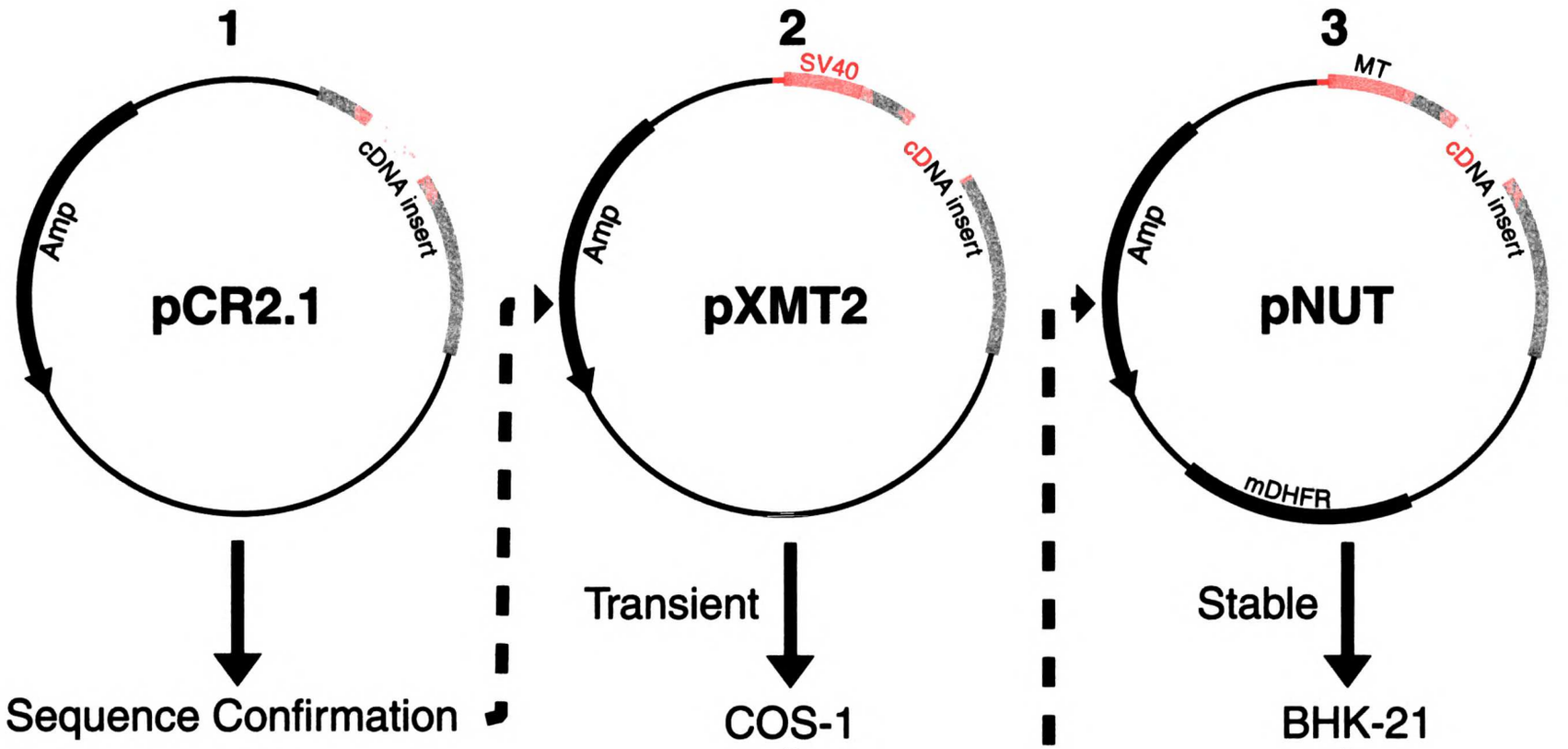

Figure 3.2. Flow diagram for cloning and expression of the wild-type and chimeric TIMPs. 1-Cloning and sequence confirmation in pCR2.1 vector. 2-Transient expression with the pXMT2 vector in COS-1 cells and analysis by reverse zymography for TIMP activity. 3-Stable transfection of BHK-21 cells with the pNUT vector and analysis by reverse zymography for TIMP activity and Western blots for confirmation of protein epitopes.

pCR2.1, to confirm the chimera sequences by fluorescent DNA sequencing. To test for functional activity, the cDNAs were transferred from pCR2.1 into the pXMT2 vector (SV40 promoter) for transient transfection in COS-1, *Cercopithecus aethiops* (African green monkey, SV40-transformed kidney fibroblasts). MMP inhibitory activity and relative protein size was determined by reverse zymography, a SDS-polyacrylamide substrate gel for detecting TIMP activity. Standard SDS-polyacrylamide gel electrophoresis (SDS-PAGE) was performed in parallel to distinguish TIMP activity from high protein expression. When the proteins were confirmed to have activity in the pXMT2/COS-1 system, the cDNAs were transferred into the pNUT vector (metallothionein promoter, methotrexate selection) for stable transfection in BHK-21, *Mesocricetus auratus* (Syrian golden hamster, normal kidney fibroblasts). The pNUT vector contains a mutated dihydrofolate reductase gene under control of the SV40 early promoter for selection. It encodes an altered enzyme with decreased affinity for the competitive inhibitor methotrexate, in comparison to the wild-type protein (6). The cDNA insert is under the control of the mouse metallothionein promoter that is inducible by zinc. Investigators have reported protein expression from pNUT transfected BHK-21 cells as high as 125 mg/L of recombinant protein in culture medium when induced with $ZnSO_4$ (7, 8). These expression levels should provide a

significant quantity of wild-type and chimeric TIMPs for purification and characterization. The ECM and conditioned media samples from the transfected cells were collected and analyzed by reverse zymography and gelatin zymography, a SDS-PAGE substrate gel for gelatinase activity. Wild-type and chimeric protein epitopes were confirmed by Western blots.

3.2 Materials and Methods

3.2.1 ***Construction of the chimeras by PCR*** – The C3 chimera was constructed using a three-step PCR process, Figure 3.3, replacing bases 136-249, Val23 to His60, of the TIMP-3 sequence with bases 145-260, Ala23 to Tyr64, of the TIMP-2 sequence.

Step 1: The first step consisted of three separate polymerase chain reactions, using overlapping primers (see Table 3.1) to create three sections, the N-terminal section that includes the signal peptide, PCR-1 in Figure 3.3, the middle section, PCR-2, and the C-terminal section, PCR-3.

PCR-1: N-terminal section: The N-terminal section was constructed by amplifying the first 135 bases of the 5′ end of TIMP-3 and 16 bases at the 3′ end of the sequence to overlap the exchanged TIMP-2 region.

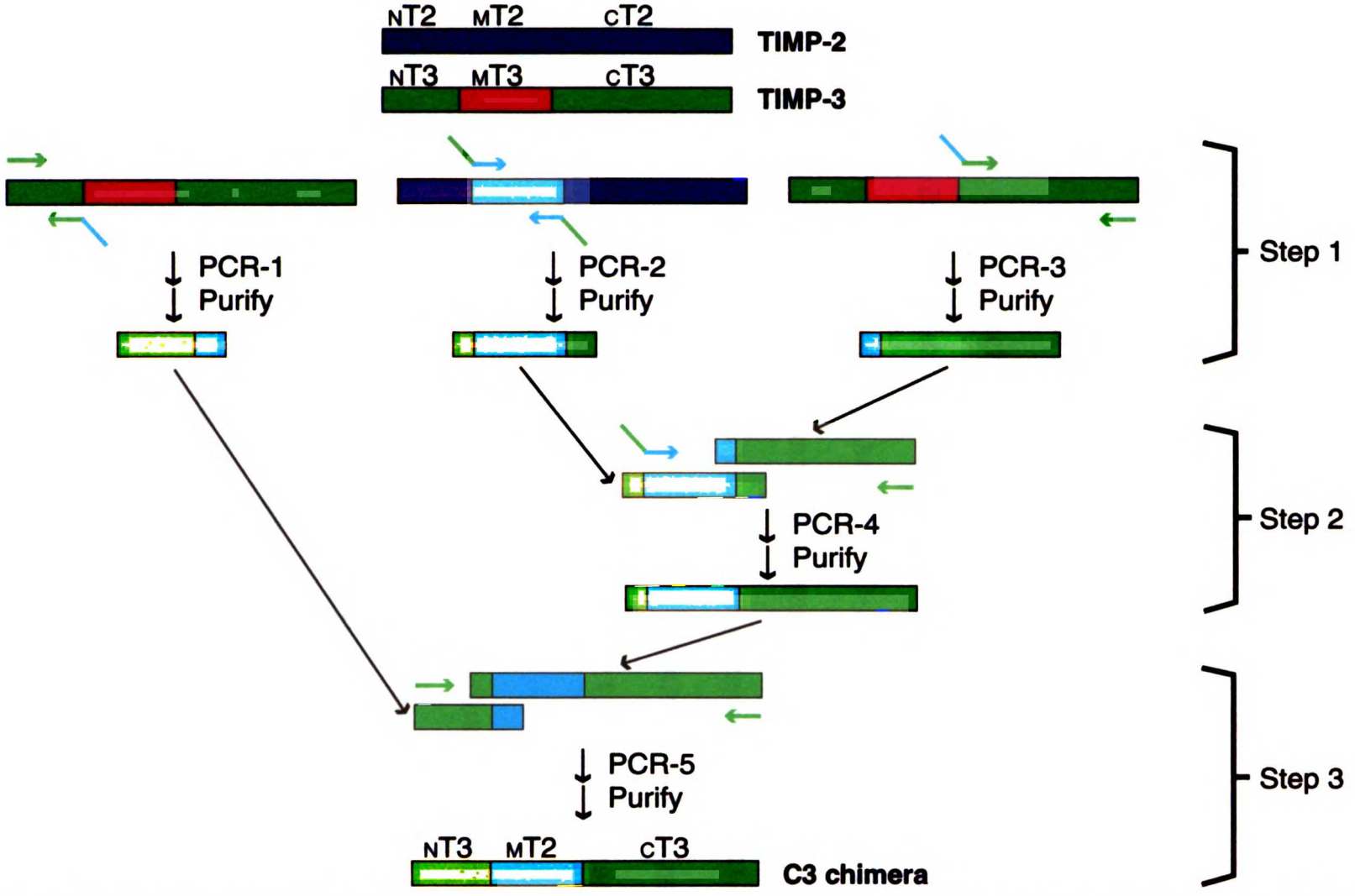

Figure 3.3: Schematic of 3-step PCR for chimera construction. Step 1 - PCR of N-terminus of C3 chimera, PCR of midsection of C3 chimera and PCR of C-terminus of C3 chimera. Step 2 - PCR to connect the midsection to the C-terminus. Step 3 - PCR to connect the N-terminus to the midsection/C-terminus.

This was accomplished by utilizing the TIMP-3 cDNA as the template and the forward NT3 and reverse NT3-MT2 primers. The *Xho*I restriction site was retained for ligation into the pXMT2 vector. An *Xma*I restriction site was created upstream of the ATG start codon of the TIMP-3 sequence for ligation into the pNUT vectors.

PCR-2: Middle section - The middle section was constructed by amplifying bases 140-260 of TIMP-2 with an additional 20 and 17 bases to overlap the TIMP-3 sequence at the 5′ and 3′ ends, respectively. This was accomplished by utilizing TIMP-2 cDNA as the template and the forward NT3-MT2 and reverse MT2-CT3 primers.

PCR-3: C-terminal section: The C-terminal section was constructed by amplifying the last 382 bases of TIMP-3 adding 18 bases at the 5′ end to overlap the TIMP-2 sequence. *Eco*RI and *Xma*I restriction sites were added downstream from the 3′ end of the coding region for ligation into the pXMT2 and pNUT vectors, respectively. This was accomplished by utilizing

TIMP-3 cDNA as the template and the forward MT2-CT3 and the reverse CT3 primers.

Step 2: The second step involved linking the middle section, PCR-2 product, to the C-terminal section, PCR-3 product, to synthesize the middle section of TIMP-2 with the TIMP-3 C-terminus. This was accomplished by utilizing the purified products of PCR-2 and PCR-3 and the forward NT3-MT2 and reverse CT3 primers. The PCR-2 and PCR-3 products acted as both templates and primers in this reaction.

Step 3: Finally, the N-terminal section from PCR-1 and the product from Step 2 were linked by PCR to create the final product, the C3 chimera cDNA. This was accomplished by using the purified products from PCR-1 and PCR-4 and the forward NT3 and reverse CT3 primers. The PCR-1 and PCR-4 products acted as both templates and primers in this reaction.

The C2 chimera, TIMP-2/TIMP-3, was constructed utilizing a similar three-step procedure replacing bases 145-273, Ala23 to Tyr64, of the TIMP-2 sequence with bases 136-252, Val23 to His60, of the TIMP-3 sequence. Primers for these reactions are shown in Table 3.2.

The cDNAs for wild-type TIMP-2 and TIMP-3 were amplified by PCR using the respective forward and reverse primers from Tables 3.1 and 3.2. As in the chimera constructs, the primers were designed to

incorporate *Xho*I and *Xma*I restriction sites upstream of the 5′ ends and *EcoR*I and *Xma*I restriction sites downstream of the 3′ ends for ligation into the pXMT2 and pNUT vectors, respectively.

The TIMP-3 template cDNA was obtained by restriction digestion of pBShTIMP-3 with *Xho*I and *Xba*I (Promega Corp.). The TIMP-2 template cDNA was obtained by restriction digestion of pBShTIMP-2 with *EcoR*I and *Not*I (Promega Corp.). Professor Dylan Edward at the University of East Anglia, UK provided the pBShTIMP-3 and pBShTIMP-2 vectors. The respective cDNA templates were purified from the vectors by agarose gel electrophoresis and the US Bioclean DNA purification kit (US Biochemicals).

Overlapping primers were designed to incorporate approximately 50% of the bases from the TIMP-3 and 50% from TIMP-2. All primers were synthesized and purified by reverse phase liquid chromatography by the UCSF Biomolecular Resource Center.

Table 3.1: Primers for the C3 chimera

Primer name	Primer sequence	Tm
Forward N-T3	5′AAACTCGAGCCCGGGCAATGACCCCTT 3′	64
Reverse NT3-	5′CCTTCTCACTGACCGCCTTGGCCCTGATCACGATG 3′	70
Forward NT3-	5′CATCGTGATCAGGGCCAAGGCGGTCAGTGAGAAG	70
Reverse MT2-	5′CTCTCGGAAGCTTCCGTGTAGATAAACTCTATAT	63
Forward MT2-	5′GATATAGAGTTTATCTACACGGAAGCTTCCGAGA	63
Reverse CT3	5′ACTAGTGAATTCCCCGGGTCAGGGGTCT 3′	64

N = N-terminus M = midsection C = C-terminus

Table 3.2: Primers for the C2 chimera

Primer name	Primer sequence	Tm
Forward N-T2	5'CTCGAGCCCGGGATGGGCGCCG 3'	68
Reverse NT2-	5'CTTCTTCCCCACCACTTTGGCCCTGATCACTAC	67
Forward NT2-	5'GTGATCAGGGCCAAAGTGGTGGGGAAGAAG 3'	66
Reverse MT3-	5'TGCCGAGGAGGGGGCCGTATGGATGTACTGCAC	71
Forward MT3-	5'GTGCAGTACATCCATACGGCCCCCTCCTCGGC	71
Reverse C-T2	5'TTTTGAATTCCCGGGTTATGGGTCCTC 3'	60

N = N-terminus M = midsection C = C-terminus

Table 3.3: Additional primers for C2cT3, T3cT2 and C3-L chimeras

Primer name	Primer sequence	Tm
Forward T3 tail for C2cT3	5'TGGTACCGCGGCGCGGCCCCCCCGGATAAA 3'	78
Forward T2 tail for T3cT2	5'ACTAGTGAATTCCCCGGGTCAGGGGTCT 3'	80
Forward primer for C3-L	5'AAGGAAGTGGACTCTGGACCTATCAAGAGGATCCAGTAT 3'	67
Reverse primer for C3-L	5'GATCCTCTTGATAGGTCCAGAGTCCACTTCCTTCTCACT 3'	68

The polymerase chain reactions were performed in a MJ Research Model 2100 Peltier thermocycler using *Pfu* DNA polymerase (Stratagene) and dNTPs (Amersham Pharmacia Biotech). Each reaction consisted of 5 cycles of heating at 94 °C for 1 min, annealing at 50 °C for 1 min, and polymerization at 74 °C for 1 min, and 30 cycles of heating 94 °C for 1 min, annealing at 55°C for 1 min, and polymerization at 74 °C for 1 min. The PCR products were purified by agarose gel electrophoresis and the US BioClean DNA purification kit (US Biochemicals) or the DNA purification kit (Qiagen Inc.). Agarose concentration ranged from 0.7% to 1.2% depending on expected product size.

3.2.2 ***Cloning and sequence confirmation*** - The C3 chimera and the TIMP-3 PCR products were ligated into the pCR2.1 TA cloning vector (Invitrogen Corp.). The C2 chimera and TIMP-2 PCR products were ligated into the pCRBlunt TA cloning vector (Invitrogen Corp.)

utilizing the Rapid DNA Ligation Kit (Boehringer-Mannheim Biochemicals). The pCR2.1 and pCRBlunt vectors were transformed into *Escherichia coli*, One Shot Top10 Competent Cells (Invitrogen Corp.), for cloning and selection. Several clones were selected by plating on 50 µg/ml ampicillin (Sigma Chemical Co.), Luria broth (LB) agar plates for the pCR2.1 clones and 50 µg/ml kanamycin (Sigma Chemical Co.), LB agar plates for the pCRBlunt clones and grown at 37 °C for 16 h. Several colonies were selected from the pCR2.1 and pCRBlunt clones and grown in 50 µg/ml ampicillin or 50 µg/ml kanamycin, respectively, in LB for 16 h at 37 °C at 225 rpm in a rotary shaking incubator. The plasmid DNA was purified from an aliquot of each culture using the Qiaprep 8 DNA Purification kit (Qiagen Inc.). Purified plasmid DNA was restriction digested with *Xho*I and *EcoR*I (Promega Corp.) and analyzed by agarose gel electrophoresis (1.2% agarose (Sigma Chemical Co.)) to determine base pair, bp, sizes. Clones were selected based on cDNA insert size from the restriction digests. The inserted cDNA sequences of selected clones were confirmed using automated fluorescent sequencing by the UCSF Biomolecular Resource Center.

3.2.3 *Transient expression in COS-1 cells for activity confirmation* - For transient transfection in COS-1 cells, cDNAs for the wild-type and chimeric proteins were ligated into the *Xho*I and

*EcoR*I sites of the pXMT2 expression vector (provided by Dylan Edward's Lab at the University of East Aglia, UK). The pXMT2 plasmids were transfected into *E. coli*, Subclone Efficiency DH5α competent cells (GibcoBRL) for subcloning and selection by plating on 50 µg/ml ampicillin LB agar plates grown at 37 °C for 16 h. Several colonies were selected and grown in 50 µg/ml ampicillin in LB for 16 h at 37 °C at 225 rpm in a rotary shaking incubator. The plasmid DNA was purified from an aliquot of each culture using the Qiaprep 8 DNA Purification kit (Qiagen Inc.). Purified plasmid DNA was restriction digested with *Xho*I and *EcoR*I (Promega Corp.) and analyzed by agarose gel electrophoresis (1.2% agarose) to determine base pair size. Clones were selected based on cDNA insert size from the restriction digests. Larger volumes of plasmid DNA were obtained by purifying the plasmid DNA from 250-500 ml of *E. coli* utilizing the Maxiprep DNA Purification kit (Promega Corp.).

The pXMT2 vectors were transiently transfected into COS-1 cells (ATCC) using the calcium phosphate method of Chen and Okayama (9) in 10% FBS (fetal bovine serum) (Sigma Chemical Co.), 50/50 Dulbecco's Modified Eagles Medium/F-12, DMEM/F-12, (GibcoBRL), see below for details of the transfection. Controls without vector and with the empty pXMT2 vector were also prepared. After transfection, the cells were maintained at 37 °C, 5% CO_2 for two days before harvesting

the conditioned media and ECM, see Appendix A for conditioned media and ECM collection. Samples were stored at -20 °C before analyzing. The conditioned media and ECM samples were analyzed by electrophoresis on a 15% SDS-polyacrylamide gel and a 15% reverse zymogram, see Appendix A for SDS-PAGE and reverse zymography.

3.2.4 *Generation of stably transfected BHK-21 cell lines and expression of wild-type and chimeric proteins* — The cDNAs for the wild-type and chimeric proteins were separately subcloned into the *Xma*I (*Sma*I) site of the pNUT expression vector for stable transfection and expression in BHK-21 cells (6). The pNUT vectors were transfected into *E. coli*, Subclone Efficiency DH5α competent cells, for subcloning and selection by plating on 50 µg/ml ampicillin LB agar plates grown at 37 °C for 16 h. Several colonies were selected and grown in 50 µg/ml ampicillin in LB for 16 h at 37 °C at 225 rpm in a rotary shaking incubator. The plasmid DNA was purified from an aliquot of each culture using the Qiaprep 8 DNA Purification kit. Clones were analyzed for correct insert size and orientation by restriction digest by *Xma*I and *Kpn*I, respectively, and agarose gel electrophoresis utilizing 0.8% agarose gels.

The pNUT clones were transfected into the BHK-21 cells utilizing the method described by Chen and Okayama in 5% FBS (Sigma Chemical Co.), 50/50 DMEM/F-12 (GibcoBRL), see below for transfection details

(9). Controls without vector and with the empty pNUT vector were also prepared. After the transfection, cells were maintained at 37 °C, 5% CO_2 for 48 h before passaging at a 1:10 split ratio into medium containing 500μM methotrexate (Calbiochem) in 5% FBS (Sigma Chemical Co.), 50/50 DMEM/F-12 (GibcoBRL). The ECM and conditioned media were collected as described in Appendix A-1.

3.2.5 ***Tansfection of COS-1 and BHK-21 cells*** – The following method is an adaptation of the procedure described by Chen and Okayama (9). Cells were seeded at 6.5 x 10^5 cells/dish and maintained in the respective growth media as described in the cell maintenance section at 37 °C and 5% CO_2. After 24 h of growth and 1 h prior to transfection, the medium was replaced with fresh medium. TE buffer (10 mM Tris(hydroxymethyl) aminomethane (US Biochemicals) pH 8.0, 1.0 mM EDTA (ethylenediaminetetraacetic acid) (Sigma Chemical Co.)) was added to 18 μg of vector DNA to a total volume of 900 μl. This was followed by the addition of 100 μl of 2.5M $CaCl_2$ (Sigma Chemical Co.) and mixed. BES saline (50 mM N,N-bis(2-hydroxyethyl)-2-aminoethanesulfonic acid (Sigma Chemical Co.), 280 mM NaCl (Fisher Scientific), pH 6.95) was slowly added dropwise (1 ml total volume of BES saline), with vortexing to mix between drops. The mixture was incubated for 20 min at room temperature. Half of the DNA mixture (1 ml) was added dropwise to each of two

dishes of cells while gently rotating. The cells were incubated at 37 °C and 3% CO_2. After 16-18 h, medium was replaced with fresh medium and the dishes were transferred to 37 °C, 5% CO_2.

3.2.6 ***Maintenance of COS-1 cells prior to transfection*** – The COS-1 cells (American Type Culture Collection) were seeded at 6.5 x 10^5 cells/100mm dish (Corning Costar) and maintained in 50/50 DMEM/F-12 (Gibco BRL) containing 10% (vol./vol.) FBS (Sigma Chemical Co.) at 37 °C under 5% CO_2. Cells were passaged by aspirating the media, washing with 1 ml of PBS-CMF (phosphate-buffered saline, calcium and magnesium free) adding 1ml 0.25% trypsin/0.02% EDTA (Sigma Chemical Co.), aspirating the excess trypsin/EDTA and incubating at 37 °C, 5% CO_2 for 5 min. The cells were removed by gentle washing with an appropriate amount of medium to be subcultured at a 1:10 split ratio every 5 days.

3.2.7 ***Maintenance of BHK-21 cells*** - The BHK-21 cells were seeded at a density of 6.5 x 10^5 cells/100mm dish (Corning Corp.) in 10 ml of 50/50 DMEM/F-12 (Gibco BRL) containing 5% (vol./vol.) FBS (Sigma Chemical Co.) at 37 °C under 5% CO_2. Cells were passaged by aspirating the media, washing with 1 ml of PBS-CMF, adding 1ml 0.25% trypsin/0.02% EDTA, aspirating the excess trypsin/EDTA and incubating at 37 °C, 5% CO_2 for 5 min. The cells were removed by gentle washing with an appropriate amount of medium to be

subcultured at a 1:20 split ratio every 3-4 days. Every fourth passage 500 μM methotrexate in 5% FBS, DMEM/F-12 selection was reapplied in order to maintain stable, high-level expression.

3.2.8 ***Induction of stably transfected BHK-21 cells*** - The stably transfected BHK-21 cells were seeded at a density of 6.5 x 10^5 cells/100mm dish (Corning Corp.) in 10 ml of 50/50 DMEM/F-12 (Gibco BRL) containing 5% (vol./vol.) FBS (Sigma Chemical Co.) at 37 °C, 5% CO_2. After another 24 h and when the cells were approximately 70-80% confluent, the medium was exchanged with fresh medium containing 80μM $ZnSO_4$. After 24 h, the conditioned medium was removed and filtered through a 0.2 μm polyethersulfone, PES, filter (Millipore Corp.). A 500 μl aliquot of the filtered conditioned medium was added to 2X Laemmli sample buffer without reducing agent, see reverse zymogram method in Appendix A-2. All samples including the ECM were stored at −20 °C prior to analysis by reverse zymography and Western blots.

3.2.9 ***Western Blots*** - Reduced samples were loaded in duplicate and electrophoresed in a 17% SDS-polyacrylamide gel utilizing a Xcell II Mini-cell SDS-PAGE apparatus (Novex) at 180V (constant voltage) for 2.5 h. The MultiMark Multicolored standard (NOVEX) was used for molecular weight standards and for monitoring the electrophoresis. The transfer to the polyvinylidenedifluoride, PVDF, membrane (Bio-Rad

Laboratories) was performed in 10 mM CAPS (3-[cyclohexylamino]-1-propanesulfonic acid) (pH 11.0) containing 10% methanol, utilizing a Mini-trans blot cell (Biorad) at 14V (constant voltage) for 16 h at 4 °C. The membrane was blocked by immersion in 5% non-fat dry milk (Bio-Rad Laboratories) in PBS-T, phosphate buffered saline with 0.1% Tween-20 (Fisher Scientific) for 1.5 h at room temperature on a rocking platform. On a rocking platform, the membrane was washed twice with PBS-T for 5 min, once with PBS-T for 15 min at room temperature and finally washed quickly with PBS-T. The membrane was cut in two and each piece was separately probed with primary antibody: 1:2000 rabbit anti-huTIMP-2 (1^{st} loop) pAb (Chemicon International, Inc.); 1:1000 mouse anti-huTIMP-2 mAb clone 69-10B11 (Fuji Chemical Co.); 1:1000 mouse anti-huTIMP-2 (C-term) mAb clone 67-4H11 (Fuji Chemical Co.); or, 1:500 rabbit anti-chickenTIMP-3 (Hawkes' Laboratory), in PBS-T for 16 h at 4 °C. The membranes were washed separately, utilizing the same washing protocol as described above. The membranes were separately probed with 1:2000 secondary antibody – horseradish peroxidase, HRP-conjugated, donkey anti-rabbit secondary antibody (Amersham Pharmacia Biotech) or HRP-conjugated goat anti-mouse antibody (Chemicon) in PBS-T for 1.5 h at room temperature on a rocking platform. The membranes were washed separately utilizing the same

washing protocol as described above. Blots were developed using the ECL-Plus kit (Amersham Pharmacia Biotech) and Hyperfilm ECL (Amersham Pharmacia Biotech).

3.2.10 ***Analysis of pNUThuTIMP-3 BHK-21 in VP-SFM*** – The pNUThuTIMP-3 BHK-21 cells were seeded on 6-100mm tissue culture plates (Corning Corp.) at a density of 6.5 x 10^5 cells/plate in 10 ml of 50/50 DMEM/F-12 (Gibco BRL) containing 2.5% (vol./vol.) FBS (Sigma Chemical Co.) and allowed to grow for 24 h. at 37 °C under 5% CO_2. The media was removed and replaced with 10 ml of media as follows:

Plate	Replacement media
1	2.5% FBS, 50/50 DMEM/F-12
2	2.5% FBS, 50/50 DMEM/F-12 containing 80 µM $ZnSO_4$
3	5% FBS, 50/50 DMEM/F-12
4	5% FBS, 50/50 DMEM/F-12 containing 80 µM $ZnSO_4$
5	VP-SFM
6	VP-SFM containing 80 µM $ZnSO_4$

The cells were allowed to grow for another 24 hours before collecting the conditioned media for analysis by reverse zymography.

3.3 Results

3.3.1 PCR Results

The C3 chimera was constructed utilizing a three-step PCR process utilizing overlapping primers, Figure 3.3, to exchange base pairs 136-249, Val23 to His60, of the TIMP-3 sequence with base pairs 145-260, Ala23 to Tyr64, of the TIMP-2 sequence. The reverse chimera, C2, was constructed utilizing a similar three-step PCR process exchanging base pairs 145-260, Ala23 to Tyr64, of the TIMP-2 sequence with base pairs 136-249, Val23 to His60, of the TIMP-3 sequence.

Products for the first three reactions in Step 1 are shown in Figures 3.4a and 3.4b for the C3 and C2 chimeras, respectively. Base pair sizes for the intense bands in lanes 2, 3 and 4 of Figure 3.4a and lanes 3, 4, and 5 in Figure 3.4b correspond to the expected size of the products shown in parentheses in the legends. These products were purified from the gels and used in subsequent PCR as both templates and primers. Step 2 (PCR-4) was performed with the purified DNA products from PCR-2 and PCR-3 of the respective C3 and C2 chimeras. The agarose gels from these reactions are shown in Figures 3.5a and 3.5b. The DNA product of PCR-4 (expected size of 550 base pairs – Figure 3.5a, lane 4) was purified and utilized in the final reaction, PCR-5, together with the DNA product from PCR-1 (Figure 3.4a, lane 2) and

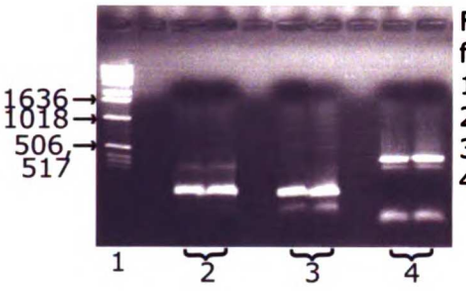

Figure 3.4a: 0.7% agarose gel of PCR products from Step 1 of the C3 chimera DNA construction.
1 - Gibco BRL 1k bp DNA std.
2 - NT3-part MT2 (169 bp) - PCR-1
3 - part NT3-MT2-part CT3 (162 bp) - PCR-2
4 - part MT2-CT3 (423 bp) - PCR-3

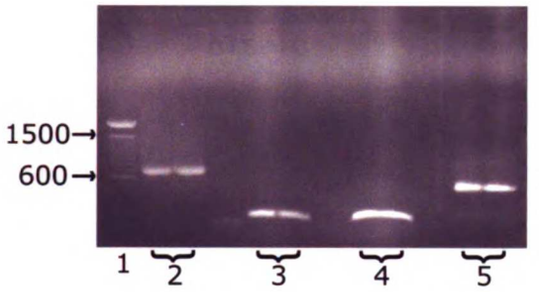

Figure 3.4b: 0.7% agarose gel of PCR products from Step 1 of the C2 chimera DNA construction.
1 - Gibco BRL 1k bp DNA ladder
2 - TIMP-2 control (690 bp)
3 - NT2-part MT3 (171 bp) - PCR-1
4 - part NT2-MT3-part CT2 (149 bp) - PCR-2
5 - part MT3-CT2 (423 bp) - PCR-3

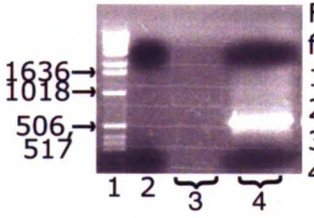

Figure 3.5a: 0.7% agarose gel of PCR products from Step 2 of the C3 chimera DNA construction.
1 - Gibco BRL 1k bp DNA std.
2 - primers and no template control
3 - blank
4 - part NT3-MT2-CT3 (550 bp) - PCR-4

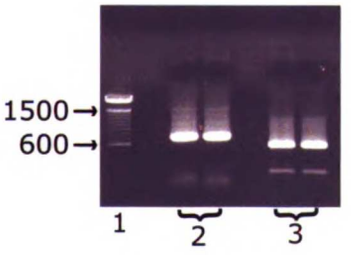

Figure 3.5b: 0.7% agarose gel of PCR products from Step 2 of the C2 chimera DNA construction.
1 - Gibco BRL 1k bp DNA ladder
2 - TIMP-2 control (690 bp)
3 - part NT2-MT3-CT2 (533 bp) - PCR-4

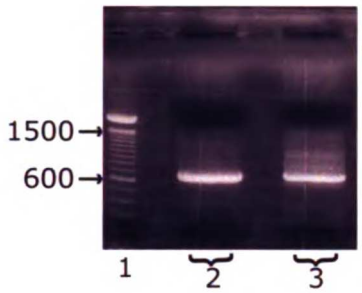

Figure 3.6a: 1% agarose gel of PCR products from Step 3 of C3 chimera DNA construction.
1 - Gibco BRL 100 bp DNA ladder
2 - huTIMP-3 (672 bp)
3 - NT3-MT2-CT3 (684 bp) - PCR-5

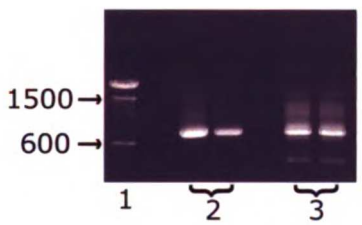

Figure 3.6b: 1% agarose gel of PCR products from Step 3 of C2 chimera DNA construction.
1 - Gibco BRL 1k bp DNA ladder
2 - TIMP-2 (690 bp)
3 - NT2-MT3-CT2 (678 bp) - PCR-5

the forward NT3 and reverse CT3 primers to create the C3 chimera. The DNA product of PCR-4 (expected size of 533 base pairs – Figure 3.5b, lane 3) was purified and utilized in the final reaction, PCR-5, together with the DNA product from PCR-1 (Figure 3.4b, lane 3) and the forward NT2 and reverse CT2 primers to create the C2 chimera. The DNA products for these final reactions are shown in Figures 3.6a and 3.6b, respectively. Again, the expected sizes (684 bp for the C3 chimera and 678 bp for the C2 chimera) are shown for the products (Figure 3.6a, lane 3, and Figure 3.6b, lane 3, respectively). The PCR products for wild-type TIMP-3 and TIMP-2 are also shown in Figures 3.6a, lane2, and 3.6b, lane 2, respectively.

3.3.2 Cloning and Sequence Confirmation of PCR Products

The final PCR products for the C3 chimera and wild-type TIMP-3 were purified from the gels and ligated into pCR2.1 vectors, a TA cloning vector for PCR products, and cloned in *E. coli* and selected for ampicillin resistance. The final PCR products for the C2 chimera and wild-type TIMP-2 were ligated into pCRBlunt vectors, another TA cloning vector for PCR products, and cloned in *E. coli* and selected for kanamycin resistance.

NOTE: The TA cloning vectors require A and T sequences at the 5′ and 3′ ends of the PCR products. The pCR2.1 vector must have sticky 5′ and 3′ ends, whereas, the pCRBlunt vector must have blunt ends.

The *Pfu* DNA polymerase was utilized for its proofreading capability for higher efficiency. This polymerase leaves blunt ends on the PCR products, whereas, *Taq* DNA polymerase creates sticky ended DNA. Therefore, an extra step utilizing *Taq* DNA polymerase was required to add A and T sticky ends to the PCR products to ligate into the PCR2.1 vector. The PCR products created with *Pfu* DNA polymerase were directly ligated into the pCRBlunt vector.

Twenty of each of the C3 chimera and TIMP-3 clones were selected and grown in overnight cultures with ampicillin. Half of each of the cultures was purified and digested with *Xho*I and *EcoR*I for characterization by restriction enzyme digest and agarose gel electrophoresis and confirmation by DNA sequencing. The expected base pair sizes for the *Xho*I and *EcoR*I restriction digests are 656 bp for TIMP-3 and 668 bp for the C3 chimera. Figures 3.7 to 3.10 show the agarose gels of the digests of the C3 chimera and TIMP-3 pCR2.1 clones. Several of the clones showed bands with the expected size, indicated by asterisks in the figures. A second enzyme, *Nar*I, was used for further confirmation. Restriction digest with *Nar*I should result in three fragments for both TIMP-3 and C3 chimera pCR2.1 vectors. The *Nar*I recognition sequence is at the 5′ end of each of the cDNA inert sequences. The pCR2.1 vector has two *Nar*I sites. The

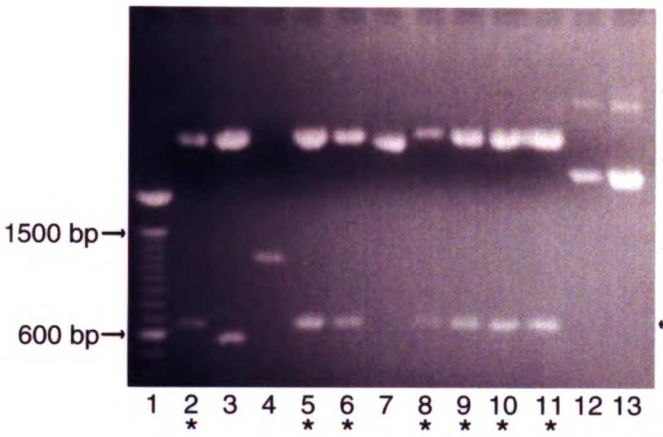

Figure 3.7: 1.0% agarose gel of *Xho*1 and *EcoR*1 restriction digest of C3 chimera pCR2.1 clones.
1 - 100 bp DNA ladder (GibcoBRL)
2-11 - Clones 1-10
12 - Clone 2 undigested
13 - Clone 1 undigested
*- Clones with expected bp size

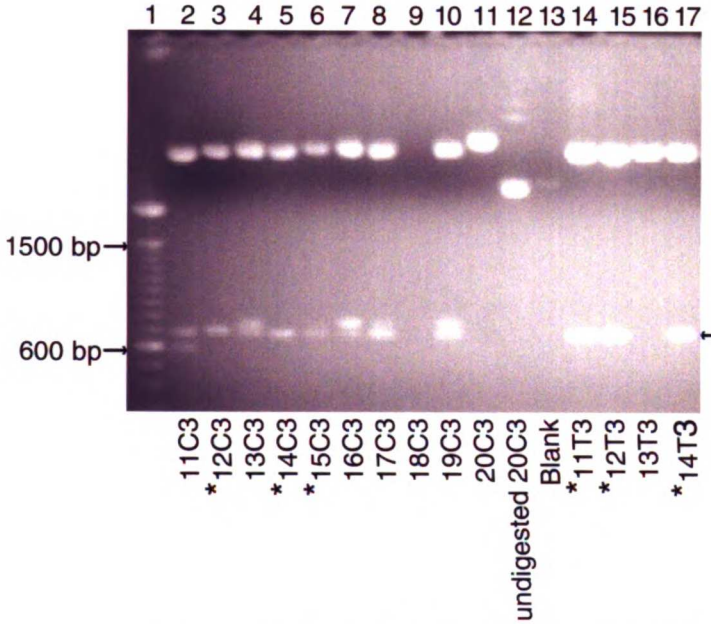

Figure 3.8: 1.0% agarose gel of *Xho*1 and *EcoR*1 restriction digest of the C3 chimera and huTIMP-3 (T3) pCR2.1 clones.
1 - 100 bp DNA ladder (GibcoBRL)
*- Clones with expected bp size

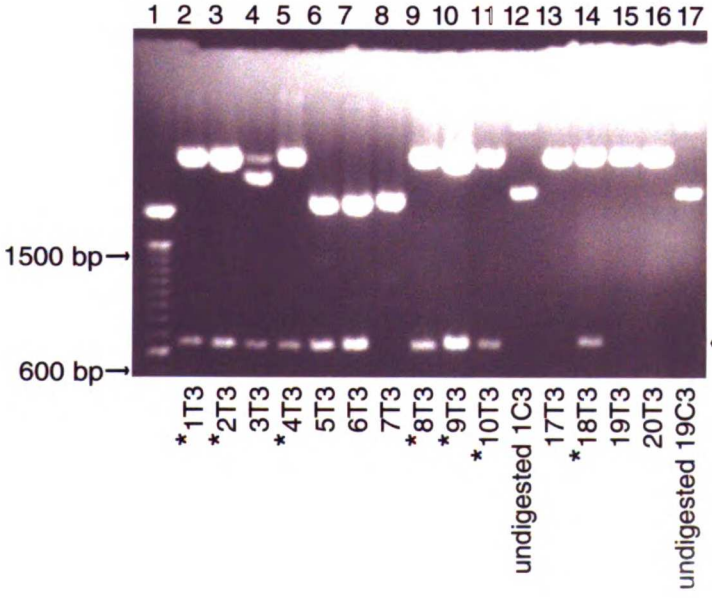

Figure 3.9: 1.0% agarose gel of *Xho*1 and *EcoR*1 restriction digest of the huTIMP-3 and C3 chimera pCR2.1 clones.
1 - 100 bp DNA ladder (GibcoBRL)
*- Clones with expected bp size

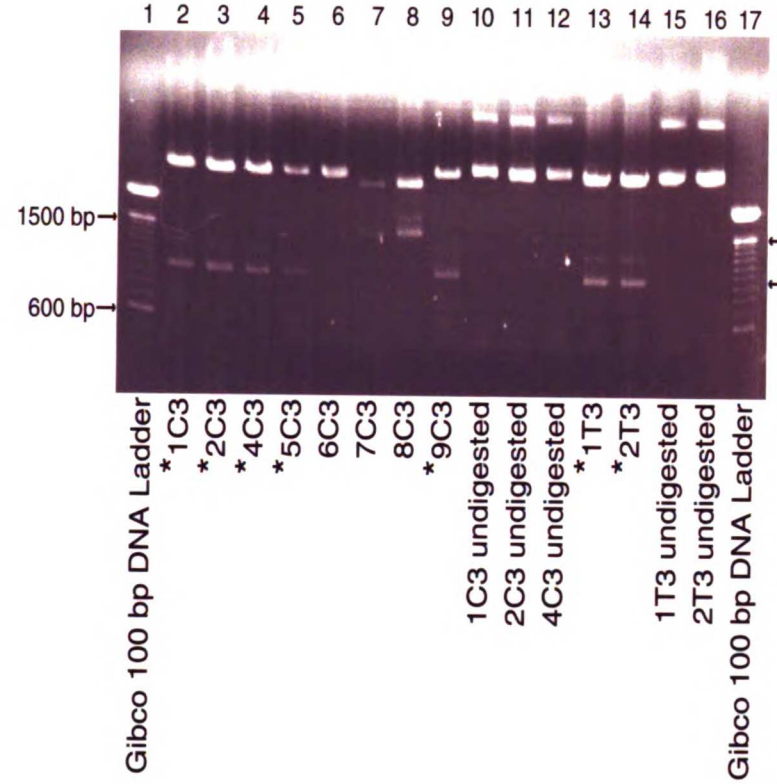

Figure 3.10: Agarose gel of *Nar*I restriction digest of the huTIMP-3 (T3) and C3 chimera pCR2.1 clones.
1, 17 - 100 bp DNA ladder
* - Clones with expected bp size.

Figure 3.11: Agarose gel of of the C2 chimera pCRBlunt clones.
1 – 100bp DNA ladder (GibcoBRL)
2-9 –Clones 1-8 undigested
10-17 – Clones 1-8 digested with *Xho*I and *EcoR*I

Figure 3.12: Agarose gel of the huTIMP-2 pCRBlunt clones
1 – 100bp DNA ladder (GibcoBRL)
2-9 –Clones 1-8 undigested
10-17 – Clones 1-8 digested with *Xho*I and *EcoR*I

insert could be ligated into the vector in either direction. Although this vector will not be used to express the protein, digestion with *Nar*I would determine which direction the insert is ligated and give further confirmation of the inserted DNA. *Nar*I digestion of the pCR2.1 clones containing the C3 chimera and TIMP-3 insert ligated in the direction of the M13 forward primer or T7 promoter would be expected to produce fragments of approximately 3440 bp, 950 bp and 248 bp. Clones with inserts ligated in the opposite direction would be digested into fragments of approximately 2910 bp , 1460 bp and 250 bp. Clones 1, 2, 4, 5, 6, 7, 8 and 9 for the C3 chimera and clones 1 and 2 for TIMP-3 were digested with *Nar*I, Figure 3.10. (Note: The smaller fragments below 300 bases are either too small to be detected or migrate from the gel. Clone 2 of C3 should not have been further characterized because it did not have the correct size when digested with *Xho*I and *EcoR*I, Figure 3.7, lane 3.) For most of these clones, the insert was in the M13 forward primer direction except for clones 7 and 8, which were in the opposite direction. All clones, except clone 2, could have been selected for DNA sequencing. Clone 2 had the correct size when digested with *Nar*I but either contained a mutation or the insert was a PCR fragment that caused it to be digested differently with *Xho*I and *EcoR*I. Clone 1 of the C3 chimera and clones 1 of TIMP-3 were

selected, confirmed by DNA sequencing and ligated into the pXMT2 vector.

*Xho*I and *EcoR*I restriction digests of pCRBlunt clones of the C2 chimera and TIMP-2 were also performed, Figures 3.11 and 3.12, respectively. All clones had the correct base pair sizes of 690 bp for TIMP-2 and 672 bp for the C2 chimera when digested with *Xho*I and *EcoR*I. *Nar*I restriction enzyme digest was not performed on these clones because it did not provide useful information. Clone 3 of the C2 chimera and clone 3 of TIMP-2 were selected and confirmed by sequencing.

3.3.3 Ligation into pXMT2 for Transient Transfection of COS-1 Cells

The cDNA inserts from the respective *Xho*I and *EcoR*I digested clones were excised from the agarose gels, purified and ligated into the *Xho*I and *EcoR*I sites of pXMT2. The pXMT2 vectors were subcloned and clones were selected. Restriction digests with *Xho*I and *EcoR*I were performed on several clones of each of the respective plasmids and analyzed by agarose gel electrophoresis for base pair size confirmation of the cDNA inserts, Figures 3.13-3.16. All clones had DNA inserts with the correct base pair size. Clone 2 was chosen for the C3 chimera, Figure 3.13, lanes 3 and 9. Clone 3 was chosen

Figure 3.13: Agarose gel of the C3 chimera pXMT2 clones.
1 – pXMT2 undigested
2-5 – Clones 1-4 undigested
6 – pXMT2 digested with *Xho*I and *EcoR*I
7 – pCR2.1 TIMP-3 digested with *Xho*I and *EcoR*I
8-17 – Clones 1-10 digested with *Xho*I and *EcoR*I

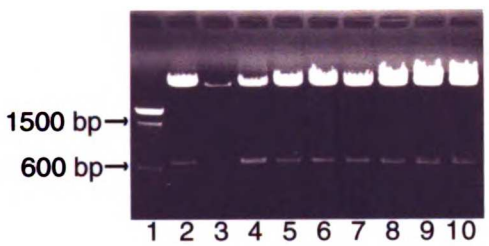

Figure 3.14: Agarose gel of the huTIMP-3 pXMT2 clones.
1 – 100bp DNA ladder (GibcoBRL)
2 – C3 chimera clone 1 digested with *Xho*I and *EcoR*I
3-10 – huTIMP-3 clones 1-8 digested with *Xho*I and *EcoR*I

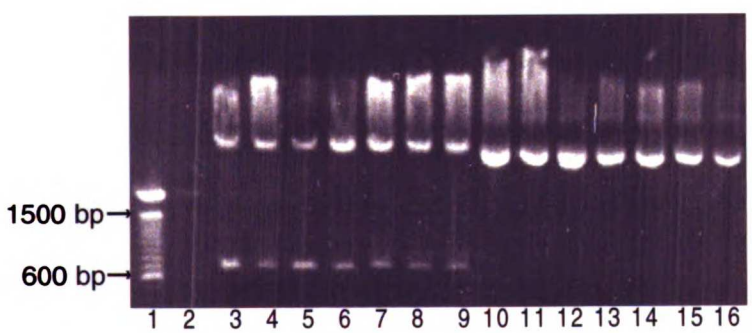

Figure 3.15: Agarose gel of the C2 chimera pXMT2 clones.
1 – 100bp DNA ladder (GibcoBRL)
2 - Blank
3-9 – Clones 1-7 digested with *Xho*I and *EcoR*I
10 – Clones 1-7 undigested

Figure 3.16: Agarose gel of the huTIMP-2 pXMT2 clones.
1 – 100bp DNA ladder (GibcoBRL)
2 - Blank
3-9 – Clones 1-7 digested with *Xho*I and *EcoR*I
10 – Clones 1-7 undigested

for TIMP-3, Figure 3.14, lane 5. Clone 1 was chosen for the C2 chimera, Figure 3.15, lanes 3 and 10. Clone 2 was chosen for TIMP-2, Figure 3.16, lanes 4 and 11. Large-scale plasmid preparations were performed with each of these clones to provide sufficient DNA for transient transfection into COS-1 cells.

The COS-1 cells were transfected with each of the pXMT2 vectors. pXMT2 without an insert and a blank transfection, no DNA, were controls. The cells were allowed to grow for 48 h after the transfection with a media change at 24 h. Analysis of the ECM and conditioned media from COS-1 controls and transfected cells by SDS-PAGE and reverse zymography is shown in Figure 3.17. The reverse zymogram, panels C and D, show TIMP activities that are not in either of the SDS-PAGE gel, panels A and B.

Table 3.4 shows the calculated molecular weights and the relative mobilities, M_r, for TIMP-1, TIMP-2, TIMP-3 and glycosylated TIMP-3 and the calculated molecular weights for the C3 and C2 chimeras.

Table 3.4: Calculated molecular weights and relative mobilities.

	MW	M_r
TIMP-1	20,708.83	~29,500
TIMP-2	21,754.80	~20,000
TIMP-3	21,689.98	~23,000
glyTIMP-3		~29,000
C3	22,170.15	
C2	21,274.64	

Note: The calculation of the MWs were made using only the amino acid sequence

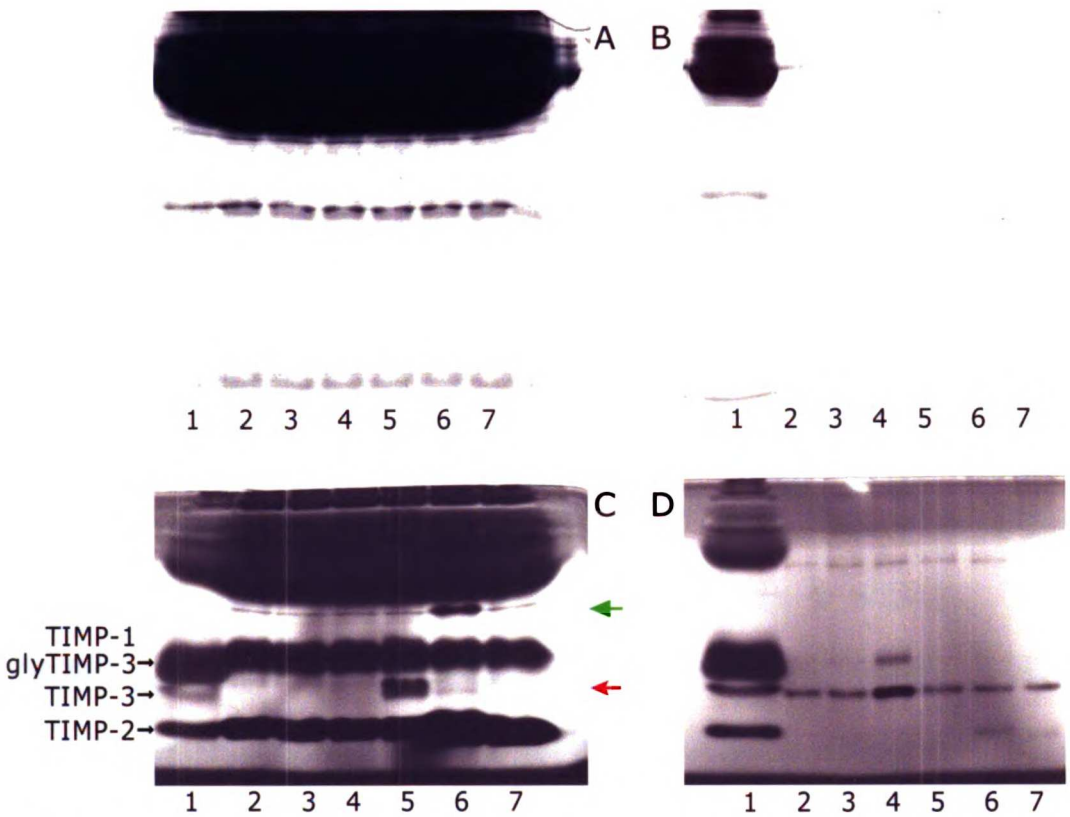

Figure 3.17: 15% SDS-PAGE of conditioned media, A, and extracellular matrix, B, and reverse zymography of conditioned media, C, and extracellular matrix, D, from transiently transfected COS-1 cells. Sample load of 40 µl for conditioned media, CM, is 1/500 of the total volume collected from each dish and 1 µl for the extracellular matrix, ECM, is 1/250 of the total volume used to extract the ECM from the dish. TIMP-1, -2 & -3 standards are from a mixture of TIMP-1 and TIMP-2 from conditioned media and TIMP-3 from extracellular matrix of pNUThuTIMP-3 BHK-21 cells. Red arrow indicates C3 chimera activity and the green arrow indicates the possible dimer of the C2 chimera.

1 - TIMP-1, -2 & -3 standards
2 - COS-1
3 - COS-1 pXMT2
4 - COS-1 pXMT2 huTIMP-3
5 - COS-1 pXMT2 C3
6 - COS-1 pXMT2 huTIMP-2
7 - COS-1 pXMT2 C2

TIMP-1 migrated with a slower mobility, M_r ~29 kDa, than the other TIMPs because of its glycosylation. Glycosylated TIMP-3 and glycosylated TIMP-1 had similar electrophoretic mobilities. Unglycosylated TIMP-3 migrates much slower than TIMP-2 even though the calculated molecular weight of TIMP-3 was 55 Daltons less than TIMP-2.

TIMP activities in conditioned media and ECM samples from the untransfected and pXMT2 transfected COS-1 cells were similar, as shown in Figure 3.17 (panels C and D, lanes 2 and 3). Each had TIMP-1 and TIMP-2 activities in the conditioned media and TIMP-3 activity in the ECM. The pXMT2huTIMP-3 transfected COS-1 cells showed similar amounts of TIMP-1 and TIMP-2 in the conditioned media (panel C, lane 4) in comparison to the conditioned media of untransfected and pXMT2 transfected cells (panel C, lanes 2 and 3) but showed an increase in activities attributed to TIMP-3 and glycosylated TIMP-3 in the ECM (compare panel C and D, lane 4). Conditioned media and ECM of pXMT2C3 transfected COS-1 cells (panel C and D, lane 5) showed similar amounts of TIMP-1, TIMP-2 and TIMP-3 activities as the controls. However, a new activity that migrated slightly slower than unglycosylated TIMP-3 was present in the conditioned media (panel C, lane 5, indicated by the red arrow). Consistent with the identification of this activity as the C3 chimera was

the fact that its theoretical molecular size is 480 Daltons more than TIMP-3. This activity was not present in the ECM (panel D, lane 5). It appears that the C3 chimera localized to the conditioned media instead of the ECM.

The conditioned media and ECM of cells transfected with pXMT2huTIMP-2 showed an increase in the level of TIMP-2 activity in the conditioned media (panel C, lane 6). Interestingly, under conditions of high level of TIMP-2 expression, an additional band was present at approximately 50 kDa. It was possible that this represented a TIMP-2 dimer, although further experimentation would be required to be certain. In addition, the low level of TIMP-2 activity detected in the ECM (panel D, lane 6), may have been due to binding to MMP-2 that is sometimes found in the ECM, although there was no evidence of MMP-2 activity as a clear band ($M_r \sim 72$ kDa) at the top of this gel.

With respect to the reverse chimera, pXMT2C2, the ECM of these transfected COS-1 cells showed a faint band of TIMP activity similar to the level of TIMP-2 in the ECM (panel D, lane 6) that migrates slightly faster than TIMP-2 (panel D, lane 7). Consistent with the identification of this activity as the C2 chimera was the fact that its theoretical molecular size is 480 Daltons less than TIMP-2. Most of this new activity was detected in the conditioned media (panel C, lane 7)

causing the TIMP-2 band to appear more intense but with a mobility slightly faster than that of TIMP-2 (panel C, lane 6).

3.3.4 Stable Transfection of BHK-21 Cells

Having established that the chimeras expressed in the COS-1 cell system displayed MMP inhibitory activity, stable transfections of BHK-21 cells utilizing the pNUT vector were performed. The BHK-21 cell system should provide sufficient wild-type TIMPs and chimeric proteins for purification and characterization. This vector has been successfully utilized by Dr. Dylan Edward's laboratory at the University of East Anglia, UK, to produce TIMP-3 and TIMP-3 mutants.

An experiment was performed to establish if the BHK-21 cells would grow in serum-free media because serum can cause interference with Western blots and hamper purification by binding to proteins. Media from Gibco-BRL called Virus Production Serum-Free Media, VP-SFM, have been demonstrated by the manufacturer to support growth of BHK-21 cells. Previous data has demonstrated that overexpression of TIMP-3 in BHK-21 cells results in localization of the protein in the conditioned media in addition to ECM. This is probably due to the saturation of the TIMP-3 binding sites in the ECM.

To test TIMP-3 expression utilizing VP-SFM, a comparison pNUThuTIMP-3 BHK-21 cells grown in 2.5% and 5% FBS DMEM/F-12 and VP-SFM was performed. Because the BHK-21 cells would not

attach to the culture dishes when seeded in VP-SFM, cells were seeded in 2.5% FBS DMEM/F-12 prior to induction. Aliquots of the conditioned media were analyzed by reverse zymography as shown in Figure 3.18. As expected, cells grown without the inducer, $ZnSO_4$, produced negligible amounts of TIMP-3 in the conditioned media, under all three conditions tested (lanes 1, 3, and 6). Induction of TIMP-3 protein expression by addition of $ZnSO_4$ resulted in significant amounts of TIMP-3 activity in the conditioned media (lanes 2, 4, and 5). TIMP-3 expression was enhanced in the cultures grown in the presence of 5% FBS (lane 4) in comparison to cultures with 2.5% FBS (lane 2). The amount of TIMP-3 activity in the conditioned media from cells induced in VP-SFM, lane 5, was comparable to that in conditioned media from cells in 5% FBS DMEM/F-12, lane 4.

The schematic of the pNUT vector (Figure 3.19) shows that there is only one site where cDNA can be inserted and this site is recognized by the *Sma*I restriction enzyme. To insert each cDNA of interest into the pNUT vector, it was first cut out of the pXMT2 vector and ligated into pNUT. The inserted DNA must be ligated in the correct direction into the pNUT vector in order to be expressed under the control of the metallothionein promoter. The resulting pNUT vector was therefore characterized using other restriction enzymes to check for the correct orientation of the inserted cDNA. *Kpn*I was utilized because the TIMP

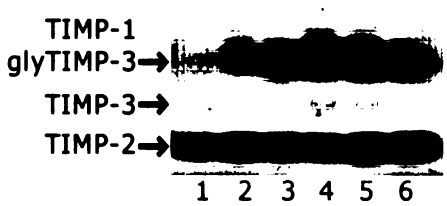

Figure 3.18: Reverse zymogram of conditioned media from pNUThuTIMP-3 BHK cells uninduced and induced in FBS DMEM/F-12 medium or virus production serum-free medium (VP-SFM).

1 - 2.5% FBS DMEM/F-12 U
2 - 2.5% FBS DMEM/F-12 I
3 - 5% FBS DMEM/F-12 U
4 - 5% FBS DMEM/F-12 I
5 - VP-SFM I
6 - VP-SFM U
U - uninduced
I - induced with 80 μM $ZnSO_4$

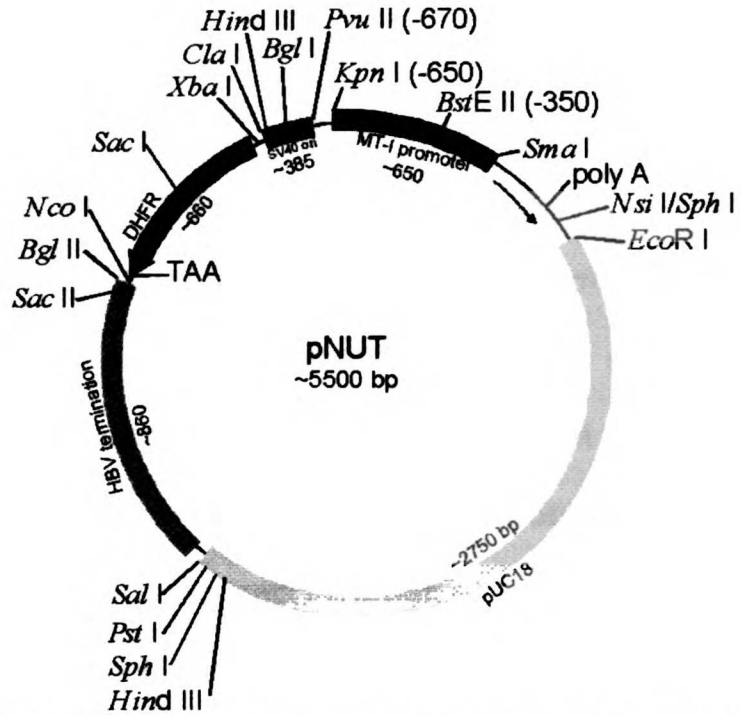

Figure 3.19: Schematic diagram of the pNUT vector.

and chimeric inserts have specific *Kpn*I restriction sites that together with the pNUT vector's *Kpn*I restriction site (Figure 3.19) would help deduce the direction of the inserted DNA.

Preliminary experiments indicated that ligation into a site created by *Sma*I digestion were not successful. This was probably due to the fact that *Sma*I creates blunt ends in cDNA that made it difficult to ligate into the vector (10). This technical problem was overcome by utilizing *Xma*I, which is an isoschizomer of *Sma*I. Both recognize the CCCGGG sequence but *Sma*I cuts in the middle and *Xma*I cuts after the first cytosine. *Xma*I leaves overhangs or sticky ends increasing the ligation efficiency.

cDNA inserts of TIMP-2, TIMP-3 and the C2 and C3 chimeras were transferred to the pNUT vector by digestion of the respective pXMT2 plasmids and ligation into pNUT. Plasmid DNA was purified from ten clones of each plasmid type and digested with *Xma*I and *Kpn*I for characterization. Tables 3.5 shows the expected size of the DNA fragments for plasmids cut with *Xma*I. Table 3.6 shows expected size of DNA fragments when they are in the correct and incorrect directions when digested with *Kpn*I.

Table 3.5: Expected size of DNA fragments generated with *Xma*I.

pNUT plasmid	Fragments
TIMP-3	5500, 644
C3 chimera	5500, 656
TIMP-2	5500, 669
C2 chimera	5500, 657

Table 3.6: Expected size of DNA fragments generated with *Kpn*I.

PNUT plasmid	Fragments for correct direction	Fragments for incorrect direction
TIMP-3	4904, 1240	5440, 704
C3 chimera	4904, 1252	5452, 704
TIMP-2	4904, 1097, 168	5297, 704, 168
C2 chimera	4904, 1085, 168	5285, 704, 168

The digestion products of the plasmids digested with *Xma*I and *Kpn*I by agarose gel electrophoresis are shown in Figures 3.20 to 3.24. Restriciton digests of clones 1-10 of pNUTTIMP-3 with *Xma*I and *Kpn*I are shown in Figure 3.20 and lanes 8-11 of Figure 3.24. Although Figure 3.20 is very dark, the original gel showed bands of the expected size (~5500 bp and 644 bp) in lanes 6 and 8 (clones 6 and 8) following digestion of pNUThuTIMP-3 with *Xma*I and (4904 bp and 1240 bp) in lanes 12 and 14 (clones 6 and 8) following digestion with *Kpn*I.

The bands in lanes 9 and 11, clone 10 of Figure 3.24, were also of the correct size for *Xma*I and *Kpn*I. Clone 10 of pNUTTIMP-3 was chosen for large-scale purification using a Qiagen Plasmid Midi Kit (Qiagen Inc.) for transfection into BHK-21 cells. Clone 3 of pNUTC3, lanes 4 and 13 of Figure 3.21, clone 8 of pNUTTIMP-2, lanes 9 and 18 of Figure 3.22, and clone 2 of pNUTC2, lanes 3 and 12 of Figure 3.23, were also used for large scale plasmid purification for stable transfection of BHK-21 cells.

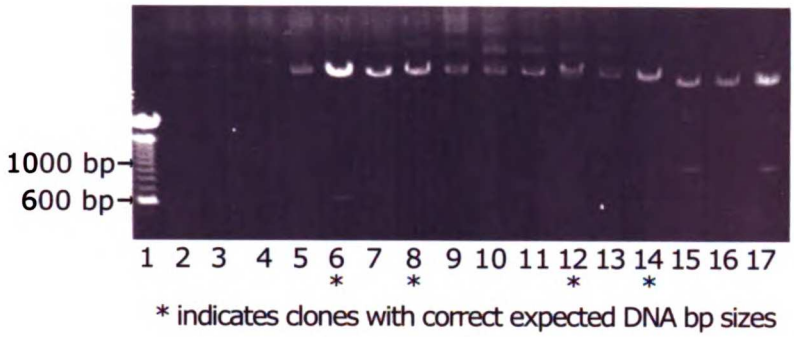

Figure 3.20: Agarose gel of *Xma*I and *Kpn*I restriction digests of pNUThuTIMP-3 clones.
1 - 100 bp DNA ladder
2-9 - Clones 1-8 digested with *Xma*I
10-17 - Clones 1-8 digested with *Kpn*I

Figure 3.21: Agarose gel of *Xma*I and *Kpn*I restriction digests of pNUTC3 clones.
1 & 20 - 100 bp DNA ladder
2-10 - Clones 1-9 digested with *Xma*I
11-19 - Clones 1-9 digested with *Kpn*I

Figure 3.22: Agarose gel of *Xma*I and *Kpn*I restriction digests of pNUThuTIMP-2 clones.
1 & 20 - 100 bp DNA ladder
2-10 - Clones 1-9 digested with *Xma*I
11-19 - Clones 1-9 digested with *Kpn*I

Figure 3.23: Agarose gel of *Xma*I and *Kpn*I restriction digests of pNUTC2 clones.
1 & 20 - 100 bp DNA ladder
2-10 - Clones 1-9 digested with *Xma*I
11-19 - Clones 1-9 digested with *Kpn*I

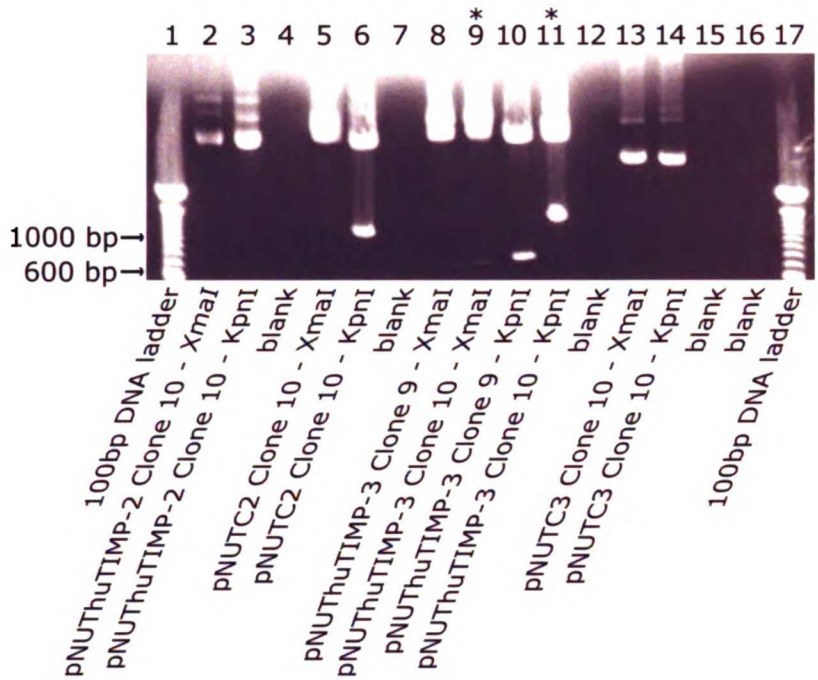

Figure 3.24: Agarose gel of *Xma*I and *Kpn*I restriction digests of pNUT clones.
* indicates clones with correct expected DNA bp sizes

3.3.5 Reverse Zymography Analysis of Condition Media and ECM of C3 and C2 Chimeras

Aliquots of conditioned media and ECM were collected from both un-induced and induced cultures of the BHK-21 cells and analyzed by SDS-PAGE and reverse zymography, Figure 3.25. Coomassie Blue stained bands in lanes 2-15 of the reverse zymograms, panels C and D (Figure 3.25), represent TIMP activities as confirmed by comparison with the control SDS polyacrylamide gels, panels A and B (Figure 3.25), where no staining was observed in the region of migration of standards ~50kDa and smaller. TIMP activities in conditioned media and ECM samples from both uninduced and induced untransfected and pNUT transfected BHK-21 cells were similar, as shown in Figure 3.25 (panels C and D, lanes 4 and 5 and lanes 6 and 7, respectively). Each had TIMP-1 and TIMP-2 activities in the conditioned media. In addition, no endogenous TIMP-3 activity was detected in the ECM of untransfected and pNUT transfected BHK-21 cells with this sample load.

The pNUThuTIMP-3 transfected BHK-21 cells showed similar amounts of TIMP-1 and TIMP-2 in the conditioned media (panel C, lanes 8 and 9) in comparison to the conditioned media of untransfected and pNUT transfected cells (panels C and D, lanes 4 and 5 and lanes 6 and 7, respectively). However, the pNUThuTIMP-3

transfected BHK-21 cells showed activities attributed to TIMP-3 and glycosylated TIMP-3 in the ECM (compare panel C and D, lanes 8 and 9). Some TIMP-3 activity was observed in the conditioned media of the pNUThuTIMP-3 transfected BHK-21 cells (panel C, lanes 8 and 9) with a higher degree of staining in the induced sample (panel C, lane 9). Again, as in the COS-1 cell system, this was believed to represent TIMP-3 that was not bound to the ECM due to the saturation of TIMP-3 ECM-binding sites. Expression of new TIMP activity in uninduced samples compared to controls is likely to be due to zinc already contained in the formulated media.

The conditioned media and ECM of cells transfected with pNUThuTIMP-2 showed an increase in the level of TIMP-2 activity in the conditioned media, Figure 3.25 (panel C, lane 12 and 13). As demonstrated in the COS-1 system, under conditions of high level of TIMP-2 expression, an additional band was present at approximately 50 kDa (indicated by red arrow, panel C, lane 13). Because the intensity of the band was higher in the induced sample (panel C, lane 13) in comparison to the uninduced sample (panel C, lane 12), this suggested that it was a form of TIMP-2. Further experimentation is needed to ascertain if this was a dimer of TIMP-2.

Conditioned media and ECM of pNUTC3 transfected BHK-21 cells (panel C and D, lanes 10 and 11) showed similar amounts of TIMP-1,

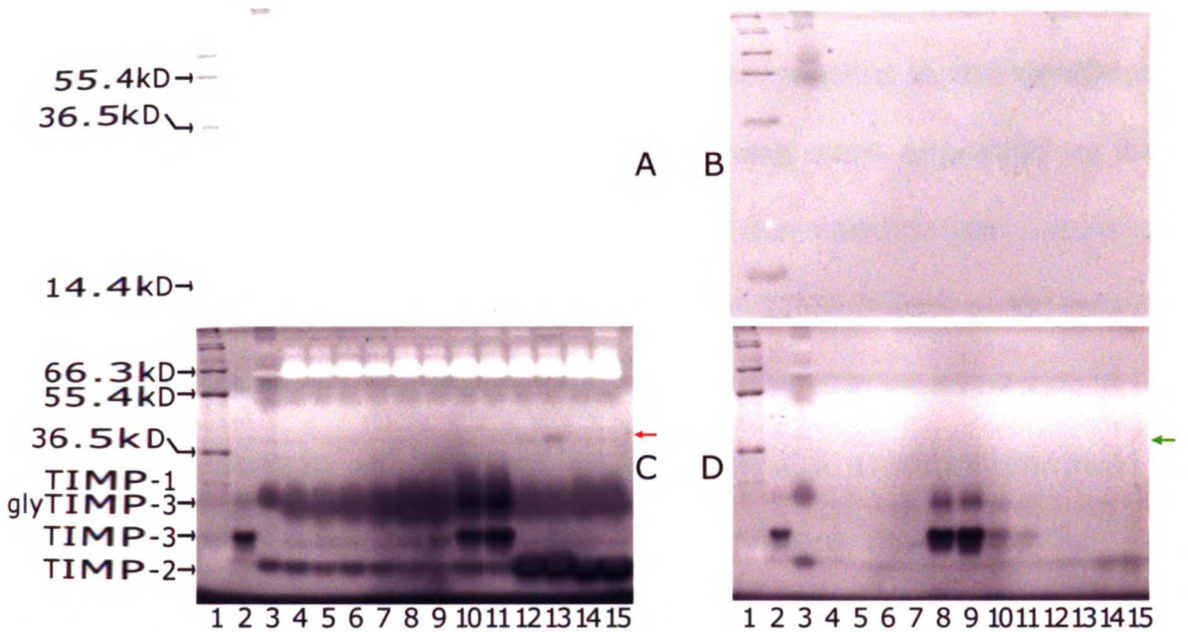

Figure 3.25: 17% SDS-PAGE of conditioned media, A, and extracellular matrix, B, and 17% reverse zymography of conditioned media, C, and extracellular matrix, D, from uninduced (U) and induced (I) BHK-21 cells. Conditioned media loads were 3 µl or 1/6666 of the 10 ml of media from each dish. ECM loads were 2 µl or 1/250 of a dish. TIMP-1, TIMP-2, and TIMP-3 standards were from conditioned media (1/6666 dish) and extracellular matrix (1/100 dish) of FHs173We cells, human embryo fibroblasts, respectively.

.

1 - Novex Mark12 Protein std.
2 - TIMP-3 std.
3 - TIMP-1 and TIMP-2 stds.
4 - BHK-21 U
5 - BHK-21 I
6 - pNUT BHK-21 U
7 - pNUT BHK-21 I
8 - pNUThuTIMP-3 BHK-21 U
9 - pNUThuTIMP-3 BHK-21 I
10 - pNUTC3 BHK-21 I
11 - pNUTC3 BHK U
12 - pNUThuTIMP-2 BHK-21 U
13 - pNUThuTIMP-2 BHK-21 I
14 - pNUTC2 BHK-21 U
15 - pNUTC2 BHK-21 I

TIMP-2 as the controls. However, a new activity migrated slightly slower than unglycosylated TIMP-3 and was present in the conditioned media (panel C, lanes 10 and 11). There also appeared to be a glycosylated form of the C3 chimera in the conditioned media that migrated slightly slower than glycosylated TIMP-3 (panel C, lanes 10 and 11). As in the transfected COS-1 system, this was consistent with the identification of this activity as the C3 chimera because its theoretical molecular size is 480 Daltons more than TIMP-3. Faint staining of a band was observed in the ECM of the pNUTC3 transfected BHK-21 cells (panel D, lanes 10 and 11) that aligns with the unglycosylated TIMP-3 standard, lane 2, and the unglycosylated TIMP-3 activity in the adjacent lane, lane 9. Further analysis of these samples by reverse zymography confirmed that this activity was due to diffusion upon sample loading.

Conditioned media and ECM from uninduced and induced pNUTC2 transfected BHK-21 cells are shown in Figure 3.25 (panel C and D, lanes 14 and 15, respectively). A new activity that migrated slightly faster than unglycosylated TIMP-2 was present in the conditioned media (panel C, lanes 14 and 15). This observation was again consistent with the identification of this activity as the C2 chimera because its theoretical molecular size is 480 Daltons less than TIMP-2. As observed in the COS-1 cell system, the C2 chimera did not

completely localize to the conditioned media (panel C, lanes 14 and 15), but was also found to a lesser extent in the ECM (panel D, lanes 14 and 15). This localization to the ECM appeared to be due to properties of the C2 chimera and not due to the overexpression of the C2 chimera because TIMP-2 was not observed in the ECM of BHK-21 cells transfected with pNUThuTIMP-2 (panel D, lanes 12 and 13). An additional band of activity was present at approximately 50 kDa in the ECM of the pNUTC2 transfected BHK-21 cells (indicated by the green arrow, panel D, lanes 14 and 15) that did not appear in the conditioned media (panel C, lanes 14 and 15). (NOTE: This was clearer in the original gel.) Analagous to the band migrating at ~50 kDa in the conditioned media of pNUThuTIMP-2 transfected BHK-21 cells (panel C, lanes 12 and 13), this band in the pNUTC2 transfect BHK-21 cells was more intense in the ECM of induced cells compared to the uninduced cells (compare panel D, lanes 14 and 15).

3.3.6 Western Blots of the C3 and C2 Chimeras

Western blots were performed to confirm the TIMP-2 and TIMP-3 epitopes of the chimeras. A rabbit polyclonal antibody to chicken TIMP-3, chkTIMP-3, that had been demonstrated to recognize human TIMP-3 and a mouse monoclonal antibody to the first loop of human TIMP-2 were utilized to probe for the C3 chimera. The mouse monoclonal antibody to huTIMP-2 (1^{st} loop) was created by

immunizing a mouse with a peptide with the amino acid sequence, DSGNDIYGNPIKRIQ. This sequence contains the first loop of TIMP-2, NDIYGN, and was part of the TIMP-2 sequence (Ala23 to Tyr64) that was exchanged into TIMP-3 to construct the C3 chimera. Figure 3.26 shows the Western blot of conditioned media from transfected BHK-21 cells. The rabbit anti-chkTIMP-3 pAb stained the TIMP-3 standard (panel B, lane 2) but did not stain the TIMP-2 (panel B, lane 1) or any proteins in the conditioned media of pNUT BHK-21 or pNUThuTIMP-3 transfected BHK-21 cells (panel B, lanes 3 and 4, respectively). The rabbit anti-chkTIMP-3 pAb stained a band in the conditioned media of pNUTC3 transfected BHK-21 cells (panel B, lane 5). This band migrated slightly faster than the TIMP-3 band (panel B, lane 2) that was consistent with the reverse zymography, Figure 3.25 (panel C, lanes 10 and 11), and the fact that the C3 chimera was 480 Daltons larger than TIMP-3. The rabbit anti-huTIMP-2 (1^{st} loop) pAb stained the TIMP-2 standard (panel A, lane 1) but did not stain proteins in the TIMP-3 standard (panel A, lane 2). The endogenous TIMP-2 in the conditioned media from pNUT or pNUThuTIMP-3 transfected BHK-21 cells (panel A, lanes 3 and 4, respectively) was not detectable. The rabbit anti-huTIMP-2 (1^{st} loop) pAb stained two bands in the conditioned media of pNUTC3 transfected BHK-21 cells (panel A,

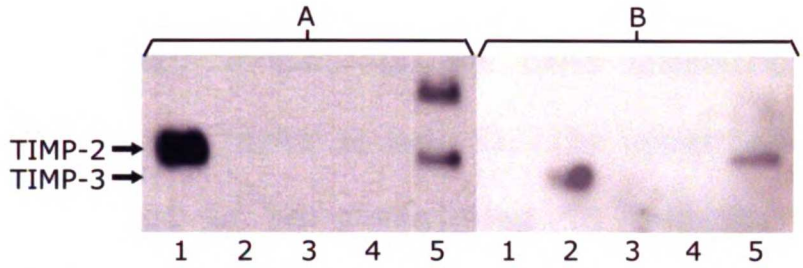

Figure 3.26: Western blots of conditioned media from transfected BHK-21 cells.

A - rabbit anti-huTIMP-2 (1st loop) pAb clone 68-6H4.
B - rabbit anti-chickenTIMP-3 pAb
1 - TIMP-2 standard
2 - TIMP-3 standard
3 - pNUT
4 - pNUThuTIMP-3
5 - pNUTC3 BHK-21

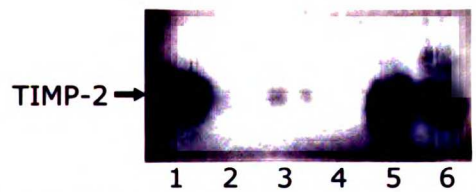

Figure 3.27: Western blot of conditioned media and extracellular matrix from pNUTC3, pNUTC3-L, pNUTT3cT2, pNUTC2, and pNUTC2cT3 transfected BHK-21 cells probed with mouse anti-huTIMP-2 mAb clone 69-10B11

1 - TIMP-2 standard
2 - CM pNUTC3
3 - CM pNUTC3-L
4 - ECM pNUTT3cT2
5 - ECM pNUTC2
6 - ECM pNUTC2cT3

lane 5). The lower band (panel A, lane 5) had the same electrophoretic mobility as the band stained by the rabbit anti-chkTIMP-3 pAb (panel B, lane 5). The upper band (panel A, lane 5) was believed to be glycosylated C3 chimera. The rabbit anti-chkTIMP-3 pAb did not stain the upper band (panel B, lane 5) nor did it stain the glycosylated TIMP-3 (panel B, lane 2).

A Western blot of the conditioned media of pNUTC2 transfected BHK-21 cells probed with the mouse anti-huTIMP-2 mAb clone 69-10B11 is shown in Figure 3.27. (NOTE: pNUTC3-L and pNUTC2cT3 will be discussed later in this chapter.) The monoclonal antibody was created by immunizing a mouse with a peptide with the amino acid sequence, DTLSTTQKKSLNHRYQ, of TIMP-2 as the antigen. The sequence is downstream of the sequence that was exchanged out of TIMP-2 to create the C2 chimera. The antibody stained the TIMP-2 standard, lane 1. Low levels of endogenous TIMP-2 were stained in both the pNUTC3 and pNUTC3-L (discussed later in the chapter), lanes 2 and 3, respectively. The mouse anti-huTIMP-2 mAb also stained a band in the conditioned media of pNUTC2 transfected BHK-21 cells, lane 5, that migrated slightly faster than TIMP-2 standard, lane 1. This was consistent with the reverse zymogram, Figure 3.25 (panel C, lanes 14 and 15) and the fact that the C2 chimera was 480 Daltons smaller than TIMP-2.

Western blot experiments utilizing the rabbit anti-chicken TIMP-3 pAb to probe for the C2 chimera were unsuccessful. A possible reason for this result is that the rabbit anti-chkTIMP-3 pAb may not recognize any of the TIMP-3 sequence (Val23 to His60) that was exchanged into the C2 chimera. The use of a mouse anti-TIMP-3 (1^{st} loop) mAb (Chemicon International) was not able to detect the TIMP-3 standard or the C2 chimera, data not shown. This was possibly due to the purity or quality of the antibody. In addition, a Western blot to demonstrate the negative control for the C2 chimera by probing conditioned media from pNUTC2 BHK-21 cells with the rabbit anti-huTIMP-2 (1^{st} loop) pAb was not shown because no staining was detected.

3.3.7 Significance of the C3 and C2 chimeras

Reverse zymography data from both the transiently transfected COS-1 cells and the stably transfected BHK-21 cells demonstrated that the C3 chimera with the first basic region, Region I (Val23 to His60), of TIMP-3 exchanged with the homologous region, (Ala23 to Tyr64), of TIMP-2 localizes to the conditioned media. The reverse chimera, C2, partially localizes to the ECM. It is clear that the basic Region I of TIMP-3 (Val23 to His60) is a major factor in the binding of this protein to the ECM because exchange of this domain with the analogous region of TIMP-2 abolishes ECM-binding. However, although this

region may be necessary for ECM-binding of TIMP-3, it is not sufficient for the complete conversion of TIMP-2 into a matrix-bound protein. That is, the C2 chimera (TIMP-2 containing basic Region I of TIMP-3), while showing some evidence of ECM-binding is still localized predominantly in the conditioned media. An explanation for these observations may be that structural features of TIMP-2 actively interfere with binding of the C2 chimera to the ECM. For example, TIMP-2 has a highly negatively charged C-terminus that could conceivably interact directly with Region I and could thus block other electrostatic interactions with molecules such as heparan sulfate. Bode *et al.* observed that the C-terminal tails of both TIMP-1 and TIMP-2 structures have many confirmations and are very flexible (11). In order to address this possibility, additional chimera constructs were analyzed.

It is conceivable that the basic Regions II and/or III in the TIMP-3 structure also contribute to its ECM-binding properties in addition to Region I. An analysis utilizing the full TIMP-2 structure, Figure 3.28, showed that chimeras incorporating Region II and/or III would not add significant positive charge to increase the capacity for ECM-binding. The areas that would undergo an electrostatic change are indicated by the white arrows in Figure 3.28 where a negatively charged glutamateis changed to a glutamine in Region II, and a negatively

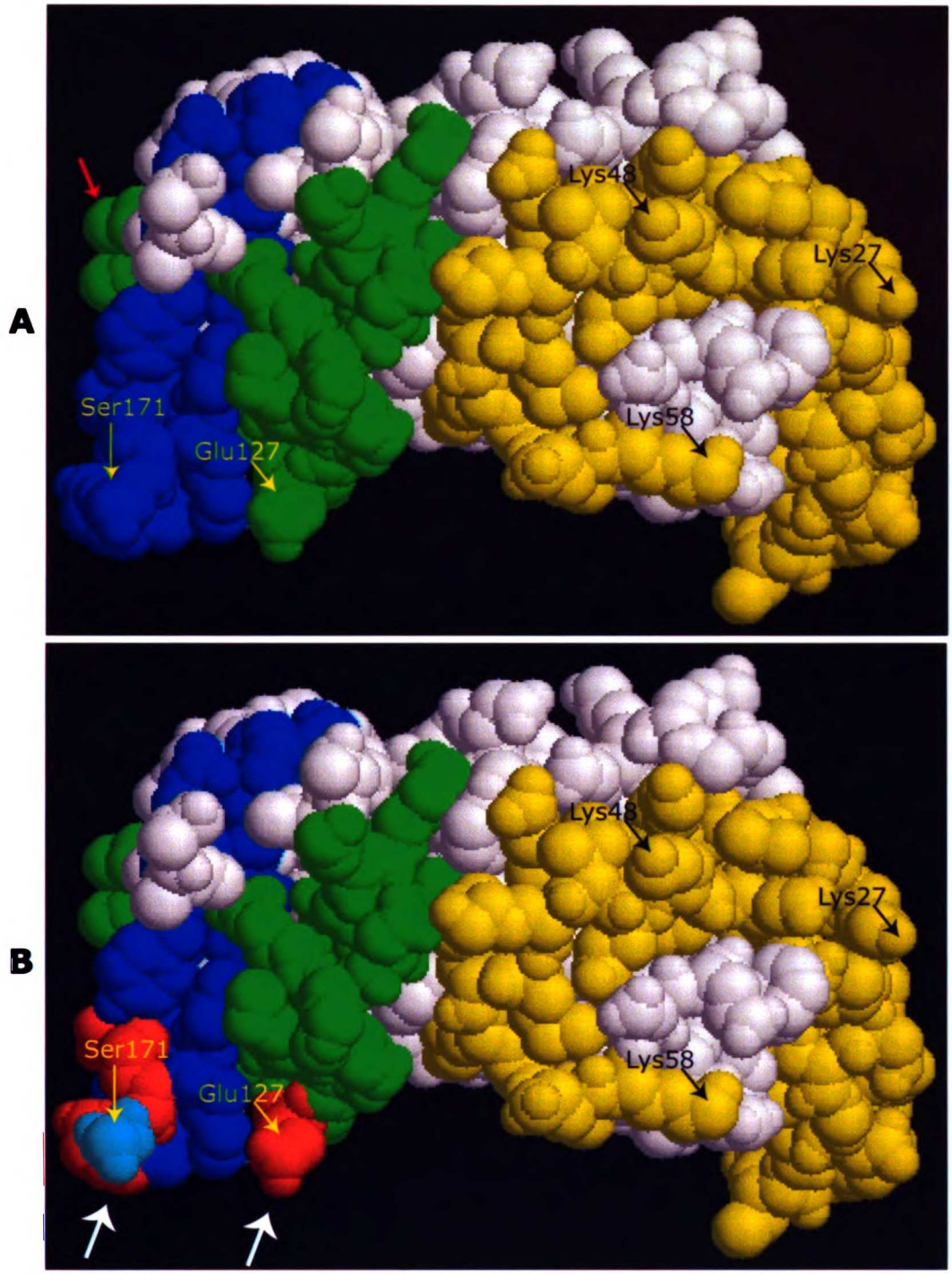

Figure 3.28: Structure of TIMP-2 with Regions I (yellow), II (green) and III (blue). A - TIMP-2 without changes made in Region II or III. Red arrow indicates part of Region II on the MMP binding side of the molecule.
B - White arrows indicate where amino acids would be changed to neutral, orange, or positively charged amino acids, cyan, if Region II and III of TIMP-2 were exchanged with Region II and III of TIMP-3.

charged aspartate is changed to a glycine and another lysine appears on the surface in Region III. Although these changes may result in a +3 change in the net charge, this did not appear to provide a significant change to the surface, therefore C2 chimeras incorporating Region II and/or III were not constructed.

Since the C-terminal tail is known to be somewhat flexible in the TIMP-1 and TIMP-2 structures, the possibility that the tail may electrostatically interact with Region I of the C2 chimera is quite plausible. To test this hypothesis, a chimera of C2 with the last 10 amino acids of TIMP-3, DKSIINATDP, designated C2cT3 (C2 chimera with the c-terminus of TIMP-3) and a chimera of TIMP-3 with the last 10 amino acids of TIMP-2, KQEFLDIEDP, designated T3cT2 (TIMP-3 with the c-terminus of TIMP-2) were constructed. It was anticipated that the tail of the C2cT3 chimera would no longer block the basic Region I and allow binding to the ECM. Conversely, the negatively charged tail of T3cT2 would electrostatically interact with the basic Region I and prevent it from binding to the ECM.

In parallel with construction and expression of the C2cT3 and T3cT2 chimeras, a third chimera was constructed and expressed that was designated C3-L (C3 chimera with the 1st Loop of TIMP-2, NDIYGN, removed). The sequence of amino acids of TIMP-2 that was exchanged into TIMP-3 to create the C3 chimera consisted of two beta

sheets connected by a long 1st loop consisting of the amino acids NDIYGN. This 1st loop of TIMP-2 is thought to confer selectivity towards interactions with MT1-MMP to form the ternary complex of MT1-MMP, TIMP-2 and proMMP-2 (11). Removing the NDIYGN sequence of amino acids from the C3 chimera should create a shorter 1st loop connecting the two beta sheets resulting in a chimera, C3-L, similar to TIMP-3 but localized to the conditioned media. It was anticipated that by removing this TIMP-2 1st loop, NDIYGN, from the C3 chimera would create a TIMP, C3-L, with similar MMP selectivity and/or sheddase selectivity as wild-type TIMP-3, but is not bound to the ECM.

3.3.8 Construction of the New Chimeras, C2cT3, T3cT2 and C3-L

The new chimeras were constructed utilizing a similar PCR protocol used in the construction of the C2 and C3 chimeras. The chimeras were cloned in pCR-Blunt vectors for cloning and sequence confirmation. After the sequences were confirmed and because previous chimeras showed activity, cDNAs were ligated directly into the pNUT vector. The pNUT plasmids were transfected into BHK-21 cells and the ECM and conditioned media were collected and analyzed by reverse zymography.

3.3.9 The C2cT3 Chimera Partially Localizes to the ECM

The reverse zymogram for the CM and ECM of the C2cT3 chimera is shown in Figure 3.29. The reverse zymogram in Figure 3.29 had contaminants migrating in each lane around glycosylated TIMP-3, just above TIMP-3 and just above TIMP-2. This did not interfere with interpretation of the gel. Unglycosylated TIMP-3, glycosylated TIMP-3 and a band that migrated slightly faster than TIMP-3 (indicated by dimer?) were observed in the standard (panel A and B, lane 1). The band that migrated slightly faster than TIMP-3 (panel A and B, lane 1) was believed to be a 'processed' form of TIMP-3. TIMP-1 and TIMP-2 activities in the conditioned media of both uninduced and induced controls of untransfected BHK-21 cells were similar, as shown in Figure 3.29 (panels A, lanes 2 and 3, respectively). Faint staining of bands that migrated with electrophoretic mobilities similar to those of TIMP-3 and its processed form were detected in the conditioned media and ECM from BHK-21 cells (panel A and B, lane 2 and 3) that were not observed in previous samples. It is interesting to note that these TIMP-3 activities were detected more in the induced BHK-21 cells (panel A and B, lane 3) than in the uninduced BHK-21 cells (panel A and B, lane 2). The conditioned media and ECM of uninduced and induced pNUTC2cT3 transfected BHK-21 cells (panel A, lanes 4 and 5) had many new TIMP activities that were not in the untransfected

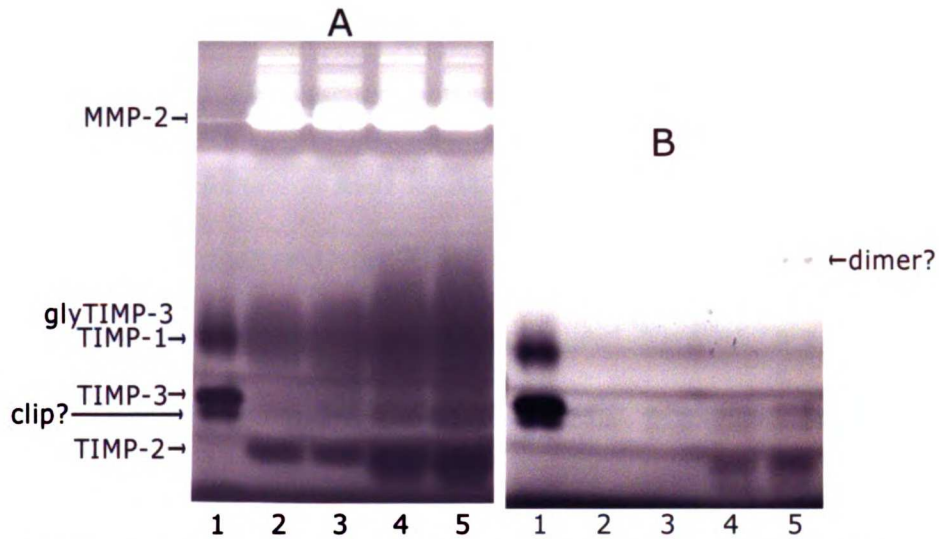

Figure 3.29: 15% Reverse zymogram of conditioned media (A) and extracellular matrix (B) from BHK-21 cells transfected with pNUTC2cT3. CM loads were 1/6666th of 10 ml of media from one dish. ECM loads were 1/1000th of a dish.

1 - TIMP-3 standard
2 - BHK-21 uninduced
3 - BHK-21 induced
4 - pNUTC2cT3 BHK-21
5 - pNUTC2cT3 BHK-21

BHK-21 cells (panel A, lanes 2 and 3). These bands were detected more in the induced samples when compared to the uninduced samples (compare panel A and B, lanes 4 and 5). The first of the new activities migrated faster than TIMP-2 and appeared predominantly in the conditioned media (panel A, lanes 4 and 5) and to a lesser extent in the ECM (panel B, lanes 4 and 5). This was consistent with the identification of this activity as the C2cT3 chimera because its theoretical molecular size is 640 Daltons less than TIMP-2. The other new activities migrated below TIMP-3 with electrophoretic mobilities similar to those of glycosylated TIMP-3 or TIMP-1, respectively, in the conditioned media of the pNUTC2cT3 transfected BHK-21 cells (panel A, lanes 4 and 5). The lower band in the conditioned media that migrated just below TIMP-3 (panel A, lanes 4 and 5), was likely to have been the glycosylated form of the C2cT3 chimera because the glycosylation was at the arginine in the C-terminal 10 amino acids of TIMP-3 that were exchanged into the C2 chimera. It was uncertain whether the band that migrated with an electrophoretic mobility similar to that of TIMP-1 was indeed TIMP-1 or another form of glycosylated C2cT3. Interestingly, two bands whose mobilities were similar to those of unglycosylated TIMP-3 and 'processed' TIMP-3 were detected more in the ECM of pNUTC2cT3 transfected BHK-21 cells (panel B, lanes 4 and 5) than in the ECM of untransfected BHK-21 cells

(panel B, lanes 2 and 3). The levels of these two activities were also higher in the induced pNUTC2cT3 BHK-21 samples compared to the uninduced samples (panel B, lanes 4 and 5). In addition, similar to previous results with the C2 chimera, a band of activity was detected around 50kDa only in the ECM of the induced pNUTC2cT3 transfected BHK-21 cells that may be a dimer of the C2cT3 chimera (indicated by dimer?, panel B, lane 5).

Western blots of the C2cT3 chimera were not conclusive, but a band was detected using the mouse anti-huTIMP-2 mAb clone 69-10B11, Figure 3.27 (page 48), lane 6, that migrated faster than the TIMP-2 control. This was consistent with the identification of this activity as the C2cT3 chimera because its theoretical molecular size is 640 Daltons less than TIMP-2.

3.3.10 The T3cT2 Chimera Does not Localize to the Conditioned Media

Reverse zymography comparing conditioned media and ECM from pNUThuTIMP-3 and pNUTT3cT2 transfected BHK-21 cells is shown in Figure 3.30. Induced and uninduced samples are not displayed because there were no significant differences other than levels of expression. TIMP-3 and glycosylated TIMP-3 activities were detected in the ECM of the pNUThuTIMP-3 BHK-21 cells with a slight amount of

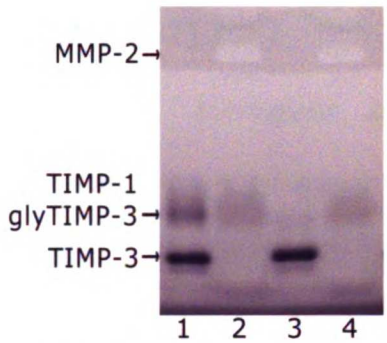

Figure 3.30: Reverse zymogram of ECM and CM from BHK-21 cells transfected with pNUTT3cT2. CM loads were 1/6000th of a dish. ECM loads were 1/200th of a dish.

1 - ECM pNUThuTIMP-3
2 - CM pNUThuTIMP-3
3 - ECM pNUTT3cT2
4 - CM pNUTT3cT2

the 'processed' TIMP-3 that migrated just below TIMP-3, lane 1. TIMP-1 and TIMP-2 activities in the conditioned media of both pNUThuTIMP-3 and pNUTT3cT2 BHK-21 cells, lanes 2 and 4, respectively, were similar. However, a new activity was detected in the ECM of the pNUTT3cT2 BHK-21 cells, lane 3, with an electrophoretic mobility that was slightly slower than that of unglycosylated TIMP-3. This was consistent with the identification of this activity as the T3cT2 chimera because its theoretical molecular size is only 160 Daltons more than TIMP-3. A very faint band in lane 3 was detected that migrated just below glycosylated TIMP-3, lane 1. This does not appear to be a glycosylated form of the T3cT2 chimera because it migrated below glycosylated TIMP-3. In addition, the T3cT2 chimera should not be glycosylated because the glycosylation site of TIMP-3 is in the C-terminal 10 amino acids that were replaced with the C-terminal 10 amino acids of TIMP-2.

3.3.11 The Localization of the C3-L Chimera is Similar to that Displayed by the C3 Chimera

Following the initial transfection of pNUTC3 into BHK-21 cells, contrary to previous observations, the C3 chimera was found to localize partially in the ECM. ECM and conditioned media samples from the initial transfection of COS-1 cells and the stable transfected

BHK-21 cells collected over a 12 month period had demonstrated localization of the C3 chimera exclusively in conditioned media. Subsequently, approximately $1/12^{th}$ of the total activity of the C3 chimera localized to the ECM.

Reverse zymography comparing conditioned media and ECM from pNUTC3 and pNUTC3-L transfected BHK-21 cells is shown in Figure 3.31. The unglosylated and glycosylated C3 chimera were detected in the conditioned media, lane 1, and to a lesser extent in the ECM, lane 2, of the pNUTC3 transfected BHK-21 cells. A new TIMP activity was detected in the conditioned media, lane 3, and to a lesser extent in the ECM, lane 4, of the pNUTC3-L transfected BHK-21 cells that migrated slightly faster than the unglycosylated C3 chimera, lane 1. This was consistent with the identification of this activity as the C3-L chimera because its theoretical molecular size is 677 Daltons less than the C3 chimera. In addition, what appeared to be the glycosylated form of the C3-L chimera was detected predominantly in the conditioned media, lane 3, but was almost undetectable in the ECM, lane 4, of the pNUTC3-L BHK-21 cells that migrated slightly faster than the glycosylated C3 chimera, lane 1. Both the conditioned media and the ECM of the pNUTC3 and pNUTC3-L BHK-21 cells, lanes 1 and 2, and lanes 3 and 4, respectively, appeared to have a 'processed' form migrating just below their respective unglycosylated forms.

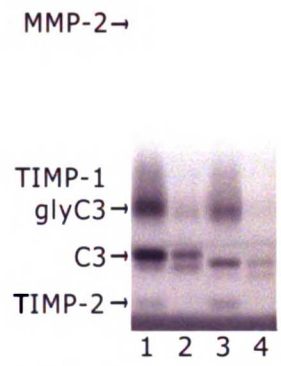

Figure 3.31: Reverse zymography of ECM and CM from BHK-21 cells transfected with pNUTC3 and pNUTC3-L. CM loads were 1/6666th of a dish. ECM loads were 1/1000th of a dish.

1 - CM pNUTC3
2 - ECM pNUTC3
3 - CM pNUTC3-L
4 - ECM pNUTC3-L

The activity of the 'processed' form of each of the chimeras appeared to be higher in the ECM, lanes 2 and 4, when compared to the conditioned media, lanes 1 and 3. The amount of C3-L chimera activity detected in the pNUTC3-L BHK-21 cells, lane 3, was about half of the amount of C3 chimera activity detected in the pNUTC3 BHK-21 cells, lane 3. It is interesting to note that the detectable amount of TIMP-2 in the conditioned media of the BHK-21 cells expressing the C3-L chimera, lane 3, was higher than the amount of TIMP-2 in the conditioned media of the BHK-21 cells expressing the C3 chimera, lane 1.

3.3.12 Gelatin Zymography of Conditioned Media from BHK-21 Cells Expressing TIMP-2 and TIMP-3 and the C2 and C3 Chimeras

TIMP-2, TIMP-3, C2 and C3 transfected BHK-21 cells were analyzed by gelatin zymography to detect MMP activity and determine if higher expression of TIMP-2 or TIMP-3 or the expression of the chimeras influences MMP activity or expression. Gelatin zymography of the C2cT3, T3cT2 and C3-L chimeras are not presented here due to the changes in C3 and C3-L chimera expression (discussed later in this chapter). Gelatin zymography of the conditioned media of untransfected and transfected BHK-21 cells is shown in Figure 3.32.

MMP-2 and MMP-9 activities and an uncharacterized gelatinase activity, A, in the conditioned media from FHs173We cells were detected in lane 1. ProMMPs are activated *in situ* presumably by the denaturation/renaturation process and autocatalytic cleavage (12). The levels of MMP-2, proMMP-2 and MMP-9 activities and 'A' appeared similarly in the conditioned media of untransfected BHK-21, pNUT BHK-21 and pNUTTIMP-3 BHK-21 cells, lanes 3, 4, and 7, respectively. Increased levels of MMP-2 and proMMP-2 activity were detected in the pNUThuTIMP-2 BHK-21 cells, lane 5, in comparison to the untransfected BHK-21, pNUT BHK-21 and pNUThuTIMP-3 BHK-21 cells, lanes 3, 4, and 7, respectively. The levels of MMP-9 and 'A' activities in the pNUThuTIMP-2 BHK-21 may have also been higher. The levels of gelatinase activities in the conditioned media of pNUTC2 and pNUTC3 transfected BHK-21 cells, lanes 6 and 8, respectively, appeared comparable to each other but higher, than those in the conditioned media of the pNUThuTIMP-2, lane 3, and much higher than those detected in the conditioned media of the other cell types, lanes 4, 5, and 7, respectively. Higher levels of gelatinase activities that migrated between proMMP-2 and MMP-9, and above A were detected in the conditioned media of pNUThuTIMP-2, pNUTC2 and pNUTC3 transfected BHK-21 cells (lanes 5, 6, and 8) than in the controls (lanes 3 and 4). While all detectable gelatinase activities

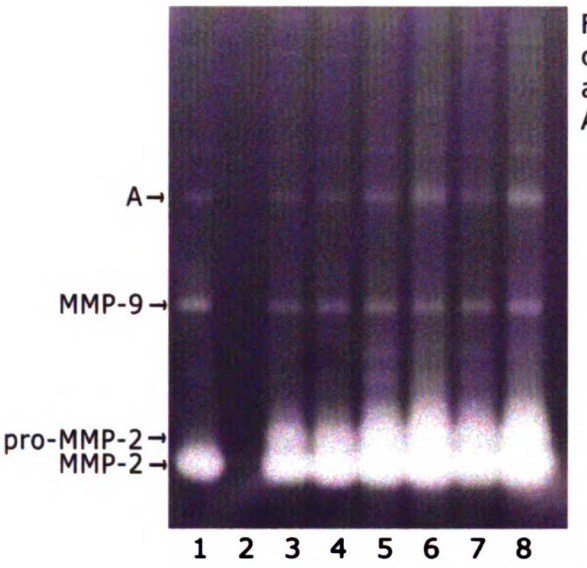

Figure 3.32: 8% zymography of conditioned media from untransfected and transfected BHK-21 cells.
A - unknown gelatinase activity.

1 - CM FHs173We
2 - ECM FHs173We
3 - CM BHK-21
4 - CM pNUT BHK-21
5 - CM pNUThuTIMP-2 BHK-21
6 - CM pNUTC2 BHK-21
7 - CM pNUThuTIMP-3 BHK-21
8 - CM pNUTC3 BHK-21

appeared to be increased in cultures of BHK-21 cells overexpressing TIMP-2 or expressing the C2 and C3 chimeras, (Figure 3.32) lanes 5, 6, and 8, respectively, the levels of proMMP-2 and MMP-2 activities appeared most affected. The detectable gelatinase activities observed in the conditioned media of BHK-21 cells overexpressing TIMP-3 did not appear to be different than the untransfected or pNUT transfected BHK-21 controls. Although this could be confirmed by mRNA analysis, the detection of this increased proMMP-2 and MMP-2 activity appeared to be due to an increase in the expression of proMMP-2 in cultures of the pNUThuTIMP-2, pNUTC2 and pNUTC3 BHK-21 cells. There are no published data relating increased TIMP expression to an increase in MMP expression. Current opinion is that TIMP-2 forms a ternary complex with proMMP-2 and MT1-MMP on the cell surface that results in the activation MMP-2 (13, 14). Butler *et al.* reported that MMP-2 activation by MT1-MMP is enhanced by low concentrations TIMP-2 but is inhibited by high concentrations of TIMP-2 (15). If the increase of TIMP-2 in the conditioned media of the pNUThuTIMP-2 BHK-21 cells only increased activation of MMP-2 then only MMP-2 levels and not proMMP-2 levels should have increased. However, the levels of proMMP-2 and MMP-2 were higher in the conditioned media of the BHK-21 cells expressing TIMP-2 and the C2 and C3 chimeras in comparison to the proMMP-2 and MMP-2 levels in the BHK-21 controls

and the BHK-21 cells expressing TIMP-3. Therefore, the proMMP-2 expression levels may have been higher in the pNUThuTIMP-2, pNUTC2 and pNUTC3 BHK-21 cells.

If the expression of proMMP-2 was indeed being induced by TIMP-2 and the C2 and C3 chimeras, are the C2 and C3 chimera forming the ternary complex with MT1-MMP and proMMP-2 to activate MMP-2? As described in Chapter 1, the ternary complex is believed to be formed by the N-terminal domain of MT1-MMP binding to the N-terminal domain of TIMP-2 and the C-terminal domain of MMP-2 binding to the C-terminal domain of TIMP-2 (14-16). The C2 chimera retains the C-terminal domain of TIMP-2 and the N-terminal binding regions of TIMP-2 except for the 1st loop, therefore, it could still form the ternary complex. TIMP-3 has been demonstrated to bind to the C-terminal domain of MMP-2 and the C3 chimera contains the 1st loop of TIMP-2 in the N-terminal domain, therefore, it could possibly form the ternary complex (17). Theoretically, both the C2 and C3 chimeras could interact with MT1-MMP and proMMP-2 to form the ternary complex to activate MMP-2.

3.4 Discussion

The C2 and C3 chimeras were constructed to determine if the first basic Region I of TIMP-3 was involved in the binding of TIMP-3 in the ECM. The basic Region I, Val23 to His60, of TIMP-3 was replaced with the analogous region, Ala23 to Tyr64, from TIMP-2 to construct the C3 chimera, and the reverse exchange was made for TIMP-2 to construct the C2 chimera. It was anticipated that the C3 chimera would localize to the conditioned media and the C2 chimera would localize to the ECM. Transiently transfected COS-1 cells and the stably transfected BHK-21 cells demonstrated that the C3 chimera localizes to the conditioned media. The reverse chimera, C2, partially localizes to the ECM. It is clear that the basic Region I of TIMP-3 (Val23 to His60) is a major factor in the binding of this protein to the ECM because exchange of this domain with the analogous region of TIMP-2 abolishes ECM-binding. However, although this region may be necessary for ECM-binding of TIMP-3, it is not sufficient for the complete conversion of TIMP-2 into a matrix binding protein. That is, the C2 chimera (TIMP-2 containing basic Region I of TIMP-3), while showing some evidence of ECM-binding is still localized predominantly in the conditioned media.

It was proposed that the negatively charged C-terminal tail of the C2 chimera could be interacting with basic Region I, blocking binding

to molecules such as heparan sulfate in the ECM. By constructing the C2cT3 chimera (C2 chimera with the c-terminus of TIMP-3) and the T3cT2 chimera (TIMP-3 with the c-terminus of TIMP-2) it was determined that the negatively charged C-terminal tail of TIMP-2 does not alter the localization of the C2 chimera or TIMP-3.

The observations made in the previous chapter only analyzed the electrostatic nature of TIMP-3 by mapping out differences of positive and negative charge. Although the interactions appear to be predominantly electrostatic, based on the TIMP models and polyanion and polycation interaction studies by Kishnani *et al.*, the possibility of hydrogen bond formation was not analyzed (18). Preliminary observations suggest that several tyrosines may also be involved in the localization of TIMP-3 to the ECM. TIMP-3 contains 16 tyrosines whereas TIMP-1, TIMP-2 and TIMP-4 contain 6, 7, and 11 tyrosines, respectively. Seven of the tyrosines found in TIMP-3 are in or near Regions II and III that appear on the same surface as the proposed heparan sulfate binding domain, Region I, in the projected TIMP-3 model (data not shown). These tyrosines are not in TIMP-1 or TIMP-2, or are near negatively charged amino acids and areas lacking positively charged amino acids in TIMP-4. In reanalyzing Region II and III with the addition of tyrosine content, it is conceivable that one or both of these regions contributes to the binding of TIMP-3 in the

ECM. In addition to the electrostatic interactions, these 'extra' tyrosines in TIMP-3 could conceivably form hydrogen bonds with many hydroxyl or amine groups in the heparan sulfate molecule.

Another possibility is that the binding of TIMPs to MMPs in the conditioned media could be localizing TIMP-2 and the C2 and C3 chimeras in the conditioned media. To what degree does MMP-binding influence localization? Although both TIMP-2 and TIMP-3 bind to MMP-2 with a K_i in the 10^{-12} M range, TIMP-2 binds to MMP-2 approximately 2-fold more than TIMP-3 (17, 19). The exchange of analogous regions of TIMP-2 and TIMP-3 to create the chimeras may have altered this selectivity towards MMP-2. The apparent expression level of MMP-2 appears to be higher in the BHK-21 cells expressing TIMP-2 and the C2 and C3 chimeras. It is conceivable that the increased amounts of proMMP-2 and MMP-2 in the conditioned media are binding to TIMP-2 and the C2 and C3 chimeras and retaining them in the conditioned media. In order to study this possibility *in vitro* the TIMP-2 and the chimeras must be expressed in cells that do not express MMP-2. Currently, these cells do not exist. MMP-2 knockout cells would need to be created.

A possible dimer of TIMP-2 was detected exclusively in the conditioned media of BHK-21 cells overexpressing TIMP-2. It is possible that the dimer is formed through disulfide linkages that do not

destroy TIMP activity. A disulfide-linked dimer would likely be through the C-terminal TIMP domains because TIMP inhibitory activity is through the N-terminal domain (11). A dimer of this type would probably lack the ability to bind the C-terminal domain of MMP-2 (20). Williamson *et al.* noted a highly hydrophobic surface region on the MMP binding face of TIMP-2 (21, 22). This surface could conceivably provide a site for dimerization of TIMP-2 or the C2 chimera through hydrophobic interactions. If this form of dimerization were to occur it would likely block N-terminal MMP interactions. The N-terminal domains of TIMP-2 and TIMP-3 interact with the N-terminal domain of MMP-2 more strongly than the C-terminal domains of TIMP-2 and TIMP-3 interact with the C-terminal domain of MMP-2 (17). Either form of a dimer, whether disulfide linked or through hydrophobic interactions, would likely decrease their combined ability to bind to MMP-2. With respect to a C2 dimer, the dimerization could be lowering its capacity for binding to MMP-2 and allowing interaction of the basic Region I with heparan sulfate and, therefore, localization to the ECM. Whereas, dimerization of TIMP-2 may lower its capacity for binding to MMP-2 but without basic Region I, it therefore localizes in the conditioned media.

The C3-L chimera may have also aided in probing the question of localization by MMP-2 interactions in the conditioned media in cell

culture. The C3 chimera contains the first loop of TIMP-2 that may be involved in MMP-2 binding (11). The C3-L chimera was constructed by removing this first loop, NDIYGN, of TIMP-2 to create a shorter loop similar to the first loop in TIMP-3. It was anticipated that the C3-L chimera would localize in the conditioned media similar to the C3 chimera but have similar TIMP-3 selectivity towards MMPs and/or ADAMs. The initial COS-1 transfections were repeated three times. Each resulted in the C3 chimera exclusively localizing in the conditioned media. The initial stable transfections of BHK-21 cells were repeated twice. Again, each resulted in the C3 chimera exclusively localizing in the conditioned media. Recently, due to unknown circumstances, the C3 chimera began to partially localize to the ECM hampering the comparison between the C3 and C3-L chimeras. During the past year, new stable transfections of BHK-21 cells with pNUTC3 and pNUTC3-L resulted in the C3 and C3-L chimeras predominantly localized in the conditioned media but approximately $1/12^{th}$ of the C3 and C3-L chimeras detected in the ECM. The pNUTC3 BHK-21 cells from the earliest stable transfections when the C3 chimera exclusively localized in the conditioned media were thawed, grown and the ECM and conditioned media were collected and analyzed by reverse zymography. The C3 chimera was observed predominantly localized in the conditioned media but approximately

$1/12^{th}$ of the C3 chimera detected in the ECM. Serum, DMEM/F-12 and tissue culture plate lot numbers have changed. It is possible that one of these changes has altered the cells or the environment of the cells causing this change in localization. This is still under investigation.

To further study the interaction of TIMP-3 and the chimeras with heparan sulfate in cell culture, we proposed transfecting the pNUT vectors in cells that do not produce heparan sulfate. Esko *et al.* have produced Chinese hamster ovary cells, PgsD-677, that lack both N-acetylglucosaminyltransferase and glucuronyltransferase activities that are required for synthesis of heparan sulfate. It was anticipated that because the cells do not produce heparan sulfate, TIMP-3 would not localize to the ECM and would be detected in the conditioned media of pNUThuTIMP-3 transfected PgsD-677 cells. Several attempts to transfect these cells with the pNUT vectors were unsuccessful. The pNUT vector may have been toxic to the cells.

Because of the change in the exclusive localization in the conditioned media by the C3 chimera, the possibility of MMP binding conveying localization, and failed attempts at transfecting the PgsD-677 cells lacking heparan sulfate, it is clear that the TIMPs and chimeras must be purified to study the interaction of heparan sulfate and the MMPs *in vitro*. Chapter 4 describes experiments performed to purify TIMP-3 and the chimeras for further characterization.

3.5 Bibliography

1. DeClerck YA, Yean TD, Chan D, Shimada H, Langley KE. Inhibition of tumor invasion of smooth muscle cell layers by recombinant human metalloproteinase inhibitor. Cancer Res. 1991;51:2151-2157.

2. Coulombe B, Skup D. In vitro synthesis of the active tissue inhibitor of metalloproteinases encoded by a complementary DNA from virus-infected murine fibroblasts. J Biol Chem 1988;263(3):1439-43.

3. Fernandez-Catalan C, Bode W, Huber R, Turk D, Calvete JJ, Lichte A, et al. Crystal structure of the complex formed by the membrane type 1-matrix metalloproteinase with the tissue inhibitor of metalloproteinases-2, the soluble progelatinase A receptor. Embo J 1998;17(17):5238-48.

4. Murphy G, Houbrechts A, Cockett MI, Williamson RA, O'Shea M, Docherty AJ. The N-terminal domain of tissue inhibitor of metalloproteinases retains metalloproteinase inhibitory activity [published erratum appears in Biochemistry 1991 Oct 22;30(42):10362]. Biochemistry 1991;30:8097-8102.

5. Wu B, Arumugam S, Gao G, Lee GI, Semenchenko V, Huang W, et al. NMR structure of tissue inhibitor of metalloproteinases-1 implicates localized induced fit in recognition of matrix metalloproteinases. Journal of Molecular Biology 2000;295(2):257-68.

6. Palmiter RD, Behringer RR, Quaife CJ, Maxwell F, Maxwell IH, Brinster RL. Cell lineage ablation in transgenic mice by cell-specific expression of a toxin gene [published erratum appears in Cell 1990 Aug 10;62(3):following 608]. Cell 1987;50(3):435-43.

7. Tweedie JW, Bain HB, Day CL, Nicholson HH, Mead PE, Sheth B, et al. Lactoferrin cDNA. Expression and in vitro mutagenesis. Adv Exp Med Biol 1994;357:197-208.

8. Mason AB, Miller MK, Funk WD, Banfield DK, Savage KJ, Oliver RW, et al. Expression of glycosylated and nonglycosylated human transferrin in mammalian cells. Characterization of the recombinant proteins with comparison to three commercially available transferrins. Biochemistry 1993;32(20):5472-9.

9. Chen CA, Okayama H. Calcium phosphate-mediated gene transfer: a highly efficient transfection system for stably transforming cells with plasmid DNA. Biotechniques 1988;6(7):632-8.

10. Bercovich JA, Grinstein S, Zorzopulos J. Effect of DNA concentration on recombinant plasmid recovery after blunt-end ligation. Biotechniques 1992;12(2):190, 192-3.

11. Bode W, Fernandez-Catalan C, Grams F, Gomis-Reuth FX, Nagase H, Tschesche H, et al. Insights into MMP-TIMP interactions. Annals of the New York Academy of Sciences 1999;878:73-91.

12. Kleiner DE, Stetler-Stevenson WG. Quantitative zymography: detection of picogram quantities of gelatinases. Anal Biochem 1994;218(2):325-9.

13. Lichte A, Kolkenbrock H, Tschesche H. The recombinant catalytic domain of membrane-type matrix metalloproteinase-1 (MT1-MMP) induces activation of progelatinase A and progelatinase A complexed with TIMP-2. FEBS Lett 1996;397(2-3):277-82.

14. Murphy G, Stanton H, Cowell S, Butler G, Knauper V, Atkinson S, et al. Mechanisms for pro matrix metalloproteinase activation. Apmis 1999;107(1):38-44.

15. Butler GS, Butler MJ, Atkinson SJ, Will H, Tamura T, van Westrum SS, et al. The TIMP2 membrane type 1 metalloproteinase "receptor" regulates the concentration and efficient activation of progelatinase A. A kinetic study. J Biol Chem 1998;273(2):871-80.

16. Seiki M. Membrane-type matrix metalloproteinases. Apmis 1999;107(1):137-43.

17. Butler GS, Apte SS, Willenbrock F, Murphy G. Human tissue inhibitor of metalloproteinases 3 interacts with both the N- and C-terminal domains of gelatinases A and B. Regulation by polyanions. Journal of Biological Chemistry 1999;274(16):10846-51.

18. Kishnani N. Characterization of Tissue Inhibitor of Metalloproteinases-3 (TIMP-3) from the Extracellular Matrices of

Cultured Human and Avian Cells [Ph.D.]. San Francisco: University of California San Francisco; 1994.

19. Murphy G, Willenbrock F. Tissue inhibitors of matrix metalloendopeptidases. Methods Enzymol 1995;248:496-510.

20. Overall CM, King AE, Sam DK, Ong AD, Lau TT, Wallon UM, et al. Identification of the tissue inhibitor of metalloproteinases-2 (TIMP-2) binding site on the hemopexin carboxyl domain of human gelatinase A by site-directed mutagenesis. The hierarchical role in binding TIMP-2 of the unique cationic clusters of hemopexin modules III and IV. J Biol Chem 1999;274(7):4421-9.

21. Williamson RA, Martorell G, Carr MD, Murphy G, Docherty AJ, Freedman RB, et al. Solution structure of the active domain of tissue inhibitor of metalloproteinases-2. A new member of the OB fold protein family. Biochemistry 1994;33:11745-11759.

22. Williamson RA, Bartels H, Murphy G, Freedman RB. Folding and stability of the active N-terminal domain of tissue inhibitor of metalloproteinases-1 and -2. Protein Eng. 1994;7:1035-1040.

Chapter 4

Purification of TIMP-3 and the C3 and C3-L Chimeras

4.1 Introduction

To further test the hypothesis that TIMP-3 binds to the ECM through interactions with heparan sulfate, TIMP-3 must be purified. In addition, because the C3 and C3-L chimeras do not bind to the ECM, these will also be purified to test whether their interactions with heparan sulfate is less than that of TIMP-3. This chapter outlines the steps taken to purify TIMP-3 and the C3 and C3-L chimeras.

Heparan sulfate has been shown to bind several proteins, such as aFGF, bFGF, interleukin-5, and lipoprotein lipase (1-3). To demonstrate the preferential binding to heparan sulfate, two of the investigators utilized purified protein and a heparan sulfate-binding assay, such as equilibrium dialysis or a heparin column with salt elution chromatography. The other utilized medium from cells expressing the protein and eluted the target protein from a heparin column using a salt gradient to demonstrate differential binding. In the latter method, the protein was impure. This approach could not be utilized with the wild-type and chimeric TIMPs because of potential complex formation with MMPs that may cause causing erroneous heparan sulfate-binding results that could interfere with the interpretation of heparan sulfate binding data. Therefore, the proteins must be purified.

Investigators have reported that TIMP-2 and TIMP-3 can be purified from the conditioned media of human gingival fibroblasts and TIMP-3 transfected NS0 myeloma cells, respectively (4, 5). These investigators used gel filtration chromatography with 1M NaCl in a neutral Tris buffer to separate the MMP and TIMP complexes followed by purification using cation exchange chromatography. Ward *et al.* have also purified TIMP-1 and TIMP-2 by reverse phase chromatography (correspondence).

Negro *et al.* demonstrated the purification of recombinant TIMP-3 from *E. coli* (6). The purification required TIMP-3 to be refolded because the recombinant TIMP-3 formed inclusion bodies of TIMP-3 with incorrect disulfide bonds and, therefore, was not active. Due to the difficulties involved in refolding proteins from inclusion bodies of *E. coli*, this method was not pursued.

In the following sections, the partial purification of minute amounts of TIMP-3 and chimeras are reported. Because of the complexity of the molecular interactions and the low levels of available material, this purification was not completed. Nevertheless, the information can aid future purification when sufficient materials become available.

4.2 Materials and Methods

4.2.1 Collection of Conditioned Media and Preparation of Extracellular Matrix – BHK-21 cells transfected with pNUThuTIMP-3, BHK-21 cells transfected with pNUTC3, and BHK-21 cells transfected with pNUTC3-L were seeded at 6.5 x 10^5 cells/10 cm dish in 5% FBS DMEM/F-12 (UCSF Cell Culture Facility) at 37 °C, 5% CO_2 for 24 h. The media were aspirated and replaced with either 5% FBS DMEM/F-12 containing 80 µM $ZnSO_4$ or Gibco-BRL VP-SFM, virus production serum-free media, containing 80 µM $ZnSO_4$ and the cells were allowed to grow for another 24 h before ECM and CM collection. The ECM from the pNUThuTIMP-3 BHK-21 cells was isolated using the method described in Appendix A by applying 500 µl of Laemmli sample buffer to each culture dish. The pooled samples were concentrated ~40:1 (unless specified) in a Centriplus-20 8000 MW cut-off concentrator (Millipore Corp.). The conditioned media from the pNUTC3-L BHK-21 cells was filtered through a 0.2 µm 0.2 µm polyethersulfone, PES, filter (Millipore Corp.) and concentrated ~40:1 (unless specified) in a Centriplus-20 8000 MW cut-off concentrator (Millipore Corp.). A sample of the ECM and CM before the concentration step was stored for analysis by reverse zymography analysis.

4.2.2 Ion Exchange Chromatography – A 16 cm x 10 mm HiLoad 16/10 SP Sepharose ion exchange column (Amersham

Pharmacia Biotech) was equilibrated in the specified buffers indicatedd in the figures, at 0.6 ml/min on a Hewlett Packard 1100 HPLC system. The Hewlett Packard 1100 system consisted of an HP1100 quaternary pump, HP1100 vacuum degasser, HP1100 UV/Visible variable wavelength detector and an HP 1100 Chemstation data system kindly provided by Quantum Analytics (Foster City, CA). Concentrated ECM or CM (500 µl) were diluted in 15 ml of ion exchange equilibration buffer and concentrated to ~500 µl in a Centriplus-20 8000 MW cut-off concentrator (Millipore Corp.). A 500 µl aliquot was injected onto the column and eluted with a sodium chloride gradient. The UV/Visible wavelength detector was set at 280 nm. Eluted fractions were collected at 0.6 ml/tube and analyzed by reverse zymography (see Appendix A).

4.2.3 Gel Filtration Chromatography – A 10 mm X 30 cm column was packed with Superdex 200 preparative grade (Amersham Pharmacia Biotech) and equilibrated in mobile phase buffer at 1.0 ml/min on the Hewlett Packard 1100 HPLC system and the UV/Visible wavelength detector was set at 280 nm. Eluted fractions were collected at 1.0 ml/tube and analyzed by reverse zymography

4.3 Results and Discussion

Preliminary experiments indicated that it was necessary to concentrate the ECM and conditioned media prior to chromatography

in order to facilitate the detection of TIMP-3 and the C3 and C3-L chimeras, respectively, by absorbance at 280 nm and their activities by reverse zymography. Apte *et al.* demonstrated the purification of TIMP-3 from TIMP-3 transfected mouse myeloma cell conditioned medium by utilizing an S-Sepharose cation exchange column with a MES buffered salt gradient (5). An SP-Sepharose cation exchange column was utilized in the initial attempt to purify TIMP-3 from the ECM of pNUThuTIMP-3 BHK-21 cells.

The chromatogram of the ion exchange chromatography of concentrated ECM from pNUThuTIMP-3 BHK-21 cells is shown in Figure 4.1 with the reverse zymogram of the eluted fractions shown in Figure 4.2. Peak 1 (Figure 4.1) contained TIMP-3 and glycosylated TIMP-3, lane 1 (Figure 4.2), with MMP activity that was determined to be MMP-2. Although, at a lower concentration, peak 2 (Figure 4.1) also contained TIMP-3 and glycosylated TIMP-3 but without any MMP activity, lane 2 (Figure 4.2). Both peaks also appeared to contain the processed form of TIMP-3 that migrated just below the unglycosylated TIMP-3.

Ion exchange chromatography and reverse zymography of concentrated conditioned media of pNUTC3 BHK-21 cells induced in 5% FBS DMEM/F-12 containing 80 μM $ZnSO_4$ showed similar results, Figures 4.3 and 4.4, respectively. The C3 chimera predominantly

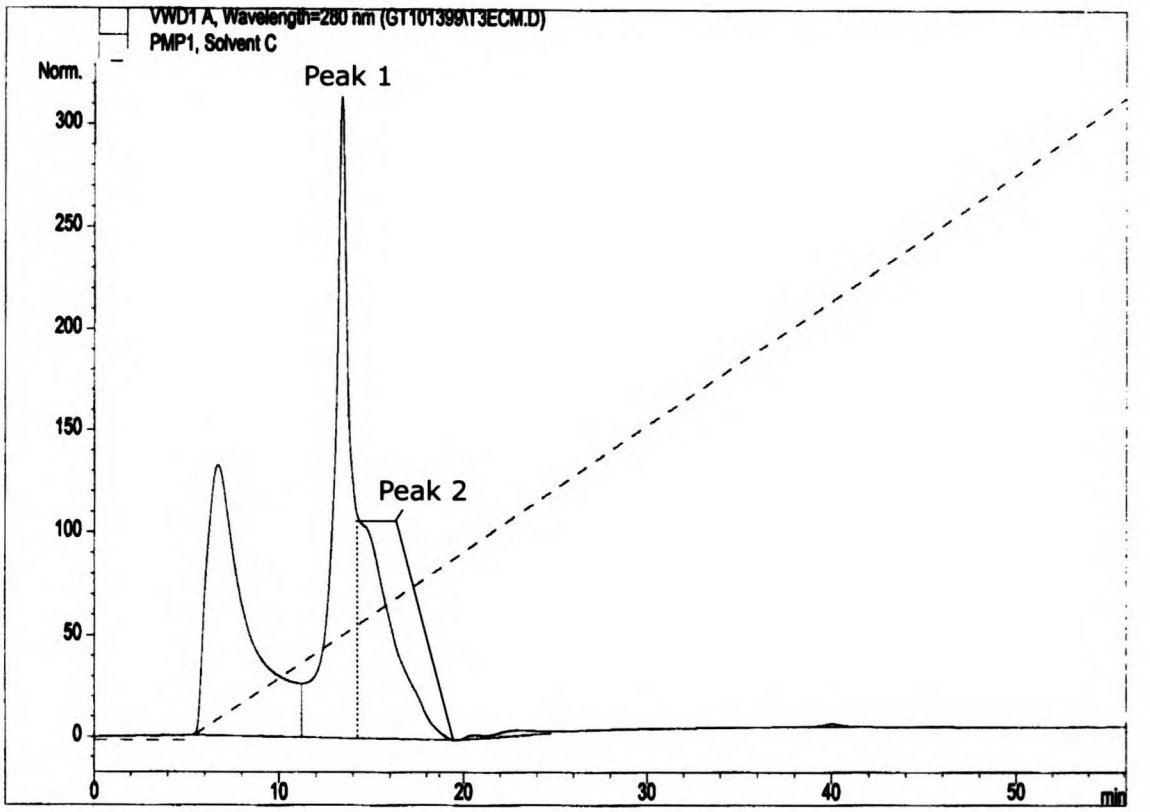

Figure 4.1: Ion exchange chromatogram of concentrated ECM from pNUThuTIMP-3 BHK-21 cells chromatographed on a HiLoad 16/10 SP Sepharose column equilibrated in 25 mM Tris (pH 7.0), 0.025% Brij35, 0.02% NaN3 and eluted with 25mM Tris (pH 7.0), 1 M NaCl, 0.025% Brij35, 0.02% NaN3 with the following gradient: 0-5 min - 5% elution buffer
5-65 min - 100% elution buffer
Flow rate: 0.6 ml/min. Injection volume: 0.5 ml.

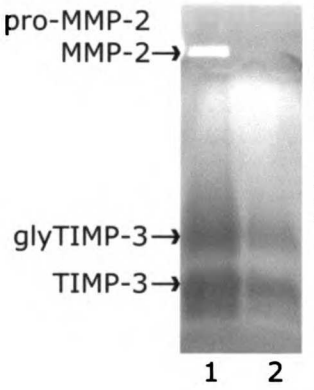

Figure 4.2: Reverse zymogram of eluted fractions from ion exchange chromatography of concentrated ECM from pNUThuTIMP-3 BHK-21 cells.

1 - 20 µl Peak 1
2 - 20 µl Peak 2

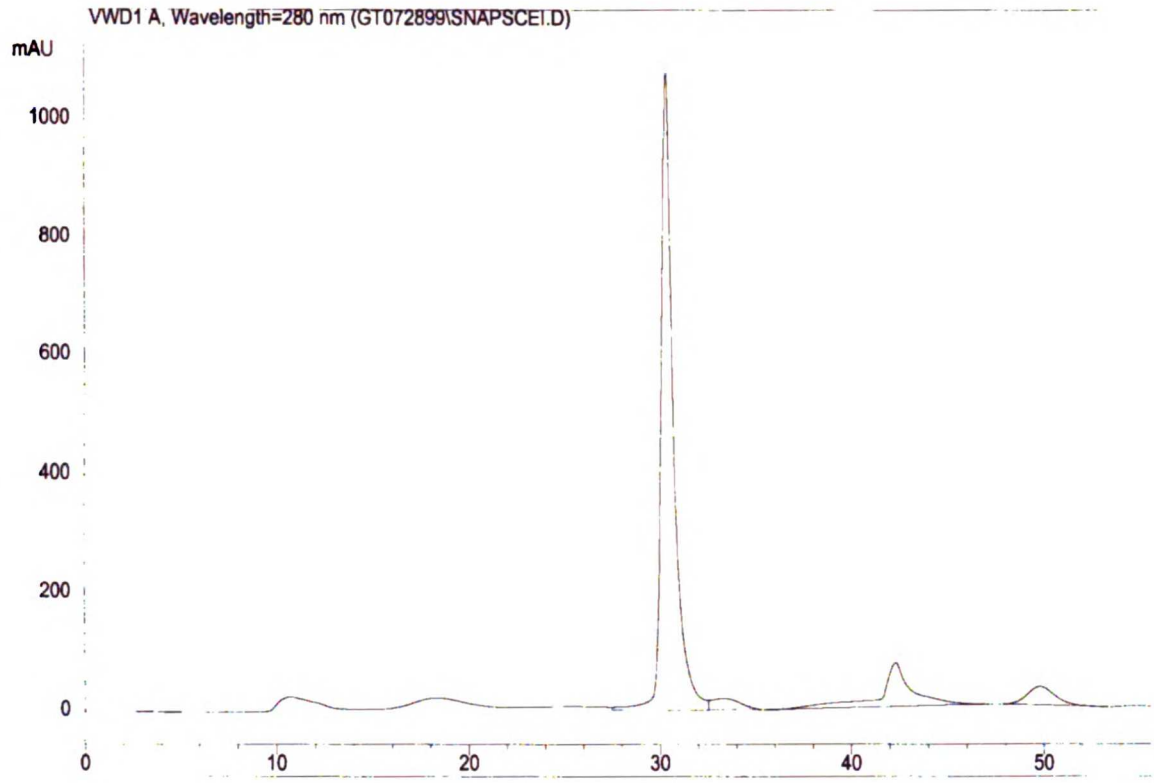

SP Sepharose column in 25 mM MES, 0.025% Brij 35, 0.02% NaN3 (pH 6.0) and eluted with 1 M NaCl, 25 mM MES (pH 6.0), 0.025% Brij 35, 0.02% NaN3 with the following gradient:

0-5 min - 5% elution buffer
5-65 min - 100% elution buffer

Flow rate: 0.6 ml/min. Injection volume: 0.5 ml.

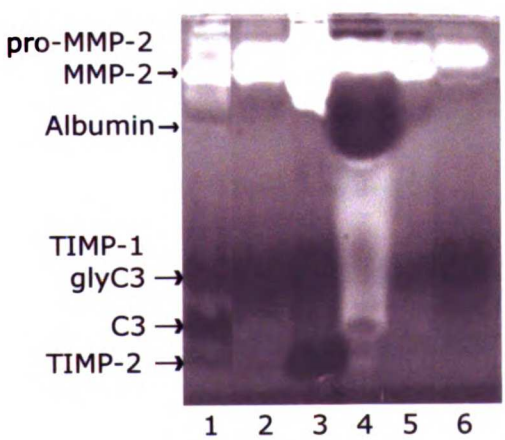

Figure 4.4: Reverse zymogram of eluted fractions from ion exchange chromatography of concentrated 5% FBS DMEM/F-12 CM from pNUTC3 BHK-21 cells.

1 - 5 µl CM from pNUTC3 BHK-21 (starting material)
2 - 25 µl Peak 1
3 - 25 µl Peak 2
4 - 25 µl Peak 3
5 - 25 µl Peak 4
6 - 25 µl Peak 5

eluted in peak 3 (Figure 4.3), lane 4 (Figure 4.4). The albumin obscured the gelatinase activity in lane 4 (Figure 4.4) and the adjacent lanes. TIMP-1 or the glycosylated form of the C3 chimera eluted at different salt concentrations. Because both TIMP-1 and the C3 chimera are glycosylated and glycosylation is usually heterogeneous, the observed elution pattern would be expected. ProMMP-2 and MMP-2 were not resolved on this gel. The band that migrated just above the proMMP-2/MMP-2 band was unresolved proMMP-9 and MMP-9, which appeared in each eluted fraction. These MMP activities were confirmed by gelatin zymography (data not shown). Their elution at different salt concentrations may have been due to heterogeneous glycosylation and/or complex formation with TIMPs. Although obscured by the gelatinase activity in lane 4 (Figure 4.4), the C3 chimera appeared to be separated from TIMP-2, lane 3 (Figure 4.4).

The TIMP-3 and C3 chimera eluted in the ion exchange experiments together with MMP activity. This co-elution may have been due to formation of MMP/TIMP complexes. Gel filtration chromatography was utilized to separate these complexes before separation by other chromatographic methods. In addition, because TIMP-3 ECM harvesting requires several dishes to collect sufficient sample for a single chromatography experiment, the purification of the C3 or C3-L chimeras from conditioned media was attempted first

because larger quantities were more easily produced and concentrated. The quantity of TIMP-3 in the conditioned media of induced pNUThuTIMP-3 BHK-21 cells is significantly lower than the quantities of C3 and C3-L chimeras in the conditioned media of pNUTC3 BHK-21 and pNUTC3-L BHK-21 cells, respectively. Although chromatographic procedures were not developed for purification of TIMP-3 from conditioned media of pNUThuTIMP-3 BHK-21 cells, gel filtration chromatography conditions for the C3 and C3-L chimeras could be applied to the purification of TIMP-3. Because the high quantity of albumin in the conditioned media of cells grown in 5% FBS DMEM/F-12 obscured the analysis by reverse zymography and may also cause purification problems, Gibco BRL's virus production serum free media, VP-SFM, was utilized for induction and expression of the chimeric proteins.

Gel filtration chromatography of VP-SFM conditioned media from BHK-21 cells expressing the C3 chimera was performed utilizing a 30 cm x 10 mm, 30/10, Superdex 200 preparative grade column with 25 mM MES, 0.025% Brij 35, 0.02% sodium azide (pH 6.0). The chromatogram and reverse zymogram in Figures 4.5 and 4.6, respectively, showed that the chimera does not separate from the MMP activities. The MMP and TIMP activities were present in each eluted

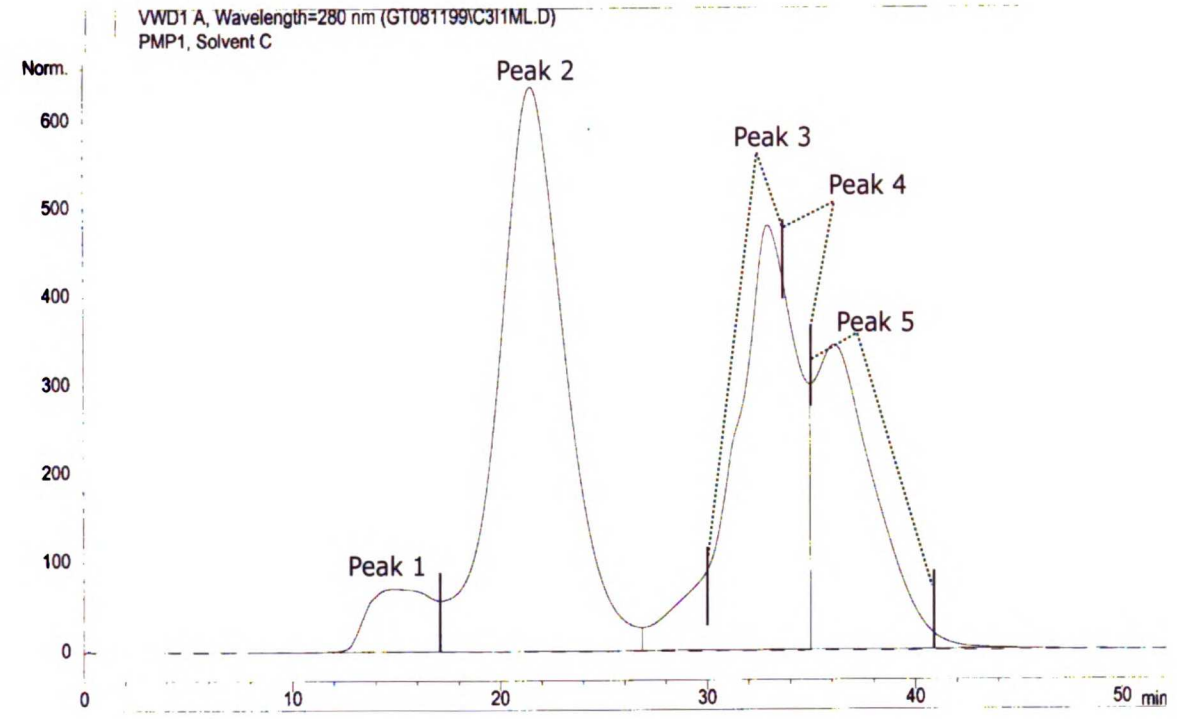

Figure 4.5: Gel filtration chromatogram of concentrated VP-SFM CM from pNUTC3 BHK-21 cells chromatographed in 25 mM MES (pH 6.0), 0.025% Brij 35, 0.02% NaN3 using a 10mm x 30 cm column packed with Superdex 200 preparative grade packing. Flow rate: 1.0 ml/min. Injection volume: 1 ml.

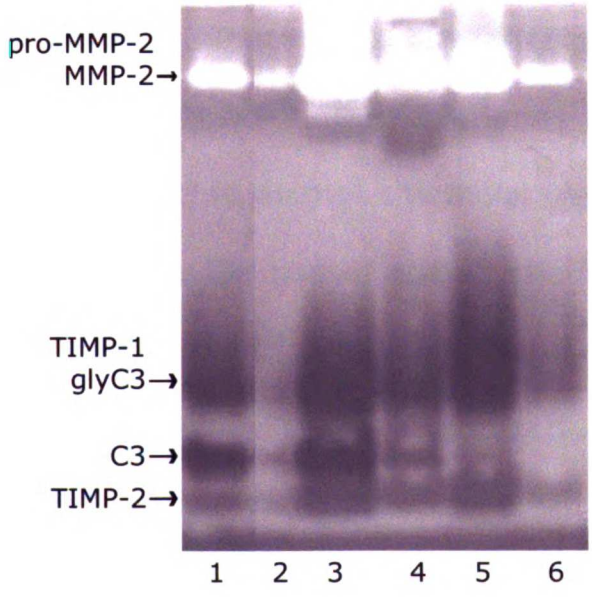

Figure 4.6: Reverse zymogram of eluted fractions from gel filtration of concentrated VP-SFM CM from pNUTC3 BHK-21 cells chromatographed in 25 mM MES (pH 6.0), 0.025% Brij 35, 0.02% NaN3.

1 - 5 µl CM pNUTC3 BHK-21 (starting material)
2 - 25 µl Peak 1
3 - 25 µl Peak 2
4 - 25 µl Peak 3
5 - 25 µl Peak 4
6 - 25 µl Peak 5

fraction. The TIMP activity in lane 2 (Figure 4.6) may have been diffusion from lane 3. Under these conditions, the MMPs and TIMPs (including the chimeras) appeared to form intermolecular and/or intramolecular complexes. For globular proteins, the fractionation range of this column packing is 10-600 kDa. If the MMPs and TIMPs did not form intermolecular and/or intramolecular complexes, the MMPs and TIMPs should have separated with some resolution and not with such a heterogeneous elution pattern. The MMPs and TIMPs may have formed complexes with other unknown proteins. The glycosylated C3, or TIMP-1, appeared to show preferential binding or other complex formations because the ratio of glycosylated C3 (or TIMP-1)/C3 was higher in peak 4 (Figure 4.5), lane 5 (Figure 4.6) than in peak 2 or 3, lane 3 and 4, and unglycosylated C3 was not contained in peak 5 (Figure 4.5), lane 6 (Figure 4.6). Where as unglycosylated C3 was in peaks 2, 3, and 4, lanes 3, 4, and 5.

In order to disrupt the molecular interactions of the MMP and TIMP complexes, the use of strong chaotropes, such as urea or guanidine, was considered. However, these chaotropes could cause a loss of TIMP activity due to denaturation and/or interference in reverse zymography. Ward *et al.* reported using 1 M NaCl in a Tris buffer to separate TIMP-2 and MMP-2 (4). Although it was not stated in the reference, it was assumed that the salt was utilized to disrupt

electrostatic interactions between TIMP-2 and MMP-2. However, the goal was to separate the chimera from the other TIMPs. A lower salt concentration may disrupt any complexes of the chimera with MMP-2 or MMP-9 and not those complexes between TIMP-2 and MMP-2 and/or MMP-9. Therefore, a lower salt concentration such as 0.5 M instead of 1 M may result in the separation of the chimera from TIMP-2 and the MMPs.

Figure 4.7 and 4.8 show the chromatogram and reverse zymogram, respectively, of gel filtration utilizing the 30/10 Superdex 200 column in 0.5 M NaCl, 25 mM MES (pH 6.0), 0.025% Brij 35, 0.02% sodium azide. Most of the C3 activity was contained in peaks 3 and 4 (Figure 4.7) shown in lanes 6 and 7 (Figure 4.8), respectively. This method appeared to separate most of the glycosylated and unglycosylated C3 chimera, lanes 6 and 7 (Figure 4.8), from the MMPs and TIMP-2 and, possibly, TIMP-1, lane 5. Very low quantities of C3 activity was detected in peaks 1, 2 and 5 (Figure 4.7), lanes 4, 5 and 8 (Figure 4.8), respectively. Peak 3 (Figure 4.7), lane 6 (Figure 4.8), contained very low levels of MMP-2 and TIMP-2 activities. Peak 4 (Figure 4.7), lane 7 (Figure 4.8) appeared to be free of TIMP-2 activity but appeared to retain a small amount of MMP-2 activity. However, because MMP-2 activity was detected in the blank lane, lane 3 (Figure

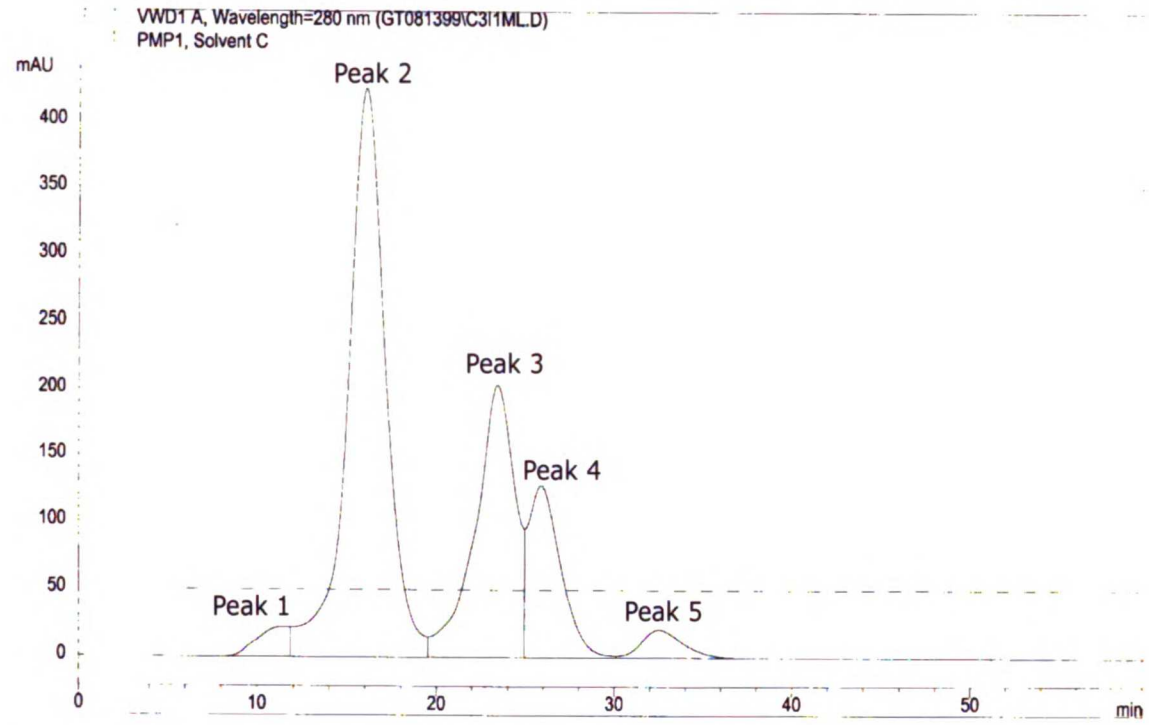

Figure 4.7: Gel filtration chromatogram of concentrated VP-SFM CM from pNUTC3 BHK-21 cells chromatographed in 0.5 M NaCl, 25 mM MES (pH 6.0), 0.025% Brij 35, 0.02% NaN3 using a 10mm x 30 cm column packed with Superdex 200 preparative grade packing. Sample: CM concentrated from 30 ml to 500 µl and diluted in running buffer to 1 ml. Flow rate: 1.0 ml/min. Injection volume: 1 ml.

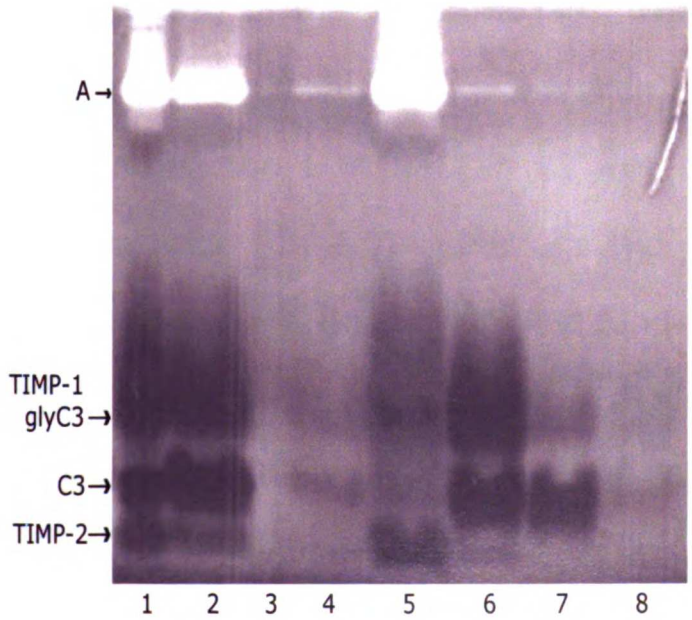

Figure 4.8: Reverse zymogram of eluted fractions from gel filtration of concentrated VP-SFM CM from pNUTC3 BHK-21 cells chromatographed in 0.5 M NaCl, 25 mM MES (pH 6.0)., 0.025% Brij 35, 0.02% NaN3

1 - 2 µl concentrated CM pNUTC3
2 - 25 µl CM pNUTC3 (starting material)
3 - blank
4 - 25 µl Peak 1
5 - 25 µl Peak 2
6 - 25 µl Peak 3
7 - 25 µl Peak 4
8 - 25 µl Peak 5

A - pro-MMP-2 and MMP-2

4.8) part of the MMP-2 activity seen in lanes 4, 6, 7, and 8 may have been due diffusion from lane 5 during sample loading.

To determine if better resolution of the MMPs and the C3 chimera could be attained, the salt concentration was raised from 0.5M to 1 M NaCl. In addition, the buffer was changed to a 25 mM Tris (pH 7.0), containing 1 M NaCl, 0.025% Brij 35, 0.02% sodium azide as in the method described by Ward *et al.* (4). Figures 4.9 and 4.10, show the chromatogram and reverse zymogram results, respectively. Although, the C3 activity was detected in all eluted fractions, the highest activity was in peaks 3 and 4 (Figure 4.9), lanes 3 and 4 (Figure 4.10). There was clearly no TIMP-2 activity in either lane 3 or 4 (Figure 4.10) and no detectable levels of MMP-2. It is of interest to note that these chromatographic conditions did not disrupt the TIMP-2/MMP-2 complex as described in the literature (4). The column began to compress during this chromatographic separation.

Utilizing the 1 M NaCl in 25 mM Tris, 0.025% Brij 35, 0.02% sodium azide (pH 7.0) buffer and two tandem 30/10 Superdex 200 preparative grade column, VP-SFM conditioned medium frompNUTC3-L BHK-21 cells was chromatographed, Figure 4.11. The tandem columns increased the number of theoretical plates and, therefore, a higher degree of separation was achieved. In addition, the assumption was that the C3 and C3-L chimeras would have similar separation

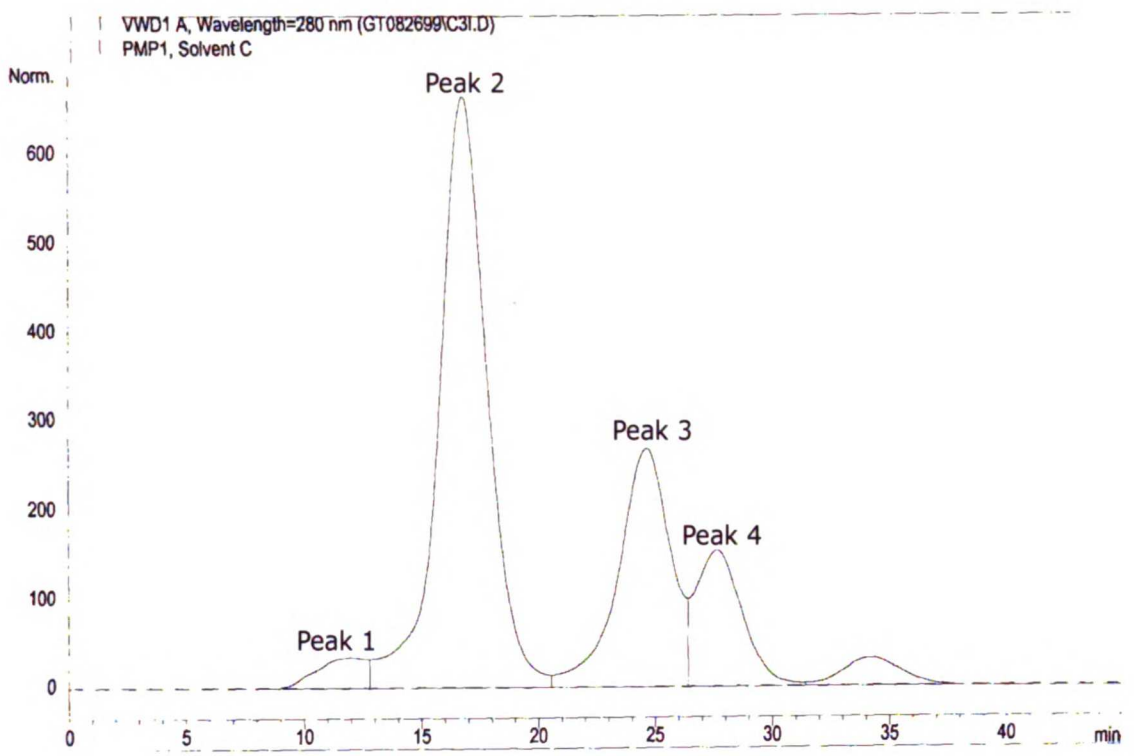

Figure 4.9: Gel filtration chromatogram of concentrated VP-SFM CM from pNUTC3 BHK-21 cells chromatographed in 1.0 M NaCl, 25 mM Tris (pH 7.0), 0.025% Brij 35, 0.02% NaN3 using a 10mm x 30 cm column packed with Superdex 200 preparative grade packing. Flow rate: 1.0 ml/min. Injection volume: 500 µl.

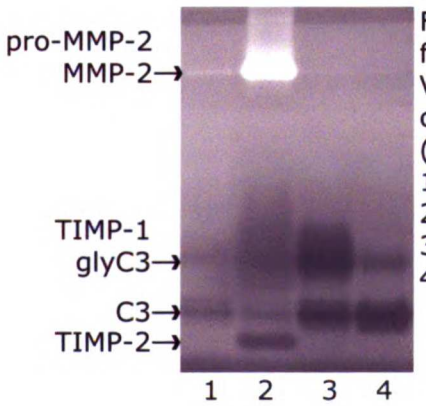

Figure 4.10: Reverse zymogram of eluted fractions from gel filtration of concentrated VP-SFM CM from pNUTC3 BHK-21 cells chromatographed in 1.0 M NaCl, 25 mM Tris (pH 7.0), 0.025% Brij 35, 0.02% NaN3 .
1 - 5 µl Peak 1
2 - 5 µl Peak 2
3 - 5 µl Peak 3
4 - 5 µl Peak 4

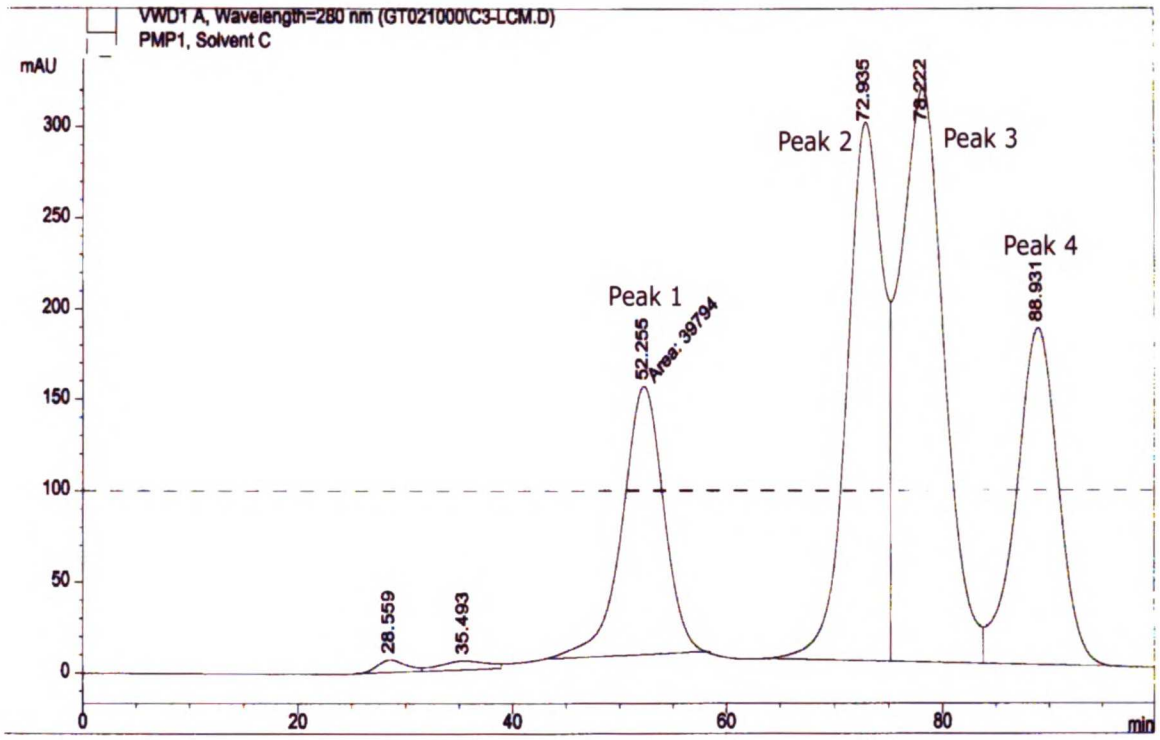

Figure 4.11: Gel filtration chromatogram of concentrated VP-SFM CM from pNUTC3-L BHK-21 cells chromatographed in 1.0 M NaCl, 25 mM Tris (pH 7.0), 0.025% Brij 35, 0.02% NaN3 using two tandem 10 mm x 30 cm column packed with Superdex 200 preparative grade packing. Flow rate: 0.6 ml/min. Injection volume: 1.0 ml.

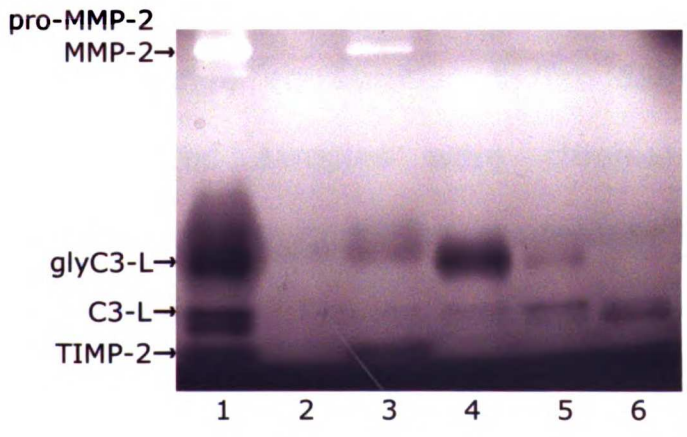

Figure 4.12: Reverse zymogram of eluted fractions from gel filtration of concentrated VP-SFM CM from pNUTC3-L BHK-21 cells chromatographed in 1.0 M NaCl, 25 mM Tris (pH 7.0), 0.025% Brij 35, 0.02% NaN3
1 - 1 µl Concentrated C3-L CM
2 - 3 µl 1X Laemmli sample buffer
3 - 3 µl Peak 1
4 - 3 µl Peak 2
5 - 3 µl Peak 3
6 - 3 µl Peak 4

characteristics because they had a difference of only 6 amino acids that form the 1st loop. Analysis by reverse zymography, Figure 4.12, demonstrated that indeed the C3-L chimera, lanes 4-6, was separated from the TIMP-1, TIMP-2 and the MMPs, lane 3. In addition, most of the glycosylated C3-L, lane 4 (Figure 4.12), was resolved from the unglycosylated C3-L, lane 5. A relatively low level of glycosylated C3-L co-eluted with the C3-L but was much less than in the previous fraction. In addition, it appeared that the processed form of C3-L, lane 6 (Figure 4.12), was separated from the full C3-L.

The separation of the VP-SFM conditioned media from pNUTC3-L BHK-21 cells was repeated twice. Eluted fractions from the three runs were pooled and concentrated. The buffer of the eluted fractions was also exchanged with ion exchange equilibration buffer containing no NaCl. This was achieved by diluting the pooled eluted fractions with ion exchange equilibration buffer during the concentration. The concentrated samples were chromatographed utilizing the ion exchange chromatography as described above and eluted fractions were collected. The ion exchange chromatogram showed extremely low levels of absorbance at 280 nm and no TIMP activity was detected in the fractions by reverse zymography (data not shown). The C3-L chimera was likely lost during the concentration and buffer exchange.

The low quantities of protein may have adhered to the walls or the filter of the 15 ml plastic concentration device.

During the last few chromatographic separations, the columns were compressing and finally collapsed. Two new columns were packed and placed in tandem but the separation could not be repeated without co-elution of MMP-2 and the chimeras. The Superdex 200 preparative grade packing is best suited for proteins between 50-200 kDa. The collapsing of the columns may have decreased the pore size, therefore, increasing their ability to discriminate smaller proteins such as the chimeras (21.5 - 22.1 kDa) resulting in the separations demonstrated in Figure 4.9 and 4.11. Superdex 75 would be a better packing for separation of the chimeras because the fractionation range is 3-70 kDa for globular proteins. To address the problem of sample loss, more VP-SFM conditioned media should be produced, concentrated, and chromatographed on a higher capacity column (26 mm x 60 cm) to obtain more chimeric protein for further purification by ion exchange and/or reverse phase chromatography.

Because TIMP-3 can be extracted from the ECM with heparan sulfate, production of TIMP-3 with VP-SFM containing 80 μM $ZnSO_4$ and heparan sulfate may result in more TIMP-3 in the conditioned medium. This conditioned medium could be concentrated and

theoretically chromatographed under similar conditions as the C3 and C3-L chimeras.

Although the goal of purifying TIMP-3 and the chimeras for binding experiments with heparan sulfate was not achieved, these gel filtration chromatography conditions provide an excellent first step towards the purification of the C3 and C3-L chimeras. Eluted fractions were not analyzed for purity by silver-stained SDS polyacrylamide gels because the primary goal of these chromatographic steps was to separate the MMP and TIMP complexes.

4.4 Bibliography

1. Lipscombe RJ, Nakhoul AM, Sanderson CJ, Coombe DR. Interleukin-5 binds to heparin/heparan sulfate. A model for an interaction with extracellular matrix. J Leukoc Biol 1998;63(3):342-50.

2. Fromm JR, Hileman RE, Weiler JM, Linhardt RJ. Interaction of fibroblast growth factor-1 and related peptides with heparan sulfate and its oligosaccharides. Arch Biochem Biophys 1997;346(2):252-62.

3. Sendak RA, Bensadoun A. Identification of a heparin-binding domain in the distal carboxyl-terminal region of lipoprotein lipase by site-directed mutagenesis. J Lipid Res 1998;39(6):1310-5.

4. Ward RV, Hembry RM, Reynolds JJ, Murphy G. The purification of tissue inhibitor of metalloproteinases-2 from its 72 kDa progelatinase complex. Demonstration of the biochemical similarities of tissue

inhibitor of metalloproteinases-2 and tissue inhibitor of metalloproteinases-1. Biochem.J. 1991;278:179-187.

5. Apte SS, Olsen BR, Murphy G. The gene structure of tissue inhibitor of metalloproteinases (TIMP)-3 and its inhibitory activities define the distinct TIMP gene family. J.Biol.Chem. 1995;270:14313-14318.

6. Negro A, Onisto M, Grassato L, Caenazzo C, Garbisa S. Recombinant human TIMP-3 from Escherichia coli: Synthesis, refolding, physico-chemical and functional insights. Protein Engineering 1997;10(5):593-599.

Chapter 5

Co-localization of TIMP-3 and Heparan Sulfate

By

Confocal Microscopy

5.1 Introduction

Part of the hypothesis is that TIMP-3 is held in the ECM by heparan sulfate chains of HSPGs. This was based on the observation by Kishnani and Hawkes that heparan sulfate-coated agarose beads could extract TIMP-3 from the ECM of cultured chicken embryo fibroblasts (1). In addition, molecular modeling of TIMP-3 and heparan sulfate demonstrated that TIMP-3 could electrostatically interact with heparan sulfate.

The heparan sulfate chains of HSPGs bind to various proteases, protease inhibitors, cytokines and growth factors such as MMP-7, anti-thrombin III, lipoprotein lipase, the FGFs, VEGF, hepatocyte growth factor, keratinocyte growth factor, and TGF-ß (2, 3). Heparan sulfate chains also bind to structural proteins in the ECM such as fibrillar collagen, fibronectin, and laminin (4). In each case HSPGs appear to function as a way of accumulating or localizing heparan sulfate binding molecules to enhance and/or promote ligand-receptor, protease-inhibitor and protease-substrate interactions. HSPGs in the the ECM include perlecan, agrin and type XVIII collagen (5). Two families of HSPGs, Syndecans-1 through –4 and glypicans-1 through –6, and two unrelated HSPGs, CD44E and the TGF-ß-receptor betaglycan have been identified on the cell surface (6, 7).

Confocal microscopy was performed to determine if TIMP-3 and heparan sulfate co-localize in cultured cells. The pNUThuTIMP-3 BHK-21 cells were also incubated with heparan sulfate to determine if Kishnani and Hawkes observations could be repeated with these cells. In addition, pNUThuTIMP-3 BHK-21 cells were incubated with heparinase III and chondroitinase ABC to determine if the degradation of heparan sulfate or chondroitinase sulfate chains would release TIMP-3 from the extracelllular matrix. Although TIMP-3 has been designated an ECM protein, Blenis and Hawkes reported that TIMP-3 also appears to be associated with the cell surface (8). The data presented in this chapter demonstrate that TIMP-3 co-localizes with heparan sulfate in the ECM and on the cell surface.

5.2 Materials and Methods

5.2.1 ***Maintenance of BHK-21 Cells*** - The BHK-21 cells were seeded at a density of 650,000 cells/100mm dish (Corning Corp.) in 10 ml of 50/50 DMEM/F-12 (Gibco BRL) containing 5% (vol./vol.) FBS (Sigma Chemical Co.) at 37 °C and 5% CO_2. Cells were passaged by aspirating the media, washing with 1 ml of PBS-CMF, adding 1ml 0.25% trypsin/0.02% EDTA, aspirating the excess trypsin/EDTA and incubating at 37 °C, 5% CO_2 for 5 min. The cells were removed by gentle washing with an appropriate amount of medium to be

subcultured at a 1:20 split ratio every 3-4 days. Every fourth passage 500 μM methotrexate in 5% FBS, DMEM/F-12 selection was reapplied in order to maintain stable, high-level expression.

5.2.2 BHK-21 Cell Growth and treatment with heparinase III - Cells were plated on 8-well Labtek glass chamber slides at 10,000 cells/well in 400 μl of 2% FBS DMEM/F-12 (UCSF Tissue Culture Facility) with 100 units/ml penicillin and 0.1 mg/ml streptomycin and maintained at 37 °C, 5% CO_2. Each cell type was plated in duplicate (BHK-21 without vector and BHK-21 transfected with pNUThuTIMP-3). After 72 h, the medium was removed from one well of each cell type and the monolayer of cells was washed with 400 μl PBS three times. Heparinase III from *Flavobacterium heparinum* (Sigma Chemical Co.), 0.5 units 100 μl of PBS was added to one well of each cell type and incubated at 37 °C, 5% CO_2 for 1.5 h. The cells were washed three times with 400 μl PBS and fixed with 400 μl of cold (4 °C) 4% paraformaldehyde in PBS for 8 min at room temperature. The wells were washed three times with 400 μl PBS.

5.2.3 Cell Growth and treatment with heparan sulfate, heparinase III and chondroitinase ABC - Cells were plated on 8-well Labtek glass chamber slides at 10,000 cells/well in 400 μl of 2% FBS DMEM/F-12 (UCSF Tissue Culture Facility) with 100 units/ml penicillin and 0.1 mg/ml streptomycin and maintained at 37 °C, 5%

CO_2, utilizing 8-wells/cell type (untransfected BHK-2 and pNUThuTIMP-3 transfected BHK-21). After 64 h, the medium was removed and an aliquot was added to 2X Laemmli sample buffer and stored at -20 °C. The monolayer of cells was rinsed three times with 400 µl PBS. The following protocol was repeated for each cell type: A 200 µl aliquot of PBS was added to two of the wells. A 200 µl aliquot of 1 mg/ml heparan sulfate (Sigma Chemical Co.) in PBS was added to two wells. A 200 µl aliquot of 5 units/ml of heparinase III from *Flavobacterium heparinum* in PBS was added to two wells. A 200 µl aliquot of 3.33 units/ml of chondroitinase ABC (Seikagaku America Inc.) was added to two wells. The slides were incubated at 37 °C, 5% CO_2 for 1.5 h. The solution from each well was mixed with an equal volume (~200 µl) 2x Laemmli sample buffer without ß-mercaptoethanol and stored at -20 °C until analyzed by reverse zymography (See Appendix). Cells were detached from one well of the two wells treated with either PBS, heparan sulfate, heparinase III, and chondroitinase ABC by rinsing the cells with PBS-CMF, adding 400 µl of 5 mM EGTA PBS-CMF and incubating the slides at 37 °C, 5% CO_2 for 15 min. The cells were rinsed off with 400 µl PBS-CMF and saved. The wells were rinsed three times with 400 µl PBS-CMF, one time with 400 µl sterile ddH_2O, and dried. The ECM was collected by pipetting 20 µl of 1x Laemmli sample buffer without ß-mercaptoethanol into the

well, moving the pipette against the bottom surface of the well and re-collecting the sample buffer. The ECM samples were stored at -20 °C until analysed by reverse zymography (See Appendix). The cells from the remaining well treated with PBS, heparan sulfate, heparinase III, and chondroitinase ABC were rinsed with 400 µl PBS and fixed with 400 µl cold (4 °C) 4% paraformaldehyde in PBS for 8 min at room temperature. The paraformaldehyde was removed and the well was rinsed three times with 400 µl PBS.

5.2.4 Staining with Anti-chkTIMP-3 Polyclonal Antibody and Anti-human Heparan Sulfate Monoclonal Antibody - The monolayer of cells was blocked with 400 µl of 0.5% BSA in PBS for 1 h on a rocking platform at room temperature. The blocking solution was aspirated from each well and replaced with rabbit anti-chkTIMP-3 pAb (Hawkes' Laboratory) diluted at 1:500 and mouse anti-human heparan sulfate mAb (Calbiochem) diluted at 1:200 in 200 µl of 0.5% BSA in PBS. The slides were incubated at 4 °C for 16 h. The primary antibody solutions were removed and the wells were gently washed three times with 300 µl 0.5% BSA PBS. Texas Red- conjugated goat anti-mouse IgG (Molecular Probes) diluted at 1:500 and Alexa Fluor 488-conjugated goat anti-rabbit IgG (Molecular Probes) diluted at 1:1000 in 200 µl of 0.5% BSA in PBS were added to each well and set on a rocking platform for 1 h at room temperature. The secondary

antibody solutions were aspirated off and the wells were washed 3 times with 300 µl PBS. The chamber dividers and seals were removed and 2-3 drops of Vector Shield (Molecular Probes) were added with a cover slip and sealed using clear nail polish. After 30 min, the slides were analyzed with the confocal microscope or stored at -20 °C.

5.2.5 Confocal Microscopy – Confocal microscopy was performed utilizing a the Bio-Rad MRC 1024 Microradiant Imaging System (Bio-Rad) with an Argon/Krypton laser tuned to an excitation wavelength of 488 nm and set to analyze emmission wavelengths of 602 nm for Texas Red and 522 nm for Alexa Fluor 488. Data were collected at 60X magnification using a sequential Z-series method with 1 µm steps.

Images from the confocal microscope were stored as *.pic files, a Bio-Rad proprietary format, on the Bio-Rad instrument. The files were transferred to a Pentium II/233MHz computer running Windows 2000 Professional and converted to *.tif (tagged image format) files using Confocal Assistant version 4.02 (Bio-Rad). Adobe Photoshop 5.5 (Adobe Systems Inc.) was utilized to merge the final images.

5.3 Results

In order to demonstrate that TIMP-3 and heparan sulfate co-localize and could interact, confocal microscopy was utilized. BHK-21 cells and BHK-21 cells transfected with pNUThuTIMP-3 were propagated on 8-well glass slides for immunofluorescence staining of TIMP-3 and heparan sulfate and analysis by confocal microscopy. TIMP-3 was detected by a rabbit anti-chicken TIMP-3 antibody and an Alexa Fluor 488-conjugated, goat anti-rabbit affinity purified secondary antibody that emits green fluorescence. Heparan sulfate was detected by a mouse anti-human heparan sulfate monoclonal antibody and a Texas Red-conjugated, goat anti-mouse affinity purified antibody that emits red fluorescence. Several fluorescent images through the plane of the cell monolayer, Z-sections, were collected sequentially to reduce fluorescent bleed from one fluorophore to the other. The green images showing TIMP-3 staining and the red images showing heparan sulfate staining were overlayed in Adobe Photoshop 5.5 to demonstrate co-localization that was depicted in yellow. Due to difficulties with color matching between the computer monitor and printer, some printed images appeared with sections of green where yellow was actually observed.

5.3.1 Confocal Microscopy of Untransfected and pNUThuTIMP-3 Transfected BHK-21 Cells

Figure 5.1 shows examples of images collected from the confocal microscope from untransfected and pNUThuTIMP-3 transfected BHK-21 cells stained with the heparan sulfate and TIMP-3 antibodies, and their respective red and green fluorescing secondary antibodies. The distribution of TIMP-3 and heparan sulfate in the untransfected BHK-21 cells appeared to be similar, Figure 5.1, A and B. However more intense staining was observed for heparan sulfate, Figure 5.1, B. Figure 5.1, C, demonstrated the complete co-localization of TIMP-3 with heparan sulfate depicted in yellow, and regions where staining was observed for heparan sulfate and not TIMP-3 depicted in red. No staining of TIMP-3 without co-localized staining of heparan sulfate, which would be depicted in green in Figure 5.1, C, was observed in the untransfected BHK-21 cells.

The detection of TIMP-3 and heparan sulfate in the pNUThuTIMP-3 transfected BHK-21 cells appeared very similar, Figure 5.1, D and E. Figure 5.1, F, demonstrates the co-localization of TIMP-3 with heparan sulfate depicted in yellow, and regions where staining was observed for heparan sulfate and not TIMP-3 depicted in red. No areas were detected where TIMP-3 staining is observed without co-localization of heparan sulfate that would be depicted in green in Figure 5.1, C. The

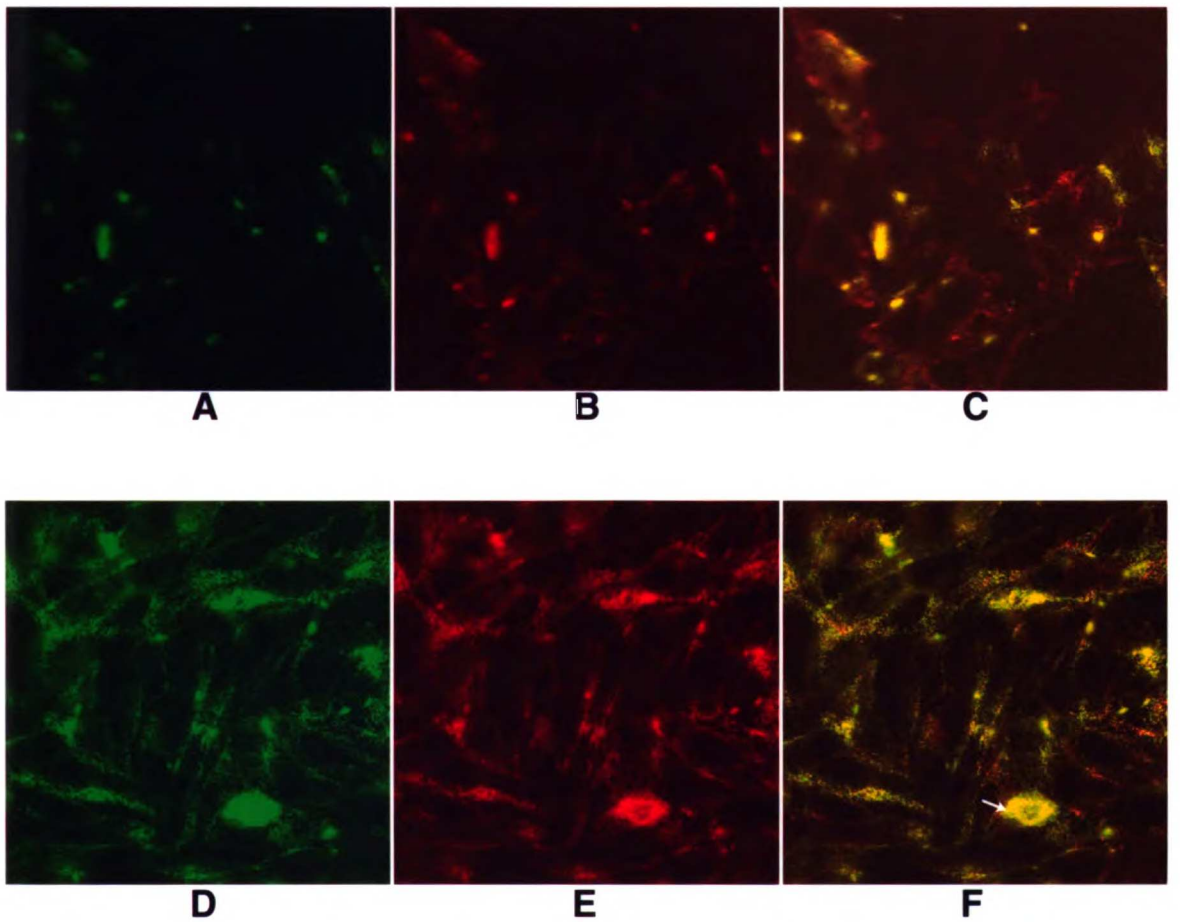

Figure 5.1: Confocal microscopy images of untransfected BHK-21 (A-C) and pNUThuTIMP-3 transfected BHK-21 (D-F). A and D - probed with rabbit anti-chicken TIMP-3 pAb and Alexa Fluor 488-conjugated, goat anti-rabbit secondary Ab emitting green fluorescence. B and E - probed with mouse anti-human heparan sulfate mAb and Texas Red-conjugated, goat anti-mouse secondary Ab emitting red fluorescence. C and F - merged images showing co-localization in yellow. All images are at 60X magnification.

relative amount of TIMP-3 observed in the pNUThuTIMP-3 BHK-21 co-localizing with heparan sulfate was much higher than that observed in the untransfected BHK-21 cells, Figure 5.1, C and F, respectively. In addition, there were significantly fewer areas of heparan sulfate staining without TIMP-3 staining observed in the pNUThuTIMP-3 than in the untransfected BHK-21 cells. Although the cell density was higher in the images of pNUThuTIMP-3 BHK-21 cells compared to the images of untransfected BHK-21 cells, the distribution of TIMP-3 and heparan sulfate was observed to be the same for other regions of each respective well. In Figure 5.1, F (white arrow), co-localization of TIMP-3 and heparan sulfate also appeared to be co-localized on the cell surface. TIMP-3 and heparan sulfate co-localization on the cell surface was observed in other images of pNUThuTIMP-3 transfected BHK-21 and untransfected BHK-21 cells.

5.3.2 Confocal Microscopy of pNUThuTIMP-3 BHK-21 Cells Incubated with Heparinase III

The pNUThuTIMP-3 transfected BHK-21 cells were incubated with heparinase III to determine if heparan sulfate degradation would release TIMP-3 from the ECM. Kishnani and Hawkes observed TIMP-3 in the conditioned media of chicken embryo fibroblasts when they were incubated with heparan sulfate (1). Heparinase III is an

endoglycosidase that specifically cleaves the 1-4 linkages between the hexosamine and glucuronic acid residues of heparan sulfate (9). The assumption was made that heparinase III would cleave the heparan sulfate binding TIMP-3 and that any TIMP-3 bound to heparan sulfate would be concomittantly released.

Figure 5.2, panels A, B and C, show examples of the untreated pNUThuTIMP-3 BHK-21 cells. The distribution of TIMP-3 and heparan sulfate in the pNUThuTIMP-3 transfected BHK-21 cells appeared very similar, Figure 5.2, A and B. Figure 5.2, C, demonstrates the complete co-localization of TIMP-3 with heparan sulfate depicted in yellow, and regions where staining was observed for heparan sulfate and not TIMP-3 depicted in red. The staining of the untreated pNUThuTIMP-3 BHK-21 cells with both antibodies appeared as a meshwork around and on the cell surface, Figure 5.2, A, B and C.

Figure 5.2, panels D, E, and F, show examples of images observed following incubation of the pNUThuTIMP-3 transfected BHK-21 cells with heparinase III in PBS. TIMP-3 and heparan sulfate staining was observed concentrated around circular areas that appeared to be partially detached cells, Figure 5.2, D and E. The co-localization of TIMP-3 and heparan sulfate is shown in Figure 5.2, F. There were no areas where TIMP-3 or heparan sulfate staining was observed alone. Small spots of intense TIMP-3 and heparan sulfate staining were also

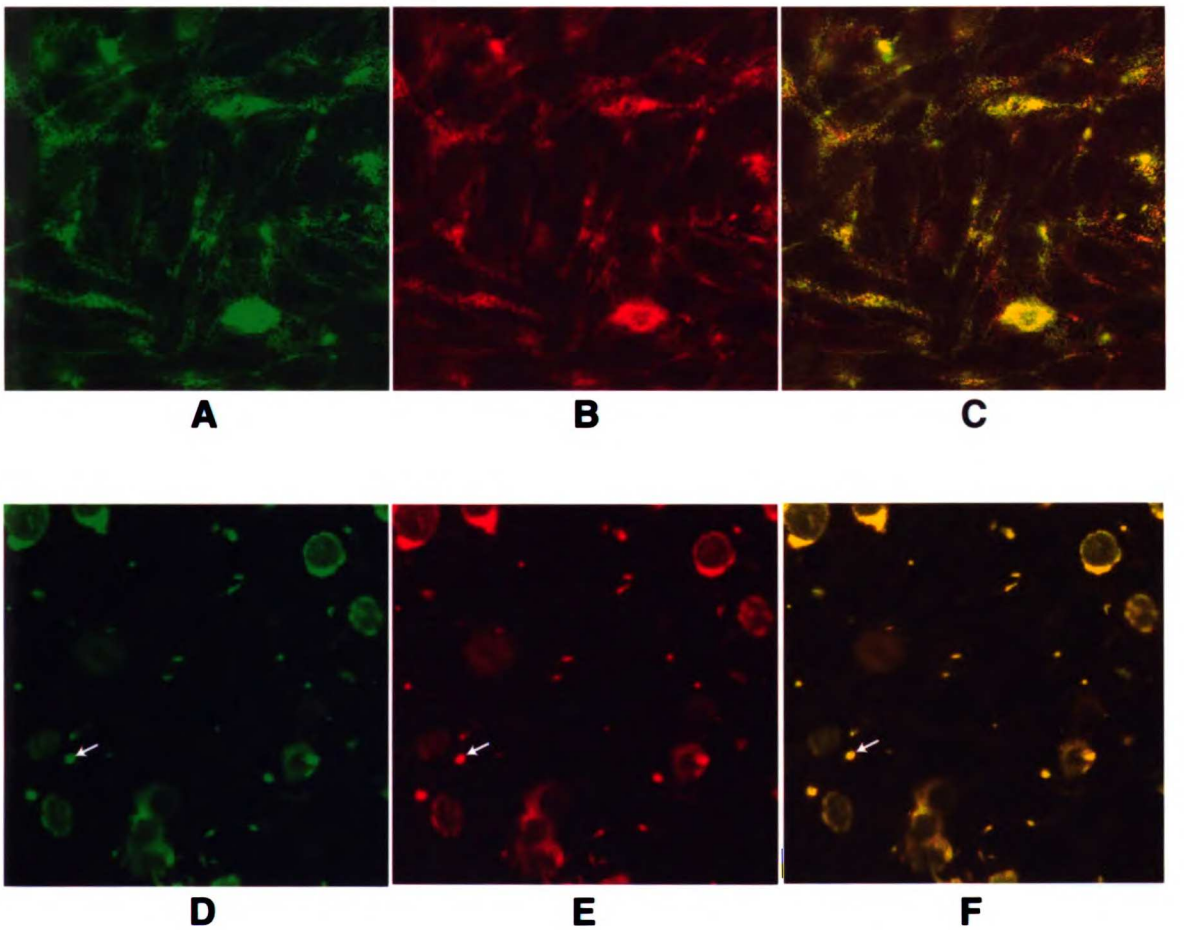

Figure 5.2: Confocal microscopy images of TIMP-3 transfected BHK-21 (A-C) and TIMP-3 transfected BHK-21 treated with heparinase III (D-F). A and D - probed with rabbit anti-chicken TIMP-3 pAb and Alexa Fluor 488-conjugated, goat anti-rabbit secondary Ab emitting green fluorescence. B and E - probed with mouse anti-human heparan sulfate mAb and Texas Red-conjugated, goat anti-mouse secondary Ab emitting red fluorescence. C and F - merged images showing co-localization in yellow. All images are at 60X magnification.

observed, Figure 5.2, D, E, and F (indicated by white arrows). These may have been anomalies or fragments of ECM or cells that concentrated in these areas. The meshwork around and on the cell surface of the heparinase III treated pNUThuTIMP-3 BHK-21 cells could barely be detected by either antibody.

5.3.3 Confocal Microscopy of pNUThuTIMP-3 BHK-21 Cells Incubated with Heparan Sulfate, Heparinase III, and Chondroitinase ABC

The heparinase III experiment was repeated. In addition, heparan sulfate and chondroitinase ABC were also incubated with the pNUThuTIMP-3 transfected BHK-21 cells. Although this did not affect the experiment, these cultures of pNUThuTIMP-3 BHK-21 cells did not appear to express much TIMP-3 as observed in the previous experiments. Figure 5.3 shows examples of confocal microscopy images observed with the incubation of the pNUThuTIMP-3 BHK-21 cells with PBS, A, heparan sulfate, B, heparinase III, C, and chondroitinase ABC. Only the co-localization images are shown in Figure 5.3. Figure 5.3, A, shows the untreated pNUThuTIMP-3 BHK-21 cells that were incubated in PBS. The co-localized staining of TIMP-3 and heparan sulfate could be seen on and around the cell surface depicted in yellow. Areas of green were actually observed as

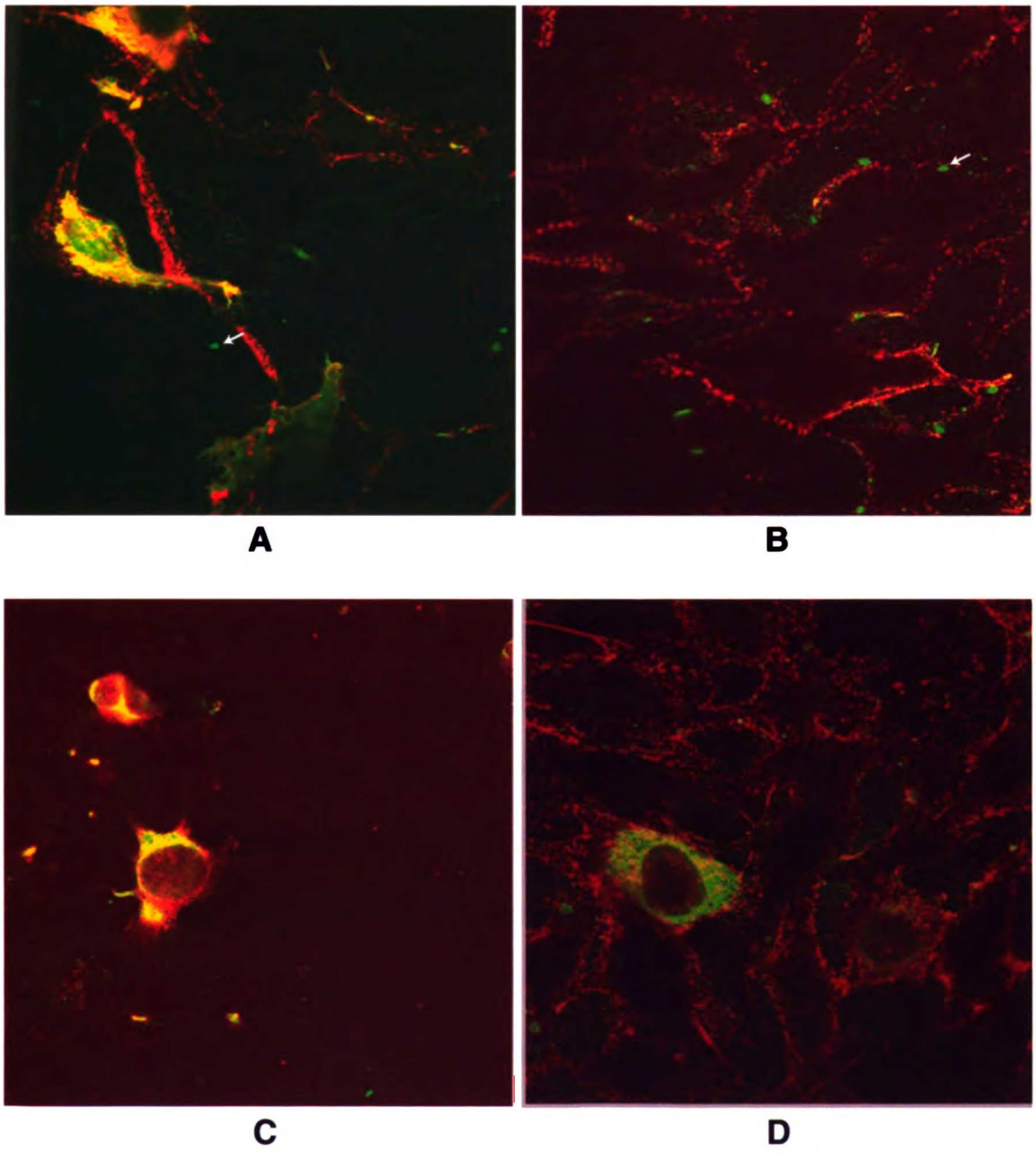

Figure 5.3: Confocal microscopy images of TIMP-3 transfected BHK-21 treated with PBS (A), heparan sulfate (B), heparinase III (C), and chondroitinase ABC (D). The cells were probed with rabbit anti-chicken TIMP-3 pAb and Alexa Fluor 488-conjugated and goat anti-rabbit secondary Ab emitting green fluorescence, and mouse anti-human heparan sulfate mAb and Texas Red-conjugated, goat anti-mouse secondary Ab emitting red fluorescence. All are merged images showing co-localization in yellow. All images are at 60X magnification.

yellow on the computer monitor except for the small green spots (indicated by white arrows) seen in Figure 5.3, A and B. These spots appeared to be anomalies from staining. Areas of heparan sulfate without TIMP-3 were observed around the untreated pNUThuTIMP-3 BHK-21 cells, Figure 5.3, A. The pNUThuTIMP-3 BHK-21 cells incubated with heparan sulfate are shown in Figure 5.3, B. Areas of co-localization, yellow (greenish) between the cells and areas staining with only heparan sulfate, red, near the edges of cells was observed. In addition, TIMP-3 or heparan sulfate staining was undetectable on the surface of the heparan sulfate treated cells.

The heparinase III treated pNUThuTIMP-3 BHK-21 cells are shown in Figure 5.3, C. This result was similar to that observed in the previous experiment except that staining was observed for heparan sulfate (depicted in red) in locations where there was no TIMP-3, Figure 5.3, C. This was possibly due to decreased expression of TIMP-3. Again intense, co-localized staining for TIMP-3 and heparan sulfate was observed around the edges of the spherical cells. In addition, the meshwork surrounding the cells and on the cell surface was not present.

The overall staining of the pNUThuTIMP-3 BHK-21 cells incubated with chondroitinase ABC appeared to be very similar to that observed for the untreated cells, Figure 5.3, D and A, respectively. Figure 5.3,

D, shows an example of the confocal microscopy images collected from pNUThuTIMP-3 BHK-21 cells incubated with chondroitinase ABC. Co-localization of TIMP-3 and heparan sulfate was observed on the surface of cells and around some of the cells. In addition, the meshwork was still intact around and on the cells.

5.3.4 Reverse Zymography of Incubation Solutions and Extracellular Matrix from pNUThuTIMP-3 BHK-21 Cells Incubated with Heparan Sulfate, Heparinase III, and Chrondroitinase ABC

The incubation solutions and ECM were collected from duplicate wells of the pNUThuTIMP-3 BHK-21 cells incubated with heparan sulfate, heparinase III, and chondroitinase ABC and analyzed by reverse zymography. Figure 5.4, panel A, shows the reverse zymogram of ECM of pNUThuTIMP-3 BHK-21 cells incubated with PBS, lane 1, heparan sulfate, lane 2, heparinase III, lane 3, and chondroitinase ABC, lane 4. All samples appeared to have similar amounts of TIMP-3 activity and glycosylated TIMP-3 activity (original gel shows gly-TIMP-3 activity to be similar among all samples). Figure 5.4, panel B, shows the reverse zymogram of the incubation solution from the pNUThuTIMP-3 BHK-21 cells incubated with PBS, lane 1, heparan sulfate, lane 2, heparinase III, lane 3, and chondroitinase

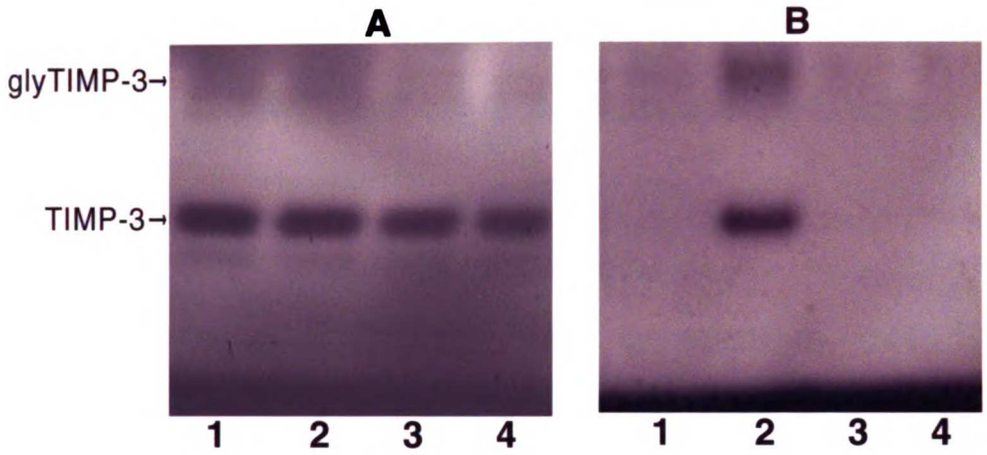

Figure 5.4. Reverse zymogram of extracellular matrix (A) and incubation solutions (B) from pNUThuTIMP-3 transfected BHK-21 cells treated with PBS (1), heparan sulfate (2), heparinase III (3), and chondroitinase ABC (4). glyTIMP-3 - glycosylated TIMP-3. Note: Gels A and B were electrophoresed separately.

ABC, lane 4. Glycosylated TIMP-3 and unglycosylated TIMP-3 activity were only detected in the heparan sulfate incubation solution, Figure 5.4, panel B, lane 2, and not in the other solutions, lanes 1, 3, and 4.

5.4 Discussion

The confocal microscopy data demonstrate that TIMP-3 and heparan sulfate co-localize in cell cultures of untransfected and pNUThuTIMP-3 transfected BHK-21 cells. In addition, they provide the first definitive demonstration of cell surface-associated TIMP-3. Heparinase III treatment of TIMP-3 BHK-21 cells results in less staining of the ECM with both TIMP-3 and heparan sulfate antibodies. In addition, as demonstrated by reverse zymography, TIMP-3 is extracted by heparan sulfate but not by PBS, heparinase III, or chondroitinase ABC. Although heparinase III treatment results in the loss of the meshwork staining of the ECM with heparan sulfate antibody, TIMP-3 is not released into the heparinase III enzyme solution.

The data reported here with pNUThuTIMP-3 transfected BHK-21 cells are in agreement with the observation of Kishnani and Hawkes that demonstrated heparan sulfate treatment of chicken embryo fibroblasts results in the extraction of TIMP-3 (1). However, in the experiments reported here, it does not appear that the TIMP-3 is

derived from the ECM but rather from the cell surface. The heparan sulfate incubation solution contained TIMP-3 activity that was not detected in the PBS control or the heparinase III and chrondroitinase ABC incubation solutions. The TIMP-3 activity in the heparan sulfate incubation solution did not appear to come from the ECM because the ECM samples collected from all of the incubation experiments appeared to have the same amount of TIMP-3 activity. Lowe-Krentz *et al.* demonstrated that addition of heparin to cultures of porcine aortic endothelial cells results in the release of approximately half of the cell surface HSPGs and none of the ECM HSPGs (10). They determined that the released HSPGs are intercalated with or possibly bound in the cell surface or are interacting through their heparan sulfate chains with some molecule on the cell surface such as a receptor. It is feasible that the heparan sulfate added to the BHK-21 cells would have a similar effect as heparin. The heparan sulfate that was added to the pNUThuTIMP-3 BHK-21 cells could have caused the release of HSPGs from the cell surface resulting in the TIMP-3 activity observed in the incubation solution.

Although heparinase III treatment does not result in TIMP-3 extraction, the cells that are treated with heparinase III appear to detach and retract, Figure 5.2, F, and 5.3, C, and the TIMP-3 appears more dense around the cells. HSPGs have been demonstrated to be

necessary for cellular attachment and have been linked to integrin-mediated cell adhesion (11). The HSPGs involved in adhesion may be accessible and cleaved by heparinase III. Degradation of this population of heparan sulfate molecules may cause the cells to detach and appear spherical. The TIMP-3 on the cell surface and in the ECM may not be released because the TIMP-3 may block the cleavage sites of heparan sulfate thus rendering them inaccessible to heparinase III. Blenis and Hawkes have demonstrated that more TIMP-3 could be radioactively labeled in the ECM when the cells are detached than when the cells are left attached (8). This suggests that the cells themselves may be limiting accessibility to TIMP-3 in the ECM beneath cells. In addition, the amount of TIMP-3 activity in the ECM of pNUThuTIMP-3 BHK-21 cells incubated in PBS, heparan sulfate, heparinase III, and chondroitinase ABC were similar. This would suggest that the TIMP-3 on the cell surface remains with the detached cells. EGTA detached pNUThuTIMP-3 cells that were lysed in Laemmli sample buffer without reducing agent have a high degree of TIMP-3 activity when analyzed by reverse zymography (data not shown). However, this activity could be attributed to newly synthesized TIMP-3 that has not been released from the cytoplasm.

Although Li and Hawkes have observed TIMP-3 in the nucleus of transformed chicken embryo fibroblasts (personal communication), a

nuclear localization was not observed in the BHK-21 cells. These data have confirmed that TIMP-3 and heparan sulfate are in the same location where they could interact. The conclusion cannot be made that the molecules indeed do interact because the resolution of these confocal microscopy experiments is only in the sub-micrometer range. To demonstrate by microscopy that TIMP-3 and heparan sulfate do interact, fluorescence resonance energy transfer microscopy would need to be performed where contact between the two molecules (within 100Å) would be necessary for fluorescence to be observed. Other methods such as immunoprecipitation and cross-linking were not utilized because of the complexity of the ECM and because the SDS that would be required to collect the ECM would undoubtedly disrupt the very interactions that were being probed.

The localization of TIMP-3 at the cell surface through interactions with membrane-anchored HSPGs such as syndecans or glypicans, would place TIMP-3 in a region where it could closely regulate MMP activity near the cell surface. Recently, Yu and Woessner demonstrated that MMP-7 and HSPGs co-localize by confocal fluorescence microscopy in the apical region of uterine glandular epithelial cells (12). Butler *et al.* demonstrated increased binding of TIMP-3 to MMP-2 in the presence of heparan sulfate (13). ProMMP-2 activation is regulated at the cell surface by the MT1-MMP/TIMP-2

complex. TIMP-3, held at the cell surface by HSPGs, could provide additional regulation of MMP-2 activity. In addition, membrane bound HSPGs may be a mechanism for the cell to localize TIMP-3 at the cell surface, where it can closely regulate the inhibitory activities of TIMP-3. The result could be focalized inhibition of MMPs preventing ECM degradation that could result in accumulation of ECM components at the contact sites allowing for other cell-matrix interactions.

Interestingly, TIMP-3 inhibits a metalloproteinase that is believed to be an ADAM, a disintegrin and metalloproteinase, involved in the shedding of syndecan-1 and -4 from the cell surface (14). Binding of TIMP-3 to heparan sulfate chains of syndecans at the cell surface could provide a mechanism for close regulation of the shedding process. This possibility is supported by the observation that shedding of both L-selectin and TNFα from the cell surface are also inhibited by TIMP-3 (15-17). This novel function of inhibiting shedding that is displayed by TIMP-3 may lead to a better understanding of apoptosis, angiogenesis, invasion, and cell-cell and cell-matrix interactions.

5.5 Bibliography

1. Kishnani N. Characterization of Tissue Inhibitor of Metalloproteinases-3 (TIMP-3) from the Extracellular Matrices of Cultured Human and Avian Cells [Ph.D.]. San Francisco: University of California San Francisco; 1994.

2. Eisenberg S, Sehayek E, Olivecrona T, Vlodavsky I. Lipoprotein lipase enhances binding of lipoproteins to heparan sulfate on cell surfaces and extracellular matrix. Journal of Clinical Investigation 1992;90(5):2013-21.

3. Tanaka Y, Kimata K, Adams DH, Eto S. Modulation of cytokine function by heparan sulfate proteoglycans: sophisticated models for the regulation of cellular responses to cytokines. Proc Assoc Am Physicians 1998;110(2):118-25.

4. Gallagher JT. Heparan sulphate and protein recognition. Binding specificities and activation mechanisms. Adv Exp Med Biol 1995;376:125-34.

5. Halfter W, Dong S, Schurer B, Cole GJ. Collagen XVIII is a basement membrane heparan sulfate proteoglycan. J Biol Chem 1998;273(39):25404-12.

6. Veugelers M, De Cat B, Ceulemans H, Bruystens AM, Coomans C, Deurr J, et al. Glypican-6, a new member of the glypican family of

cell surface heparan sulfate proteoglycans. Journal of Biological Chemistry 1999;274(38):26968-77.

7. Tumova S, Woods A, Couchman JR. Heparan sulfate proteoglycans on the cell surface: versatile coordinators of cellular functions. Int J Biochem Cell Biol 2000;32(3):269-88.

8. Blenis J, Hawkes SP. Characterization of a transformation-sensitive protein in the extracellular matrix of chicken embryo fibroblasts. J Biol Chem 1984;259(18):11563-70.

9. Desai UR, Wang HM, Linhardt RJ. Substrate specificity of the heparin lyases from Flavobacterium heparinum. Arch Biochem Biophys 1993;306(2):461-8.

10. Lowe-Krentz LJ, Thompson K, Patton WAd. Heparin releasable and nonreleasable forms of heparan sulfate proteoglycan are found on the surfaces of cultured porcine aortic endothelial cells. Mol Cell Biochem 1992;109(1):51-60.

11. Klaśs CM, Couchman JR, Woods A. Control of extracellular matrix assembly by syndecan-2 proteoglycan. Journal of Cell Science 2000;113(Pt 3)):493-506.

12. Yu WH, Woessner JF, Jr. Heparan sulfate proteoglycans as extracellular docking molecules for matrilysin (matrix metalloproteinase 7). Journal of Biological Chemistry 2000;275(6):4183-91.

13. Butler GS, Apte SS, Willenbrock F, Murphy G. Human tissue inhibitor of metalloproteinases 3 interacts with both the N- and C-terminal domains of gelatinases A and B. Regulation by polyanions. Journal of Biological Chemistry 1999;274(16):10846-51.

14. Fitzgerald ML, Wang Z, Park PW, Murphy G, Bernfield M. Shedding of syndecan-1 and -4 ectodomains is regulated by multiple signaling pathways and mediated by a TIMP-3-sensitive metalloproteinase. Journal of Cell Biology 2000;148(4):811-24.

15. Amour A, Slocombe PM, Webster A, Butler M, Knight CG, Smith BJ, et al. TNF-alpha converting enzyme (TACE) is inhibited by TIMP-3. FEBS Lett 1998;435(1):39-44.

16. Borland G, Murphy G, Ager A. Tissue inhibitor of metalloproteinases-3 inhibits shedding of L-selectin from leukocytes. J Biol Chem 1999;274(5):2810-5.

17. Smith MR, Kung H, Durum SK, Colburn NH, Sun Y. TIMP-3 induces cell death by stabilizing TNF-alpha receptors on the surface of human colon carcinoma cells. Cytokine 1997;9(10):770-80.

Chapter 6

Growth Effects of the Wild-Type and Chimeric TIMPs

6.1 Introduction

In 1975, Bauer *et al.* and McCroskery *et al.* first described a natural inhibitor of MMPs that was later designated TIMP and eventually, TIMP-1 (1, 2). Two years later, while studying erythropoiesis, a protein with erythroid-potentiating activity, EPA, was discovered in leukoctye-conditioned media free of erythropoietin (3, 4). It was not until eight years later that Docherty *et al.* sequenced TIMP and discovered that EPA and TIMP were identical (5, 6). Other proteins, originally described by their cytokine effects, such as tumor promoting factor, TPA-S1, phorbin, and embryogenin-1 were later found to be TIMP-1 (7, 8). In 1992, TIMP-2 was also demonstrated to have erythroid potentiating activity (9).

Hayakawa *et al.* demonstrated that TIMP-1 and TIMP-2 promote the growth of several types of adherent and non-adherent human and bovine cells (10). These authors postulated that the MMP activity and growth-promoting activity were independent and in 1994, they did indeed demonstrate that reduction and alkylation of TIMP-1 destroys its MMP inhibitory activity but not its growth-promoting activity (11). In addition, Chesler et al. demonstrated that point mutations of TIMP-1 abolish the MMP inhibitory activity while retaining the growth-promoting activity (12). Utilizing a TIMP-2 variant with an alanine on the amino terminus that abolishes MMP inhibitory, Wingfield

et al. have also reported that the two actvities are separate (13). Corcoran *et al.* further characterized the cytokine activity of TIMP-2 by demonstrating that it activates adenylate cyclase through a G-protein coupled receptor that increases cAMP dependent protein kinase activity, resulting in cell proliferation (14).

In contrast, TIMP-3 has been shown to induce apoptosis in HeLa, HT1080, colon carcinoma and vascular smooth muscle cell lines (15-17). By using synthetic MMP inhibitors, the investigators demonstrated that the effect was independent of MMP inhibition. Although, in 1992, Yang and Hawkes reported that TIMP-3 stimulates the proliferation of chicken embryo fibroblasts, this could be interpreted as apoptosis because DNA synthesis was slowed by addition of TIMP-3 to transformed cells (18). Smith *et al.* suggested that TIMP-3 might induce apoptosis by stabilizing the TNFalpha receptor and preventing shedding of the TNFalpha receptor from the surface of the cell (15). A year later, it was discovered that TIMP-3, and not TIMP-1 or TIMP-2, inhibits TNFalpha converting enzyme, TACE (19). In contrast to the ability of TIMP-3 to induce apoptosis, TIMP-1 and TIMP-2 have the ability to rescue cells from apoptosis. Li *et al.* demonstrated that TIMP-1 inhibits MCF10A cell death induced by hydrogen peroxide, adriamycin, or X-ray irradiation (20). The inhibition of apoptosis occurred after the MCF10A cells detached and,

therefore, was not dependent on the stabilization of the matrix by TIMP-1. Valente *et al.* reported that B16F10 melanoma cells are also protected from apoptosis by TIMP-2 (21).

Experiments were performed to study the effects of wild-type and chimeric TIMP proteins on the growth of the BHK-21 cells. All nine cell lines, BHK-21 without pNUT vector, pNUT BHK-21, pNUThuTIMP-3 BHK-21, pNUThuTIMP-2 BHK-21, pNUTC3 BHK-21, pNUTC2 BHK-21, pNUTC2cT3 BHK-21, pNUTC3-L BHK-21, and pNUTT3cT2 BHK-21, were grown over a six day period to analyze their relative growth rates and determine if any cells were undergoing apoptosis.

6.2 Materials and Methods

6.2.1 Seeding and growth of BHK-21 cell lines - BHK-21 without pNUT vector, pNUT BHK-21, pNUThuTIMP-3 BHK-21, pNUThuTIMP-2 BHK-21, pNUTC3 BHK-21, pNUTC2 BHK-21, pNUTC2cT3 BHK-21, pNUTC3-L BHK-21, and pNUTT3cT2 BHK-21 cells were thawed from stocks stored at -80 °C. Cells had been stored frozen in 50% FBS, 5% DMSO DMEM/F-12 with 100 units/ml penicillin and 0.1 mg/ml streptomycin. The cells were seeded in 10 cm dishes in DMEM/F-12 with a final FBS concentration of ~5%. The cells were maintained at 37 °C and 5% CO_2 for 24 h before and then passaged 1:20 in 1% FBS DMEM/F-12 with 100 units/ml penicillin and 0.1 mg/ml

streptomycin. Twenty fours h before the next passage, the media were changed to 0.5% FBS DMEM/F-12 with 100 units/ml penicillin and 0.1 mg/ml streptomycin. Each cell line was passaged into 0.5% DMEM/F-12 with 100 units/ml penicillin and 0.1 mg/ml streptomycin into 6 wells of a 6-well plate (Falcon) at 25,000 cells/well.

6.2.2 Cell Proliferation Assay - Cells were counted at approximately 24 h intervals over a 6-day period. The media were removed, checked for volume and saved. The cells were gently washed with 500 µl of PBS-CMF, that was aspirated and replaced with 500 µl of 0.25% trypsin, 0.02% EDTA solution. The trypsin-EDTA solution was removed after 15-30 sec and the plates were incubated at 37 °C and 5% CO_2 for 4 min. The cells were washed from the plate using the saved conditioned media and were added to 50 µl of 0.4% trypan blue in PBS. After 5 min the number of viable cells was determined with a hemocytometer.

6.3 Results

Several preliminary experiments were performed to determine optimal parameters of serum concentration, cell density, and time points. Initially, the experiment was performed using two different cell densities, 1 x 10^5 and 2 x 10^5 cells/9.6 cm^2 well, in 2.5% FBS DMEM/F-12, Figures 6.1 and 6.2. Data points were collected only for a

48 h period. This was not sufficient time to obtain saturated growth data. Therefore, an extended experiment using 5 x 10^4 cells/9.6 cm^2 well, in 1% FBS DMEM/F-12 was performed over a 6 day period, Figure 6.3. In this experiment, it appeared that the pNUT BHK-21 cells were seeded higher than the expected 5 x 10^4 cells/well. Although the data in Figures 6.1-6.3 clearly overlap, a trend can be determined. In each of these experiments, Figures 6.1-6.3, the pNUThuTIMP-3 BHK-21 cells exhibited the lower growth rate. However, these cells did not appear to be apoptotic because less than 1% of the cells were not viable as assessed by the trypan blue assay. The untransfected BHK-21 cells proliferated faster than any of the cell types including the pNUT BHK-21 cells. The cells transfected with TIMP-2, C2, or C2cT3 appeared to grow faster than those transfected with C3, C3-L, or T3cT2. They were clearly more prolific than the TIMP-3 transfected cells. After 4 days of growth, it became difficult to determine the correct cell counts because the cells would stack and clump. Trypsinization would disperse the clumped cells but many cells would lyse. Therefore, another experiment starting at a lower density was performed.

Figure 6.4 is the graph of the growth experiment for cells seeded at 2.5 x 10^4 cells/well. At this density, cells would still clump and stack after 4 days of growth. Some would form mounds that

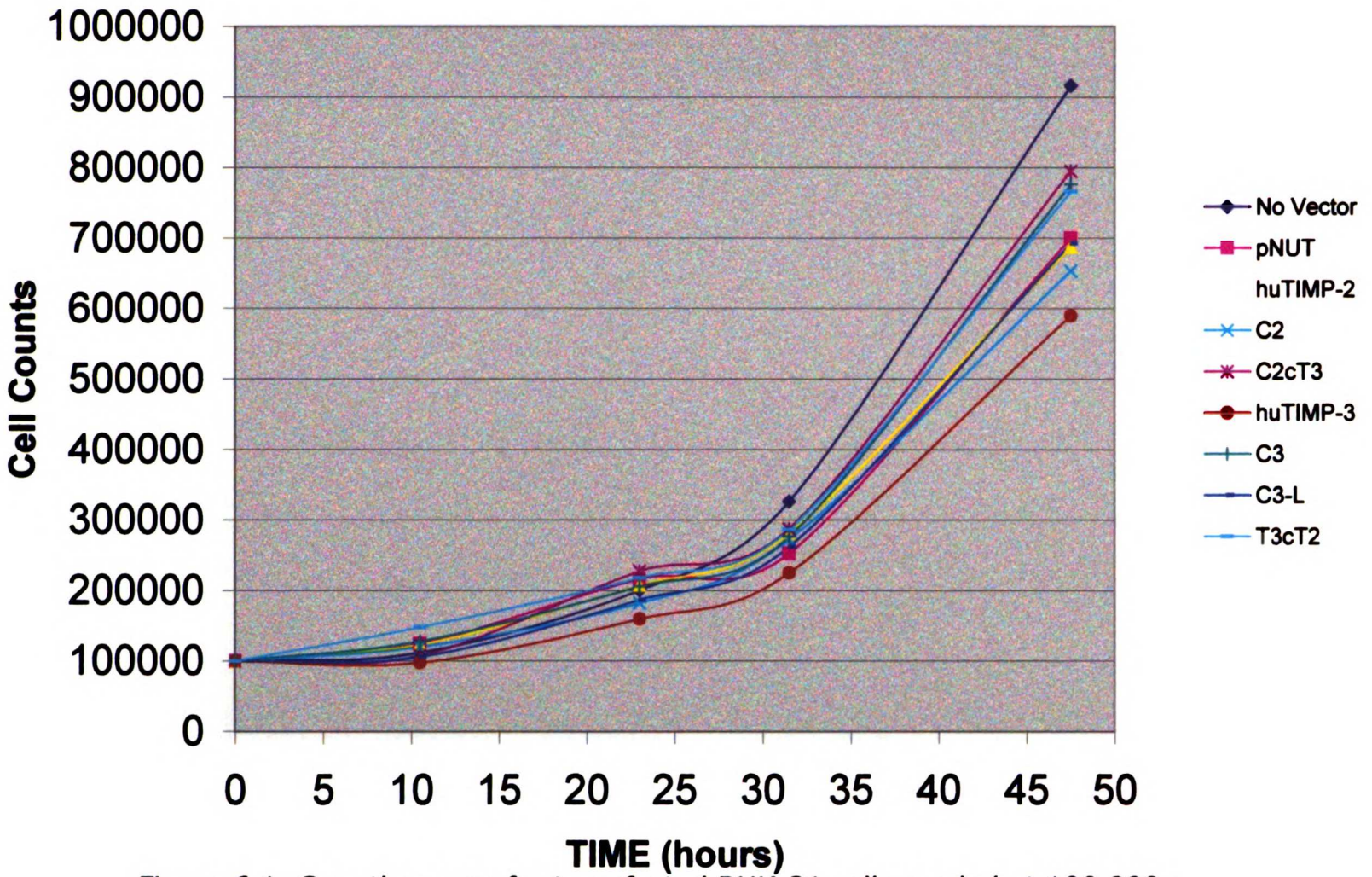

Figure 6.1. Growth curves for transfected BHK-21 cells seeded at 100,000 cells/well in 2.5% FBS DMEM/F-12.

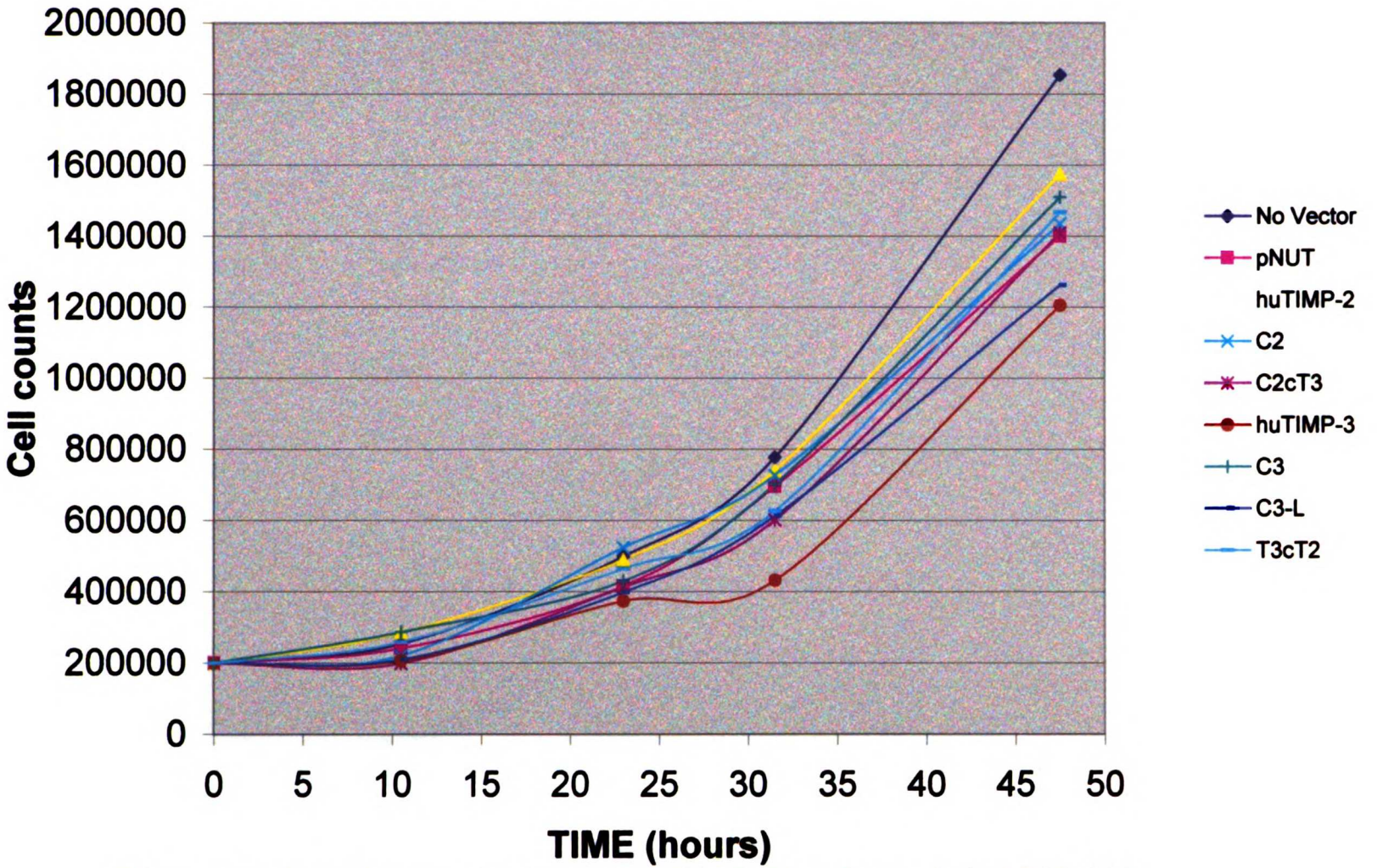

Figure 6.2. Growth curves for transfected BHK-21 cells seeded at 200,000 cells/well in 2.5% FBS DMEM/F-12.

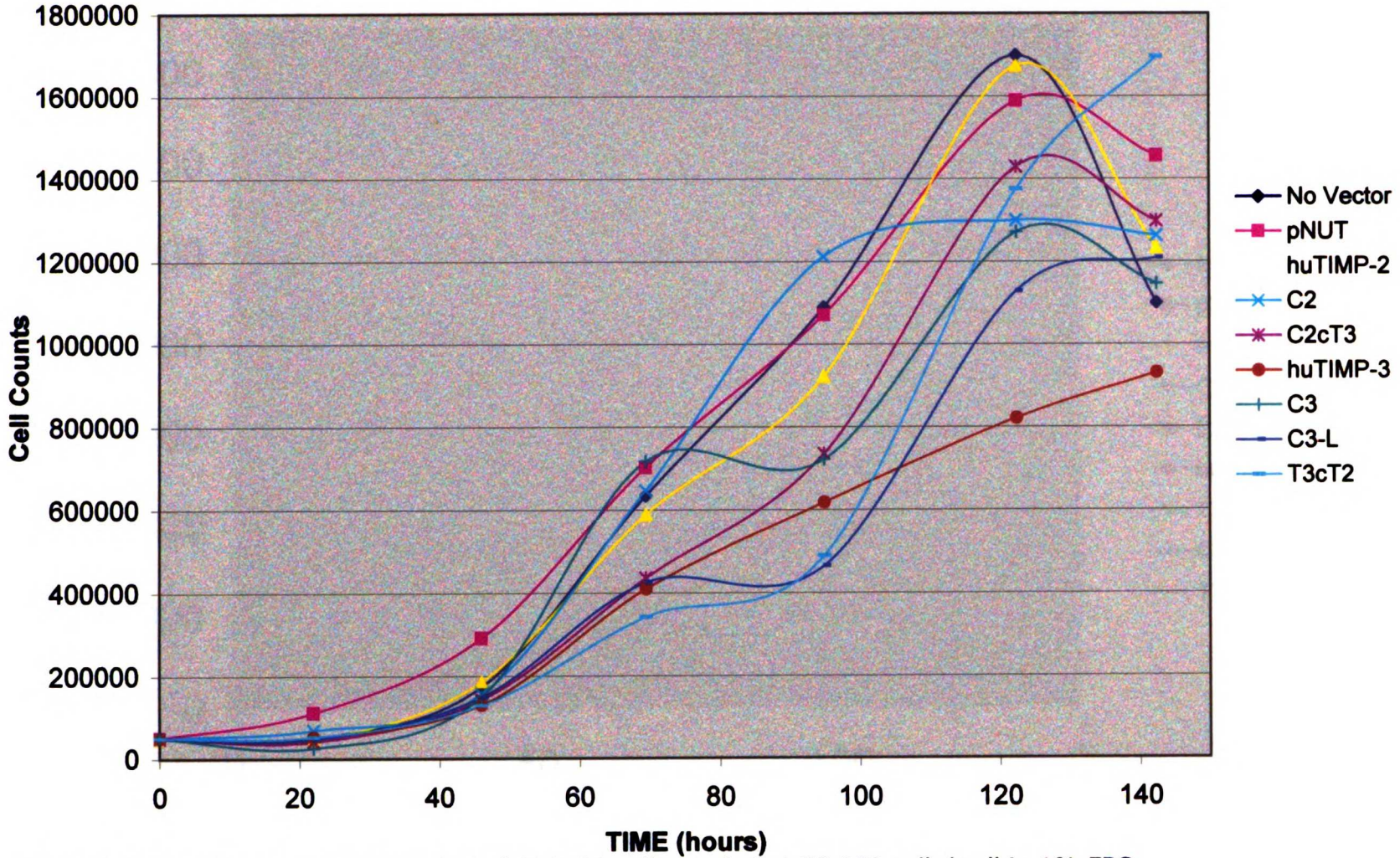

Figure 6.3. Growth curves for transfected BHK-21 cells seeded at 50,000 cells/well in 1% FBS DMEM/F-12.

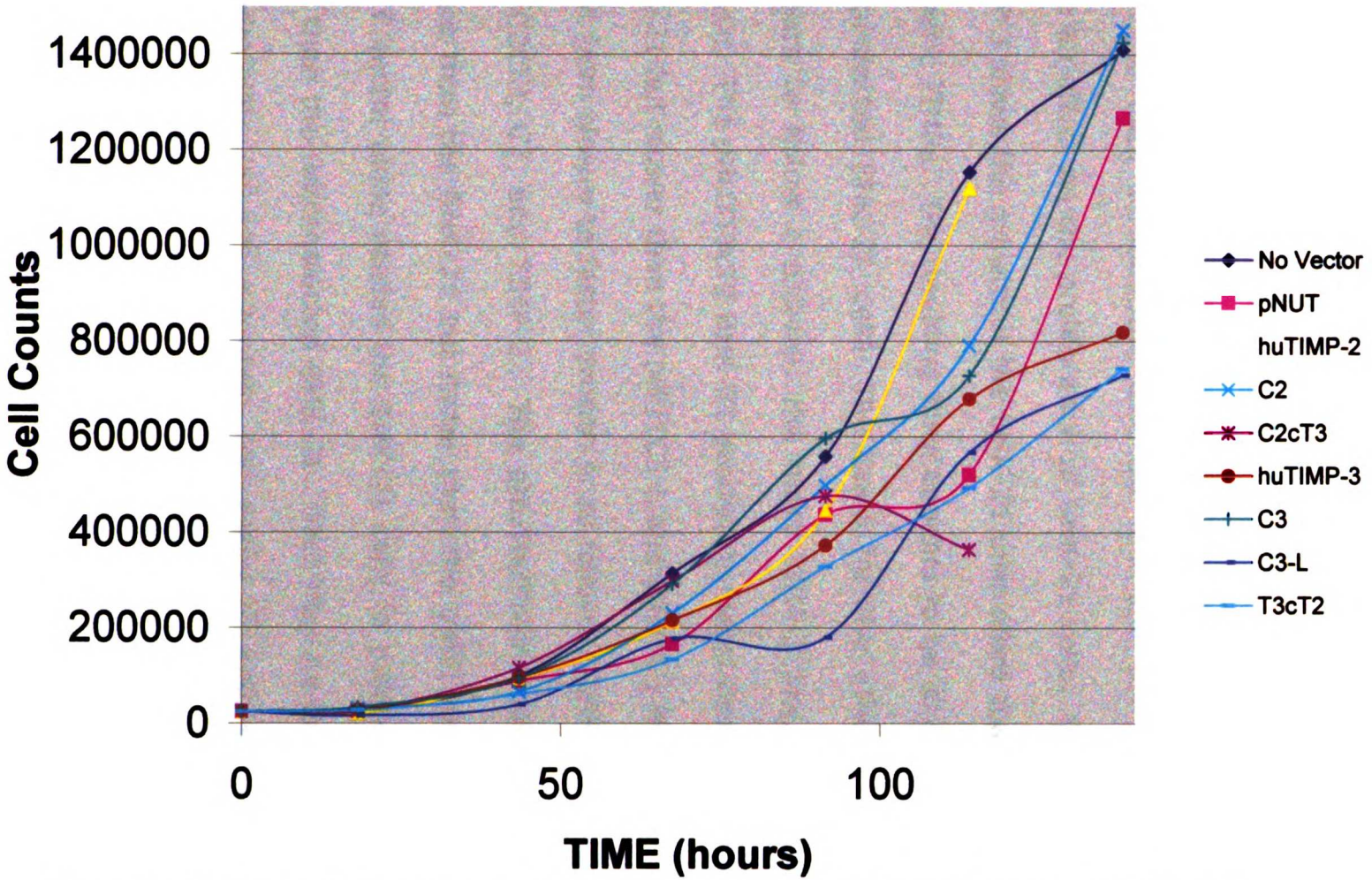

Figure 6.4. Growth curves for transfected BHK-21 cells seeded at 25,000 cell/well in 0.5% FBS DMEM/F-12. pNUTC2cT3 BHK-21 were contaminated after 120 hours.

appeared as islands in the media. This stacking was not dependent on the type of TIMP protein being expressed. The growth trend was similar to the previous experiment.

6.4 Discussion

These data demonstrate that the chimeric and wild-type TIMPs have an effect on the proliferation of BHK-21 cells. Clearly, wild-type TIMP-3 slows the growth of the BHK-21 cells more than TIMP-2 or the chimeric TIMPs. The doubling time appears to be almost twice that of untransfected BHK-21 cells. The trend for the other TIMP proteins appears to follow a pattern: the more TIMP-3 like, the slower the growth. The pNUTT3cT2 BHK-21 proliferate faster than pNUThuTIMP-3 BHK-21 but slower than the pNUTC3-L and pNUTC3 BHK-21 cells. The trend from slower to faster growth is as follows: TIMP-3, T3cT2, C3-L, C3, C2cT3, C2, and TIMP-2. The pNUThuTIMP-2 BHK-21 cells grow slower than the BHK-21 but faster than the pNUT BHK-21 cells. The pNUT vector alone causes the BHK-21 cells to proliferate at a slower rate than the untransfected BHK-21. This may be due to the mutant dihydrofolate reductase protein, expressed through the pNUT vector slowing the normal turnover of the folic acid system. The TIMP-2 transfected BHK-21 cells apparently have the ability to overcome this, possibly through the adenylate cyclase activation.

Although all cell types were viable over the 6-day period using the trypan blue test, apoptosis cannot be ruled out. A 6-day period may have not been enough time to observe cell death. An apoptosis assay such as the TUNEL assay (Terminal deoxynucleotidyl Transferase-mediated dUTP nick end labeling) may be able to detect early stages of apoptosis.

The BHK-21 cells expressing the wild-type and chimeric TIMPs is not an optimal system to study the growth effects of these proteins. Because MMP inhibitory activity and cytokine activities are separate functions of the TIMPs, the effects of these activities cannot be distinguished in the BHK-21 cells expressing the wild-type TIMPs and chimeras. The protein would be most usefully expressed in TIMP-3 -/- and/or TIMP-2 -/- cells. In order to make a distinction between the inhibitory and cytokine effects, the expressed proteins should be purified and added to cells in both reduced and non-reduced forms. Alternatively, the TIMP or chimera could be expressed with an additional alanine on the N-terminus (13).

These chimeras may provide useful tools to probe the effect of localization of the TIMPs on the cellular microenvironment. For example, two immediate questions are: 1) Does the unique localization of TIMP-3 on the cell surface and to the ECM affect its ability to induce apoptosis or is this due to its inhibitory selectivity? 2) Does the

localization of TIMP-1 and TIMP-2 affect their ability to inhibit apoptosis? Because the C3-L chimera does not localize to the cell surface or ECM and if it has the same inhibitory selectivity as wild-type TIMP-3, experiments with the C3-L chimera may be able to answer the first question.

The MMP inhibitory and cell proliferation activities of the TIMPs are separate functions (10, 12, 13). The unique property of TIMP-3 to localize to the ECM and cell surface may focalize these activities. Chimeras such as those reported in this thesis may aid in understanding the effects these separate functions have on cells and their environment.

6.5 Bibliography

1. Bauer EA, Stricklin GP, Jeffrey JJ, Eisen AZ. Collagenase production by human skin fibroblasts. Biochemical and Biophysical Research Communications 1975;64(1):232-40.

2. McCroskery PA, Richards JF, Harris ED, Jr. Purification and characterization of a collagenase extracted from rabbit tumours. Biochemical Journal 1975;152(1):131-42.

3. Johnson GR, Metcalf D. Pure and mixed erythroid colony formation in vitro stimulated by spleen conditioned medium with no detectable erythropoietin. Proceedings of the National Academy of Sciences of the United States of America 1977;74(9):3879-82.

4. Aye MT. Erythroid colony formation in cultures of human marrow: effect of leukocyte conditioned medium. Journal of Cellular Physiology 1977;91(1):69-77.

5. Docherty AJ, Lyons A, Smith BJ, Wright EM, Stephens PE, Harris TJ, et al. Sequence of human tissue inhibitor of metalloproteinases and its identity to erythroid-potentiating activity. Nature 1985;318(6041):66-9.

6. Gasson JC, Bersch N, Golde DW. Characterization of purified human erythroid-potentiating activity. Prog Clin Biol Res 1985;184:95-104.

7. Johnson MD, Housey GM, O'Brian CA, Kirschmeier PT, Weinstein IB. Role of protein kinase C in regulation of gene expression and relevance to tumor promotion. Environ Health Perspect 1987;76:89-95.

8. Satoh T, Kobayashi K, Yamashita S, Kikuchi M, Sendai Y, Hoshi H. Tissue inhibitor of metalloproteinases (TIMP-1) produced by granulosa and oviduct cells enhances in vitro development of bovine embryo. Biol.Reprod. 1994;50:835-844.

9. Stetler-Stevenson WG, Bersch N, Golde DW. Tissue inhibitor of metalloproteinase-2 (TIMP-2) has erythroid-potentiating activity. FEBS Lett. 1992;296:231-234.

10. Hayakawa T, Yamashita K, Tanzawa K, Uchijima E, Iwata K. Growth-promoting activity of tissue inhibitor of metalloproteinases-1 (TIMP-1) for a wide range of cells. A possible new growth factor in serum. FEBS Lett. 1992;298:29-32.

11. Hayakawa T, Yamashita K, Ohuchi E, Shinagawa A. Cell growth-promoting activity of tissue inhibitor of metalloproteinases-2 (TIMP-2). J.Cell Sci. 1994;107:2373-2379.

12. Chesler L, Golde DW, Bersch N, Johnson MD. Metalloproteinase inhibition and erythroid potentiation are independent activities of tissue inhibitor of metalloproteinases-1. Blood 1995;86(12):4506-15.

13. Wingfield PT, Sax JK, Stahl SJ, Kaufman J, Palmer I, Chung V, et al. Biophysical and functional characterization of full-length, recombinant human tissue inhibitor of metalloproteinases-2 TIMP-2 produced in Escherichia coli. Comparison of wild type and amino-terminal alanine appended variant with implications for the mechanism of TIMP functions. Journal of Biological Chemistry 1999;274(30):21362-8.

14. Corcoran ML, Stetler-Stevenson WG. Tissue inhibitor of metalloproteinase-2 stimulates fibroblast proliferation via a cAMP-dependent mechanism. J.Biol.Chem. 1995;270:13453-13459.

15. Smith MR, Kung H, Durum SK, Colburn NH, Sun Y. TIMP-3 induces cell death by stabilizing TNF-alpha receptors on the surface of human colon carcinoma cells. Cytokine 1997;9(10):770-80.

16. Baker AH, Zaltsman AB, George SJ, Newby AC. Divergent effects of tissue inhibitor of metalloproteinase-1, -2, or -3 overexpression on rat vascular smooth muscle cell invasion, proliferation, and death in vitro. TIMP-3 promotes apoptosis. J Clin Invest 1998;101(6):1478-87.

17. Baker AH, George SJ, Zaltsman AB, Murphy G, Newby AC. Inhibition of invasion and induction of apoptotic cell death of cancer cell lines by overexpression of TIMP-3. Br J Cancer 1999;79(9-10):1347-55.

18. Yang TT, Hawkes SP. Role of the 21-kDa protein TIMP-3 in Oncogenic transformation of cultured chicken embryo fibroblasts. Proc.Natl.Acad.Sci.U.S.A. 1992;89:10676-10680.

19. Amour A, Slocombe PM, Webster A, Butler M, Knight CG, Smith BJ, et al. TNF-alpha converting enzyme (TACE) is inhibited by TIMP-3. FEBS Lett 1998;435(1):39-44.

20. Li G, Fridman R, Kim HR. Tissue inhibitor of metalloproteinase-1 inhibits apoptosis of human breast epithelial cells. Cancer Research 1999;59(24):6267-75.

21. Valente P, Fasina G, Melchiori A, Masiello L, Cilli M, Vacca A, et al. TIMP-2 over-expression reduces invasion and angiogenesis and protects B16F10 melanoma cells from apoptosis (vol 75, pg 246, 1998). International Journal of Cancer 1999;80(3):485.

Chapter 7

Conclusion

7.1 Conclusion

Experiments reported in this thesis determined and demonstrated:

a) By sequence analysis and homology modeling basic Region I, Arg20 to Lys 52, of TIMP-3 that forms two anti-parallel beta sheets connected by a short loop, appears as a basic surface on the TIMP-3 model that could interact with heparan sulfate. The negatively charged sulfate groups of heparan sulfate are separated by distances similar to the positively charged amines of the TIMP-3 model where they could electrostatically interact. The GAGs, keratan sulfate, chondroitin sulfate and hyaluronate do not appear to be able to form as many close interactions.

b) The C2 and C3 chimeras were constructed to determine if the first basic Region I, Arg20 to Lys52, of TIMP-3 was involved in the binding of TIMP-3 in the ECM. The basic Region I, Val23 to His60, of TIMP-3 was replaced with the analogous region, Ala23 to Tyr64, from TIMP-2 to construct the C3 chimera, and the reverse exchange was made for TIMP-2 to construct the C2 chimera. It was anticipated that the C3 chimera would localize to the conditioned media and the C2 chimera would localize to the ECM. Transient transfections in COS-1 cells and the stable transfections in BHK-21 cells demonstrated that the C3 chimera localizes to the conditioned media. The reverse chimera, C2, partially localizes to the ECM. It

is clear that the basic Region I of TIMP-3 (Val23 to His60) is a major factor in the binding of this protein to the ECM because exchange of this domain with the analogous region of TIMP-2 abolishes ECM-binding. However, although this region may be necessary for ECM-binding of TIMP-3, it is not sufficient for the complete conversion of TIMP-2 into a matrix bound protein. That is, the C2 chimera, while showing some evidence of ECM-binding, is still localized predominantly in the conditioned media.

c) The preliminary gel filtration and ion exchange chromatographic experiments demonstrate that it is possible to purify the C3 and C3-L chimeras from the conditioned medium. In addition, from these experiments, it appears that the affinity of MMP-2 for the C3 and C3-L chimeras is less than for TIMP-2, to which it binds avidly. Heparan sulfate was demonstrated to release TIMP-3 from the cell surface of the BHK-21 cells in Chapter 5. The heparan sulfate could be utilized to extract TIMP-3 into the conditioned media for purification.

d) The confocal microscopy experiments are the first definitive demonstration of TIMP-3 on the cell surface. If the findings that heparin causes the release of cell-surface HSPGs from endothelial cells by Lowe-Krentz *et al.* is applied to the interpretation of the data from the incubation of heparan sulfate with pNUThuTIMP-3

BHK-21 cells, then it can be concluded that TIMP-3 binds to HSPGs on the cell surface and in the ECM (1).

e) Growth experiments have determined that wild-type TIMP-2 and TIMP-3 and the chimeras have an effect on the proliferation of the transfected BHK-21 cells. However, because the TIMPs have separate inhibitory and cell proliferation activities, their relative contributions to the growth differences cannot be ascertained. Because both cell-cell and cell-matrix interactions affect cell proliferation, these MMP and/or sheddase inhibition and cytokine activities of the TIMPs may, in concert, affect cell proliferaction.

The binding experiments of TIMP-3 with heparan sulfate-coated agarose beads by Kishnani and Hawkes and the confocal microscopy experiments reported in Chapter 5, demonstrate that TIMP-3 binds to HSPGs on the cell surface and the ECM. However, even though basic Region I, Arg20 to Lys52, of TIMP-3 has been demonstrated to be important for its ECM localization, this is not proof that Region I binds to heparan sulfate. Binding experiments of purified wild-type and chimeric proteins with heparan sulfate would aid in determining if Region I does indeed preferentially bind to heparan sulfate. Site-directed mutagenesis along with binding experiments could determine which amino acids are necessary for the interactions of Region I of TIMP-3 and heparan sulfate. The mutagenesis experiments should not

be limited to lysines and arginines, because amino acids such as glutamate, aspartate, tyrosine and histidine may form hydrogen bonds with proton donors and acceptors on heparan sulfate. In addition, the TIMP-3 and heparin interaction could be observed by X-ray crystallography. Heparan sulfate-binding proteins such as FGF are dependent on the sulfation patterns on the heparan sulfate chains (2-4). A comparison of the binding of differentially sulfated forms of heparan sulfate with TIMP-3 should also be investigated. It should also be noted that the HSPG-binding could also occur through interactions with the core protein. Herndon *et al.* showed that laminin-1 can bind to glypican-1 and syndecan-3 independent of their GAG chains (5).

The localization of TIMP-3 at the cell surface is important and significant in that this localization positions it where TIMP-3 can directly interact with MT-MMPs, sheddases such as TACE and other ADAMs, syndecans and glypicans. Investigators have many times postulated that the ECM localization of TIMP-3 placed it in a location to directly effect the homeostasis of the ECM (6-9). The cell surface localization of TIMP-3 places it in a location to directly interact with and possibly be controlled by the cell. The expression patterns of membrane-bound HSPGs such as syndecans and glypicans could focalize the inhibitory effects of TIMP-3 at the cell surface. Recently,

Hotary *et al.* demonstrated that MT1-MMP and MT2-MMP, and not MT3-MMP were able to convert the phenotype of MDCK cells from noninvasive to invasive in a three-dimensional matrix (10). This activity was shown to be independent of proMMP-2 activation. Interactions of TIMP-3 on the cell surface with MT-MMPs and sheddases could be a method of focalizing the inhibition of these membrane bound enzymes and their invasive and apoptotic effects (8, 11, 12). The interaction of TIMP-3 with syndecans and/or glypicans may function as a mechanism for the cell to concentrate or control TIMP-3 at the cell surface. In addition, because MT-MMPs, ADAMs, and syndecans have transmembrane domains that may be involved in cytoplasmic signaling, and because the glypicans have membrane spanning GPI anchors, these direct interactions of TIMP-3 may be mechanisms of inside-out and outside-in signals of the cell (13, 14).

In the case of tumor metastasis and angiogenesis, these cell signals could aid in the orchestration of the degradation of and cell migration through the basal laminae and/or ECM (14-17). MMP-2 and MT1-MMP have been determined to separately interact with $\alpha V\beta 3$ integrins on the cells surface (18-20). This may be a mechanism for invasion and migration to be focused at the leading edge of migrating cells analogous to the concentration of plasmin activity by the uPAR receptors at the cell surface (21, 22). The potential for TIMP-3 to

inhibit MT-MMPs, MMP-2, and ADAMs such as TACE at the cells surface through its binding to the heparan sulfate chains of syndecans and/ or glypicans is diagrammed in Figure 7.1. In each of these scenarios cell signaling could have effects on migration, proliferation, and invasiveness (11, 12, 18, 20, 23, 24).

Recently, Fitzgerald *et al.* demonstrated that the shedding of syndecan-1 and -4 is inhibited by TIMP-3 (25). The investigators determined that a metalloproteinase was responsible for enzymatic cleavage of the ectodomain from the cell surface. The significance of syndecan shedding is still not well understood. However, Park *et al.* demonstrated that accelerated syndecan-1 shedding accompanies host cell invasion by microbial pathogens such as *Peudomonas aeruginosa* (26). TIMP-3 inhibition of shedding of the IL-6 receptor and L-selectin have also been demonstrated (11). ADAM-7, A Disintegrin And Metalloproteinse, also known as TACE, TNFalpha converting enzyme, is inhibited by TIMP-3 and is believed to be the enzyme responsible for TNFalpha shedding (11). In addition, ADAM-10 is also inhibited by TIMP-3 and TIMP-1 (12). The unique localization of TIMP-3 may be the critical property that determines its ability to inhibit the shedding of molecules from the cell surface.

Because of the unique localization of TIMP-3 on the cell surface, further investigation of the specific HSPGs to which TIMP-3 is binding

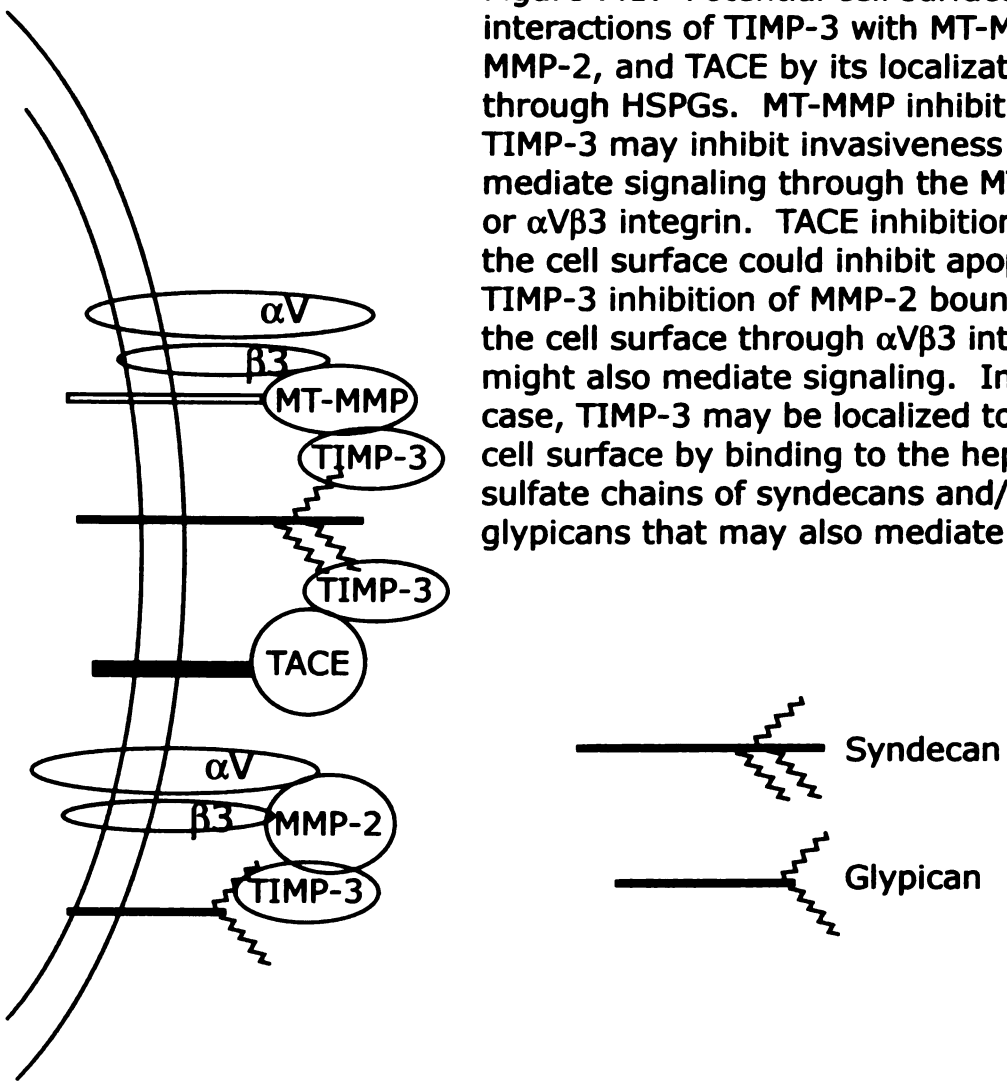

Figure 7.1: Potential cell surface interactions of TIMP-3 with MT-MMP, MMP-2, and TACE by its localization through HSPGs. MT-MMP inhibition by TIMP-3 may inhibit invasiveness and mediate signaling through the MT-MMP or αVβ3 integrin. TACE inhibition at the cell surface could inhibit apoptosis. TIMP-3 inhibition of MMP-2 bound to the cell surface through αVβ3 integrin might also mediate signaling. In each case, TIMP-3 may be localized to the cell surface by binding to the heparan sulfate chains of syndecans and/or glypicans that may also mediate signals.

is warranted. It will also be important to characterize the precise activities of TIMP-3 at the cell surface and to determine the downstream effects these cell surface activities may have. These experiments may lead to a better understanding of the role of TIMP-3 in metastasis, angiogenesis and apoptosis and possibly utilizing TIMP-3 as a focalized inhibitor for cancer metastasis and angiogenesis.

7.2 Bibliography

1. Lowe-Krentz LJ, Thompson K, Patton WAd. Heparin releasable and nonreleasable forms of heparan sulfate proteoglycan are found on the surfaces of cultured porcine aortic endothelial cells. Mol Cell Biochem 1992;109(1):51-60.

2. Lindahl U, Kusche-Gullberg M, Kjellen L. Regulated diversity of heparan sulfate. J Biol Chem 1998;273(39):24979-82.

3. Gallagher JT. Structure-activity relationship of heparan sulphate. Biochem Soc Trans 1997;25(4):1206-9.

4. Gallagher JT. Heparan sulphate and protein recognition. Binding specificities and activation mechanisms. Adv Exp Med Biol 1995;376:125-34.

5. Herndon ME, Stipp CS, Lander AD. Interactions of neural glycosaminoglycans and proteoglycans with protein ligands:

assessment of selectivity, heterogeneity and the participation of core proteins in binding. Glycobiology 1999;9(2):143-55.

6. Blenis J, Hawkes SP. Characterization of a transformation-sensitive protein in the extracellular matrix of chicken embryo fibroblasts. J Biol Chem 1984;259(18):11563-70.

7. Edwards DR, Beaudry PP, Laing TD, Kowal V, Leco KJ, Leco PA, et al. The roles of tissue inhibitors of metalloproteinases in tissue remodelling and cell growth. Int J Obes Relat Metab Disord 1996;20 Suppl 3:S9-15.

8. Butler GS, Apte SS, Willenbrock F, Murphy G. Human tissue inhibitor of metalloproteinases 3 interacts with both the N- and C-terminal domains of gelatinases A and B. Regulation by polyanions. Journal of Biological Chemistry 1999;274(16):10846-51.

9. Denhardt DT. On the Paradoxical Ability of TIMPs Either to Inhibit of to Promote the Development and Progression of the Malignant Phenotype. In: Hawkes SP, Edwards DR, Khokha R, editors. Tissue Inhibitors of Metalloproteinases in Development and Disease: Proceedings of the Inhibitor of Metalloproteinases Conference, Banff, Alberta, Canada, September 25-29, 1996. Amsterdam, The Netherlands: Harwood Academic Publishers; 2000. p. 260.

10. Hotary K, Allen E, Punturieri A, Yana I, Weiss SJ. Regulation of cell invasion and morphogenesis in a three-dimensional type I collagen

matrix by membrane-type matrix metalloproteinases 1, 2, and 3. Journal of Cell Biology 2000;149(6):1309-23.

11. Amour A, Slocombe PM, Webster A, Butler M, Knight CG, Smith BJ, et al. TNF-alpha converting enzyme (TACE) is inhibited by TIMP-3. FEBS Lett 1998;435(1):39-44.

12. Amour A, Knight CG, Webster A, Slocombe PM, Stephens PE, Knauper V, et al. The in vitro activity of ADAM-10 is inhibited by TIMP-1 and TIMP-3 [In Process Citation]. FEBS Lett 2000;473(3):275-9.

13. Tumova S, Woods A, Couchman JR. Heparan sulfate proteoglycans on the cell surface: versatile coordinators of cellular functions. Int J Biochem Cell Biol 2000;32(3):269-88.

14. Boudreau N, Bissell MJ. Extracellular matrix signaling: integration of form and function in normal and malignant cells. Curr Opin Cell Biol 1998;10(5):640-6.

15. Lelievre S, Weaver VM, Bissell MJ. Extracellular matrix signaling from the cellular membrane skeleton to the nuclear skeleton: a model of gene regulation. Recent Prog Horm Res 1996;51:417-32.

16. Fidler IJ. Angiogenesis and cancer metastasis. Cancer Journal from Scientific American 2000;6 Suppl 2(8):S134-41.

17. Folkman J. Seminars in Medicine of the Beth Israel Hospital, Boston. Clinical applications of research on angiogenesis [see comments]. New England Journal of Medicine 1995;333(26):1757-63.

18. Hofmann UB, Westphal JR, Van Kraats AA, Ruiter DJ, Van Muijen GN. Expression of integrin alpha(v)beta(3) correlates with activation of membrane-type matrix metalloproteinase-1 (MT1-MMP) and matrix metalloproteinase-2 (MMP-2) in human melanoma cells in vitro and in vivo. International Journal of Cancer 2000;87(1):12-9.

19. Daemi N, Thomasset N, Lissitzky JC, Dumortier J, Jacquier MF, Pourreyron C, et al. Anti-beta4 integrin antibodies enhance migratory and invasive abilities of human colon adenocarcinoma cells and their MMP-2 expression. International Journal of Cancer 2000;85(6):850-6.

20. Brooks PC, Stromblad S, Sanders LC, von Schalscha TL, Aimes RT, Stetler-Stevenson WG, et al. Localization of matrix metalloproteinase MMP-2 to the surface of invasive cells by interaction with integrin alpha v beta 3. Cell 1996;85(5):683-93.

21. Andreasen PA, Kjøller L, Christensen L, Duffy MJ. The urokinase-type plasminogen activator system in cancer metastasis: a review. International Journal of Cancer 1997;72(1):1-22.

22. Murphy G, Gavrilovic J. Proteolysis and cell migration: creating a path? Current Opinion in Cell Biology 1999;11(5):614-21.

23. Klass CM, Couchman JR, Woods A. Control of extracellular matrix assembly by syndecan-2 proteoglycan. Journal of Cell Science 2000;113(Pt 3)):493-506.

24. Woods A, Couchman JR. Syndecans: synergistic activators of cell adhesion. Trends in Cell Biology 1998;8(5):189-92.

25. Fitzgerald ML, Wang Z, Park PW, Murphy G, Bernfield M. Shedding of syndecan-1 and -4 ectodomains is regulated by multiple signaling pathways and mediated by a TIMP-3-sensitive metalloproteinase. Journal of Cell Biology 2000;148(4):811-24.

26. Park PW, Pier GB, Preston MJ, Goldberger O, Fitzgerald ML, Bernfield M. Syndecan-1 shedding is enhanced by LasA, a secreted virulence factor of Pseudomonas aeruginosa. J Biol Chem 2000;275(5):3057-64.

APPENDIX

A-1: Extracellular Matrix and Conditioned Media Collection
Adapted from the method described by Blenis and Hawkes (1).

Materials

10x PBS-CMF (calcium and magnesium free phosphate buffered saline)

(100mL)

- 8.0 g NaCl
- 0.2 g KCl
- 1.25 g Na_2HPO_4
- 0.2 g KH_2PO_4
- adjust pH to 7.2 with 1M NaOH
- distilled and deionized water, ddH_2O, q.s. to 100ml

1x PBS-CMF + 5mM EGTA (ethylene glycol-bis(b-aminoethyl ether)

N,N,N',N' tetraacetic acid) (300mL)

- 30 ml 10X PBS-CMF
- 570.6 mg EGTA (MW=380.4)
- ddH_2O, to 250ml
- adjust pH to 7.2 with 1M NaOH
- q.s. to 300ml with ddH_2O

2x Laemmli sample buffer, LSB, without reducing agent (10 ml)

- 2.5 ml 0.5mM TrisHCl pH 6.8
- 3 ml glycerol
- 4.0 ml 10% SDS
- 100 µl 0.1% Bromophenol Blue
- 400 µl ddH_2O

0.1% SDS, 100mM Tris-HCl (pH 7.2)

RQ1 RNase-Free DNase (Promega Corp.) in 100 mM Tris-HCl (pH 7.2), 100mM NaCl, 60 mM MgCl2, 100 mM CaCl2

Method

NOTE: The following method was written for 10 cm tissue culture dishes. Cell densities and solution volumes were adjusted for higher or lower tissue culture surface areas.

Cell Culture:

- Cells were seeded at 6.5 x 10^5/10 cm dish and incubated at 37 °C, 5% CO_2 for 16-20 h.
- Transfected BHK-21 cells were induced and incubated another 16-20 h. at 37 °C, 5% CO_2 prior to ECM and CM collection.

Conditioned media, cell, and ECM harvesting:

- Conditioned medium was removed and an aliquot was diluted with an equal volume of 2x Laemmli sample buffer, LSB, without reducing agent.
- The dishes were rinsed with 10 ml PBS-CMF, which was removed by aspiration.
- A 10 ml aliquot of 5mM EGTA PBS-CMF was added and the dishes were incubated at 37 °C, 5% CO_2 for ~15 min for BHK-21 or ~20 min for COS-1.
- Cells were detached by repeatedly pipetting the 5 mM EGTA PBS-CMF solution over the surface of the dish until all cells were detached. The cells were collected by centrifugation at 800 *x g* for

10 min. Cells were lysed in 1 ml 0.1% SDS 100 mM Tris-HCl (pH 7.2)/dish at room temperature for 5 min. An aliquot of 100 µl of 0.05 units/µl RQ1 RNase-Free DNase (Promega Corp.) in 100 mM Tris-HCl (pH 7.2), 100 mM NaCl, 60 mM $MgCl_2$, 100 mM $CaCl_2$ was added to the lysate and incubated at 37 °C for 15 min. The samples were diluted with an equal volume of 2x LSB without reducing agent.

- The dishes were rinsed 3-4 times with 10 ml PBS-CMF to remove all cells.
- The dishes were rinsed once with 10 ml ddH_2O, aspirated, and set to dry.
- A 500 µl aliquot of 1x LSB without reducing agent was added to each dish. A cell scraper was used to evenly move the LSB over the surface for approximately 30 sec to extract the ECM. The sample was placed in a 1.5 ml eppendorf tube.
- All conditioned media, cell, and ECM samples were stored at -20 °C prior to analysis.

A-2: Reverse Zymography Method
(Includes SDS-PAGE and zymography methods)

Materials

- X Cell II Mini cell SDS-PAGE Gel apparatus (NOVEX)
- Model 3000Xi Power Supply (Bio-Rad)
- Vacuum source
- Rocking platform or rotary shaker
- Contrad 70 (Fisher Scientific)
- Acrylamide (Bio-Rad)
- 1.5% (w/v) agarose (Sigma Chemical Co.)
- N, N'- methylene-bis-acrylamide (Bio-Rad)
- Tris(hydroxymethyl) aminomethane (US Biochemicals)
- Glycine (Bio-Rad)
- Gelatin - Type A, from porcine skin, bloom 175 (Sigma Chemical Co.)
- 10% (w/v) Ammonium persulfate (Bio-Rad)
- N,N,N',N'-tetramethylethylenediamine (TEMED) (Bio-Rad)
- Glycerol (Gibco-BRL)
- 10% (w/v) sodium dodecylsulfate, SDS, (US Biochemicals)
- 1M Calcium Chloride, $CaCl_2$ (Mallinckrodt)
- 0.1% (w/v) Bromophenol blue (Bio-Rad)
- 2.5% (v/v) Triton X-100 (US Biochemicals)
- Hydrochloric acid (Fisher Scientific)
- 1 M NaOH (Fisher Scientific)
- Sodium azide, NaN_3, (US Biochemicals)
- MultiMark Multicolor molecular weight standards (NOVEX)
- TIMP-1, TIMP-2, TIMP-3, MMP-2 and MMP-9 standards (See NOTE-1)
- Coomasie Brilliant Blue R-250 (Bio-Rad)
- Destaining solution (45% (v/v) methanol, 10% (v/v) acetic acid in ddH_2O) (Fisher Scientific)
- Cellophane (NOVEX)
- Gel drying apparatus (NOVEX)
- Gel drying solution (15% (v/v) ethanol, 5% (v/v) glycerol in ddH_2O)

NOTE-1: TIMP-1 and TIMP-2 standards and TIMP-3 standards were from conditioned media and ECM of pNUThuTIMP-3 BHK-21 cells, respectively, unless indicated in the figures. The MMP-2 and MMP-9 standards were from the conditioned media of pNUThuTIMP-3

transfected BHK-21 cells and pNUTm92kDMMP transfected BHK-21 cells, respectively. Conditioned medium and ECM were sometimes mixed to give proportionate quantities of TIMP-1, TIMP-2 and TIMP-3 when stained with Coomasie Blue.

Preparation of Reagents

10X Laemmli Running Buffer (Tris-glycine (pH 8.3), 10% SDS)

- 144.1 g glycine
- 30.3 g Tris(hydroxymethyl) aminomethane
- 10 g sodium dodecyl sulfate
- mix into 900 ml of ddH_2O
- adjust pH to 8.3 with concentated hydrochloric acid
- q.s. to 1000mL with ddH_20

2x Laemmli sample buffer, LSB, without reducing agent (10 ml)

- 2.5 ml 0.5mM TrisHCl (pH 6.8)
- 3 ml glycerol
- 4.0 ml 10% SDS
- 100 µl 0.1% Bromophenol Blue
- 400 µl ddH_2O

40% (w/v) acrylamide/bis (38.93% acrylamide, 1.07% bis-acrylamide)

- 19.47 g acrylamide
- 535 mg bis-acrylamide
- q.s. to 50 ml with ddH2O
- store in translucent container at 4 °C

0.5M Tris-HCl (pH 6.8)

- 60.57 g Tris(hydroxymethyl) aminomethane
- dissolve in 900 ml of ddH_2O
- adjust pH to 6.8 with concentrated hydrochloric acid
- q.s. to 1000 ml with ddH_2O and filter through a sterile 0.22 µm polyether sulfone sterile filter

1.5M Tris-HCl (pH 8.8)

- 181.7 g Tris(hydroxymethyl) aminomethane
- dissolve in 900 ml of ddH_2O
- adjust pH to 8.8 with concentrated hydrochloric acid
- q.s. to 1000 ml with ddH_2O and filter through a sterile 0.22 µm polyether sulfone filter

10% (w/v) gelatin

- 10 g gelatin
- dissolve 100 ml ddH_2O at 60 °C

Development Buffer (50 mM Tris-HCl (pH 8.8), 0.2% (w/v) NaN_3, 5 mM $CaCl_2$)

- 3.33 ml 1.5 M Tris-HCl (pH 8.8)
- 200 mg sodium azide
- 3 ml 2.5% Triton X-100
- 500 µl 1 M $CaCl_2$
- q.s. to 100 ml with ddH_2O

Coomasie Staining Solution (0.1% w/v Coomasie Blue)

- dissolve 500 mg Coomasie Brilliant Blue R-250 in 500 ml of destaining solution

Method

- Glass gel plates were soaked in 0.1% (v/v) Contrad 70 for 1 h and rinsed thoroughly before assembly and sealing with 1.5% agarose.
- Depending on the gels being poured, the following mixtures were added to a 50 ml vacuum flask and vacuum degassed.

Reagent	15% rev. zym.	15% SDS-PAGE	8% zym.	5% stack
40% Bis/Acrylamide	5.63 ml	5.63 ml	3.0 ml	1.25 ml
0.5M Tris-Hcl, pH 6.8	0	0	0	2.50 ml
1.5M Tris-Hcl, pH 8.8	3.75 ml	3.75ml	3.75 ml	0
Conditioned Media	3.50 ml	0	0	0
100X Gelatin	150 µl	0	150 µl	0
10% SDS	0	150 µl		100 µl
dd H2O	1.86 ml	5.36 ml	8.00 ml	6.04 ml

* provides enough for 2 NOVEX gels (15mL)

- A 100 µl aliquot of 10% ammonium persulfate and 10 µl TEMED were added to the gel mixture that was poured to a level 2.5 cm from the top of the plates. ddH_2O was carefully overlayed on top of the polymerizing gel. The gel was allowed to polymerize for approximately 45 min.
- The ddH_2O was removed.
- A 100 µl aliquot of 10% ammonium persulfate and 10 µl TEMED were added to the stacking gel mixture that was poured on top of the polymerized gel and a gel loading comb was inserted between the

glass plates. The stacking gel was allowed to polymerize for approximate 30 min.

- The comb was carefully removed and the wells were rinsed with 1x Laemmli running buffer.
- The gel box was assembled, 1x Laemmli running buffer was added and standards and samples were loaded.
- Electrophoresis was performed at 180V for 2.5 h.
- Reverse zymogram gels were removed and placed in glass containers with 100 ml of 2.5% Triton X-100 for 15 min on a rocking platform to exchange the SDS. This was repeated once. The 2.5% Triton X-100 was replaced with 100 ml of development buffer and incubated in a 37 °C water bath with shaking for 20 h.
- The gels were transferred to a plastic container with 0.1% Coomasie Blue in destaining solution.
- After an adequate amount of time for staining (2-24 h.), Coomasie Blue solution was removed and the gels were destained with destaining solution for approximately 2 h.
- Gels were scanned before sealing in cellophane.
- Gels were soaked in gel drying solution for 10 min.
- Cellophane was soaked in gel drying solution for 2 min before assembling the gel drying apparatus. Gels were dried for more than 24 h.

For a more detailed description of this method see Hawkes *et al.* (2).

Bibliography

1. Blenis J, Hawkes SP. Characterization of a transformation-sensitive protein in the extracellular matrix of chicken embryo fibroblasts. J Biol Chem 1984;259(18):11563-70.

2. Hawkes SP, Li H, Taniguchi GT. Zymography and Reverse Zymography for Detecting MMPs and TIMPs; 2000.